Soddyian Triangles

Frank M. Jackson

Abstract. A Soddyian triangle is a triangle whose outer Soddy circle has degenerated into a straight line. This paper examines some properties of Soddyian triangles, including the facts that no Soddyian triangle can be right angled and all integer Soddyian triangles are Heronian. A generating formula is developed to produce all primitive integer Soddyian triangles. A ruler and compass construction of a Soddyian triangle concludes the paper.

1. The outer Soddy circle

In 1936 the chemist Frederick Soddy re-discovered the Descartes' theorem that relates the radii of two tangential circles to the radii of three touching circles and applied the problem to the three contact circles of a general triangle.
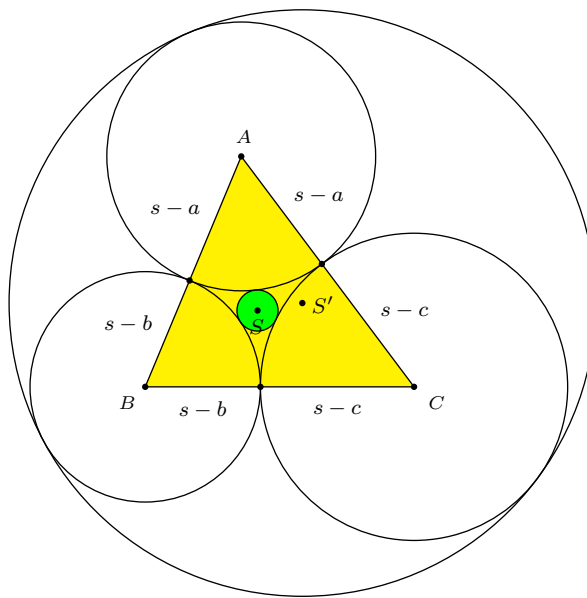

Figure 1

The tangential circles with centers S and S' are called the inner and outer Soddy circles of the reference triangle ABC. If r_i and r_o are the radii of the inner and outer Soddy circles, then

$$r_i = \frac{\Delta}{4R + r + 2s} \quad \text{and} \quad r_o = \frac{\Delta}{4R + r - 2s}. \tag{1}$$

where Δ is the area of the triangle, R its circumradius, r its inradius, s its semi-perimeter, and $s - a$, $s - b$, $s - c$ the radii of the touching circles (see [1]). By adjusting the side lengths of the reference triangle it is possible to fashion a triangle with contact circles such that the outer Soddy circle degenerates into a straight line. This occurs when $4R + r = 2s$ and is demonstrated in Figure 2 below, where it is assumed that $a \le b \le c$.

Note that for a Soddyian triangle, the radius of the inner Soddy circle is $\frac{r}{4}$. This follows from

$$r_i = \frac{\Delta}{4R + r + 2s} = \frac{\Delta}{4s} = \frac{r}{4}$$
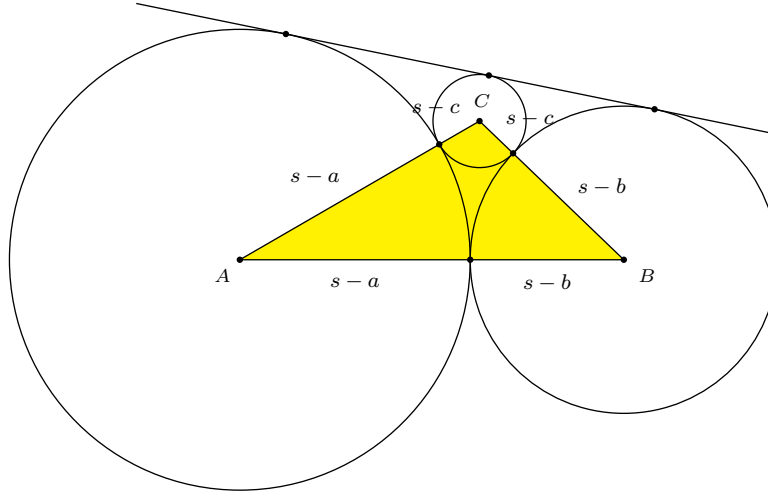
provided $4R + r = 2s$.

Figure 2

Now the common tangent to the three circles is the outer Soddy circle. Consequently a class of triangles can be defined as Soddyian if their outer Soddy radius is infinite. However from the above diagram it is possible to derive a relationship that is equivalent to the condition that the outer Soddy circle is infinite by considering the length of the common tangents between pairs of touching circles. Given two touching circles of radii u and v, their common tangent has a length of $2\sqrt{uv}$ and applying this to the three touching circle with a common tangent gives

$$\frac{1}{\sqrt{s - c}} = \frac{1}{\sqrt{s - a}} + \frac{1}{\sqrt{s - b}}. \tag{2}$$

2. Can a Soddyian triangle be right angled?

If triangle ABC has a right angle at C, then

$$R = \frac{c}{2} \quad \text{and} \quad r = s - c.$$

If $4R + r = 2s$, then $2c + s - c = 2s$. This resolves to $c = a + b$, an impossibility. Therefore, no Soddyian triangle is right angled.

3. Can a Soddyian triangle be isosceles?

A Soddy triangle with side lengths $a \leq b \leq c$ is isosceles only if $a = b$. Since $s = a + \frac{c}{2}$ and $\frac{1}{\sqrt{s-c}} = \frac{2}{\sqrt{s-a}}$, we have $\frac{c}{2} = 4a - 2c$. Hence $a : c = 5 : 8$, and the only primitive integer isosceles Soddyian triangle has sides 5, 5, 8. Note that this has integer area 12.

4. Are all integer Soddyian triangles Heronian?

Now consider the Soddyian constraint $4R + r = 2s$ expressed in terms of the area Δ:

$$\frac{abc}{\Delta} + \frac{\Delta}{s} = 2s.$$

This is quadratic in Δ and

$$\Delta = s^2 \pm \sqrt{s^4 - abcs}$$

Since s is greater than any of the sides, $\Delta < s^2$ and we must have

$$\Delta = s^2 - \sqrt{s^4 - abcs}.$$

By the Heron formula, $16\Delta^2 = (a + b + c)(b + c - a)(c + a - b)(a + b - c)$ is an integer. This can only happen if $s^4 - abcs$ is also a square integer. Hence all integer Soddyian triangles are Heronian.

5. Construction of integer Soddyian triangles

It is well known that for a Heronian triangle, the semiperimeter s is an integer. From (2),

$$s - c = \frac{(s - a)(s - b)}{(s - a) + (s - b) + 2\sqrt{(s - a)(s - b)}}.$$

This requires $\sqrt{(s - a)(s - b)}$ to be an integer. We write $s - a = km^2$ and $s - b = kn^2$ for integers k, m, n, and obtain

$$s - c = \frac{km^2n^2}{(m + n)^2}.$$

Therefore,

$$s - a : s - b : s - c : s = m^2(m+n)^2 : n^2(m+n)^2 : m^2n^2 : (m^2 + mn + n^2)^2,$$

and we may take

$$\begin{aligned}
a &= n^2((m + n)^2 + m^2), \\
b &= m^2((m + n)^2 + n^2), \\
c &= (m + n)^2(m^2 + n^2).
\end{aligned}$$

For this triangle,

$$\Delta = m^2 n^2 (m+n)^2 (m^2 + mn + n^2),$$

$$R = \frac{(m^2 + n^2)((m+n)^2 + m^2)((m+n)^2 + n^2)}{4(m^2 + mn + n^2)},$$

$$r = \frac{m^2 n^2 (m+n)^2}{m^2 + mn + n^2},$$

$$s = (m^2 + mn + n^2)^2.$$

Here are some examples of integer Soddyian triangles.

m	n	a	b	c	s	Δ	r	R
1	1	5	5	8	9	12	$\frac{4}{3}$	$\frac{25}{6}$
2	1	13	40	45	49	252	$\frac{36}{7}$	$\frac{325}{14}$
3	1	25	153	160	169	1872	$\frac{144}{13}$	$\frac{2125}{26}$
4	1	41	416	425	441	8400	$\frac{400}{21}$	$\frac{9061}{42}$
3	2	136	261	325	361	17100	$\frac{900}{19}$	$\frac{6409}{38}$
5	1	61	925	936	961	27900	$\frac{900}{31}$	$\frac{29341}{62}$
6	1	85	1800	1813	1849	75852	$\frac{1764}{43}$	$\frac{78625}{86}$
5	2	296	1325	1421	1521	191100	$\frac{4900}{39}$	$\frac{56869}{78}$
4	3	585	928	1225	1369	261072	$\frac{7056}{37}$	$\frac{47125}{74}$
7	1	113	3185	3200	3249	178752	$\frac{3136}{57}$	$\frac{183625}{114}$
5	3	801	1825	2176	2401	705600	$\frac{14400}{49}$	$\frac{110449}{98}$
8	1	145	5248	5265	5329	378432	$\frac{5184}{73}$	$\frac{386425}{146}$
7	2	520	4165	4293	4489	1063692	$\frac{15876}{67}$	$\frac{292825}{134}$
5	4	1696	2425	3321	3721	1976400	$\frac{32400}{61}$	$\frac{210781}{122}$
9	1	181	8181	8200	8281	737100	$\frac{8100}{91}$	$\frac{749521}{182}$
7	3	1341	5341	5800	6241	3483900	$\frac{44100}{79}$	$\frac{470989}{158}$

6. Soddyian triangles with a given side

Consider Soddyian triangles with a given base AB in a rectangular coordinate system with origin at A and $B = (c, 0)$ on the x-axis. Suppose the vertex C has coordinates (x, y). Using the expressions in §5 in terms of m and n, allowing them to take on positive real values, we have

$$\frac{x}{c} = \frac{b^2 + c^2 - a^2}{2c^2} = \frac{m^3(m^2 + mn + 2n^2)}{(m+n)(m^2 + n^2)^2},$$

$$\frac{y}{c} = \frac{2\Delta}{c^2} = \frac{2m^2 n^2 (m^2 + mn + n^2)}{(m+n)^2 (m^2 + n^2)^2}.$$

Writing $n = tm$, we obtain a parametrization of the locus of C as follows (see Figure 3).

$$(x, y) = c\left(\frac{1 + t + 2t^2}{(1+t)(1+t^2)^2}, \frac{2t^2(1 + t + t^2)}{(1+t)^2(1+t^2)^2} \right).$$
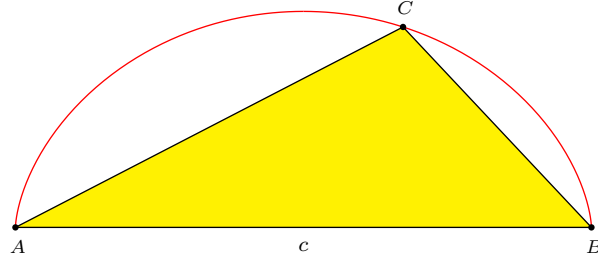
Figure 3.

In fact, given $s - a$ and $s - b$, there is a simple ruler and compass construction for the Soddyian triangle.

Construction 1. *Given a segment AB and a point Z on it (with $AZ = s - a$ and $BZ = s - b$),*
(1) construct the perpendicular to AB at Z, to intersect the semicircle with diameter AB at P;
(2) let A' and B' be points on the same side of AB such that AA', $BB' \perp AB$ and $AA' = AZ$, $BB' = BZ$;
(3) join PA' and PB' to intersect AB at X and Y respectively;
(4) construct the circle through P, X, Y to intersect the line PZ again at Q;
(5) let X' and Y' be point on AZ and ZB such that $X'Z = ZY' = ZQ$;
(6) construct the circles centers A and B, passing through Y' and X' respectively, to intersect at C.
The triangle ABC is Soddyian with incircle touching AB at Z (see Figure 4).
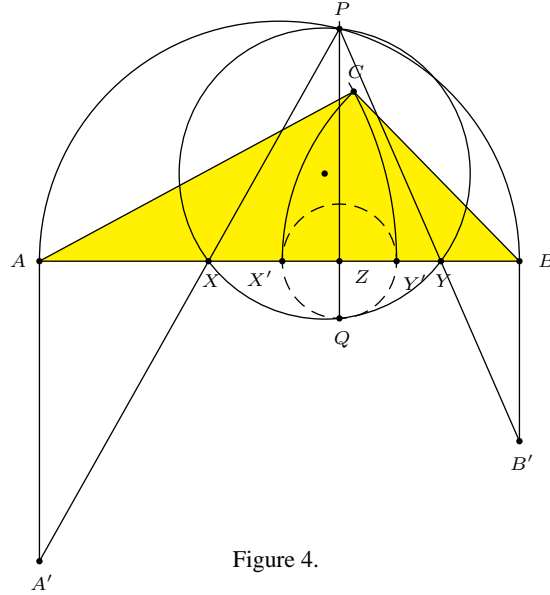

Figure 4.

Proof. Let $AZ = u$ and $BZ = v$. From (1), $ZP = \sqrt{uv}$. From (2),

$$ZX = ZA \cdot \frac{ZP}{ZP + AA'} = u \cdot \frac{\sqrt{uv}}{u + \sqrt{uv}} = \frac{u\sqrt{v}}{\sqrt{u} + \sqrt{v}}.$$

Similarly, $ZY = \frac{v\sqrt{u}}{\sqrt{u}+\sqrt{v}}$. By the intersecting chords theorem,

$$ZQ = \frac{ZX \cdot ZY}{ZP} = \frac{uv}{(\sqrt{u}+\sqrt{v})^2}.$$

It follows that

$$\frac{1}{\sqrt{ZQ}} = \frac{\sqrt{u}+\sqrt{v}}{\sqrt{uv}} = \frac{1}{\sqrt{u}} + \frac{1}{\sqrt{v}} = \frac{1}{\sqrt{AZ}} + \frac{1}{\sqrt{ZB}}.$$

Therefore, triangle ABC satisfies

$$\begin{aligned}
BC &= BX' = BZ + ZX' = BZ + ZQ, \\
AC &= AY' = AZ + ZY' = AZ + ZQ, \\
AB &= AZ + ZB,
\end{aligned}$$

with

$$\frac{1}{\sqrt{s-c}} = \frac{1}{\sqrt{ZQ}} = \frac{1}{\sqrt{AZ}} + \frac{1}{\sqrt{ZB}} = \frac{1}{\sqrt{s-a}} + \frac{1}{\sqrt{s-b}}.$$

It is Soddyian and with incircle tangent to AB at Z. $\qquad\square$

Reference

[1] N. Dergiades, The Soddy circles, *Forum Geom.*, 7 (2007) 191–197.

Frank M. Jackson: Aldebaran, Mixbury, Northamptonshire NN13 5RR United Kingdom
E-mail address: fjackson@matrix-logic.co.uk

A Triad of Circles Tangent Internally to the Nine-Point Circle

Nikolaos Dergiades and Alexei Myakishev

Abstract. Given an acute triangle, we construct the three circles each tangent to two sides and to the nine point circle internally. We show that the centers of these three circles are collinear.

In this note we construct, for a given acute triangle, the three circles each tangent to two sides of the triangle and tangent to the nine point circle internally. We show that the centers of these three circles are collinear ([1, 3]).
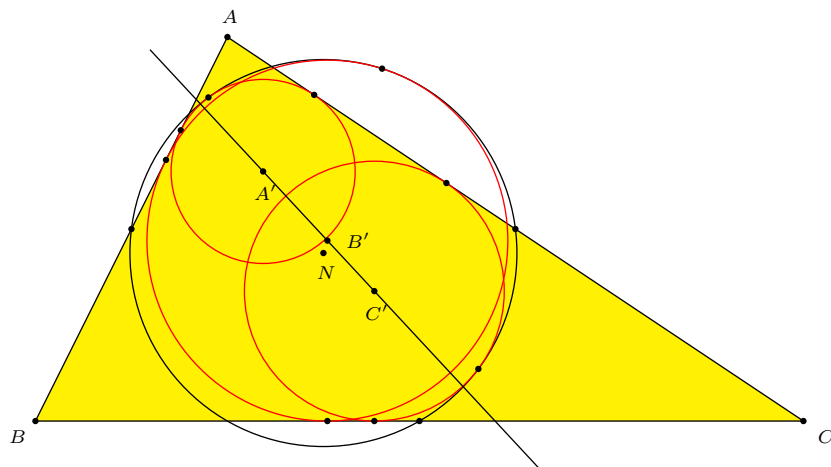

Figure 1.

Let ABC be the given triangle with incenter I. For three points A', B', C' on the respective angle bisectors, write the vectors

$$\mathbf{IA}' = p\mathbf{IA}, \quad \mathbf{IB}' = q\mathbf{IB}, \quad \mathbf{IC}' = r\mathbf{IC}.$$

Since

$$\left(\frac{a}{p}\right)\mathbf{IA}' + \left(\frac{b}{q}\right)\mathbf{IB}' + \left(\frac{c}{r}\right)\mathbf{IC}' = a\mathbf{IA} + b\mathbf{IB} + c\mathbf{IC} = 0,$$

the three points A', B', C' are collinear if and only if $\frac{a}{p} + \frac{b}{q} + \frac{c}{r} = 0$.

Now consider the nine-point circle of triangle ABC. This is tangent to the incircle at the Feuerbach point F_{e}. The power of A is $d^2 = \frac{1}{2}S_A$. If we apply

inversion with center A and power d^2, the inverse of the incircle is a circle (A') tangent to AB, AC and the nine-point circle at the second intersection F_1 of the line AF_e. We have

$$\frac{AA'}{AI} = \frac{d^2}{(s-a)^2}.$$

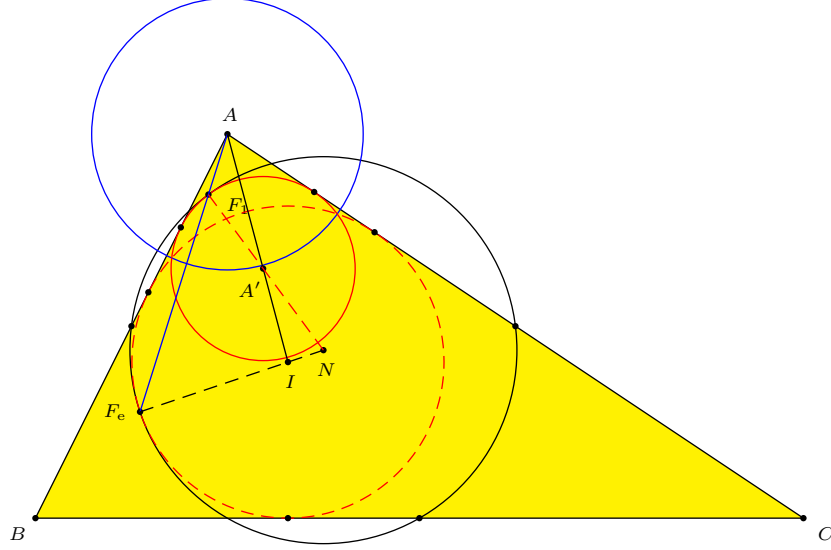Hence, $p = \frac{IA'}{IA} = \frac{2(a-b)(a-c)}{(b+c-a)^2}$.

Figure 2.

Similarly for the other centers B', C' we have

$$q = \frac{2(b-c)(b-a)}{(c+a-b)^2}, \qquad r = \frac{2(c-a)(c-b)}{(a+b-c)^2}.$$

It is easy to prove that

$$\frac{a}{p} + \frac{b}{q} + \frac{c}{r} = 0.$$

Therefore, the three centers A', B', C' are collinear.

These centers are

$$A' = pA + (1-p)I = \left(\frac{p(a+b+c)}{1-p} + a \; : \; b \; : \; c \right),$$

$$B' = qB + (1-q)I = \left(a \; : \; \frac{q(a+b+c)}{1-q} + b \; : \; c \right),$$

$$C' = rC + (1-r)I = \left(a \; : \; b \; : \; \frac{r(a+b+c)}{1-r} + c \right).$$

If the line containing these centers has barycentric equation $ux + vy + wz = 0$ with reference to triangle ABC, then

$$A' = \left(-\frac{bv + cw}{u} : b : c \right), \quad B' = \left(a : -\frac{au + cw}{v} : c \right), \quad C' = \left(a : b : -\frac{au + bv}{w} \right).$$

It follows that

$$\frac{p-1}{p} = \frac{(a+b+c)u}{au+bv+cw}, \qquad \frac{q-1}{q} = \frac{(a+b+c)v}{au+bv+cw}, \qquad \frac{r-1}{r} = \frac{(a+b+c)w}{au+bv+cw},$$

and

$$\begin{aligned}
u : v : w &= \frac{p-1}{p} : \frac{q-1}{q} : \frac{r-1}{r} \\
&= \frac{b^2 + c^2 - a^2}{2(c-a)(a-b)} : \frac{c^2 + a^2 - b^2}{2(a-b)(b-c)} : \frac{a^2 + b^2 - c^2}{2(b-c)(c-a)} \\
&= (b-c)S_A : (c-a)S_B : (a-b)S_C.
\end{aligned}$$

The line containing these points has equation

$$(b-c)S_A x + (c-a)S_B y + (a-b)S_C z = 0.$$

This line contains the orthocenter $\left(\frac{1}{S_A} : \frac{1}{S_B} : \frac{1}{S_C} \right)$ and the Spieker center. As such, it is the Soddy line of the inferior triangle. It is perpendicular to the Gergonne axis, and is the trilinear polar of X_{1897}. Randy Hutson [2] has remarked that this is also the Brocard axis of the excentral triangle.
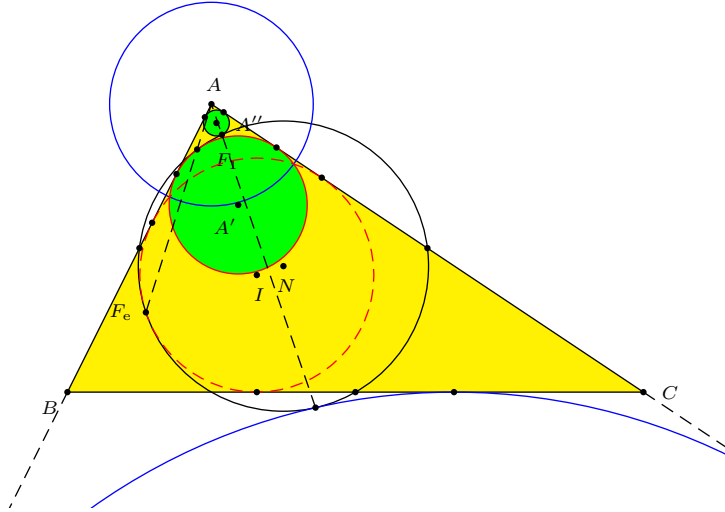

Figure 3.

We conclude with two remarks about the constructions in this note.

(1) If angle A is acute, then the circle (A') is tangent internally to the nine-point circle, and the circle (A'') inverse to the A-excircle is tangent externally to the nine-point circle (see Figure 3).

(2) The constructions apply also to obtuse triangles. If angle A is obtuse, the points A', A'' are on the extention of IA. The circle (A') is tangent externally to the nine-point circle, and the inverse of the A-excircle is a circle tangent internally to the nine-point circle (see Figure 4).
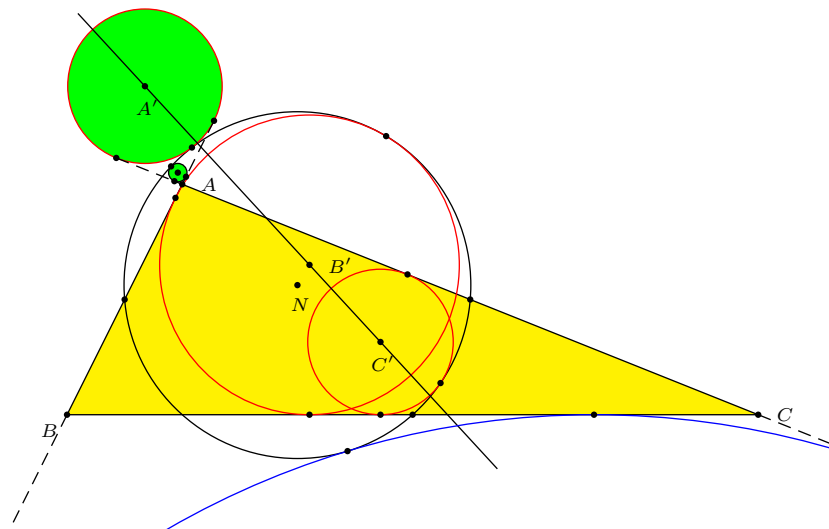

Figure 4.

References

[1] N. Dergiades, Hyacinthos, message 21408, January 12, 2013.
[2] R. Hutson, Hyacinthos, message 21411, January 12, 2013.
[3] A. Myakishev, Hyacinthos, messages 21396, 21404, January 11, 2013.

Nikolaos Dergiades: I. Zanna 27, Thessaloniki 54643, Greece
E-mail address: ndergiades@yahoo.gr

Alexei Myakishev: Belomorskaia-12-1-133,Moscow, Russia, 125445
E-mail address: amyakishev@yahoo.com

Bicentric Quadrilaterals through Inversion

Albrecht Hess

Abstract. We show that inversion is a delightful tool for making some recent and some older results on bicentric quadrilaterals more transparent and to smoothen their proofs. As a main result we give an illustrative interpretation of Yun's inequality and derive a sharper form.

1. Introduction

Figure 1 shows a bicentric quadrilateral $ABCD$, its circumcircle $\mathcal{C}$ with center O and radius R, and its incircle $\mathscr{C}$ with center Z and radius r, $OZ = d$. The sides of $ABCD$ are tangent to $\mathscr{C}$ at E, F, G, H. Apply an inversion with respect to $\mathscr{C}$.
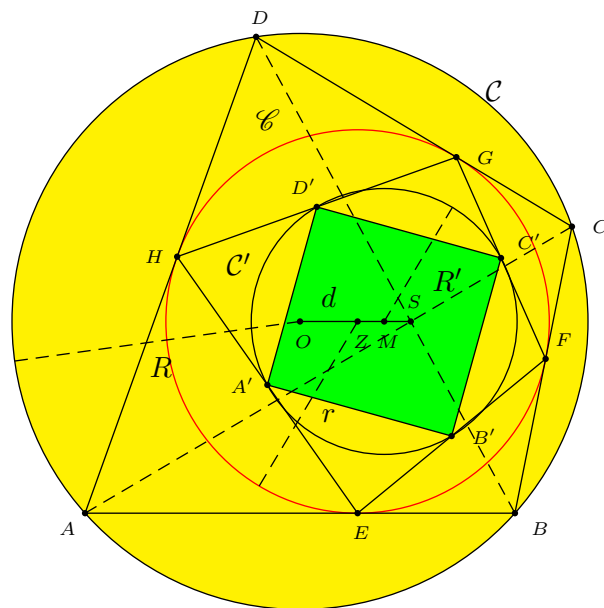
Figure 1

The images A', B', C', D' of the vertices lie on the circle $\mathcal{C}'$ with center M and radius R', $MZ = d'$. The image A' lies on the polar of A with respect to $\mathscr{C}$ and is therefore the midpoint of EH. The same applies to the other images. $A'B'C'D'$ is a rectangle, because being the quadrilateral of the midpoints of $EFGH$ it is a cyclic parallelogram. The diagonals EG and HF are orthogonal, since they are parallel to the sides of $A'B'C'D'$. Cf. [14, step 2] and [7, 837 ff.].

2. Orthogonality of Newton lines

Theorem 1 (9, Theorem 6). *A tangential quadrilateral $ABCD$ - without axes of symmetry - is cyclic if and only if its Newton line is perpendicular to the Newton line of its contact quadrilateral.*

The restriction is included, since Newton lines do not exist in tangential quadrilaterals with several axes of symmetry, for isosceles tangential trapezoids the theorem is obvious and it is false for kites. Let I and J be the points of intersection of AB and CD, respectively. BC and AD. The midpoints M_{AC}, M_{BD}, M_{IJ} are collinear in any quadrilateral. The line passing through these points is called the Newton line. To prove the collinearity one could use barycentric coordinates. For a visual proof, connect some midpoints of the quadrilateral sides and the appearing parallelograms will guide you. More information about Newton lines can be found in [1, pp. 116–118] and [2]. The points X on the Newton line have a special property: The sum of the signed areas of AXB and CXD equals the sum of the signed areas of AXD and BXC. This can be seen easily from the equivalence of both

$$\overrightarrow{XM_{AC}} \times (\overrightarrow{AB} + \overrightarrow{CD}) = 0 \quad \text{and} \quad \overrightarrow{XM_{BD}} \times (\overrightarrow{AB} + \overrightarrow{CD}) = 0$$

to

$$\overrightarrow{XA} \times \overrightarrow{XB} + \overrightarrow{XC} \times \overrightarrow{XD} = \overrightarrow{XD} \times \overrightarrow{XA} + \overrightarrow{XB} \times \overrightarrow{XC}.$$

If $ABCD$ is a tangential quadrilateral its consecutive sides a, b, c and d satisfy $a + c = b + d$, and therefore the center Z of its incircle share the property that the sum of the areas of AZB and CZD equals the sum of the areas of AZD and BZC. Hence Z belongs to the Newton line.

Proof of Theorem 1. Suppose that the Newton line of $ABCD$, *i.e.*, the line n_1 through M_{AC}, Z, M_{BD}, M_{IJ}, and the Newton line of $EFGH$, *i.e.*, the line n_2 through M_{EG}, M_{FH}, are perpendicular. Apply the inversion with respect to the incircle $\mathcal{C}$. The images of I and J of M_{EG} and M_{FH} lie on the image of n_2, which is a circle through Z orthogonal to n_1, whose center lies on n_1. If $M_{IJ} \in n_1$ is not the center of this circle, then I and J are symmetrical with respect to n_1 and $ABCD$ is a kite, which was excluded. Hence M_{IJ} is the center of the image of n_2, $\angle IZJ = 90°$, $EG \perp FH$, $A'B'C'D'$ is a rectangle and $ABCD$ cyclic. This argument can be reversed easily.

3. Fuss' formula

We derive Fuss' theorem (cf. [3], [7, 837 ff.], [8, Theorem 125], [11, p.1],) by inversion. I found no other place in literature, except the quoted book [7], where Fuss' theorem is proved with inversion. But the calculations in F. G.-M.'s book are somewhat cumbersome.

Observe - with Thales' theorem or angle chasing - that $B'SD'Z$ is a parallelogram. M being the midpoint of ZS, the parallelogram law says

$$4R'^2 + 4d'^2 = 4MD'^2 + 4d'^2 = 2ZD'^2 + 2SD'^2 = 2r^2.$$

Newton's line

Newton's line

Figure 2

The formulae for radius and midpoint distance of an inverted circle $R' = \frac{r^2 R}{R^2 - d^2}$ and $d' = \frac{r^2 d}{R^2 - d^2}$, [8, p. 51], substituted into $2R'^2 + 2d'^2 = r^2$ lead to Fuss' formula

$$\frac{1}{(R-d)^2} + \frac{1}{(R+d)^2} = \frac{1}{r^2}.$$

4. Poncelet's porism

Theorem 2. *$ABCD$ is a bicentric quadrilateral with circumcircle $\mathcal{C}$ and incircle $\mathscr{C}$. Then bicentric quadrilaterals with circumcircle $\mathcal{C}$ and incircle $\mathscr{C}$ can be constructed starting from any point of the circumcircle $\mathcal{C}$ (cf. [4], [6], [12], [13]).*

Proof. If $ABCD$ is bicentric (see Figure 1), R, r and d obey Fuss' formula. Using inversion with respect to $\mathscr{C}$, the circumcircle $\mathcal{C}$ of $ABCD$ is mapped onto the circle $\mathcal{C}'$ with center M and $2R'^2 + 2d'^2 = r^2$, just reverse the substitutions above. Let S be a point such that M is the midpoint between the center Z of the incircle and this point S. Choose any point A' on $\mathcal{C}'$. This point A' and its diametrically opposite point C' form with Z and S a parallelogram. From the parallelogram law follows that A' is the midpoint of a chord HE of $\mathscr{C}$ which forms together with S a right triangle. G and F are the endpoints of the chords from E and H through S and B', C' and D' the midpoints of the corresponding chords. Inversion with respect to $\mathscr{C}$ converts the circles with diameters ZE, ZF, ZG, ZH into the sides of the bicentric quadrilateral whose vertices are the images of A', B', C' and D'.   □

5. Carlitz' inequality

Furthermore, from $2R'^2 + 2d'^2 = r^2$ we get $\sqrt{2}R' \leq r$. Substituted into $R = \frac{r^2 R'}{R'^2 - d'^2} \geq \frac{r^2}{R'} \geq \sqrt{2}r$, Carlitz' inequality [5] is obtained.

6. Coaxial system of circles

Writing $2R'^2 + 2d'^2 = r^2$ as $\frac{R'^2}{d'} + d' = \frac{r^2}{2d'}$, we see that in a bicentric quadrilateral $ABCD$ the image S' of the point S of intersection of GE and FH - and also of AC and BD by Pascal's theorem applied to a degenerated hexagon - is the same when inverted with respect to $\mathscr{C}$ or when inverted with respect to $\mathcal{C}'$. This means that the circle with diameter SS' is orthogonal to $\mathscr{C}$ and to $\mathcal{C}'$ - and also to $\mathcal{C}$ by inversion with respect to $\mathscr{C}$. This reveals $\mathcal{C}, \mathscr{C}$ and $\mathcal{C}'$ as members of a coaxial system of circles with limiting points S and S'. The perpendicular bisector of SS' is the radical axis of this coaxial system, [8, chapter III].

7. Yun's inequality revisited

With $\frac{A+B}{2} = E$, $\frac{B+C}{2} = F$ and the law of sines $2r \sin E = FH$, $2r \sin F = EG$, Yun's inequality

$$\frac{\sqrt{2}r}{R} \leq \frac{1}{2}\left(\sin\frac{A}{2}\cos\frac{B}{2} + \sin\frac{B}{2}\cos\frac{C}{2} + \sin\frac{C}{2}\cos\frac{D}{2} + \sin\frac{D}{2}\cos\frac{A}{2}\right) \leq 1,$$

[10], [15], is converted by multiplication with $2r$ into $\frac{2\sqrt{2}r^2}{R} \leq \frac{EG+FH}{2} \leq 2r$. The right hand side is obvious. We increase the left hand side applying the formula for the radius of an inverted circle $R = \frac{r^2 R'}{R'^2 - d^2} \geq \frac{r^2}{\sqrt{R'^2 - d'^2}}$ to $\frac{2\sqrt{2}r^2}{R} \leq 2\sqrt{2R'^2 - 2d'^2}$. From $2R'^2 + 2d'^2 = r^2$ we get $\frac{2\sqrt{2}r^2}{R} \leq 2\sqrt{r^2 - (2d')^2}$. But $2\sqrt{r^2 - (2d')^2}$ is the length of the minimum chord of the circle $\mathscr{C}$ through S and $\frac{EG+FH}{2}$ is the mean of any two orthogonal chords through S, which is obviously greater, equality occurs only for squares $ABCD$ when $S = Z$.

Comparing one chord instead of the mean of two orthogonal chords with the minimum chord we get the inequality

$$\frac{\sqrt{2}r}{R} \leq \sin\frac{A+B}{2} = \sin\frac{A}{2}\sin\frac{D}{2} + \sin\frac{B}{2}\sin\frac{C}{2},$$

of which Yun's inequality is a consequence.

References

[1] C. Alsina and R. B. Nelsen, *Charming Proofs*, MAA, 2010.
[2] A. Bogomolny, Newton's and Léon Anne's Theorems,
   http://www.cut-the-knot.org/Curriculum/Geometry/NewtonTheorem.shtml
[3] A. Bogomolny, Poncelet Porism, Fuss' Theorem,
   http://www.cut-the-knot.org/Curriculum/Geometry/Fuss.shtml
[4] A. Bogomolny, Poncelet Porism,
   http://www.cut-the-knot.org/Curriculum/Geometry/PonceletChain.shtml
[5] L. Carlitz, A note on circonscriptible cyclic quadrilaterals, *Math. Mag.*, 38 (1965) 33–35.
[6] L. Flatto, *Poncelet's Theorem*, AMS, Providence RI, 2008.

[7] F. G.-M., *Exercices de géométrie*, A. Mame et fils, Tours, 1912.

[8] R. A. Johnson, *Advanced Euclidean Geometry*, Dover, 2007.

[9] M. Josefsson, Characterizations of bicentric quadrilaterals, *Forum Geom.*, 10 (2010) 165–173.

[10] M. Josefsson, A new proof of Yun's inequality for bicentric quadrilaterals, *Forum Geom.*, 12 (2012) 79–82.

[11] J. C. Salazar, Algunos teoremas y sus demostraciones, *Rev. Esc. Olimpíada Iberoamericana de Matemática*, 13 (2003) 1–8.

[12] D. Speyer, Poncelet Porism,
    `http://sbseminar.wordpress.com/2007/07/16/poncelets-porism/`

[13] Wolfram MathWorld, Poncelet's Porism,
    `http://mathworld.wolfram.com/PonceletsPorism.html`

[14] yetti (username), `www.artofproblemsolving.com/Forum/viewtopic.php?p=148226`

[15] Z. Yun, Euler's inequality revisited, *Mathematical Spectrum*, 40 (2008) 119–121.

Albrecht Hess: Deutsche Schule Madrid, Avenida Concha Espina 32, 28016 Madrid, Spain

E-mail address: `albrecht.hess@gmail.com`

FORUM GEOM

Five Proofs of an Area Characterization of Rectangles

Martin Josefsson

Abstract. We prove in five different ways a necessary and sufficient condition for a convex quadrilateral to be a rectangle regarding its area expressed in terms of its sides.

There are a handful of well known characterizations of rectangles, most of which concerns one or all four of the angles of the quadrilateral (see [8, p.34]). One example is that a parallelogram is a rectangle if and only if it has (at least) one right angle. Here we shall prove that *a convex quadrilateral with consecutive sides a, b, c, d is a rectangle if and only if its area K satisfies*

$$K = \tfrac{1}{2}\sqrt{(a^2 + c^2)(b^2 + d^2)}. \tag{1}$$

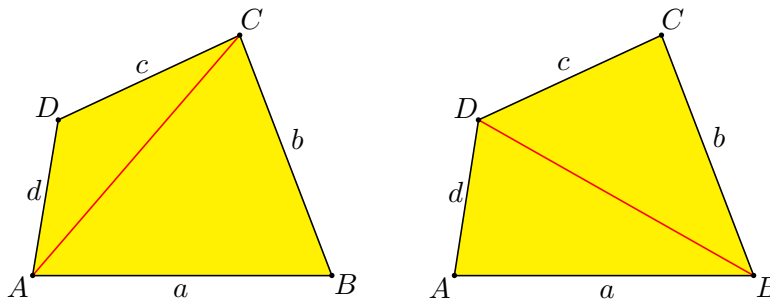We give five different proofs of this area characterization.

Figure 1. Dividing a quadrilateral into two triangles

First proof. For the area of a convex quadrilateral, we have (see the left half of Figure 1)

$$K = \tfrac{1}{2}ab\sin B + \tfrac{1}{2}cd\sin D \leq \tfrac{1}{2}(ab + cd),$$

where there is equality if and only if $B = D = \frac{\pi}{2}$. Using the following algebraic identity due to Diophantus of Alexandria

$$(ab + cd)^2 + (ad - bc)^2 = (a^2 + c^2)(b^2 + d^2)$$

directly yields the two dimensional Cauchy-Schwarz inequality

$$ab + cd \leq \sqrt{(a^2 + c^2)(b^2 + d^2)}$$

with equality if and only if $ad = bc$. Hence the area of a convex quadrilateral satisfies

$$K \leq \tfrac{1}{2}\sqrt{(a^2 + c^2)(b^2 + d^2)} \tag{2}$$

with equality if and only if $B = D = \frac{\pi}{2}$ and $ad = bc$. The third equality is equivalent to $\frac{a}{c} = \frac{b}{d}$, which together with $B = D$ yields that triangles ABC and CDA are similar. But these triangles have the side AC in common, so they are in fact congruent right triangles (since $B = D = \frac{\pi}{2}$). Then the angles at A and C in the quadrilateral must also be right angles, so $ABCD$ is a rectangle. Conversely it is trivial, that in a rectangle $B = D = \frac{\pi}{2}$ and $ad = bc$. Hence there is equality in (2) if and only if the quadrilateral is a rectangle.
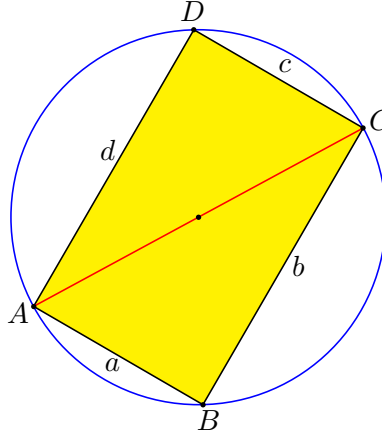

Figure 2. Congruent right triangles ABC and CDA

Second proof. A diagonal can divide a convex quadrilateral into two triangles in two different ways (see Figure 1). Adding these four triangle areas yields that the area K of the quadrilateral satisfies

$$2K = \tfrac{1}{2}ab\sin B + \tfrac{1}{2}bc\sin C + \tfrac{1}{2}cd\sin D + \tfrac{1}{2}da\sin A$$

$$\leq \tfrac{1}{2}ab + \tfrac{1}{2}bc + \tfrac{1}{2}cd + \tfrac{1}{2}da = \tfrac{1}{2}(a+c)(b+d)$$

where there is equality if and only if $A = B = C = D = \frac{\pi}{2}$. Thus

$$K \leq \tfrac{1}{4}(a+c)(b+d), \tag{3}$$

which is a known inequality for the area of a quadrilateral (see [2, p.129]), with equality if and only if it is a rectangle.[1] According to the AM-GM inequality,

$$(a+c)^2 = a^2 + c^2 + 2ac \leq 2(a^2 + c^2)$$

---

[1] An interesting historical remark is that the formula $K = \frac{a+c}{2} \cdot \frac{b+d}{2}$ (this is another area characterization of rectangles) was used by the ancient Egyptians to calculate the area of a quadrilateral, but it's only a good approximation if the angles of the quadrilateral are close to being right angles. In all quadrilaterals but rectangles the formula gives an overestimate of the area, which the tax collectors probably didn't mind.

with equality if and only if $a = c$. Similarly, $(b + d)^2 \leq 2(b^2 + d^2)$. Using these two inequalities in (3), which we first rewrite, we get

$$K \leq \tfrac{1}{4}\sqrt{(a + c)^2(b + d)^2}$$
$$\leq \tfrac{1}{4}\sqrt{2(a^2 + c^2) \cdot 2(b^2 + d^2)} = \tfrac{1}{2}\sqrt{(a^2 + c^2)(b^2 + d^2)}.$$

There is equality if and only if $a = c$, $b = d$, and $A = B = C = D = \frac{\pi}{2}$, that is, only when the quadrilateral is a rectangle.
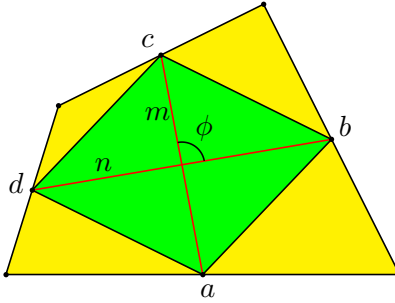

Figure 3. The Varignon parallelogram and the bimedians

Third proof. The area of a convex quadrilateral is twice the area of its Varignon parallelogram [3, p.53]. The diagonals in that parallelogram are the bimedians m and n in the quadrilateral, that is, the line segments connecting the midpoints of opposite sides (see Figure 3). Using that the area K of a convex quadrilateral is given by one half the product of its diagonals and sine for the angle between the diagonals (this was proved in [5]), we have that

$$K = mn \sin \phi \tag{4}$$

where ϕ is the angle between the bimedians. In [7, p.19] we proved that the diagonals of a convex quadrilateral are congruent if and only if the bimedians are perpendicular. Hence the area of a convex quadrilateral is

$$K = mn \tag{5}$$

if and only if the diagonals are congruent (it is an equidiagonal quadrilateral). The length of the bimedians in a convex quadrilateral can be expressed in terms of two opposite sides and the distance v between the midpoints of the diagonals as

$$m = \tfrac{1}{2}\sqrt{2(b^2 + d^2) - 4v^2},$$
$$n = \tfrac{1}{2}\sqrt{2(a^2 + c^2) - 4v^2} \tag{6}$$

(see [6, p.162]). Using these expressions in (5), we have that the area of a convex quadrilateral is given by

$$K = \tfrac{1}{4}\sqrt{(2(a^2 + c^2) - 4v^2)(2(b^2 + d^2) - 4v^2)}$$

if and only if the diagonals are congruent. Now solving the equation

$$\tfrac{1}{2}\sqrt{(a^2+c^2)(b^2+d^2)} = \tfrac{1}{4}\sqrt{(2(a^2+c^2)-4v^2)(2(b^2+d^2)-4v^2)}$$

yields $8v^2 = 0$ or $a^2+b^2+c^2+d^2 = 2v^2$. The second equality is not satisfied in any quadrilateral, since according to Euler's extension of the parallelogram law, in all convex quadrilaterals

$$a^2+b^2+c^2+d^2 = p^2+q^2+4v^2 > 2v^2$$

where p and q are the lengths of the diagonals [1, p.126]. Thus we conclude that $v = 0$ is the only valid solution. Hence a convex quadrilateral has the area given by (1) if and only if the diagonals are congruent and bisect each other. A parallelogram, the quadrilateral characterized by bisecting diagonals ($v = 0$), has congruent diagonals if and only if it is a rectangle.

Fourth proof. Combining equations (4) and (6) yields that the area of a convex quadrilateral with consecutive sides a, b, c, d is given by

$$K = \tfrac{1}{4}\sqrt{(2(a^2+c^2)-4v^2)(2(b^2+d^2)-4v^2)}\sin\phi$$

where v is the the distance between the midpoints of the diagonals and ϕ is the angle between the bimedians. Since parallelograms are characterized by $v = 0$, we have that the area is

$$K = \tfrac{1}{2}\sqrt{(a^2+c^2)(b^2+d^2)}\sin\phi$$

if and only if the quadrilateral is a parallelogram. In a parallelogram, ϕ is equal to one of the vertex angles since each bimedian is parallel to two opposite sides (see Figure 4). A parallelogram is a rectangle if and only if one of the vertex angles is a right angle. The equation $\sin\phi = 1$ only has one possible solution $\phi = \frac{\pi}{2}$; hence we have that the area of a convex quadrilateral is given by (1) if and only if it is a rectangle.
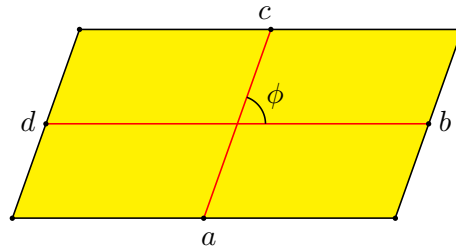

Figure 4. The angle between the bimedians in a parallelogram

Fifth proof. A convex quadrilateral with consecutive sides a, b, c, d and diagonals p, q has the area [4, p.27]

$$K = \tfrac{1}{4}\sqrt{4p^2q^2 - (a^2 - b^2 + c^2 - d^2)^2}.$$

Now solving the equation

$$\tfrac{1}{2}\sqrt{(a^2 + c^2)(b^2 + d^2)} = \tfrac{1}{4}\sqrt{4p^2q^2 - (a^2 - b^2 + c^2 - d^2)^2}$$

we get

$$(2pq)^2 - (a^2 + b^2 + c^2 + d^2)^2 = 0$$

with only one positive solution $a^2 + b^2 + c^2 + d^2 = 2pq$. Using again Euler's extension of the parallelogram law

$$a^2 + b^2 + c^2 + d^2 = p^2 + q^2 + 4v^2,$$

where v is the distance between the midpoints of the diagonals p and q, yields

$$p^2 + q^2 + 4v^2 = 2pq \quad \Leftrightarrow \quad (2v)^2 = -(p - q)^2.$$

Here the left hand side is never negative, whereas the right hand side is never positive. Thus for equality to hold, both sides must be zero. Hence $v = 0$ and $p = q$. This is equivalent to that the quadrilateral is a parallelogram with congruent diagonals, *i.e.*, a rectangle.

References

[1] N. Altshiller-Court, *College Geometry*, Barnes & Nobel, 1952. New edition by Dover Publications, 2007.

[2] O. Bottema, R. Z. Djordjević, R. R. Janić, D. S. Mitrinović, and P. M. Vasić, *Geometric Inequalities*, Wolters-Noordhoff publishing, Groningen, 1969.

[3] H. S. M. Coxeter and S. L. Greitzer, *Geometry revisited*, Math. Assoc. Amer., 1967.

[4] C. V. Durell and A. Robson, *Advanced Trigonometry*, Dover reprint, 2003.

[5] J. Harries, Area of a Quadrilateral, *The Mathematical Gazette* 86 (2002) 310–311.

[6] M. Josefsson, The area of a bicentric quadrilateral, *Forum Geom.* 11 (2011) 155–164.

[7] M. Josefsson, Characterizations of orthodiagonal quadrilaterals, *Forum Geom.* 12 (2012) 13–25.

[8] Z. Usiskin and J. Griffin, *The Classification of Quadrilaterals. A Study of Definition*, Information Age Publishing, Charlotte, 2008.

Martin Josefsson: Västergatan 25d, 285 37 Markaryd, Sweden

E-mail address: `martin.markaryd@hotmail.com`

Characterizations of Trapezoids

Martin Josefsson

Abstract. We review eight and prove an additional 13 necessary and sufficient conditions for a convex quadrilateral to be a trapezoid. One aim for this paper is to show that many of the known properties of trapezoids are in fact characterizations.

1. Introduction

A trapezoid (in British English it is called a trapezium) is a quadrilateral with a pair of opposite parallel sides. But there is some disagreement if the definition shall state *exactly* one pair or *at least* one pair. The former is called an exclusive definition and the latter an inclusive definition. The exclusive seems to be common in textbooks at lower levels of education, whereas the inclusive is common among mathematicians and at higher levels of education (beyond high school) [10, p. xiii]. What is the reason for and significance of the two possible definitions?

One likely explanation for the exclusive definition is that when students first encounter shapes like a trapezoid or a rhombus, they could get confused if a rhombus also can be called a trapezoid. When proving properties of a trapezoid it is important to actually draw it with only one pair of opposite parallel sides, so the proof covers the general case. Here the exclusive definition has its merits. But when students are to progress in their mathematical education, the exclusive definition has some drawbacks.

First of all, the main strength of the inclusive definition is the fact that a property that is proved to hold for a trapezoid automatically also holds for all quadrilaterals with two pairs of opposite parallel sides, that is, for parallelograms, rhombi, rectangles, and squares. This is a major advantage, since then we do not have to repeat arguments for those classes. Other benefits are that the taxonomy for quadrilaterals is more perspicuous within the inclusive definition, and features like symmetry and duality becomes more prominent. Also, there is the trapezoid rule for calculating integrals. But these trapezoids do not always just have one pair of opposite parallel sides; sometimes they are in fact rectangles. That would make the name of the rule confusing if a rectangle was not considered to be a special case of a trapezoid. These are some of the reasons why mathematicians nowadays prefer the inclusive definition, that is, *a trapezoid is a quadrilateral with* at least *one pair of opposite parallel sides*.

We claim that many geometry textbooks do not put much effort into summarizing even the most basic characterizations of trapezoids. The trapezoid is one of the six simplest types of quadrilaterals, so it is usually covered in books at lower levels of education. In those texts the authors often covers quite extensively methods for proving that a quadrilateral is one of the other five types: parallelograms, rhombi, rectangles, squares, and isosceles trapezoids.[1] But not the general trapezoid. Why is that? One reason could be that authors consider the topic already covered in connection with the treatment of parallel lines. But if so, then why not instead take this opportunity to connect that theory with quadrilaterals to show how it all fits together?

Anyway, we will now summarize a handful of the simplest characterizations of trapezoids. These are the ones that rely only upon the theory of parallel lines or similarity. Then we shall prove a dozen of other characterizations, and in doing so we will demonstrate that most of the well known properties of trapezoids are in fact necessary and sufficient conditions for a quadrilateral to be a trapezoid.

First a comment on notations. The consecutive sides of a convex quadrilateral $ABCD$ will be denoted $a = AB$, $b = BC$, $c = CD$, and $d = DA$. In most of the characterizations we only consider the case when $a \parallel c$ and $a \geq c$. We trust the reader can then reformulate the characterizations in the other main case $b \parallel d$ using symmetry.
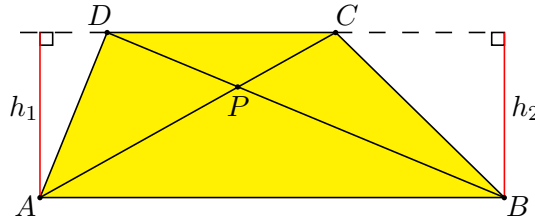

Figure 1. Two altitudes to the side CD

If the extensions of opposite sides AB and CD in a convex quadrilateral intersect at an angle ξ, then the quadrilateral is a trapezoid if and only if $\xi = 0$. A second characterization is that *the quadrilateral $ABCD$ is a trapezoid with parallel sides AB and CD if and only if $\angle ABD = \angle CDB$,* see Figure 1. An equivalent necessary and sufficient condition is that *a convex quadrilateral is a trapezoid if and only if two pairs of adjacent angles are supplementary, that is*

$$A + D = \pi = B + C. \tag{1}$$

---

[1]The kite must also be considered to be one of the basic quadrilaterals. Perhaps since there are only a few known characterizations of these, it usually don't get that much attention. If we are to include the possibility of a tangential quadrilateral as well (i.e. one that has an incircle), then there are a further dozen of (less well known) characterizations of kites, see [6]. We note that Theorem 2 (ix) in that paper contained a misprint. It should state: The incenter lies on the diagonal that is a line of symmetry (which is not necessarily the longest one).

From the theory of parallel lines we also have that *the line segments AB and CD are the bases of a trapezoid $ABCD$ if and only if the triangles ACD and BCD have equal altitudes to the common side CD ($h_1 = h_2$ in Figure 1).*

Two characterizations concerning similarity are the following. *A convex quadrilateral $ABCD$ is a trapezoid if and only if the diagonals divide each other in the same ratio, that is*

$$\frac{AP}{CP} = \frac{BP}{DP}, \tag{2}$$

where P is the intersection of the diagonals. A closely related necessary and sufficient condition states that *the diagonals divide a convex quadrilateral into four non-overlapping triangles, of which two opposite are similar if and only if the quadrilateral is a trapezoid* ($ABP \sim CDP$ in Figure 1).

2. Trigonometric characterizations

As part of the proof of Theorem 2 in [7] we have already proved two trigonometric characterizations of trapezoids, so we just restate them here. A convex quadrilateral $ABCD$ is a trapezoid if and only if

$$\sin A \sin C = \sin B \sin D.$$

An equivalent necessary and sufficient condition is

$$\cos (A - C) = \cos (B - D).$$

In fact, both of these conditions incorporate the possibility for either pair of opposite sides to be parallel, not just $a \parallel c$.

The first theorem and the subsequent proposition are trigonometric versions of the adjacent angle characterization (1).

Theorem 1. *A convex quadrilateral $ABCD$ is a trapezoid with parallel sides AB and CD if and only if*

$$\cos A + \cos D = \cos B + \cos C = 0.$$

Proof. ($\Rightarrow$) If the quadrilateral is a trapezoid, then $A + D = \pi$. Hence

$$\cos A + \cos D = \cos A + \cos (\pi - A) = \cos A - \cos A = 0.$$

The second equality is proved in the same way.

($\Leftarrow$) We do an indirect proof of the converse. Assume the quadrilateral is not a trapezoid and without loss of generality that $A > \pi - D$. Since $0 < A < \pi$ and the cosine function is decreasing on that interval, we get $\cos A < \cos (\pi - D)$. Hence

$$\cos A + \cos D < \cos (\pi - D) + \cos D = 0.$$

From the sum of angles in a quadrilateral we also have that

$$A > \pi - D \quad \Rightarrow \quad B < \pi - C \quad \Rightarrow \quad \cos B + \cos C > 0.$$

So if the quadrilateral is not a trapezoid, then $\cos A + \cos D \neq \cos B + \cos C$, and neither side is equal to 0. This completes the indirect proof. $\qquad\square$

Proposition 2. *A convex quadrilateral $ABCD$ is a trapezoid with parallel sides AB and CD if and only if*

$$\cot A + \cot D = \cot B + \cot C = 0.$$

Proof. Since the cotangent function is decreasing on the interval $0 < x < \pi$ and $\cot(\pi - x) = -\cot x$, the proof is identical to that of Theorem 1. $\qquad\square$

So far we have characterizations with sine, cosine and cotangent. Next we prove one for the tangents of the half angles.

Theorem 3. *A convex quadrilateral $ABCD$ is a trapezoid with parallel sides AB and CD if and only if*

$$\tan\frac{A}{2}\tan\frac{D}{2} = \tan\frac{B}{2}\tan\frac{C}{2} = 1.$$

Proof. ($\Rightarrow$) If the quadrilateral is a trapezoid, then $A + D = \pi = B + C$. Using these, the equalities in the theorem directly follows since $\tan\frac{D}{2} = \cot\frac{A}{2}$ and $\tan\frac{C}{2} = \cot\frac{B}{2}$.

($\Leftarrow$) Assume the quadrilateral is not a trapezoid and without loss of generality that $A + D > \pi$ and $B + C < \pi$. From the addition formula for tangent, we get

$$0 > \tan\left(\frac{A}{2} + \frac{D}{2}\right) = \frac{\tan\frac{A}{2} + \tan\frac{D}{2}}{1 - \tan\frac{A}{2}\tan\frac{D}{2}}.$$

The angles $\frac{A}{2}$ and $\frac{C}{2}$ are acute, so the numerator is positive. Then the denominator must be negative, so $\tan\frac{A}{2}\tan\frac{D}{2} > 1$. In the same way $\tan\frac{B}{2}\tan\frac{C}{2} < 1$. Hence

$$\tan\frac{A}{2}\tan\frac{D}{2} \neq \tan\frac{B}{2}\tan\frac{C}{2}$$

and neither side is equal to 1. $\qquad\square$

3. Characterizations concerning areas

The first proposition about areas concerns a bimedian, that is, a line segment that connects the midpoints of two opposite sides.

Proposition 4. *A convex quadrilateral is a trapezoid if and only if one bimedian divide it into two quadrilaterals with equal areas.*

Proof. ($\Rightarrow$) In a trapezoid, the bimedian between the bases (see the left half of Figure 2) divide it into two quadrilaterals with equal altitudes and two pairs of equal bases. Hence these two quadrilaterals, which are also trapezoids, have equal areas according to the well known formula for the area of a trapezoid.[2]

($\Leftarrow$) If $T_1 + T_2 = T_3 + T_4$ in a convex quadrilateral with notations as in the right half of Figure 2, then we have $T_1 = T_4$ since T_2 and T_3 are equal due to equal bases and equal altitudes. But T_1 and T_4 also have equal bases, so then their altitudes must be equal as well. This means that the quadrilateral is a trapezoid. $\quad\square$

---

[2] The area of a trapezoid is the arithmetic mean of the bases times the altitude.
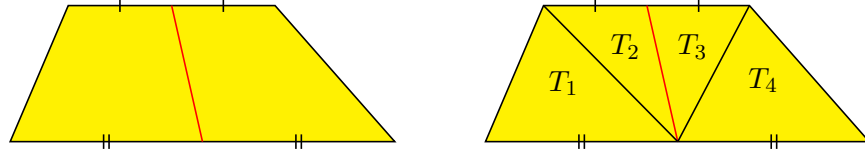
Figure 2. A trapezoid (left) and $T_1 + T_2 = T_3 + T_4$ (right)

We will need the next proposition in the proofs of the following two characterizations. A different proof was given as the solution to Problem 4.14 in [9, pp.80, 89].

Proposition 5. *If the diagonals in a convex quadrilateral $ABCD$ intersect at P, then it is a trapezoid with parallel sides AB and CD if and only if the areas of the triangles APD and BPC are equal.*

Proof. We have that the sides AB and CD are parallel if and only if (see Figure 1)

$$h_{ACD} = h_{BCD} \quad \Leftrightarrow \quad T_{ACD} = T_{BCD} \quad \Leftrightarrow \quad T_{APD} = T_{BPC}$$

where h_{XYZ} and T_{XYZ} stands for the altitude and area of triangle XYZ respectively. $\qquad \square$

The following theorem was proved by us using trigonometry as Theorem 2 in [7]. Here we give a different proof using the previous characterization.

Theorem 6. *A convex quadrilateral is a trapezoid if and only if the product of the areas of the triangles formed by one diagonal is equal to the product of the areas of the triangles formed by the other diagonal.*

Proof. We use notations on the subtriangle areas as in Figure 3. Then we have

$$(S + U_1)(T + U_2) = (S + U_2)(T + U_1)$$
$$\Leftrightarrow \quad SU_2 + TU_1 = SU_1 + TU_2$$
$$\Leftrightarrow \quad S(U_2 - U_1) = T(U_2 - U_1)$$
$$\Leftrightarrow \quad (S - T)(U_2 - U_1) = 0.$$

The last equality is equivalent to $S = T$ or $U_2 = U_1$, where either of these equalities is equivalent to that the quadrilateral is a trapezoid according to Proposition 5. $\qquad \square$

In the proof of the next theorem we will use the following lemma about a property that all convex quadrilaterals have. Observe that the triangles in this lemma are not the same as the ones in Theorem 6.

Lemma 7. *The diagonals of a convex quadrilateral divide it into four non-overlapping triangles. The product of the areas of two opposite triangles is equal to the product of the areas of the other two triangles.*
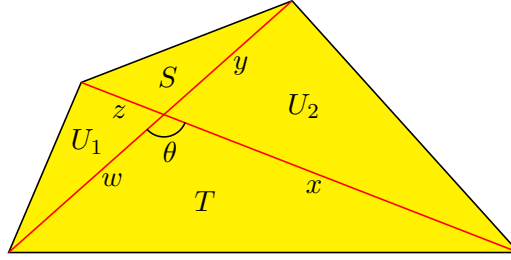
Figure 3. The diagonal parts and subtriangle areas

Proof. We denote the diagonal parts by w, x, y, z and the consecutive subtriangle areas by S, U_1, T, U_2, see Figure 3. These areas satisfy

$$ST = \tfrac{1}{4}wxyz \sin^2\theta = U_1U_2$$

where θ is the angle between the diagonals.[3] $\qquad\square$

Our last characterization concerning areas is a beautiful formula for the area of a trapezoid. It can be proved using similarity as in [1, p.50]. We give a short proof establishing it to be both a necessary and sufficient condition.

Theorem 8. *The diagonals of a convex quadrilateral divide it into four non-over-lapping triangles. If two opposite of these have areas S and T, then the quadrilateral has the area*

$$K = \left(\sqrt{S} + \sqrt{T}\right)^2$$

if and only if it is a trapezoid whose parallel sides are the two sides in the triangles in question that are not parts of the diagonals.

Proof. A convex quadrilateral has the area (see Figure 3)

$$\begin{aligned}
K &= S + T + U_1 + U_2 \\
&= S + T + 2\sqrt{ST} - 2\sqrt{U_1U_2} + U_1 + U_2 \\
&= \left(\sqrt{S} + \sqrt{T}\right)^2 + \left(\sqrt{U_1} - \sqrt{U_2}\right)^2
\end{aligned}$$

where we in the second equality used that $ST = U_1U_2$ according to the Lemma. We have that the quadrilateral is a trapezoid if and only if $U_1 = U_2$ (by Proposition 5), so it is a trapezoid if and only if it has the area $K = \left(\sqrt{S} + \sqrt{T}\right)^2$. $\qquad\square$

As a corollary we note that the area K of a convex quadrilateral satisfies the inequality [4]

$$\sqrt{K} \geq \sqrt{S} + \sqrt{T},$$

---

[3]This equality can also be proved without trigonometry. If the altitudes in the two triangles on respective side of the diagonal $w + y$ are h_1 and h_2, then we have that $ST = \tfrac{1}{4}wyh_1h_2 = U_1U_2$.

[4]We have seen this inequality before, but we cannot recall a reference.

where there is equality if and only if the quadrilateral is a trapezoid.

Theorem 8 was formulated as if there could be only one pair of opposite parallel sides (a general trapezoid). If there are two pairs of opposite parallel sides, then the two triangles with areas S and T could be be any one of the two pairs of opposite triangles formed by the diagonals.

4. Characterizations concerning sides and distances

The following simple characterization concerns the ratio of two opposite sides and the ratio of the sine of two adjacent angles.

Proposition 9. *The convex quadrilateral $ABCD$ is a trapezoid with parallel sides AB and CD if and only if*

$$\frac{DA}{BC} = \frac{\sin C}{\sin D}.$$

Proof. The quadrilateral is a trapezoid if and only if the triangles ACD and BCD have equal altitudes to the side CD, which is equivalent to that the areas of these two triangles are equal. This in turn is equivalent to

$$\tfrac{1}{2}CD \cdot DA \sin D = \tfrac{1}{2}CD \cdot BC \sin C,$$

which is equivalent to the equality in the theorem. $\square$

The parallelogram law states that in a parallelogram, the sum of the squares of the four sides equals the sum of the squares of the two diagonals. Euler generalized this to a convex quadrilateral with sides a, b, c, d and diagonals p, q as

$$a^2 + b^2 + c^2 + d^2 = p^2 + q^2 + 4v^2 \tag{3}$$

where v is the distance between the midpoints of the diagonals. A proof can be found in [2, p.126]. We shall now derive another generalization of the parallelogram law, that will give us a characterization of trapezoids as a special case. This equality was stated in [4, p.249], but Dostor's derivation was very scarce.

Theorem 10. *If a convex quadrilateral has consecutive sides a, b, c, d and diagonals p, q, then*

$$p^2 + q^2 = b^2 + d^2 + 2ac \cos \xi$$

where ξ is the angle between the extensions of the sides a and c.

Proof. In a convex quadrilateral $ABCD$, let the extensions of AB and CD intersect at J. Other notations are as in Figure 4, where $AC = p$, $BD = q$, $AB = a$, and $AE = x$. We construct GC parallel to AB. Then $\angle DCG = \angle BJC$. We also have $EF = GC = c \cos \xi$, $DG = c \sin \xi$, $ED = h - c \sin \xi$, and $FB = a - c \cos \xi - x$.
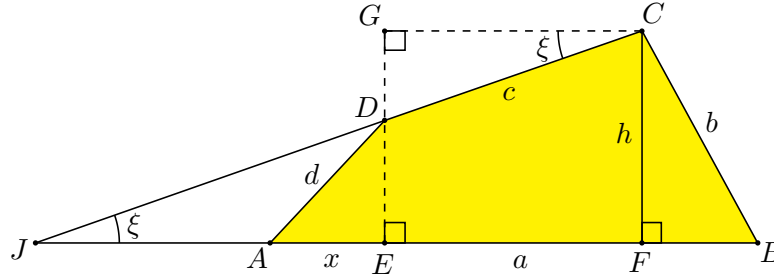
Figure 4. The alternate angles ξ

Applying the Pythagorean theorem in triangles ACF, BDE, BCF, AED, we get respectively

$$p^2 = h^2 + (x + c\cos\xi)^2, \tag{4}$$

$$q^2 = (a - x)^2 + (h - c\sin\xi)^2, \tag{5}$$

$$b^2 = h^2 + (a - c\cos\xi - x)^2, \tag{6}$$

$$d^2 = x^2 + (h - c\sin\xi)^2. \tag{7}$$

Expanding the parentheses and adding (4) and (5), we get

$$p^2 + q^2 = 2(h^2 + x^2) + 2x(c\cos\xi - a) + a^2 + c^2 - 2hc\sin\xi. \tag{8}$$

From (6) and (7),

$$b^2 + d^2 = 2(h^2 + x^2) + a^2 + c^2 - 2hc\sin\xi - 2ac\cos\xi + 2x(c\cos\xi - a). \tag{9}$$

Comparing (9) and (8), we see that

$$b^2 + d^2 = p^2 + q^2 - 2ac\cos\xi$$

and the equation in the theorem follows. $\square$

Corollary 11. *A convex quadrilateral with consecutive sides a, b, c, d and diagonals p, q is a trapezoid with parallel sides a and c if and only if*

$$p^2 + q^2 = b^2 + d^2 + 2ac.$$

Proof. This characterization is a direct consequence of Theorem 10, since the quadrilateral is a trapezoid if and only if $\xi = 0$. $\square$

The next two theorems concerns the distances between the midpoints of the diagonals and the midpoints of two opposite sides (a bimedian).

Theorem 12. *A convex quadrilateral is a trapezoid with parallel sides a and c if and only if the distance v between the midpoints of the diagonals has the length*

$$v = \frac{|a - c|}{2}.$$

Proof. Inserting the equation in Corollary 11 into (3), we get that a convex quadrilateral is a trapezoid if and only if

$$a^2 + b^2 + c^2 + d^2 = b^2 + d^2 + 2ac + 4v^2 \quad \Leftrightarrow \quad (a - c)^2 = 4v^2.$$

Hence we get the characterization $v = \frac{1}{2}|a - c|$.   □

Remark. According to the formula, the diagonals bisect each other ($v = 0$) if and only if $a = c$. In this case the quadrilateral is a parallelogram, which is a special case of a trapezoid within the inclusive definition.

Theorem 13. *A convex quadrilateral with consecutive sides a, b, c, d is a trapezoid with parallel sides a and c if and only if the bimedian n that connects the midpoints of the sides b and d has the length*

$$n = \frac{a + c}{2}.$$

Proof. The length of the bimedian n that connects the midpoints of the sides b and d in a convex quadrilateral is given by

$$4n^2 = p^2 + q^2 + a^2 - b^2 + c^2 - d^2$$

according to [3, p.231] and post no 2 at [5] (both with other notations). Substituting $p^2 + q^2$ from Corollary 11, we get that a convex quadrilateral is a trapezoid if and only if

$$4n^2 = b^2 + d^2 + 2ac + a^2 - b^2 + c^2 - d^2 \quad \Leftrightarrow \quad 4n^2 = (a + c)^2.$$

Hence $n = \frac{1}{2}(a + c)$.   □

The last characterization on sides and distances is about formulas for the length of the diagonals.

Theorem 14. *A convex quadrilateral $ABCD$ with consecutive sides a, b, c, d is a trapezoid with $a \parallel c$ and $a \neq c$ if and only if the length of the diagonals AC and BD are respectively*

$$p = \sqrt{\frac{ac(a - c) + ad^2 - cb^2}{a - c}},$$

$$q = \sqrt{\frac{ac(a - c) + ab^2 - cd^2}{a - c}}.$$

Proof. We prove the second formula first. Using the law of cosines in the two triangles formed by diagonal $BD = q$ in a convex quadrilateral, we have $d^2 = a^2 + q^2 - 2aq \cos u$ and $b^2 = c^2 + q^2 - 2cq \cos v$ (see Figure 5). Thus

$$\cos u = \frac{a^2 + q^2 - d^2}{2aq}$$

and

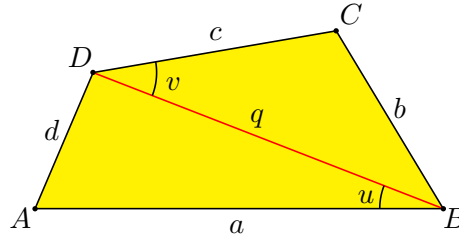$$\cos v = \frac{c^2 + q^2 - b^2}{2cq}.$$

Figure 5. A diagonal and two alternate angles

The quadrilateral is a trapezoid with $a \parallel c$ if and only if $u = v$, which is equivalent to $\cos u = \cos v$. This in turn is equivalent to

$$\frac{a^2 + q^2 - d^2}{2aq} = \frac{c^2 + q^2 - b^2}{2cq}$$

which we can rewrite as

$$ac(a - c) + ab^2 - cd^2 = (a - c)q^2.$$

Now if $a \neq c$, the second formula follows.

The first formula can be proved in the same way, or we can use symmetry and need only to make the change $b \leftrightarrow d$ in the formula we just proved. $\square$

Remark. The quadrilateral is a trapezoid with $a \parallel c$ and $a = c$ if and only if it is a parallelogram. In that case the sides alone do not uniquely determine neither the quadrilateral nor the length of the diagonals.

5. A collinearity characterization

The following theorem has been stated as a collinearity, but another possibility is to state it as a concurrency: *a convex quadrilateral is a trapezoid if and only if the two diagonals and one bimedian are concurrent, in which case the two sides that the bimedian connects are parallel.* The proof of the converse is cited from [11].

Theorem 15. *Two opposite sides in a convex quadrilateral are parallel if and only if the midpoints of those sides and the intersection of the diagonals are three collinear points.*

Proof. ($\Rightarrow$) In a trapezoid, let E and G be the midpoints of the sides AB and CD respectively, and P the intersection of the diagonals. Triangles CDP and ABP are similar due to two pairs of equal angles (see Figure 6). Note that PG and PE are medians in those triangles, but we do not yet know that $\angle DPG = \angle BPE$. This is what we shall prove. From the similarity, we get

$$\frac{PD}{PB} = \frac{CD}{AB} = \frac{2GD}{2EB} = \frac{GD}{EB}.$$
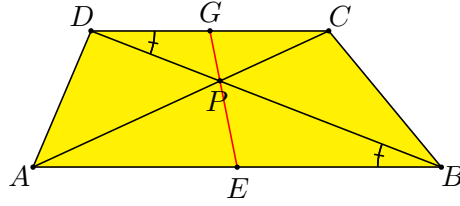
Figure 6. Are E, P and G collinear?

Also $\angle PDG = \angle PBE$, so triangles PDG and PBE are similar. Hence $\angle DPG = \angle BPE$, and since BPD is a straight line, then so is EPG.
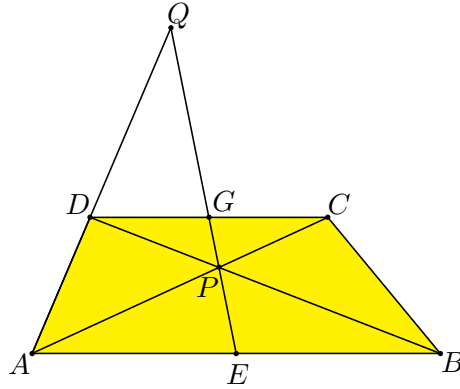
Figure 7. Is $ABCD$ a trapezoid?

($\Longleftarrow$) In a convex quadrilateral $ABCD$ where E and G are the midpoints of AB and CD and P is the intersection of the diagonals, we know that E, P and G are collinear. We shall prove that AB and CD are parallel. Extend AD and EG to intersect at Q (see Figure 7). We apply Menelaus' theorem to triangles ABD and ACD using the transversal $EPGQ$. Then

$$\frac{AE}{EB} \cdot \frac{BP}{PD} \cdot \frac{DQ}{QA} = 1 \tag{10}$$

and

$$\frac{AP}{PC} \cdot \frac{CG}{GD} \cdot \frac{DQ}{QA} = 1. \tag{11}$$

Since $AE = EB$ and $CG = GD$, equations (10) and (11) yields

$$\frac{BP}{PD} = \frac{AP}{PC}.$$

This equality states that the diagonals divide each other in the same ratio, which is the well known sufficient condition (2) for the sides AB and CD to be parallel. $\square$

6. Can all convex quadrilaterals be folded into a trapezoid?

A convex quadrilateral is not uniquely determined by its sides alone. This means that there can be different types of quadrilaterals having the same consecutive sides.[5] Let us make a model of a convex quadrilateral as four very thin rods connected by hinges at their endpoints. We assume that the length of any rod is shorter that the sum of the other three, which ensures that the rods can be the sides of a convex quadrilateral. What we shall explore is if it's always possible to fold the model into a trapezoid?
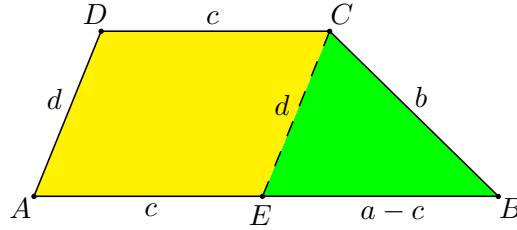

Figure 8. $AECD$ is a parallelogram

In a general trapezoid where $a \parallel c$ and $a \neq c$, we construct the triangle BCE in Figure 8 such that $CE \parallel DA$. This triangle exists whenever its sides satisfy the three triangle inequalities $a - c < b + d$, $d < a - c + b$, and $b < a - c + d$. The first of these is always satisfied if the quadrilateral exists. The second and third can be merged into

$$|a - c| > |b - d|,$$

which is a necessary condition for $a \parallel c$ when $a \neq c$. But it is also a sufficient condition, since if it is satisfied, it is possible to construct the triangle BCE and then the trapezoid. In the same way, we have that

$$|a - c| < |b - d|$$

is a necessary and sufficient condition for $b \parallel d$ when $b \neq d$. Thus the only case when we can't fold a convex quadrilateral into a trapezoid is when

$$|a - c| = |b - d|.$$

This is the characterization for when the quadrilateral has an excircle (so it is an extangential quadrilateral) according to [8, p.64].

Let us examine why we can't get a trapezoid in this case. We use the "semi factored" version of Heron's formula for the area T of a triangle to get a formula for the altitude in a trapezoid. In a triangle with sides x, y, z, the altitude h to the side x has the length

$$h = \frac{2T}{x} = \frac{\sqrt{((y+z)^2 - x^2)(x^2 - (y-z)^2)}}{2x}.$$

[5]For instance, a quadrilateral having the sides a, b, a, b can be either a (general) parallelogram or a rectangle.

The triangle BCE has the same altitude as the trapezoid. Inserting $x = a - c$, $y = b$, and $z = d$ yields the trapezoid altitude

$$h = \frac{\sqrt{((b+d)^2 - (a-c)^2)((a-c)^2 - (b-d)^2)}}{2|a-c|}$$

which is valid when $a \neq c$. Here we see that when $|a - c| = |b - d|$, the trapezoid altitude is zero. This means that the trapezoid has collapsed into a line segment. If we don't consider that degenerate case to be a trapezoid, this is the reason why an extangential quadrilateral (with a finite exradius) can never be folded into a trapezoid.

Finally we have the case $|a - c| = |b - d| = 0$. Then both pairs of opposite sides have equal length, so the quadrilateral is a parallelogram.[6] This is already a trapezoid (within the inclusive definition), so no folding is needed.

We conclude by stating the conclusions above in the following theorem.

Theorem 16. *If four line segments a, b, c, d have the property that any one of them is shorter than the sum of the other three, then they can always constitute the consecutive sides of a non-degenerate trapezoid except when $|a-c| = |b-d| \neq 0$. In that case they will be the sides of an extangential quadrilateral.*

References

[1] C. Alsina and R. B. Nelsen, *Icons of Mathematics. An exploration of twenty key images*, Math. Ass. Amer., 2011.
[2] N. Altshiller-Court, *College Geometry*, Dover reprint, 2007.
[3] C. A. Bretschneider, Untersuchung der trigonometrischen Relationen des geradlinigen Viereckes (in German), *Archiv der Mathematik und Physik* 2 (1842) 225–261.
[4] G. Dostor, Propriétés nouvelle du quadrilatère en général, avec application aux quadrilatères inscriptibles, circonscriptibles, etc. (in French), *Archiv der Mathematik und Physik* 48 (1868) 245–348.
[5] Headhunter (username) and M. Constantin, Inequality Of Diagonal, *Art of Problem Solving*, 2010, available at
    `http://www.artofproblemsolving.com/Forum/viewtopic.php?t=363253`
[6] M. Josefsson, When is a tangential quadrilateral a kite?, *Forum Geom.* 11 (2011) 165–174.
[7] M. Josefsson, The area of the diagonal point triangle, *Forum Geom.* 11 (2011) 213–216.
[8] M. Josefsson, Similar metric characterizations of tangential and extangential quadrilaterals, *Forum Geom.* 12 (2012) 63–77.
[9] V. Prasolov, *Problems in Plane and Solid Geometry*, translated and edited by D. Leites, 2006, available at `http://students.imsa.edu/~tliu/Math/planegeo.pdf`
[10] Z. Usiskin and J. Griffin, *The Classification of Quadrilaterals. A Study of Definition*, Information age publishing, Charlotte, 2008.
[11] xxxxtt and abhinavzandubalm (usernames), Convex quadrilateral is trapesoid, *Art of Problem Solving*, 2011, available at
    `http://www.artofproblemsolving.com/Forum/viewtopic.php?t=387022`

Martin Josefsson: Västergatan 25d, 285 37 Markaryd, Sweden
E-mail address: `martin.markaryd@hotmail.com`

---

[6]Note that parallelograms can be considered to be extangential quadrilateral with infinite exradius, see [8, p.76].

The Most Inaccessible Point of a Convex Domain

María Calvo and Vicente Muñoz

Abstract. The inaccessibility of a point p in a bounded domain $D \subset \mathbb{R}^n$ is the minimum of the lengths of segments through p with boundary at ∂D. The points of maximum inaccessibility I_D are those where the inaccessibility achieves its maximum. We prove that for strictly convex domains, I_D is either a point or a segment, and that for a planar polygon I_D is in general a point. We study the case of a triangle, showing that this point is not any of the classical notable points.

1. Introduction

The story of this paper starts when the second author was staring at some workers spreading cement over the floor of a square place to construct a new floor over the existing one. The procedure was the following: first they divided the area into triangular areas (actually quite irregular triangles, of around 50 square meters of area). They put bricks all along the sides of the triangles and then poured the liquid cement in the interior. To make the floor flat, they took a big rod of metal, and putting it over the bricks on two of the sides, they moved the rod to flatten the cement. Of course, they had to be careful as they were reaching the most inner part of the triangle.

The question that arose in this situation is: *What is the minimum size for the rod? Even more, which is the most inaccessible point, i.e. the one that requires the full length of the rod? Is it a notable point of the triangle?*

The purpose of this paper is to introduce the concept of maximum inaccessibility for a domain. This is done in full generality for a bounded domain in $\mathbb{R}^n$. The inaccessibility function $\mathbf{r}$ assigns to a point of the domain D the minimum length of a segment through it with boundary in ∂D. We introduce the sets $D_r = \{x \mid \mathbf{r}(x) > r\}$ and the most inaccessible set I_D given by the points where the inaccessibility function achieves its maximum value (the notion has to be suitable modified for the case where $\mathbf{r}$ only has suppremum).

Then we restrict to convex domains to prove convexity properties of the sets D_r and I_D. For strictly convex domains, I_D is either a point or a segment. For planar convex domains not containing pairs of regular points with parallel tangent lines (e.g. polygons without parallel sides), I_D is a point. In some sense, domains for which I_D is not a point are of very special nature. When $I_D = \{p_D\}$ is a point, we call p_D *the point of maximum inaccessibility* of D.

In the final section, we shall study in detail the case of a polygonal domain in the plane, and more specifically the case of a triangle, going back to the original problem. One of the results is that the point p_T, for a triangle T, is not a notable point of T. It would be nice to determine explicitly this point in terms of the coordinates of the vertices. We do it in the case of an isosceles triangle.

2. Accessibility for domains

Let $D \subset \mathbb{R}^n$ be a bounded domain, that is an open subset such that $\overline{D}$ is compact. Clearly also ∂D is compact. For a point $p \in D$, we consider the function:

$$f_p : S^{n-1} \to \mathbb{R}_+ \,,$$

which assigns to every unit vector v the length $l(\gamma)$ of the segment γ given as the connected component of $(p + \mathbb{R}v) \cap D$ containing p.

Lemma 1. f_p *is lower-semicontinuous, hence it achieves its minimum.*

Proof. Let us introduce some notation: for $p \in D$ and $v \in S^{n-1}$, we denote $\gamma_{p,v}$ the connected component of $(p + \mathbb{R}v) \cap D$ containing p. (So $\overline{\gamma_{p,v}} = [P, Q]$ for some $P, Q \in \partial D$.) Now define the function

$$H : D \times S^{n-1} \to \mathbb{R}_+ \,,$$

by $H(p, v) = f_p(v)$. Let us see that H is lower-semicontinuous (see [3] for general definitions of continuity). Suppose that $(p_n, v_n) \to (p, v)$. Let $\overline{\gamma_{p_n,v_n}} = [P_n, Q_n]$, where $P_n, Q_n \in \partial D$. As ∂D is compact, then there are convergent subsequences (which we denote as the original sequence), $P_n \to P$, $Q_n \to Q$. Clearly $P, Q \in \partial D$. Let γ be the open segment with $\overline{\gamma} = [P, Q]$. Then $p \in \gamma \subset (p + \mathbb{R}v)$. So $\gamma_{p,v} \subset \gamma$ and

$$H(p_n, v_n) = l(\gamma_{p_n,v_n}) = ||P_n - Q_n|| \to ||P - Q|| = l(\gamma) \geq l(\gamma_{p,v}) = H(p, v)\,.$$

Clearly, $f_p(v) = H(p, v)$, obtained by freezing p, is also lower-semicontinuous. $\square$

Remark. In Lemma 1, if D is moreover convex, then H is continuous. This follows from the observation that a closed segment $\sigma = [P, Q]$ with endpoints $P, Q \in \partial D$ either is fully contained in ∂D or $\sigma \cap \partial D = \{P, Q\}$. The segment γ in the proof of Lemma 1 has endpoints in ∂D and goes through p, therefore it coincides with $\gamma_{p,v}$. So $H(p_n, v_n) \to H(p, v)$, proving the continuity of H.

We say that a point $p \in D$ is *r-accessible* if there is a segment of length at most r with boundary at ∂D and containing p. Equivalently, let

$$\mathbf{r}(p) = \min_{v \in S^{n-1}} f_p(v)\,,$$

which is called *accessibility* of p. Then p is r-accessible if $\mathbf{r}(p) \leq r$. Extend $\mathbf{r}$ to $\overline{D}$ by setting $\mathbf{r}(p) = 0$ for $p \in \partial D$.

Proposition 2. *The function* $\mathbf{r} : \overline{D} \to \mathbb{R}_{\geq 0}$ *is lower-semicontinuous.*

Proof. We first study the function $\mathbf{r} : D \to \mathbb{R}_+$. As $\mathbf{r}(p) = \min_v H(p, v)$, the lower-semicontinuity of H gives the lower-semicontinuity of $\mathbf{r}$: If $p_n \to p$, take v_n such that $\mathbf{r}(p_n) = H(p_n, v_n)$. After taking a subsequence, we can assume that $(p_n, v_n) \to (p, v)$. So

$$\underline{\lim}\, \mathbf{r}(p_n) = \underline{\lim}\, H(p_n, v_n) \geq H(p, v) \geq \mathbf{r}(p)\,,$$

as required.

Finally, as we define $\mathbf{r}(p) = 0$ if $p \in \partial D$, those points give no problem to lower-semicontinuity. $\qquad\square$

We have some easy examples where f_p or $\mathbf{r}$ are not continuous. For instance, if we consider the domain

$$D = \{(x, y)|x^2 + y^2 < 1, x \leq 0\} \cup \{(x, y)|x^2 + y^2 < 4, x > 0\}\,,$$

and let $p = (0, 0)$. Then $f_p : S^1 \to \mathbb{R}^+$ has constant value 3 except at the horizontal vectors where it has value 2. Also $\mathbf{r}$ is not continuous, since $\mathbf{r}(p) = 2$, but $\mathbf{r}((\epsilon, 0)) \approx 3$, for $\epsilon > 0$ small.

Remark. If D is convex, then $\mathbf{r} : D \to \mathbb{R}_+$ is continuous. Let $p_n \to p$. Take w so that $H(p, w) = \mathbf{r}(p)$. Then $\mathbf{r}(p) = H(p, w) = \lim H(p_n, w) \geq \overline{\lim}\, \mathbf{r}(p_n)$, using the continuity of H and $H(p_n, w) \geq \mathbf{r}(p_n)$. So $\mathbf{r}$ is upper-semicontinuous, and hence continuous.

The function $\mathbf{r} : \overline{D} \to \mathbb{R}_{\geq 0}$ may not be continuous, even for convex domains. Take a semicircle $\{(x, y)|x^2 + y^2 < 1, x > 0\}$. Then $\mathbf{r}((\epsilon, 0)) = 1$, for $x > 0$ small, but $\mathbf{r}((0, 0)) = 0$.

We introduce the sets:

$$
\begin{aligned}
D_r &= \{p \in D \mid \mathbf{r}(p) > r\}, \\
E_r &= \overline{\{p \in D \mid \mathbf{r}(p) \geq r\}}.
\end{aligned}
$$

D_r is open by Proposition 2, and E_r is compact. The function $\mathbf{r}$ is clearly bounded, so it has a suppremum.

Definition. We call $R = \sup \mathbf{r}$ the *inaccessibility* of D. We call

$$I_D := \bigcap_{r < R} E_r$$

the set of points of *maximum inaccessibility* of D.

The set I_D may intersect the boundary of D. For instance, $D = \{(x, y)|x^2 + y^2 < 1, x > 0\}$. Then $R = 1$. It can be seen that $I_D = E_R = \{(x, 0)|0 \leq x \leq \frac{\sqrt{3}}{2}\}$.

Moreover, I_D can be a point of the boundary. Take $D = \{(x,y)|\frac{x^2}{4} + y^2 < 1\} - \{(x,0)|x \leq 0\}$. Then $R = 2$, and $I_D = \{(0,0)\}$. The sets D_r, for $1 < r < 2$ are petals with vertex at the origin.

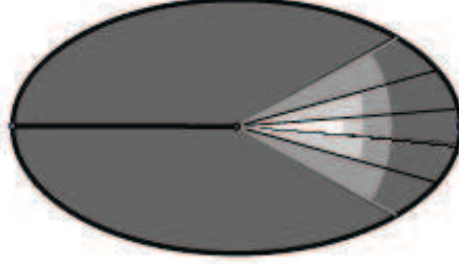Figure 1. The sets D_r for the ellipse with a long axis removed. The set I_D is in the boundary

Note that **r** does not achieve the maximum is equivalent to $I_D \subset \partial D$. This does not happen for convex D, as will be seen in the next section.

3. Convex domains

From now on, we shall suppose that D is a convex bounded domain (see [4] for general results on convex sets). This means that if $x, y \in D$, then the segment $[x, y]$ is completely included in D. There are several easy facts: $\overline{D}$ is a compact convex set, the interior of $\overline{D}$ is D, and $\overline{D}$ is the convex hull of ∂D.

There is an alternative characterization for convex sets. Let v be a unit vector in $\mathbb{R}^n$. Then the function $f(x) = \langle x, v \rangle$ achieves its maximum in ∂D, say c. Then $f(x) \leq c$ for $x \in D$. Consider the half-space

$$H_v^- = \{x \in \mathbb{R}^n \mid f(x) < c\}.$$

Then $D \subset H_v^-$. We call

$$H_v = \{x \in \mathbb{R}^n \mid f(x) = c\}$$

a *supporting hyperplane* for D (see [2, p. 129]). Note that $\partial D \cap H_v \neq \varnothing$. Let also $H_v^+ = \{x \in \mathbb{R}^n \mid f(x) > c\}$.

Lemma 3. *The convex set D is the intersection*

$$\bigcap_{|v|=1} H_v^- \, ,$$

and conversely, any such intersection is a convex set. Moreover,

$$\overline{D} = \bigcap_{|v|=1} \overline{H_v^-} \, .$$

Proof. The second assertion is clear, since the intersection of convex sets is convex.

For the first assertion, we have the trivial inclusion $D \subset \bigcap_{|v|=1} H_v$. Now suppose $p \notin D$. We have two cases:

- $p \notin \overline{D}$. Then take $q \in \overline{D}$ such that $d(p,q)$ achieves its minimum, say $s > 0$. Let v be the unit vector from p to q. Let H_v be the hyperplane through q determined by v. It is enough to see that the half-space H_v^+ is disjoint from D, since $p \in H_v^+$. Suppose that $x \in D \cap H_v^+$. Then the segment from q to x should be entirely included in $\overline{D}$, but it intersects the interior of the ball of centre p and radius s. This contradicts the choice of q.

- $p \in \partial D$. Consider $p_n \to p$, $p_n \notin \overline{D}$. By the above, there are $q_n \in \partial D$ and vectors v_n such that $D \subset H_{v_n}^- = \{\langle x - q_n, v_n \rangle < 0\}$. We take subsequences so that $q_n \to q \in \partial D$ and $v_n \to v$. So $D \subset \overline{H}_v^- = \{\langle x - q, v\rangle \leq 0\}$. But D is open, so $D \subset H_v^-$. Moreover, as $d(p_n, D) \to 0$, then $d(p_n, q_n) \to 0$, so $p = q$, and the hyperplane determining H_v goes through p, so $p \notin H_v^-$ (actually $p \in H_v$).

$\square$

Remark. The proof of Lemma 3 shows that if $p \in \partial D$, then there is a supporting hyperplane H_v through p. We call it a *supporting hyperplane at p*, and we call v a *supporting vector at p*. When a point p has several supporting hyperplanes, it is called a *corner point*. The set

$$\mathbb{R}_+ \cdot \{v | v \text{ is supporting vector at } p\} \subset \mathbb{R}^n$$

is convex. Note that if ∂D is piecewise smooth, and $p \in \partial D$ is a smooth point, then p is non-corner and the tangent space to ∂D is the supporting hyperplane.

Now we want to study the sets D_r and E_r. First note that $\mathbf{r}$ is continuous on D. Therefore

$$E_r \cap D = \{x | \mathbf{r}(x) \geq r\}$$

is closed on D.

Proposition 4. *If D is convex, then $\mathbf{r}$ achieves its supremum R at D. Moreover, $I_D \cap D = E_R \cap D = \{p \,|\, \mathbf{r}(p) = R\}$ and $I_D = E_R$ (which is the closure of $E_R \cap D$).*

Proof. Let $p \in I_D \cap \partial D$, and take a supporting hyperplane H_v at p. We claim that the open semiball $B_R(p) \cap H_v^- \subset D$. If not, then there is a point $q \in \partial D$, $d(p,q) < R$, $q \in H_v^-$. Then all the segments $[q,x]$, with $x \in B_\epsilon(p) \cap \partial D$, have length $\leq r_0 <$ (for suitable small ϵ). Therefore, there is neighbourhood U of p such that $\mathbf{r}(x) \leq r_0, \forall x \in U \cap D$. Contradiction.

Now all points in the ray $p + tv$, $t \in (0, \epsilon)$ are not r-accessible for any $r < R$. Therefore they belong to $\mathbf{r}^{-1}(R)$. So p is in the closure of $\mathbf{r}^{-1}(R)$, which is E_R.

Therefore $I_D \cap \partial D \subset E_R$. Also, by continuity of $\mathbf{r}$ on D, we have that $E_r \cap D = \mathbf{r}^{-1}[r, \infty)$. Thus $I_D \cap D = \bigcap_{r < R} \mathbf{r}^{-1}[r, \infty) = \mathbf{r}^{-1}(R) = E_R \cap D$. All together, $I_D \subset E_R$. Obviously, $E_R \cap D = \mathbf{r}^{-1}(R) \subset I_D$, and taking closures,

$E_R = \overline{E_R \cap D} \subset I_D$. So $I_D = E_R$. Finally, as I_D is always non-empty, we have that R is achieved by **r**. $\square$

Now we prove a useful result. Given two points P, Q, we denote $\overrightarrow{PQ} = Q - P$ the vector from P to Q.

Lemma 5. *Let $p \in D$ and $r = \mathbf{r}(p)$. Let $[P, Q]$ be a segment of length r with $P, Q \in \partial D$ and $p \in [P, Q]$. Let v_P, v_Q be supporting vectors at P, Q respectively. Then*

> (1) *If v_P, v_Q are parallel, then: $v_P = -v_Q$, P, Q are non-corner points, $\overrightarrow{PQ} \parallel v_P$, and $r = R$.*
> (2) *If v_P, v_Q are not parallel, then: $\overrightarrow{PQ}$ is in the plane π spanned by them, there is a unit vector $v \perp \overrightarrow{PQ}$, $v \in \pi$, such that for $H_v = \{\langle x - p, v\rangle = 0\}$, it is $E_r \subset \overline{H_v^-}$; and $\mathbf{r}(x) < r$ for $x \in [P, Q] - \{p\}$ close to p.*

Proof. (1) Suppose first that v_P, v_Q are parallel. So D is inside the region between the parallel hyperplanes H_{v_P} and H_{v_Q}. Clearly $v_P = -v_Q$. Let $x \in D$, and draw the segment parallel to $[P, Q]$ through x with endpoints in the hyperplanes. It has length r. The intersection of this segment with D is of length $\leq r$. Therefore $\mathbf{r}(x) \leq r$, for all $x \in D$, so $R = r$.

If $\overrightarrow{PQ}$ is not parallel to v_P, take a small vector w such that $\langle w, v_P\rangle = 0$, $\langle w, \overrightarrow{PQ}\rangle > 0$. Let $t \in (0, 1)$ so that $p = (1-t)P + tQ$. Then $P' = P + tw \in H_{v_P}$ and $Q' = Q - (1-t)w \in H_{v_Q}$, and $p \in [P', Q']$. First, $||\overrightarrow{P'Q'}|| = ||\overrightarrow{PQ} - w|| < ||\overrightarrow{PQ}|| = r$. Also $P', Q' \notin D$, so the segment $[P', Q'] \cap D$ is of length at most $||\overrightarrow{P'Q'}||$. Therefore $\mathbf{r}(p) < r$, a contradiction.

The assertion that P, Q are non-corner points is proved below.

(2) Suppose now that v_P, v_Q are not parallel. Again D is inside the region between the hyperplanes H_{v_P} and H_{v_Q}. Let π be the plane spanned by v_P, v_Q. Let w be the projection of $\overrightarrow{PQ}$ on the orthogonal complement to π, and suppose $w \neq 0$. Clearly $\langle w, \overrightarrow{PQ}\rangle > 0$. Let $t \in (0, 1)$ so that $p = (1 - t)P + tQ$. Then $P' = P + tw \in H_{v_P}$ and $Q' = Q - (1 - t)w \in H_{v_Q}$, and $p \in [P', Q']$. So $l([P', Q'] \cap D) \leq ||\overrightarrow{P'Q'}|| < ||\overrightarrow{PQ}|| = r$, which is a contradiction. Therefore $\overrightarrow{PQ} \in \pi$.

Let $v \in \pi$ be a unit vector such that $v \perp \overrightarrow{PQ}$. Now consider unit vectors e_1, e_2 in π so that $e_1 \perp v_P$, $e_2 \perp v_Q$, The vector

$$u = \frac{1}{\langle e_1, v\rangle \langle e_2, v\rangle}(\langle e_1, v\rangle e_2 - \langle e_2, v\rangle e_1)$$

is perpendicular to v, hence parallel to $\overrightarrow{PQ}$. We arrange that $\langle u, \overrightarrow{PQ}\rangle < 0$ by changing the sign of v if necessary. Denote $H_v = \{\langle x - p, v\rangle = 0\}$. Let us see that this satisfies the statement. Consider w so that $\langle w, v\rangle > 0$. Let $w_1 = \frac{\langle w, v\rangle}{\langle e_1, v\rangle} e_1 \in$

H_{v_P} and $w_2 = \frac{\langle w, v \rangle}{\langle e_2, v \rangle} e_2 \in H_{v_Q}$. Then

$$w_2 - w_1 = \frac{\langle w, v \rangle}{\langle e_1, v \rangle \langle e_2, v \rangle} (\langle e_1, v \rangle e_2 - \langle e_2, v \rangle e_1) = \langle w, v \rangle u \,,$$

so $\langle w_2 - w_1, \overrightarrow{PQ} \rangle = \langle w, v \rangle \langle u, \overrightarrow{PQ} \rangle < 0$. Set $P' = P + w_1$, $Q' = Q + w_2$. So $[P', Q']$ is parallel to $[P, Q]$, it goes through $p + w$, and it is shorter than $[P, Q]$. So $H_v^+ \cap E_r = \varnothing$.

For the last assertion, we write $\overrightarrow{PQ} = a_1 e_1 + a_2 e_2$, where $a_1, a_2 \neq 0$. Let $P' = P + x e_1 \in H_{v_P}$, $Q' = Q + y e_2 \in H_{v_Q}$. The condition $p \in [P', Q']$ is equivalent to p, P', Q' being aligned, which is rewritten as

$$xy + (1 - t)a_2 x - t a_1 y = 0 \,. \tag{1}$$

Now, the condition $||\overrightarrow{P'Q'}|| = ||\overrightarrow{PQ} + y e_2 - x e_1|| < ||\overrightarrow{PQ}|| = r$ for small r is achieved if $\langle \overrightarrow{PQ}, y e_2 - x e_1 \rangle < 0$. This is a linear equation of the form $\alpha_1 x + \alpha_2 y < 0$. The intersection of such half-plane with the hyperbola (1) is non-empty except if $\alpha_1 x + \alpha_2 y = 0$ is tangent to the hyperbola at the origin. So (α_1, α_2) is a multiple of $((1 - t)a_2, -t a_1)$. This determines t uniquely. So for $s \neq t$ (and close to t), we have that $p_s = (1 - s)P + sQ$ satisfies $\mathbf{r}(p_s) < r$. (Note incidentally, that it cannot be $\overrightarrow{PQ} \parallel v_P$. If so, then $\alpha_1 = 0$, and then $(1 - t)a_2 = 0$, so $t = 1$, which is not possible.)

Now we finish the proof of (1). Suppose that Q is a corner point. Then we can choose another supporting vector v_Q'. On the one hand $\overrightarrow{PQ} \parallel v_P = -v_Q$. On the other, as $v_P \nparallel v_Q'$, we must have $\overrightarrow{PQ} \nparallel v_P$, by the discussion above. Contradiction. $\square$

Theorem 6. *The sets D_r, E_r are convex sets, for $r \in [0, R]$, $R = \max \mathbf{r}$. Moreover, $\partial D_r \cap D$ is $\mathbf{r}^{-1}(r)$, for $r \in (0, R)$.*

Proof. The assertion for E_r follows from that of D_r: knowing that D_r is convex, then

$$E_r = \overline{\bigcap_{\epsilon > 0} D_{r - \epsilon}}$$

is convex since the intersection of convex sets is convex, and the closure of a convex set is convex.

Let $0 < r < R$, and let us see that D_r is convex. Let $p \notin D_r$. Then $\mathbf{r}(p) \leq r$. By Lemma 5, there is a segment $[P, Q]$ of length r, with $P, Q \in \partial D$, $v_P \nparallel v_Q$, and a vector $v \perp \overrightarrow{PQ}$ such that $E_r \subset \overline{H_v^-}$. Then $D_r \subset H_v^-$, and $p \notin H_v^-$. So D_r is the intersection of half-spaces, hence convex.

For the last assertion, note that the continuity of $\mathbf{r}$ implies that $D \cap \partial D_r \subset \mathbf{r}^{-1}(r)$. For the reversed inclusion, suppose that $\mathbf{r}(p) = r$, but $p \notin \partial D_r$. Then there is some $\epsilon > 0$ so that $B_\epsilon(p) \subset \mathbf{r}^{-1}(0, r]$. Now $\mathbf{r}^{-1}[r, \infty)$ is convex, so it is the closure of its interior, call it V. Therefore $V \cap B_\epsilon(p)$ is open, convex, and contains p in its adherence. Moreover $V \cap B_\epsilon(p) \subset \mathbf{r}^{-1}(r)$. But this is

impossible, since an easy consequence of Lemma 5 is that $\mathbf{r}^{-1}(r)$ has no interior for any $r \in (0, R)$. □

Proposition 7. *Suppose D is a convex* planar *set. Let $r \in (0, R)$. Then ∂D_r is the envelope of the segments of length r with endpoints at ∂D.*

Proof. As we proved before, the boundary of D_r is $\mathbf{r}^{-1}(r)$, so the points of ∂D_r are r-accessible, but not r'-accessible for $r' < r$. Let $p \in \partial D_r$ be a smooth point. Then there is a segment of length r and D_r is at one side of it. Therefore the segment is tangent to ∂D_r at p. □

4. Strictly convex domains

Recall that D is *strictly convex* if there is no segment included in its boundary. We assume that D is strictly convex in this section. Therefore, for each unit vector v, there is a unique point of contact $H_v \cap \partial D$. We define the function

$$g : S^{n-1} \to \partial D \,.$$

Lemma 8. *If D is strictly convex, then g is continuous.*

Proof. Let $v_n \in S^{n-1}$, $v_n \to v$. Consider $p_n = g(v_n) \in \partial D$, and the supporting hyperplane $\langle x - p_n, v_n \rangle \leq 0$. Let $p = g(v)$, with supporting hyperplane $\langle x - p, v \rangle \leq 0$. After taking a subsequence, we can suppose $p_n \to q \in \partial D$. Now $p \in \overline{D} \implies \langle p - p_n, v_n \rangle \leq 0$, and taking limits, $\langle p - q, v \rangle \leq 0$. On the other hand, $p_n \in \overline{D} \implies \langle p_n - p, v \rangle \leq 0$, and taking limits, $\langle q - p, v \rangle \leq 0$. So $\langle q - p, v \rangle = 0$. By strict convexity, $q = p$, so $g(v_n) \to g(v)$, and g is continuous. □

Now suppose that ∂D is C^1. Then for each point $p \in \partial D$, there is a normal vector $\mathbf{n}(p)$. We have a well defined function

$$\phi : \partial D \to S^{n-1}, \quad \phi(p) = \mathbf{n}(p) \,.$$

Note that $p \in H_{\mathbf{n}(p)} \cap \overline{D}$. Therefore if D is C^1 and strictly convex, both ϕ and g are defined and inverse to each other.

In general, for D convex, there are pseudo-functions $g : S^n \to \partial D$, $\phi : \partial D \to S^n$. A pseudo-function assigns to each point $v \in S^n$ a subset $g(v) \subset \partial D$ in such a way that the graph $\{(v, p) \mid p \in g(v)\}$ is closed. The inverse of a pseudo-function is well-defined, and g and ϕ are inverse to each other. The set $\phi(p)$ is the set of supporting vectors at p (see Remark 3).

Lemma 9. *Suppose D strictly convex. For all $0 < r < R$, $\partial D_r \cap \partial D = \varnothing$, so $\partial D_r = \mathbf{r}^{-1}(r)$.*

Proof. Take a point $p \in \partial D$, and let H_v be a supporting hyperplante. Consider a small ball B around p of radius $\leq r/2$. By strict convexity, $d(\partial B \cap D, H) = \epsilon_0 > 0$. Now we claim that $B_{\epsilon_0}(p) \cap D$ does not intersect D_r, so $p \notin \overline{D}_r$. Let $q \in B_{\epsilon_0}(p) \cap D$, and consider a line l parallel to H through q. The segment $l \cap B$ has endpoints $P, Q \in \partial B$. But $d(P, H) = d(Q, H) < \epsilon_0$, so $P, Q \notin D$. So the connected component $[P, Q] \cap D$ has length $< ||\overrightarrow{PQ}|| < r$, and q is r'-accessible for some $r' < r$. □

Corollary 10. *For D strictly convex, $\mathbf{r} : \overline{D} \to \mathbb{R}_{\geq 0}$ is continuous.*

Proof. By Remark 2, $\mathbf{r}$ is continuous on D. The continuity at ∂D follows from the proof of Lemma 9. □

Therefore, if D is strictly convex, then

$$I_D = E_R = \mathbf{r}^{-1}(R)\,.$$

As $I_D \subset D$, we have that I_D does not touch ∂D.

Theorem 11. *Let D be strictly convex. For all $0 < r < R$, D_r is strictly convex.*

Proof. Suppose that ∂D_r contains a segment l. Let p be a point in the interior of l. As it is r-accessible, there is a segment $[P, Q]$ of length r through p, where $P, Q \in \partial D$. By Lemma 5, v_P, v_Q are not parallel, and all points in $[P, Q]$ different from p are r'-accessible for some $r' < r$. Therefore l is transversal to $[P, Q]$. Let H_v be the hyperplane produced by Lemma 5 (2). Then all points at one side of H_v are r'-accessible for some $r' < r$, hence l cannot be transversal to H_v, so $l \subset H_v$.

Now let $x \in l$, $x \neq p$. Consider the segment parallel to $[P, Q]$ through x, call it σ. It has length r and endpoints at H_{v_P}, H_{v_Q}. But D is strictly convex, so it only touches the supporting hyperplanes at one point. Hence $\sigma \cap D$ is strictly contained in σ. Therefore $\mathbf{r}(x) < r$. Contradiction. □

5. Set of maximum inaccessibility

In this section we suppose that D is convex. Then $\mathbf{r}$ is continuous on D and it achieves its maximum R on D. Then $I_D = E_R$ and $I_D \cap D = E_R \cap D = \mathbf{r}^{-1}(R)$, by Proposition 4.

We want to characterize the case where I_D contains interior. Let us see an example where this situation happens. Let D be a rectangle. In this case R is the length of the shortest edge of the rectangle, and we have an open set with $\mathbf{r}(p) = R$ (see Figure 5). Note that it might happen that ∂E_R intersects ∂D.

Proposition 12. *If I_D has non-empty interior, then ∂D contains two open subsets which are included in parallel hyperplanes, which are at distance R.*

Proof. Consider an interior point $p \in I_D$, so $\mathbf{r}(p) = R$. Take a segment $l = [P, Q]$ of length R with endpoints $P, Q \in \partial D$. Let v_P, v_Q be vectors orthogonal to the supporting hyperplanes at P, Q. By Lemma 5, if they are not parallel, then there is a hyperplane through p such that E_R is contained in one (closed) half-space. This is not possible, as p is an interior point of E_R. So v_P, v_Q are parallel, and $\overrightarrow{PQ} \parallel v_P$. Now take any point x close to p, and consider the segment $[P', Q']$ through x parallel to $[P, Q]$, which has endpoints in H_{v_P}, H_{v_Q}. If $[P', Q'] \cap D$ is properly contained in $[P', Q']$, then $\mathbf{r}(x) < R$, which contradicts that $x \in E_R$. So $P' \in H_{v_P}$, $Q' \in H_{v_Q}$, and ∂D contains two open subsets in H_{v_P}, H_{v_Q} around P, Q, respectively. □

Theorem 13. *Let D be a strictly convex bounded domain, $R = \max \mathbf{r}$. Then I_D is a point or a segment.*

Proof. Suppose that I_D is not a point. As it is convex by Theorem 6, it contains a maximal segment σ. Let us see that it cannot contain two different (intersecting) segments. Let $p \in \sigma$ be an interior point of the segment. By Lemma 5, if we draw the segment $[P, Q]$ of length R through p, we have the following possibilities:

- v_P, v_Q are parallel. Then $\overrightarrow{PQ} \parallel v_P$. Then any point $x \notin [P, Q]$ lies in a segment $[P', Q']$ parallel to $[P, Q]$, with $P' \in H_{v_P}$ and $Q' \in H_{v_Q}$. By strict convexity, $l([P', Q'] \cap D) < R$, so $\mathbf{r}(x) < R$. That is, $E_R \subset [P, Q]$.
- v_P, v_Q are non-parallel. Then there is a hyperplane H_v through p such that $E_R \subset \overline{H_v^-}$. As p is an interior point of σ, σ does not cross H_v, so $\sigma \subset H_v$. Now let $x \in \sigma$, and consider the segment $[P', Q']$ parallel to $[P, Q]$ through x, with length R, $P' \in H_{v_P}$ and $Q' \in H_{v_Q}$. If $x \notin [P, Q]$ then strict convexity gives $l([P', Q'] \cap D) < R$, so $\mathbf{r}(x) < R$. That is, $E_R \subset [P, Q]$. Note that Lemma 5 (2) gives in this case that $E_R = \{p\}$.

□

Let us see an example where E_R is a segment. Let D be the ellipse with equation $\frac{x^2}{a^2} + \frac{y^2}{b^2} < 1$, where $2a > 2b$. Then $R = 2b$ and E_R is a segment contained in the short axis, delimited by the intersection of the axis with the perpendicular segments of length R with endpoints in the ellipse.
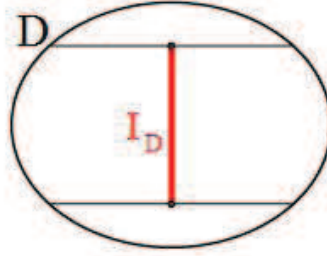
Figure 2. Ellipse

All points $(x, y) \in D$ with $x \neq 0$ can be reached by vertical segments of length $< R = 2b$. Now let $x_0 = b$, $y_0 = b\sqrt{a^2 - b^2}/a$. If $y \in (-b, -y_0) \cup (y_0, b)$ then the point $(0, y)$ is r-accessible (with a horizontal segment) with $r < R$. Now let $y \in [-y_0, y_0)$, and consider a line through $(0, y)$. Let us parametrize it as

$$r(s) = (s\, a\, \cos\theta, y + s\, b\, \sin\theta),$$

with θ fixed. The intersection with the ellipse are given by $s = -\frac{y}{b}\sin\theta \pm \sqrt{1 - \frac{y^2}{b^2}\cos^2\theta}$. So the square of the distance between the two points is

$$
\begin{aligned}
l(\theta)^2 &= 4(1 - \frac{y^2}{b^2}\cos^2\theta)(a^2\cos^2\theta + b^2\sin^2\theta) \\
&= 4(1 - \frac{y^2}{b^2}T)((a^2 - b^2)T + b^2),
\end{aligned}
$$

where $T = \cos^2 \theta \in [0, 1]$. The minimum of this degree 2 expression on T happens for a negative value of T, therefore, we only need to check the values $T = 0, 1$. For $T = 0$, we get $4b^2$; for $T = 1$, we get $4(1 - \frac{y^2}{b^2})a^2 \geq 4(1 - \frac{y_0^2}{b^2})a^2 = 4b^2$. So $l(\theta)^2 \geq 4b^2$.

A consequence of Theorem 13 is the following: for a strictly convex bounded domain D, if I_D is not a point then there are two non-corner points $P, Q \in \partial D$ with parallel tangent hyperplanes which are moreover perpendicular to $\overrightarrow{PQ}$.

Corollary 14. *Suppose D is a* planar *convex bounded domain (not necessarily strictly convex). If I_D is not a point then there are two non-corner points $P, Q \in \partial D$ with parallel tangent hyperplanes which are moreover perpendicular to $\overrightarrow{PQ}$.*

Proof. Following the proof of Theorem 13, we only have to rule out case (2). As the hyperplane H_v is now of dimension 1, we have $\sigma \subset [P, Q] = H_v \cap \overline{D}$. But Lemma 5 says also that $E_R \cap [P, Q] = \{p\}$. So E_R does not contain a segment, i.e. it is a point. $\qquad\square$

So, for a convex polygon D, if it does not have parallel sides, then I_D is a point.

Corollary 14 is not true in dimension ≥ 3. Take a triangle $T \subset \mathbb{R}^2$ and consider $D = T \times [0, L]$ for large L. For T, denote $I_T = \{p\}$. Then D has $I_D = \{p\} \times [a, b]$, for some $0 < a < b < L$. Certainly, there are two parallel faces (base and top), but we slightly move one of them to make them non-parallel, and I_D is still a segment.
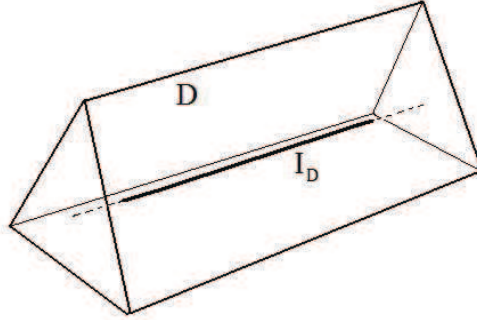

Figure 3. I_D can be positive dimensional

One can make this construction to have I_D of higher dimension (not just a segment), e.g. by considering $T \times [0, L]^N$, $N > 1$.

6. Polygons

In this section we want to study in detail the case of convex polygons in the plane, and to give some answers in the case of triangles. The starting point is the case of a sector.

Lemma 15. *Fix $\lambda \in \mathbb{R}$. Let D be the domain with boundary the half-lines $(x, 0)$, $x \geq 0$ and $(\lambda y, y)$, $y \geq 0$. Let $r > 0$. Then the boundary of D_r is the curve:*

$$\begin{cases} x = r(\cos^3 \theta + \lambda(\sin^3 \theta + 2 \sin \theta \cos^2 \theta)) \\ y = r(\sin^3 \theta - \lambda \sin^2 \theta \cos \theta) \end{cases} \tag{2}$$

Proof. D is not a bounded domain, but the theory works as well in this case. To find the boundary of D_r, we need to take the envelope of the segments of length r with endpoints laying on the half-rays, according to Proposition 7. Two points at $(a, 0)$ and $(\lambda b, b)$ are at distance r if

$$(\lambda b - a)^2 + b^2 = r^2 .$$

So $\lambda b - a = -r \cos \theta$, $b = r \sin \theta$, i.e. $a = \lambda r \sin \theta + r \cos \theta$. The line which passes through $(\lambda b, b)$ and $(a, 0)$ is

$$r \sin \theta \, x + r \cos \theta \, y = r^2 \sin \theta \cos \theta + r^2 \lambda \sin^2 \theta .$$

We are going to calculate the envelope of these lines (see pp. 75-80 in [5]). Take the derivative and solve the system:

$$\begin{cases} r \sin \theta \, x + r \cos \theta \, y = r^2 \sin \theta \cos \theta + r^2 \lambda \sin^2 \theta \\ r \cos \theta \, x - r \sin \theta \, y = -r^2 \sin^2 \theta + r^2 \cos^2 \theta + 2r^2 \lambda \sin \theta \cos \theta . \end{cases}$$

We easily get the expression in the statement. The region D_r is the unbounded region with boundary the curve (2) and the two half-rays. $\qquad\square$

We call the curve in Lemma 15 a λ-*bow* (or just a bow). Let $\lambda = \cot \alpha$, $\alpha \in (0, \pi)$. If $\lambda < 0$, we are dealing with an obtuse angle, and $\theta \in [0, \pi - \alpha]$. If $\lambda = 0$, we have a right angle, and $\theta \in [0, \frac{\pi}{2}]$. Finally, an acute angle happens for $\lambda > 0$. In this case, $\theta \in [\frac{\pi}{2} - \alpha, \frac{\pi}{2}]$. (Note that θ is the angle between the segment and the negative horizontal axis, in the proof of Lemma 15.)
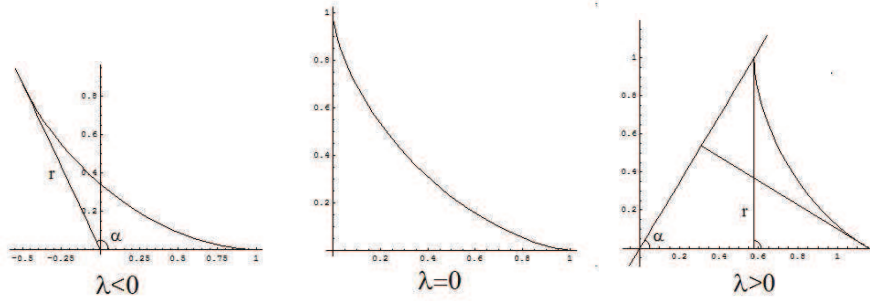
Figure 4. λ-bows with $r = 1$

As an application, we prove the following:

Corollary 16. *Let D be a planar convex polygon. Then the sets D_r, $0 < r < R$, and I_D if it is not a point, have boundaries which are piecewise C^1, and whose pieces are λ-bows and (possibly) segments in the sides of ∂D. In particular, these domains are strictly convex when ∂D_r does not intersect ∂D.*

Proof. Let $l_1, \ldots, l_k$ be the lines determined by prolonging the sides of the polygon. Consider l_i, l_j. If they intersect, consider the sector that they determine in which D is contained. Lemma 15 provides us with a (convex) region D_r^{ij}. If l_i, l_j are parallel and $r < d(l_i, l_j)$ then set $D_r^{ij} = D$, and if l_i, l_j are parallel and $r \geq d(l_i, l_j)$ then set $D_r^{ij} = \varnothing$. It is fairly clear that

$$D_r = \bigcap_{i \neq j} D_r^{ij} \, .$$

To see the last assertion, note that at any smooth point $p \in \partial D_r$, we have strict convexity because of the shape of the bows given in Lemma 15. If $p \in \partial D_r$ is a non-smooth point, then it is in the intersection of two such curves. This means that there are segments σ_1, σ_2 of length r where σ_1 has endpoints at lines l_{i_1}, l_{j_1} and σ_2 has endpoints at lines l_{i_2}, l_{j_2}. Moreover, the endpoints should be actually in the sides of D (otherwise p would be r'-accessible for some $r' < r$). In particular, this means that σ_1, σ_2 cannot be parallel. As such segments are tangent to the bows, the curves intersect transversely at p, and p is a corner point.

A similar statement holds for $I_D = E_R$, when it is not a point, by doing the above reasoning for $r = R$. $\qquad\square$

In particular, we see that I_D cannot be a segment for polygons.

For instance, when D is a rectangle of sides $a \geq b$, then $R = b$. We draw the bows at the vertices, to draw the set $I_D = E_R$.
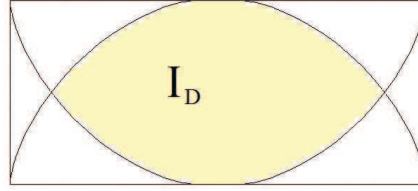
Figure 5. For a rectangle, I_D has interior

Note that I_D intersects ∂D if and only if $a \geq 2b$.

It would be nice to have a function

$$I_D = (I_1, I_2) = I_D((x_1, y_1), (x_2, y_2), \ldots, (x_k, y_k)) \in \mathbb{R}^2 \, ,$$

which assigns the value of I_D given the vertices (x_i, y_i) of a k-polygon. Such function is only defined for polygons with non-parallel sides.

We shall produce the formula for I_D for the case of an *isosceles triangle*. Consider an isosceles triangle of height 1, and base $2\lambda > 0$. Put the vertices at the points $A = (0,0)$, $B = (2\lambda, 0)$ and $C = (\lambda, 1)$. By symmetry, the point I_D must lie in the vertical axis $x = \lambda$. Moreover, the segment of length R through

I_D tangent to the bow corresponding to C must be horizontal. This means that $I_D = (\lambda, I_2)$ where $\frac{R}{2} = \lambda(1 - I_2)$. So

$$I_D = (I_1, I_2) = (\lambda, I_2(\lambda)) = \left(\lambda, 1 - \frac{R}{2\lambda}\right).$$

The sector corresponding to A is that of Lemma 15, and the point I_D should lie in its λ-bow, which is the curve given in Lemma 15 for the value $r = R$. Hence

$$\lambda = R(\cos^3\theta + \lambda(\sin^3\theta + 2\sin\theta\cos^2\theta)),$$
$$1 - \frac{R}{2\lambda} = R(\sin^3\theta - \lambda\sin^2\theta\cos\theta).$$

Eliminating R, we get

$$\lambda^2 \sin^2\theta\cos\theta + 2\lambda\sin\theta\cos^2\theta + \cos^3\theta - \frac{1}{2} = 0$$

i.e.

$$\lambda = \frac{-2\cos^2\theta + \sqrt{2\cos\theta}}{2\sin\theta\cos\theta} \tag{3}$$

(the sign should be plus, since $\lambda > 0$). Note that for an equilateral triangle, $\lambda = \frac{1}{\sqrt{3}}$, $I_2 = \frac{1}{3}$, $\theta = \frac{\pi}{3}$ and $R = \frac{4}{3\sqrt{3}}$.

Also

$$R = \frac{\lambda}{\cos^3\theta + \lambda(\sin^3\theta + 2\sin\theta\cos^2\theta)}. \tag{4}$$

One can check the following formula:

$$I_2 = 1 - \frac{R}{2\lambda} = \lambda\frac{\sin^3\theta - \lambda\sin^2\theta\cos\theta}{\cos^3\theta + \lambda(\sin^3\theta + 2\sin\theta\cos^2\theta)}. \tag{5}$$

This locates the point $I_D = (\lambda(\theta), I_2(\lambda(\theta)))$.

Remark. Do the change of variables $\cos\theta = \frac{1-u^2}{1+u^2}$, $\sin\theta = \frac{2u}{1+u^2}$, to get algebraic expressions for I_D. It is to be expected that this algebraicity property holds for a general triangle.

Recall the position of the ortocentre, incentre, baricentre and circumcentre [1]

$$H = \left(\lambda, \lambda^2\right).$$
$$I = \left(\lambda, \frac{\lambda}{\lambda + \sqrt{\lambda^2 + 1}}\right).$$
$$G = \left(\lambda, \frac{1}{3}\right),$$
$$O = \left(\lambda, \frac{1 - \lambda^2}{2}\right).$$

We draw the height of the point H, I, G, O, I_D as a function of λ:

A simple consequence is that these 5 points are distinct for an isosceles triangle which is not equilateral. We conjecture that this is true for a non-isosceles triangle.
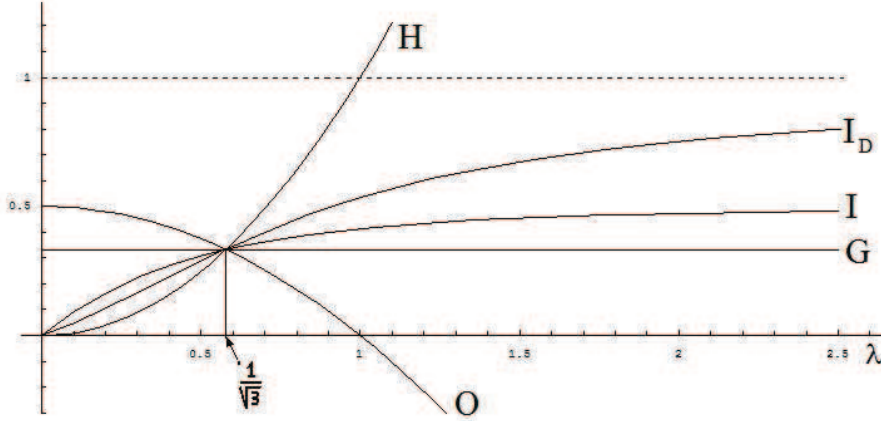
Figure 6. Notable points of a triangle of height 1 and base 2λ

Note the asymptotic for an isosceles triangle. For $\lambda \sim 0$, we have that (3) implies $\cos^3 \theta \sim \frac{1}{2}$. Now (4) and (5) give that $R \sim 2\lambda$ and

$$I_2(\lambda) \sim \frac{\sin^3 \theta}{\cos^3 \theta} \lambda \sim (2^{2/3} - 1)^{3/2} \lambda \,.$$

Rescale the triangle to have base $b = 2$ and height $h = \frac{1}{\lambda}$. Then when h is large, the point I_D approaches to be at distance $(2^{2/3} - 1)^{3/2} = 0.4502$ to the base, and $R \sim 2$. Also, for $\lambda \to \infty$, we have $I_2(\lambda) \to 1$.

Remark. Consider a rectangle D with vertices $(\pm a, \pm 1)$, with $a \gg 1$. Then I_D has interior (see Figure 5). Moving slightly the vertices at the left, we get an isosceles trapezoid Z_ϵ, with vertices $(-a, \pm(1 - \epsilon)), (a, \pm 1)$, for $\epsilon > 0$. Consider the triangle T_ϵ obtained by prolonging the long sides of Z_ϵ, i.e. with vertices $(a - 2a/\epsilon, 0), (a, \pm 1)$. By the above, the point $I_{T_\epsilon} \sim (a - 0.4502, 0)$. As $R \sim 2$, we have that $I_{Z_\epsilon} = I_{T_\epsilon}$.

By symmetry, if we consider the isosceles trapezoid Z'_ϵ with vertices $(-a, \pm 1)$, $(a, \pm(1 - \epsilon))$, then $I_{Z'_\epsilon} \sim (-a + 0.4502, 0)$.

The polygons Z_ϵ and Z'_ϵ are nearby, but their points of maximum inaccessibility are quite far apart. So the map $D \mapsto I_D$ cannot be extended continuously (in any reasonable topology) to all polygons with 4 sides.

References

[1] C. Kimberling, Triangle centers and central triangles, *Congressus Numerantium*, 129 (1998) 1–285.

[2] A. Ostaszewski, *Advanced mathematical methods*. Cambridge University Press, 1990.

[3] K. R. Stromberg, *Introduction to classical real analysis*. Wadsworth, 1981.

[4] F. Valentine, *Convex sets*, McGraw-Hill, 1964.

[5] R. C. Yates, *A Handbook on Curves and Their Properties*. J. W. Edwards, 1952.

María Calvo: Departamento de Álgebra, Facultad de Ciencias, Universidad de Granada, 18071 Granada, Spain

E-mail address: mariacc88@gmail.com

Vicente Muñoz: Facultad de Matemáticas, Universidad Complutense de Madrid, Plaza de Ciencias 3, 28040 Madrid, Spain

E-mail address: vicente.munoz@mat.ucm.es

Perpendicular Bisectors of Triangle Sides

Douglas W. Mitchell

Abstract. Formulas, in terms of the sidelengths and area, are given for the lengths of the segments of the perpendicular bisectors of the sides of a triangle in its interior. The ratios of perpendicular bisector segments to each other are given, and the ratios of the segments into which the perpendicular bisectors are divided by the circumcenter are considered. Then we ask whether a set of three perpendicular bisector lengths uniquely determines a triangle. The answer is no in general: depending on the set of bisectors, anywhere from zero to four (but no more than four) triangles can share the same perpendicular bisector segments.

1. Introduction

It is well-known that the perpendicular bisectors of the sides of a triangle meet at a single point, which is the center of the circumcircle. Bui [1] gives results for similar triangles associated with the perpendicular bisectors. In this paper we first find formulas for the lengths of the segments of the perpendicular bisectors in the *interior* of a given triangle. Then we study the question of existence of triangles with prescribed lengths of perpendicular bisector segments.

Lemma 1. *The perpendicular bisector segment through the midpoint of one side terminates at a point on the longer of the remaining two sides* (or at their intersection if these sides are equal).
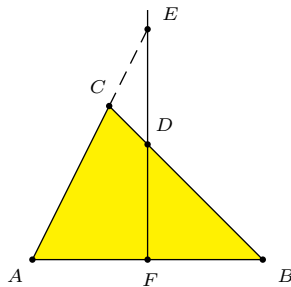

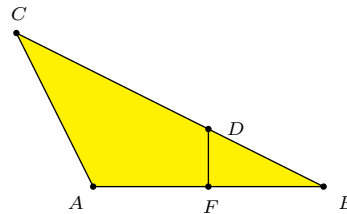Figure 1   Figure 2

Proof. Let the perpendicular bisector pass through the midpoint F of the side AB of triangle ABC. Consider the case when both angles A and B are acute. In Figure 1, $AF = FB$ and $FE \geq FD$. We show that $BC \geq AC$. Now,

$$\tan A = \frac{EF}{AF} \geq \frac{DF}{AF} = \frac{DF}{BF} = \tan B.$$

Since $\tan A \geq \tan B$ and angles A and B are both acute, $\angle A \geq \angle B$. It follows that $BC \geq AC$.

The other cases (when one of angles A and B is obtuse or a right angle) are clear (see Figure 2 in the case of an obtuse angle A). $\qquad\square$

Lemma 1 will be used in constructing the perpendicular bisectors in Figures 3-5. Henceforth we will adopt the notational convention that the sides a, b, and c opposite to angles A, B, and C are such that $a \geq b \geq c$ (and hence $A \geq B \geq C$). We denote by p_a, p_b, p_c the lengths of the perpendicular bisector segments on the sides BC, CA, AB respectively. Also, Δ denotes the area of the triangle.

Theorem 2. *Let $a \geq b \geq c$.*

$$p_a = \frac{2a\Delta}{a^2 + b^2 - c^2}, \qquad p_b = \frac{2b\Delta}{a^2 + b^2 - c^2}, \qquad p_c = \frac{2c\Delta}{a^2 - b^2 + c^2}.$$
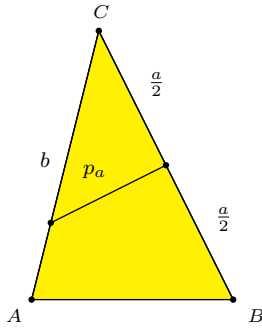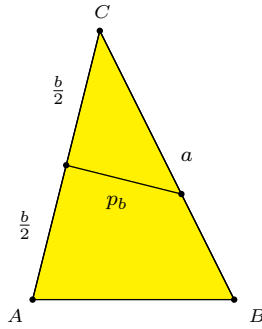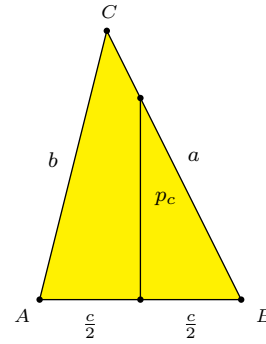
Figure 3   Figure 4   Figure 5

Proof. (i) Figure 3 illustrates the case where $\angle A$ is acute; the proof is identical when $\angle A$ is right or obtuse. We have $\tan C = \frac{p_a}{\frac{a}{2}}$ since by Lemma 1 bisector p_a meets side b because $b \geq c$. We know from [2] (which applies since $\angle C$ is oblique since $\angle A \geq \angle C$) that $\Delta = \frac{\tan C}{4}(a^2 + b^2 - c^2)$. Combining these gives $p_a = \frac{2a\Delta}{a^2 + b^2 - c^2}$.

(ii) Figure 4 illustrates the case where $\angle A$ is acute; the proof is again identical when $\angle A$ is right or obtuse. We have $\tan C = \frac{p_b}{\frac{b}{2}}$ (since by Lemma 1 bisector p_b intersets side a because $a \geq c$). Again $\Delta = \frac{\tan C}{4}(a^2 + b^2 - c^2)$. Combining these gives $p_b = \frac{2b\Delta}{a^2 + b^2 - c^2}$.

(iii) Figure 5 illustrates the case where $\angle A$ is acute; the proof is again identical when $\angle A$ is right or obtuse. We have $\tan B = \frac{p_c}{\frac{c}{2}}$ since by Lemma 1 bisector p_c intersects side a because $a \geq b$. By [2] (which applies since $\angle B$ is oblique since $\angle A \geq \angle B$) we have $\Delta = \frac{\tan B}{4}(a^2 - b^2 + c^2)$. Combining these gives $p_c = \frac{2c\Delta}{a^2 - b^2 + c^2}$. $\qquad\square$

Since Heron's well-known formula gives Δ in terms of a, b, and c, Theorem 2 gives each of the perpendicular bisectors in terms of the three sides. Moreover, we can apply the law of cosines for each angle to obtain these symmetric area formulas in terms of one side, another perpendicular bisector and a third angle.

Corollary 3. $\Delta = p_a b \cos C = p_b a \cos C = p_c a \cos B.$

Theorem 4. *Let $a \geq b \geq c$.*
(i) $p_a \geq p_b$;
(ii) $p_c \geq p_b$;
(iii) $p_a \geq p_c$, $p_a = p_c$ and $p_a < p_c$ are all possible.

Proof. (i) By Theorem 2, $\frac{p_a}{p_b} = \frac{a}{b} = \frac{\sin A}{\sin B}$. Since $A \geq B$ and $A + B < \pi$, $\sin A \geq \sin B$. It follows that $p_a \geq p_b$.

(ii) From Figures 4 and 5,

$$\frac{p_b}{p_c} = \frac{\frac{b}{2}\tan C}{\frac{c}{2}\tan B} = \frac{b\sin C}{\cos C} \cdot \frac{\cos B}{c\sin B} = \frac{\cos B}{\cos C} \leq 1$$

since $B \geq C$ are acute angles.

(iii) We show that all scenarios are possible by examples. Let $a = 6$ and $c = 4$, so that $4 \leq b \leq 6$.

b	Δ	p_a	p_c	
4	$3\sqrt{7}$	$\frac{\Delta}{3}$	$\frac{2\Delta}{9}$	$p_a > p_c$
$2\sqrt{\frac{29}{5}}$	$\frac{48}{5}$	$\frac{5\Delta}{18}$	$\frac{5\Delta}{18}$	$p_a = p_c$
5	$\frac{15\sqrt{7}}{4}$	$\frac{4\Delta}{15}$	$\frac{8\Delta}{27}$	$p_a < p_c$

$\square$

Since we also know [3] that the distances from the circumcenter - which is the intersection of the perpendicular bisectors - to the sides AC and AB are in the ratios $\frac{\cos B}{\cos C}$, we have in Figure 6 that $\frac{OE}{OF} = \frac{\cos B}{\cos C} = \frac{ED'}{FD}$ (by Theorem 4(ii)) so $\frac{OE}{ED'} = \frac{OF}{FD}$. Hence:
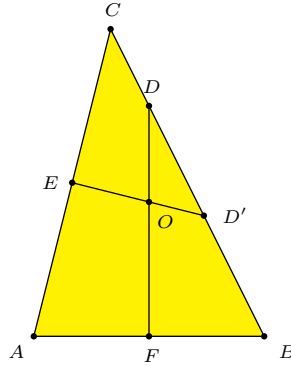
Figure 6

Corollary 5. *In an acute triangle the circumcenter divides the perpendicular bisectors p_b and p_c in equal proportions.*

A similar result applies when the triangle is obtuse (in which case the circumcenter lies outside the triangle):

Corollary 6. *In an obtuse triangle, the perpendicular bisectors p_b and p_c extended to the circumcenter are divided by their respective intersecting triangle sides in equal proportions.*

2. Do the perpendicular bisectors uniquely determine a triangle?

Theorem 7. *Given positive p_a, p_b, p_c satisfying $p_a \geq p_b$ and $p_c \geq p_b$, there are no more than two non-congruent triangles with $a \geq b \geq c$ and perpendicular bisector segments of lengths p_a, p_b, p_c.*

Proof. By Theorem 2, $\frac{p_a}{p_b} = \frac{a}{b}$, and

$$\frac{p_c}{p_b} = \frac{\frac{c}{b} \cdot (a^2 + b^2 - c^2)}{a^2 - b^2 + c^2} = \frac{\frac{c}{b}\left(\left(\frac{a}{b}\right)^2 + 1 - \left(\frac{c}{b}\right)^2\right)}{\left(\frac{a}{b}\right)^2 - 1 + \left(\frac{c}{b}\right)^2}$$

Putting $\alpha := \frac{p_a}{p_b} \geq 1$, $\gamma := \frac{p_c}{p_b} \geq 1$, and $x := \frac{c}{b}$, we rearrange this as

$$f(x) = x^3 + \gamma x^2 - (\alpha^2 + 1)x + \gamma(\alpha^2 - 1) = 0. \tag{1}$$

Since x is a ratio of sides, and $a - b < c \leq b$, we must have $x \in (\alpha - 1, \ 1]$.

If $\alpha - 1 = 0$ (the isosceles case of $\frac{a}{b} = \frac{p_a}{p_b} = 1$), (1) becomes $x(x^2 + \gamma x - 2) = 0$, and has exactly one solution in the interval $(\alpha - 1, \ 1]$.

If $\alpha - 1 > 0$, (1) exhibits two switches in the signs of parameters, so by Descartes' rule the cubic has either 2 or 0 positive roots. Thus the number of non-similar triangles cannot be more than 2. Since similar but non-congruent triangles cannot share the same absolute sizes of perpendicular bisectors, the number of non-congruent triangles sharing the same (p_a, p_b, p_c) can be no more than 2. □

Remark. Since $c > a - b$, we must have $x > \alpha - 1$. If $\gamma = 1$, (1) becomes

$$(x + \alpha + 1)(x - 1)(x - (\alpha - 1)) = 0.$$

It follows that $x = 1$ is the only admissible root. This results in an isosceles triangle.

Having already given an exact number of triangles above for the cases of $p_a = p_b$ and $p_c = p_b$, we next find specific parameter conditions that are necessary and sufficient for the number of triangles with specified (p_a, p_b, p_c), *i.e.*, the number of admissible solutions of (1) - to be 0, 1, or 2 when α and γ both exceed 1, *i.e.*, $p_a > p_b$ and $p_c > p_b$.

It is easy to see that the cubic $f(x)$ in (1) has a local minimum at

$$x_0 = \frac{-\gamma + \sqrt{\gamma^2 + 3(\alpha^2 + 1)}}{3} > 0,$$

and a local maximum at $x_1 = \frac{-\gamma - \sqrt{\gamma^2 + 3(\alpha^2 + 1)}}{3} < 0$.

It is routine to verify that the local minimum $x_0 \in (\alpha - 1, 1)$ if and only if $\gamma \in \left(\frac{\alpha^2 - 2}{2}, \ \frac{-\alpha^2 + 3\alpha - 1}{\alpha - 1}\right)$.

Theorem 8. *Given $p_a > p_b$ and $p_c > p_b$, let $\alpha = \frac{p_a}{p_b}$ and $\gamma = \frac{p_c}{p_b}$. The number of triangles with perpendicular bisector segments of lengths p_a, p_b, p_c is*

2 if and only if $\gamma \in \left(\frac{\alpha^2-2}{2}, \frac{-\alpha^2+3\alpha-1}{\alpha-1} \right)$ and $f(x_0) < 0$,

1 if and only if $\gamma \in \left(\frac{\alpha^2-2}{2}, \frac{-\alpha^2+3\alpha-1}{\alpha-1} \right)$ and $f(x_0) = 0$,

0 otherwise.

Proof. Note that $f(\alpha - 1) = 2\alpha(\alpha - 1)(\gamma - 1) > 0$ and $f(1) = \alpha^2(\gamma - 1) > 0$.

If the local minimum $x_0 \in (\alpha - 1, \ 1)$, then the number of roots of $f(x)$ in the interval 2, 1, or 0 according as $f(x_0) < 0, = 0$, or > 0.

If $x_0 \notin (\alpha - 1, \ 1)$, then $f(x)$ is monotonic and has no root in the interval. $\square$

While no more than two distinct triangles can share the same p_a, p_b, p_c, one must also consider the possibility that up to two more triangles could share the same three perpendicular bisectors segments $\{p_1, p_2, p_3\}$ with different assignments of the bisectors to the long, medium, and short sides of the triangle. This is because, by Theorem 4, the medium-length side b has the shortest perpendicular bisector but either the longest side a or the shortest side c can have the longest bisector. Therefore, given segments of lengths $p_1 \geq p_2 \geq p_3$, we seek triangles (a, b, c) with $a \geq b \geq c$ and $(p_a, p_b, p_c) = (p_1, p_3, p_2)$ or (p_2, p_3, p_1). Thus:

Corollary 9. *There are a maximum of four triangles with the three segments of given lengths as perpendicular bisector segments.*

We conclude this paper by giving explicit examples showing that the number of triangles in Corollary 9 can be any of 0, 1, 2, 3, 4.

(i) $n = 4$: Consider $(p_1, p_2, p_3) = (20, \ 18, \ 15)$.

If $(p_a, p_b, p_c) = (20, 15, 18)$, $\alpha = \frac{4}{3}$, $\gamma = \frac{6}{5}$, and

$$f_1(x) = x^3 + \frac{6}{5}x^2 - \frac{25}{9}x + \frac{14}{15} = \left(x - \frac{7}{15} \right) \left(x - \frac{\sqrt{97} - 5}{6} \right) \left(x + \frac{\sqrt{97} + 5}{6} \right).$$

This gives two triangles similar to $(20, 15, 7)$ and $(8, 6, \sqrt{97} - 5)$.

On the other hand, if $(p_a, p_b, p_c) = (18, 15, 20)$, $\alpha = \frac{6}{5}$, $\gamma = \frac{4}{3}$, and

$$f_2(x) = x^3 + \frac{4}{3}x^2 - \frac{61}{25}x + \frac{44}{75} = \left(x - \frac{4}{5} \right) \left(x - \frac{\sqrt{421} - 16}{15} \right) \left(x + \frac{\sqrt{421} + 16}{15} \right).$$

This gives two triangles similar to $(6, 5, 4)$ and $(18, 15, \sqrt{421} - 16)$.

(ii) For $n = 3$, let $(p_1, p_2, p_3) = (3, \ 2\sqrt{2}, \ \sqrt{5})$.

If $(p_a, p_b, p_c) = (3, \sqrt{5}, \ 2\sqrt{2})$, $\alpha = \frac{\sqrt{5}}{3}$, $\gamma = \frac{2\sqrt{2}}{\sqrt{5}}$, and

$$f_3(x) = x^3 + \frac{2\sqrt{2}}{\sqrt{5}}x^2 - \frac{14}{5}x + \frac{8\sqrt{2}}{5\sqrt{5}} = \left(x + \frac{4\sqrt{2}}{\sqrt{5}} \right) \left(x - \frac{\sqrt{2}}{\sqrt{5}} \right)^2.$$

This gives a triangle similar to $(3, \sqrt{5}, \ \sqrt{2})$.

If $(p_a, p_b, p_c) = (2\sqrt{2}, \sqrt{5}, 3)$, then

$$f_4(x) = x^3 + \frac{3}{\sqrt{5}}x^2 - \frac{13}{5}x + \frac{9}{5\sqrt{5}} = \left(x - \frac{1}{\sqrt{5}}\right)\left(x - \frac{\sqrt{13}-2}{\sqrt{5}}\right)\left(x + \frac{\sqrt{13}+2}{\sqrt{5}}\right).$$

The two roots in the interval $(0, 1)$ give the triangles similar to $(2\sqrt{2}, \sqrt{5}, 1)$ and $(2\sqrt{2}, \sqrt{5}, \sqrt{13} - 2)$.

(iii) For $n = 2$, let $(p_1, p_2, p_3) = (39, 30, 25)$. If $(p_a, p_b, p_c) = (30, 25, 39)$, then $\alpha = \frac{6}{5}, \gamma = \frac{39}{25}$, and

$$f_5(x) = x^3 + \frac{39}{25}x^2 - \frac{61}{25}x + \frac{429}{625} = \left(x + \frac{13}{5}\right)\left(x - \frac{11}{25}\right)\left(x - \frac{3}{5}\right).$$

The two positive roots are in $(\alpha - 1, 1) = \left(\frac{1}{5}, 1\right)$. These give two triangles similar to $(30, 25, 11)$ and $(6, 5, 3)$.

On the other hand, if $(p_a, p_b, p_c) = (39, 25, 30)$, the cubic

$$f_6(x) = x^3 + \frac{6}{5}x^2 - \frac{2146}{625}x + \frac{5376}{3125}$$

has only one real root which is negative (see Figure 7). There is no triangle with $(p_a, p_b, p_c) = (39, 25, 30)$.
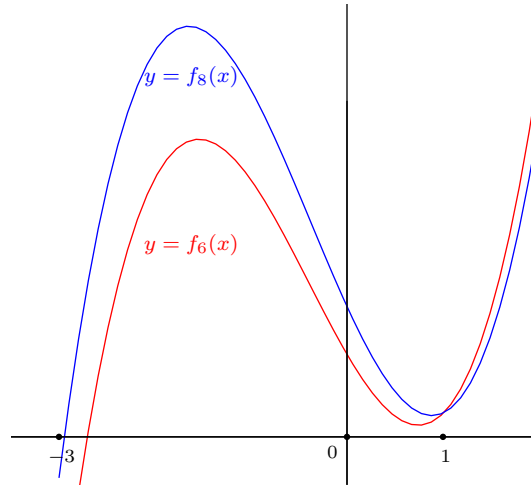
Figure 7

(iv) For $n = 1$, consider $(p_1, p_2, p_3) = (8, 5, \sqrt{19})$. If $(p_a, p_b, p_c) = (5, \sqrt{19}, 8)$, then $(\alpha, \gamma) = \left(\frac{5}{\sqrt{19}}, \frac{8}{\sqrt{19}}\right)$, and

$$f_7(x) = x^3 + \frac{8}{\sqrt{19}}x^2 - \frac{44}{19}x + \frac{48}{19\sqrt{19}} = \left(x + \frac{12}{\sqrt{19}}\right)\left(x - \frac{2}{\sqrt{19}}\right)^2.$$

This give a single triangle similar to $(5, \sqrt{19}, 2)$.

On the other hand, with $(p_a, p_b, p_c) = (8, \sqrt{19}, 5)$, we have $(\alpha, \gamma) = \left(\frac{8}{\sqrt{19}}, \frac{5}{\sqrt{19}} \right)$, and

$$f_8(x) = x^3 + \frac{5}{\sqrt{19}}x^2 - \frac{83}{19}x + \frac{225}{19\sqrt{19}}$$

has only one real root which is negative (see Figure 7). There is no such triangle.

(v) Finally, for $n = 0$, we take $(p_1, p_2, p_3) = (5, 4, 1)$. The two cubic polynomials are $f_9(x) = x^3 + 5x^2 - 17x + 75$ and $f_{10}(x) = x^3 + 4x^2 - 26x + 96$. Each of these has exactly one real root which is negative (see Figure 8). Therefore, there is no triangle with perpendicular bisector segments $(5, 4, 1)$.
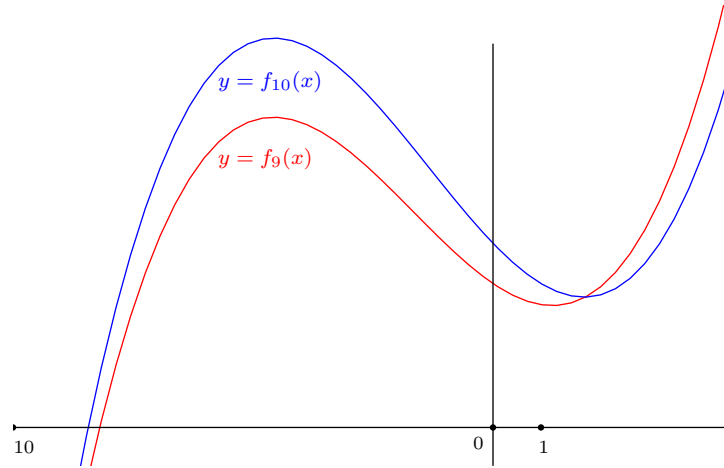
References

[1] Q. T. Bui, On a triad of similar triangles associated with the perpendicular bisectors of the sides off a triangle, *Forum Geom.*, 10 (2010) 1–6.

[2] D. Mitchell, The area of a quadrilateral, *Math. Gazette*, 93 (2009) 306–309.

[3] E. W. Weisstein, Exact trilinear coordinates, from *MathWorld - A Wolfram Web Resource*, http://mathworld.wolfram.com/ExactTrilinearCoordinates.html.

Douglas W. Mitchell: 1002 Saman, Carambola, Christiansted, St. Croix, US Virgin Islands
E-mail address: doug.mitchell.1234@hotmail.com

Convolution Filters for Triangles

Grégoire Nicollier

Abstract. The construction of a new triangle by erecting similar ears on the sides of a given triangle (as in Napoleon's theorem) can be considered as the convolution of the initial triangle with another triangle. We use the discrete Fourier transformation and a shape function to give a complete and explicit description of such convolution filters and their iterates. Our method leads to many old and new results in a very direct way.

1. Introduction

Johnson [17, pp. 284, 294], citing Emmerich [5, p. 129], formulates and proves the following property: "If points divide the sides of a given triangle in equal ratios, they are vertices of a triangle having the same Brocard angle as the given triangle. [. . .] The triangles whose vertices divide in equal ratios the sides of a given triangle constitute all the different forms of triangle having the same Brocard angle." (See also [29, 11] and our Theorem 2.) We analyze this kind of transformations of an initial triangle into a new triangle by considering convolutions of two triangles: with one exception, such a convolution simply erects three similar triangular ears on the sides of the initial triangle before transforming the triangle of the ears' apices by a direct similarity. A circulant linear transformation of a triangle in the complex plane, given by the coefficients c_0, c_1, c_2 of the circulant linear combination of the vertices, is simply the convolution of the initial triangle and the triangle with vertices c_0, c_2, c_1.

Here is a sketch of our method. We use the spectral decomposition in the Fourier base of $\mathbf{C}^3$ to represent any triangle of the complex plane as the sum of its centroid and of two positively and negatively oriented equilateral triangles: the convolution with this triangle is then a diagonal linear map, and we call *shape* of the triangle the quotient of the eigenvalues belonging to the negatively and positively oriented equilateral base vectors; this shape is also the quotient of the corresponding spectral values of the convolving triangle, *i.e.*, the ratio of the negatively and positively oriented equilateral quantities in this triangle. It is then immediate that the shape of a convolution product of two triangles is equal to the product of the triangles' shapes. Two directly similar triangles (with vertices in order) have the same shape; moreover, when restricted to normalized triangles with vertices 0, 1, and z, the

shape function is a Möbius transformation as function of z: the equivalence classes of directly similar triangles (with respect to the given order of their vertices) are thus parametrized by their shape. Every triangle transformation given by a convolution can be described by analyzing this Möbius transformation. Emmerich's introducing result, for example, becomes almost immediate (see also [11]): the transformation is a convolution with a degenerate triangle; since degenerate triangles are characterized by shapes of modulus 1, the convolution acts on the shape of the initial triangle as a rotation and does not change the shape's modulus; since triangles are equibrocardal and equally oriented exactly when their shapes have the same modulus, the Brocard angle is invariant under a convolution with a degenerate triangle; the converse follows from the fact that the shapes of the degenerate triangles needed for the Emmerich transformations cover the whole unit circle (-1 being half an exception). By iterating the convolution with a degenerate triangle, one simply rotates the shape by a constant angle at each step: the successive triangles are directly similar to triangles with a common base whose apices turn on the same Neuberg circle, and these apices are periodic or dense on the Neuberg circle according as the rotation angle for the shape is a rational or irrational multiple of π.

Many triangle transformations in the literature are in fact convolutions with a fixed triangle and could thus have been analyzed by the present method in a very efficient and standardized way. Moreover, if the convolving triangle is degenerate, *i.e.*, if the shape of the convolving triangle lies on the unit circle, the transformation behaves as the Emmerich transformation with the same shape (as far as only the triangle's form is concerned), and the work is done as soon as the rotation angle, *i.e.*, the argument of the shape of the convolving degenerate triangle, is determined! The s-Rooth triangles of [11] for example, which already appear in [22], are in fact given by the convolution with a degenerate triangle, like any circulant transformation of a triangle where the new vertices are a *real* linear combination of the old ones, and such convolutions are included once for all in the Emmerich transformations (as far as only the triangle's form is concerned).

The Fourier decomposition of a triangle or polygon and circulant matrices have been used for a long time for studying triangle and polygon transformations with a circulant structure, beginning with Darboux in 1878 [3], [1, 4, 6, 7, 8, 14, 25, 27, 28, 30, 31, 32, 33, 36]; they are in general more efficient than purely geometric and trigonometric approaches [16, 34, 35]. Our presentation is free from matrix algebra since we only need convolutions. The shape function we use seems to appear for the first time in 2003 in a paper by Nakamura and Oguiso [22] (from a sixteen years older preprint), and later independently in [10]: we found only in [10] an indirect relation between the shape function and some eigenfunction as tentative explanation of the nature of this shape function. As far as we know, the fact that the shape of a convolution product is the product of the shapes is noticed and exploited here for the first time, and this is the key point for the success of our method. Note that Hajja *et al.* [10, 11, 12, 13], and Nakamura and Oguiso [22] establish *ad hoc* for each analyzed transformation that the shape of the transformed triangle is the shape of the initial triangle multiplied by some function independent of the initial

triangle, without noticing that this function is in fact the shape of a triangle and that the transformation is a convolution. We extended this shape function to polygons in [24].

2. Fourier transform of a triangle

Consider a triangle Δ of the complex plane as a point $\Delta = (z_0, z_1, z_2) \in \mathbf{C}^3$ representing the closed polygonal line $z_0 \to z_1 \to z_2 \to z_0$ starting at z_0: there are up to six triangles with the same vertices. A triangle is called *degenerate* when its vertices are collinear, *trivial* when it is reduced to a triple point, and *proper* when it is nondegenerate; a degenerate triangle is both positively and negatively oriented.

Endow $\mathbf{C}^3$ with the inner product $\langle (z_0, z_1, z_2), (w_0, w_1, w_2) \rangle = \frac{1}{3} \sum_{k=0}^{2} z_k \overline{w_k}$ and set $\zeta = e^{i2\pi/3}$. The vectors

$$e_0 = (1, 1, 1), \quad e_1 = (1, \zeta, \zeta^2), \quad e_2 = (1, \zeta^2, \zeta^4) = (1, \zeta^2, \zeta) = \overline{e_1}$$

form the orthonormal *Fourier base* of $\mathbf{C}^3$: e_0 is a trivial triangle; e_1 and e_2 are a positively and a negatively oriented equilateral triangle centered at the origin, respectively. The *discrete Fourier transform* or *spectrum* of Δ is the triangle $\widehat{\Delta} = (\hat{z}_0, \hat{z}_1, \hat{z}_2)$ given by the *spectral representation* of Δ in the Fourier base:

$$\Delta = \sum_{k=0}^{2} \hat{z}_k e_k \quad \text{with} \quad \hat{z}_k = \langle \Delta, e_k \rangle, \ k = 0, 1, 2.$$

$\hat{z}_0 = \frac{1}{3}(z_0 + z_1 + z_2)$ is the centroid of Δ, and

$$\hat{z}_1 = \tfrac{1}{3}(z_0 + \zeta^2 z_1 + \zeta z_2), \quad \hat{z}_2 = \tfrac{1}{3}(z_0 + \zeta z_1 + \zeta^2 z_2).$$

A triangle is trivial if $\hat{z}_1 = \hat{z}_2 = 0$; it is *pequilateral* if it is equilateral and positively oriented, *i.e.*, if $\hat{z}_1 \neq 0$, $\hat{z}_2 = 0$; it is *nequilateral* if it is equilateral and negatively oriented, *i.e.*, if $\hat{z}_1 = 0$, $\hat{z}_2 \neq 0$; it is *mixed* if $\hat{z}_1 \neq 0$, $\hat{z}_2 \neq 0$, *i.e.*, if it is neither trivial nor equilateral. A spectrum is *full* if all *Fourier coefficients* $\hat{z}_k$ are different from 0.

3. Shape of a triangle

We define the shape of a nontrivial triangle Δ by

$$\sigma_\Delta = \sigma(z_0, z_1, z_2) = \frac{\hat{z}_2}{\hat{z}_1} = \frac{z_0 + \zeta z_1 + \zeta^2 z_2}{z_0 + \zeta^2 z_1 + \zeta z_2} \in \mathbf{C} \cup \{\infty\},$$

the ratio of the contributions to Δ of the nequilateral e_2 and of the pequilateral e_1 [22, 10]. Note that [22, 10] define this shape function without any reference to Fourier transforms or circulant matrices. The first properties of the shape function presented below can already be found in [10]: some errors are corrected in [13]. Since $(w_0, w_1, w_2) = a(z_0, z_1, z_2) + be_0$ for some b is equivalent to $(\hat{w}_1, \hat{w}_2) = a(\hat{z}_1, \hat{z}_2)$, Δ_1 has the shape of Δ if and only if $\Delta_1 = a\Delta + be_0$ with $a, b \in \mathbf{C}$, $a \neq 0$: $\Delta = (z_0, z_1, z_2)$ has thus the shape of a unique (directly similar) normalized triangle $\Delta' = \Delta'(z) = (0, 1, z)$, namely $\Delta'\left(\frac{z_2 - z_0}{z_1 - z_0}\right)$, where $\Delta'(\infty) = (0, 1, \infty)$

means $\Delta' = (0, 0, 1)$ for $z_0 = z_1$. The shape $f(z)$ of the normalized triangle $\Delta'(z)$ is the Möbius transformation

$$s = \sigma_{\Delta'(z)} = f(z) = \frac{\zeta z + 1}{z + \zeta} = \zeta \frac{z - e^{i\pi/3}}{z - e^{-i\pi/3}} = \frac{1}{f(\overline{z})}$$

of the extended complex plane with inverse

$$z = f^{-1}(s) = \frac{\zeta s - 1}{\zeta - s} = -\zeta \frac{s - \zeta^2}{s - \zeta} = -f(-s) = \frac{1}{f^{-1}(\overline{s})}.$$

Triangles corresponding to different normalized triangles have different shapes: the equivalence classes of triangles are parametrized by their shape. $\sigma_\Delta = 0$ or ∞ if and only if Δ is pequilateral or nequilateral, respectively. A cyclic left shift $(z_0, z_1, z_2) \mapsto (z_1, z_2, z_0)$, *i.e.*, a start from the next vertex of the triangle, causes a change $(\hat{z}_0, \hat{z}_1, \hat{z}_2) \mapsto (\hat{z}_0, \zeta\hat{z}_1, \zeta^2\hat{z}_2)$ in the spectrum; an orientation reversing, *i.e.*, a permutation of the last two vertices $\Delta = (z_0, z_1, z_2) \mapsto (z_0, z_2, z_1) = 3\widehat{\widehat{\Delta}}$, causes the same permutation of the Fourier coefficients:

$$\sigma(z_1, z_2, z_0) = \zeta\sigma(z_0, z_1, z_2), \quad \sigma(z_0, z_2, z_1) = \frac{1}{\sigma(z_0, z_1, z_2)}, \quad \sigma_{\overline{\Delta}} = \frac{1}{\overline{\sigma_\Delta}}.$$

A triangle Δ_1 is thus directly similar to the proper Δ of shape $\sigma_\Delta = s$ with the same orientation if and only if $\sigma_{\Delta_1} = \zeta^k s$, $k \in \{0, 1, 2\}$; Δ_1 is directly similar to the proper Δ with the inverse orientation if and only if $\sigma_{\Delta_1} = \zeta^k \frac{1}{s}$; Δ_1 is inversely similar to the proper Δ with the same orientation if and only if $\sigma_{\Delta_1} = \zeta^k \overline{s}$; and Δ_1 is inversely similar to the proper Δ with the inverse orientation if and only if $\sigma_{\Delta_1} = \zeta^k \frac{1}{\overline{s}}$.

Since $f(0) = \zeta^2$, $f(1) = 1$, $f(\infty) = \zeta$, and $f(e^{i\pi/3}) = 0$, f maps the extended real axis (corresponding to the normalized degenerate triangles) to the unit circle and the extended upper half-plane to the unit disc: the modulus $|\sigma_\Delta|$ is thus < 1, > 1, or $= 1$ according as Δ is positively oriented and proper, negatively oriented and proper, or degenerate, respectively. Two nontrivial degenerate triangles Δ and Δ_1 are similar if and only if $\sigma_{\Delta_1} = \zeta^k \sigma_\Delta$ or $\sigma_{\Delta_1} = \zeta^k \overline{\sigma_\Delta}$, $k \in \{0, 1, 2\}$. The degenerate normalized triangle $\Delta'(x)$, $x \in \mathbf{R} \cup \{\infty\}$, and its shape $e^{i\varphi}$ are linked by

$$\varphi = \arg \sigma_{\Delta'(x)} = \frac{2\pi}{3} + 2\arg(x - e^{i\pi/3}) = \frac{2\pi}{3} + 2\arctan\frac{\sqrt{3}}{1 - 2x} \quad (1)$$

and $x = \frac{\sin\left(\frac{\pi}{3} + \frac{\varphi}{2}\right)}{\sin\left(\frac{\pi}{3} - \frac{\varphi}{2}\right)}$: when x runs rightwards over the whole extended real axis, $f(x) = \sigma_{\Delta'(x)}$ turns counterclockwise on the unit circle starting and ending at ζ, which is the shape of $\Delta'(\infty) = (0, 0, 1)$.

For the normalized right-angled triangles (Figure 1), f maps the extended imaginary axis to the circle $\mathcal{C}$ of radius $\sqrt{3}$ centered at -2, the circle of radius $\frac{1}{2}$ centered at $\frac{1}{2}$ to the circle $\zeta\mathcal{C}$ of radius $\sqrt{3}$ centered at $1 - i\sqrt{3}$, and the extended vertical line through 1 to the circle $\zeta^2\mathcal{C}$ of radius $\sqrt{3}$ centered at $1 + i\sqrt{3}$: the shape function σ maps thus the right-angled triangles to the three circles $\mathcal{C}$, $\zeta\mathcal{C}$, and $\zeta^2\mathcal{C}$.
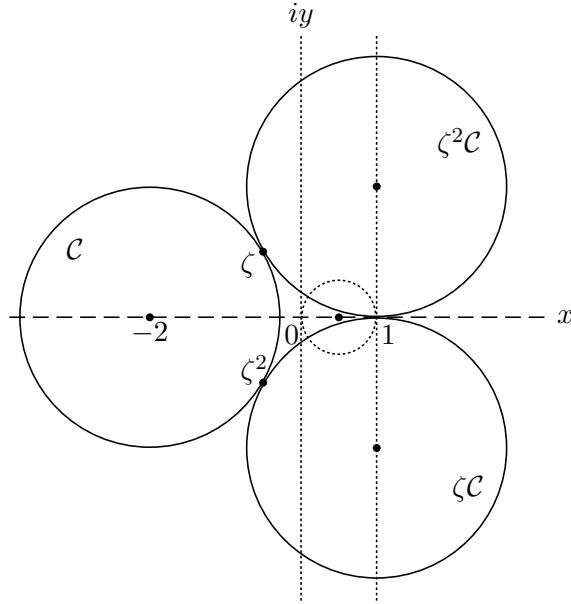
Figure 1. Normalized right-angled triangles $(0, 1, z)$: loci of their vertex z (dotted curves) and of their shape (plain circles)
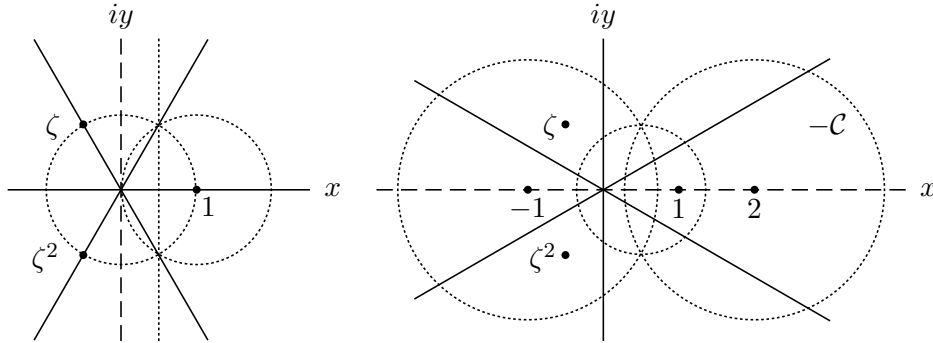
Figure 2. Normalized isosceles (on the left) and automedian triangles $(0, 1, z)$: loci of their vertex z (dotted curves) and of their shape (plain straight lines)

For the normalized isosceles triangles (Figure 2), f maps the unit circle to the extended real axis, the extended vertical line through $\frac{1}{2}$ to the extended line through 0 and ζ, and the circle of radius 1 centered at 1 to the extended line through 0 and ζ^2: σ maps thus the nonequilateral isosceles triangles to the punctured lines $\lambda\zeta^k$, $\lambda \in \mathbf{R} \setminus \{0\}$, $k = 0, 1, 2$. s is the shape of an isosceles triangle if and only if $\overline{s} \in \{s, \zeta s, \zeta^2 s\}$. The normalized isosceles $\Delta'(z)$ with apex $z = \frac{1 + i\tan\theta}{2}$, $|\theta| < \frac{\pi}{2}$, and base angles θ (< 0 when $\operatorname{Im} z < 0$) has the shape $f(z) = \frac{\tan\theta - \sqrt{3}}{\tan\theta + \sqrt{3}}\zeta$; the shape
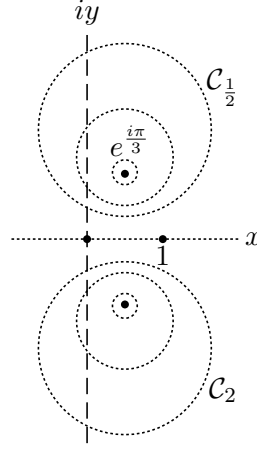
Figure 3. Neuberg circles $\mathcal{C}_R$: $|\sigma_{\Delta'}| = \left|\frac{z - e^{i\pi/3}}{z - e^{-i\pi/3}}\right| = R$ for the normalized triangles $\Delta' = (0, 1, z)$, $R = 0, \frac{1}{10}, \frac{1}{3}, \frac{1}{2}, 1, 2, 3, 10, \infty$

of the isosceles $\Delta'\left(\frac{1}{\sqrt{3}}e^{i\pi/6}\right)$ with base angles $\frac{\pi}{6}$ is $-\frac{\zeta}{2}$. We set $\xi = \frac{1}{\sqrt{3}}e^{i\pi/6} = \frac{1}{2} + \frac{i}{2\sqrt{3}} = \frac{1}{1-\zeta} = \frac{-1}{\sqrt{3}}i\zeta$.

A nontrivial triangle is *automedian* when it is (inversely) similar to its median triangle: by the median theorem, this is the case if and only if the vertex opposite to the middle side u lies on the circle of radius $\frac{\sqrt{3}}{2}u$ centered at the midpoint of u (as does the apex of the equilateral triangle erected on u), and also if and only if $2u^2$ is the sum of the other squared sides. The sides of a right-angled automedian triangle are proportional to $1 : \sqrt{2} : \sqrt{3}$, and an isosceles triangle is automedian exactly when it is equilateral. For the normalized automedian triangles (Figure 2), f maps the circle of radius $\frac{\sqrt{3}}{2}$ centered at $\frac{1}{2}$ to the extended line through 0 and $i\zeta = -e^{i\pi/6}$, the circle of radius $\sqrt{3}$ centered at -1 to the extended line through 0 and $i\zeta^2$, and the circle $-\mathcal{C}$ of radius $\sqrt{3}$ centered at 2 to the extended imaginary axis: σ maps thus the nonequilateral automedian triangles to the punctured lines $\lambda i \zeta^k$, $\lambda \in \mathbf{R} \setminus \{0\}$, $k = 0, 1, 2$. s is the shape of an automedian triangle if and only if $-\overline{s} \in \{s, \zeta s, \zeta^2 s\}$. The normalized automedian triangle with vertex $z = \frac{1}{2} + \frac{\sqrt{3}}{2}e^{i\varphi}$ has the shape $f(z) = \tan(\frac{\pi}{4} - \frac{\varphi}{2})e^{i\pi/6}$.

For $R \in [0, \infty]$, f maps the circle $|z| = R$ to the Apollonius circle $\left|\frac{s - \zeta^2}{s - \zeta}\right| = R$, *i.e.*, to the circle $\left|s + \frac{1}{2} - i\frac{\sqrt{3}}{2}\frac{R^2+1}{R^2-1}\right| = \frac{\sqrt{3}R}{|R^2-1|}$ if $R \neq 1$ and to the extended real axis if $R = 1$. Conversely, f^{-1} maps the circle $|s| = R$ to the Apollonius circle

$$\mathcal{C}_R: \left|\frac{z + \zeta^2}{z + \zeta}\right| = \left|\frac{z - e^{i\pi/3}}{z - e^{-i\pi/3}}\right| = R, \qquad (2)$$

i.e., to the circle $\left|z - \frac{1}{2} + i\frac{\sqrt{3}}{2}\frac{R^2+1}{R^2-1}\right| = \frac{\sqrt{3}R}{|R^2-1|}$ if $R \neq 1$ and to the extended real axis if $R = 1$ (Figure 3). If $R \neq 1$, $\mathcal{C}_R$ is a Neuberg circle [17, p. 287], [29],

i.e., the locus of the vertex z of the triangles $\Delta'(z)$ with an appropriate constant Brocard angle ω in the upper or lower half-plane according as $R < 1$ or $R > 1$: since the base side 1 of $\Delta'(z)$ subtends the angle 2ω from the center of $\mathcal{C}_R$, one has (see also [10])

$$\cot \omega = \sqrt{3} \left| \frac{R^2 + 1}{R^2 - 1} \right| \text{ for } R = \left| \sigma_{\Delta'(z)} \right|. \tag{3}$$

If $\left| \sigma_{\Delta'(z_0)} \right| = R \neq 0, 1, \infty$, the sides of $\Delta'(z_0)$ issued from $z_0 \in \mathcal{C}_R$ cut $\mathcal{C}_R$ in one or two other points: these are vertices of normalized triangles inversely similar to $\Delta'(z_0)$; the reflections of z_0 and of these vertices in the line $\operatorname{Re} z = \frac{1}{2}$ give the other normalized triangles similar to $\Delta'(z_0)$ with the same orientation [17, p. 289].

Figures 1, 2, and 3 show how many right-angled, isosceles, and automedian normalized triangles are equibrocardal with a shape of given modulus $R \neq 0, 1, \infty$. There are two inversely similar automedian triangles with opposite shapes (and their companions with cyclically shifted vertices); there are two isosceles triangles with opposite shapes (and their companions), whose base angles are

$$\theta_1 = \arctan \frac{\sqrt{3}(1 - R)}{1 + R}, \quad \theta_2 = \arctan \frac{\sqrt{3}(1 + R)}{1 - R}. \tag{4}$$

Note that $\tan \theta_1 \cdot \tan \theta_2 = 3$ and that θ_1, θ_2 are < 0 when the orientation is negative. For $R = 2 \pm \sqrt{3}$ or $R \in \left] 2 - \sqrt{3}, 2 + \sqrt{3} \right[$ there are one (isosceles) right-angled triangle or two inversely similar right-angled triangles with conjugate shapes (and their companions), respectively. Note that some of the above triangles may be simultaneously right-angled and isosceles or automedian.

We will prove later that two nontrivial triangles have opposite shapes (possibly after multiplying one of the shapes by $\zeta^{\pm 1}$) if and only if they are directly similar to the median triangle of each other.

f maps the circle $\mathcal{C}'$ through $e^{i\pi/3}$, $e^{-i\pi/3}$, and $z_0 \in \mathbf{C} \setminus \left\{ e^{i\pi/3}, e^{-i\pi/3} \right\}$ to the line $\lambda f(z_0)$, $\lambda \in \mathbf{R} \cup \{\infty\}$, and $Z_0 = \frac{z_0 - 2}{2z_0 - 1}$ lies on this circle since $f\left(\frac{z-2}{2z-1} \right) = -f(z)$. When z_0 is not real, $\Delta'(z_0)$ is automedian if and only if the line through z_0 and Z_0 is horizontal or contains 0 or 1, because two equibrocardal triangles with a common angle are similar and because $\Delta'(Z_0)$ is directly similar to the median triangle of $\Delta'(z_0)$. For each $L \geq 0$, f admits the values $\pm L f(z_0)$ at the points $z_\pm$ given by the intersections of $\mathcal{C}'$ with the Apollonius circle $\mathcal{C}_{L|f(z_0)|}$ (Figure 4).

$\widetilde{\sigma}(z_0, z_1, z_2) = \frac{z_2 - z_0}{z_1 - z_0}$ [36], which is invariant under triangle translation and under homothety and rotation, is a shape function that is more intuitive than σ. One has $\widetilde{\sigma}(0, 1, z) = z$, $\sigma(0, 1, z) = \zeta \widetilde{\sigma}(z, e^{-i\pi/3}, e^{i\pi/3})$, and $\sigma(z_0, z_1, z_2) = \sigma(0, 1, \widetilde{\sigma}(z_0, z_1, z_2))$.

4. Convolution filters

We consider a *filter* $T_\Gamma \colon \mathbf{C}^3 \to \mathbf{C}^3$ given by the cyclic convolution $*$ with a fixed triangle $\Gamma = (c_0, c_1, c_2)$, *i.e.*, by a circulant matrix:

$$T_\Gamma \colon \Delta \mapsto \Delta * \Gamma = (z_0, z_1, z_2) * (c_0, c_1, c_2) = (z_0, z_1, z_2) \begin{pmatrix} c_0 & c_1 & c_2 \\ c_2 & c_0 & c_1 \\ c_1 & c_2 & c_0 \end{pmatrix}.$$
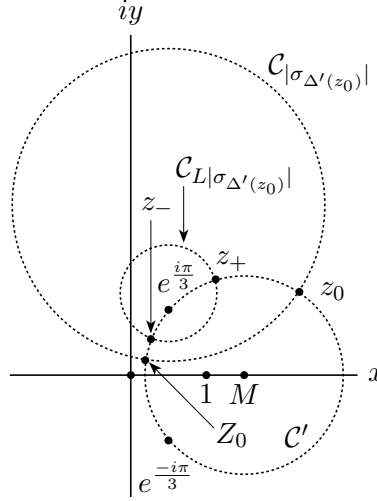
Figure 4. $\Delta'(z_0)$ and $\Delta'(Z_0)$ have opposite shapes; $\Delta'(z_\pm)$ have opposite shapes $\pm L\sigma_{\Delta'(z_0)}$ for $L = \frac{1}{2}$.

The kth entry of $\Delta * \Gamma = \Gamma * \Delta$ is $\sum_{\ell=0}^{2} z_\ell c_{k-\ell \,(\mathrm{mod}\ 3)}$, $k = 0, 1, 2$.

Since the operator $*$ is bilinear and since $e_k * e_\ell = \begin{cases} 3e_k & (k = \ell) \\ (0,0,0) & (k \neq \ell) \end{cases}$, one has

$$T_\Gamma(\Delta) = \Delta * \Gamma = \left(\sum_{k=0}^{2} \hat{z}_k e_k \right) * \left(\sum_{\ell=0}^{2} \hat{c}_\ell e_\ell \right) = \sum_{k=0}^{2} 3\hat{c}_k \hat{z}_k e_k,$$

i.e., $\widehat{\Delta * \Gamma} = 3\widehat{\Delta} \cdot \widehat{\Gamma}$, where $\cdot$ is the entrywise product: the Fourier base is a base of eigenvectors of the convolution T_Γ with eigenvalues $3\hat{c}_k$ (and the ratio $\frac{3\hat{c}_2}{3\hat{c}_1}$ of the two "equilateral" eigenvalues is the shape of Γ). T_Γ maps thus trivial, pequilateral and nequilateral triangles to triangles of the same category or to trivial triangles. $T_\Gamma(\Delta)$ and Δ always have the same centroid if and only if $c_0 + c_1 + c_2 = 1$, which means $\hat{c}_0 = \frac{1}{3}$; the centroid is always translated to the origin if and only if $\hat{c}_0 = 0$. The image by T_Γ of the *Dirac triangle* $(1,0,0) = \frac{1}{3}(e_0 + e_1 + e_2)$ of shape 1 is Γ, the *impulse response* of the filter T_Γ, and the filter output is the convolution of the input with the impulse response, as for every linear time-invariant filter; the convolution with the Dirac triangle is the identity. It is immediate that

$$\sigma_{\Delta * \Gamma} = \sigma_\Delta \sigma_\Gamma$$

when Γ and Δ are not trivial, except that $\Delta * \Gamma$ is trivial when Γ and Δ are equilateral with opposite orientations (*i.e.*, $0 \cdot \infty = $ trivial). When Γ and Δ are mixed, $\Delta * \Gamma$ is degenerate if and only if $|\sigma_\Delta \sigma_\Gamma| = 1$. When Δ is mixed, $T_\Gamma(\Delta)$ can have any prescribed shape σ_{Δ_1}, and this is the case if and only if $\sigma_\Gamma = \frac{\sigma_{\Delta_1}}{\sigma_\Delta}$.

One has $T_{\Gamma_1} \circ T_{\Gamma_2} = T_{\Gamma_2} \circ T_{\Gamma_1} = T_{\Gamma_1 * \Gamma_2}$. The iterates of T_Γ are the convolution filters $T_\Gamma^n \colon (z_0, z_1, z_2) \mapsto \sum_{k=0}^{2} (3\hat{c}_k)^n \hat{z}_k e_k$, $n \in \mathbf{N}$, with centroid $(3\hat{c}_0)^n \hat{z}_0$. The sum of the squared distances between the centroid and the vertices of $T_\Gamma^n(\Delta)$ is

$3 \sum_{k=1}^{2} (3|\hat{c}_k|)^{2n} |\hat{z}_k|^2$: the diameter of $T_\Gamma^n(\Delta)$ tends to 0 for all Δ when $n \to \infty$ if and only if $|\hat{c}_1| < \frac{1}{3}$ and $|\hat{c}_2| < \frac{1}{3}$; this diameter remains bounded for every Δ exactly when $|\hat{c}_1| \leq \frac{1}{3}$ and $|\hat{c}_2| \leq \frac{1}{3}$, and it tends to ∞ for all nontrivial Δ if and only if $|\hat{c}_1| > \frac{1}{3}$ and $|\hat{c}_2| > \frac{1}{3}$. When Γ and Δ are neither trivial nor both equilateral with opposite orientations, $T_\Gamma^n(\Delta)$ has the shape $\sigma_\Delta \sigma_\Gamma^n$ for $n \geq 1$. The behavior of the shape of a mixed triangle under iterated convolution with Γ is thus a matter of domination between the eigenvalues $3\hat{c}_1$ and $3\hat{c}_2$, *i.e.*, this behavior depends on $|\sigma_\Gamma|$ (Theorem 2). We call the filter trivial, equilateral, degenerate, and so on when Γ is trivial, equilateral, degenerate, and so on. A trivial filter maps any triangle to a trivial one.

We now show that a nontrivial convolution filter (with half an exception) simply adds three similar ears of fixed shape to every triangle $\Delta = (z_0, z_1, z_2)$ before submitting the triangle Δ_1 of the ears' apices to a direct similarity $a\Delta_1 + b\hat{z}_0 e_0$ with fixed $a \neq 0$ and fixed b. A (generalized) *Kiepert triangle* consists of the apices of ears that are erected on the sides of the initial triangle (opposite to the vertices in order) and that all have the shape of the normalized $\Delta'(z) = (0, 1, z)$ with apex $z \in \mathbf{C}$: the ear's apex for the side $z_1 \to z_2$ is defined as $z_2 + z(z_1 - z_2)$; it is a right-hand ear if $\operatorname{Im} z > 0$. The corresponding Kiepert triangle is thus given by the centroid-preserving convolution with $K(z) = (0, 1 - z, z)$ of spectrum $\frac{1}{3}(1, \zeta^2 + \sqrt{3}iz, \zeta - \sqrt{3}iz)$ and of shape $\frac{\xi - z}{z - \bar{\xi}} = -\tilde{\sigma}(z, \bar{\xi}, \xi)$, where $\xi = \frac{1}{\sqrt{3}}e^{i\pi/6}$. One has $\sigma_{K(1-z)} = 1/\sigma_{K(z)}$, since $K(1 - z) = (0, z, 1 - z)$, and $K(\bar{z}) = \overline{K(z)}$. Thus $\sigma_{K(1-x)} = \overline{\sigma_{K(x)}}$ if $x \in \mathbf{R}$.

$K(z)$ is orthogonal to e_2, hence pequilateral since nontrivial, exactly for $z = \xi = \frac{1}{1-\zeta}$; $K(z)$ is orthogonal to $e_1 = \overline{e_2}$, hence nequilateral, exactly for $z = \bar{\xi} = \frac{1}{1-\zeta^2}$. The filters $T_{K(\xi)}$ and $T_{K(\bar{\xi})}$ add right-hand and left-hand isosceles ears with base angles $\frac{\pi}{6}$ and shape $-\frac{\zeta}{2}$ and -2ζ, respectively. Napoleon's theorem [9, 26] is now obvious: the convolution of the initial triangle with the pequilateral triangle $K(\xi) = (0, \bar{\xi}, \xi) = \frac{1}{3}(e_0 - e_1)$ and with the nequilateral triangle $K(\bar{\xi}) = \overline{K(\xi)} = \frac{1}{3}(e_0 - e_2)$, respectively, are equilateral (or trivial).

Since $(0, 1, z) = (z + 1)\left(0, 1 - \frac{z}{z+1}, \frac{z}{z+1}\right)$ for $z \in \mathbf{C} \setminus \{-1\}$, every normalized triangle $\Delta'(z)$ different from $(0, 1, -1)$ and from $(0, 0, 1)$ has the shape of $K\left(\frac{z}{z+1}\right)$. One has further $(0, 0, 1) = K(1) = \lim_{z \to \infty} K\left(\frac{z}{z+1}\right)$, and $(0, 1, -1) = \frac{i}{\sqrt{3}}(e_2 - e_1)$ of shape -1 is equal to $\lim_{z \to -1}(z + 1)K\left(\frac{z}{z+1}\right)$.

Theorem 1. *A nontrivial filter T_Γ of shape $\sigma_\Gamma \neq -1$ is the convolution with $\Gamma =$*

$$aK\left(\frac{\bar{\xi}\sigma_\Gamma + \xi}{\sigma_\Gamma + 1}\right) + be_0 \text{ for some fixed complex } a \neq 0 \text{ and } b, \text{ where } \xi = \frac{1}{\sqrt{3}}e^{i\pi/6}.$$

If $\sigma_\Gamma = -1$, T_Γ is the convolution with some $\Gamma = a(0, 1, -1) + be_0$, $a \neq 0$.

A triangle $\Gamma = (c_0, c_1, c_2)$ can be written as $\Gamma = (c_1 - c_0)(0, 1, -1) + c_0 e_0$ if $c_1 + c_2 = 2c_0$ and as $\Gamma = (c_1 + c_2 - 2c_0)K\left(\frac{c_2 - c_0}{c_1 + c_2 - 2c_0}\right) + c_0 e_0$ otherwise.

The convolutions with $K(1) = (0, 0, 1)$ of shape ζ and $K(0) = (0, 1, 0)$ of shape ζ^2 are simply a left and a right cyclic shift of the vertices, respectively; the

only shape-preserving Kiepert filter is the convolution with $K\left(\frac{1}{2}\right) = \left(0, \frac{1}{2}, \frac{1}{2}\right) = \frac{1}{6}(2e_0 - e_1 - e_2)$ of shape 1, which maps a triangle Δ to its medial triangle, *i.e.*, to $\frac{1}{2}$ times the half-turned Δ (shrunk and rotated about the centroid). More generally, $T_{K(x)}(\Delta)$, $x \in \mathbf{R}$, is the $(1-x)$-medial triangle of Δ [11]: this is the introducing Emmerich transformation! Since $K(x)$ has the shape of $\Delta'\left(\frac{x}{1-x}\right)$, $\sigma_{K(x)}$ turns anticlockwise on the unit circle, starting and ending at $-1 = \sigma(0, 1, -1)$ excluded, as x grows on the real axis.

Note that $\sigma_{K(z)}$ is real if and only if $\operatorname{Re} z = \frac{1}{2}$, *i.e.*, if and only if the added ears are isosceles with equal angles at 0 and 1 (this corresponds to the *classical* Kiepert triangles). To get isosceles ears with base angles $|\theta| < \frac{\pi}{2}$, one has to convolve with the isosceles $K_{\text{iso}}(\theta) = K\left(\frac{1+i\tan\theta}{2}\right)$ with apex angle $2|\theta|$ and shape $\frac{1-\sqrt{3}\tan\theta}{1+\sqrt{3}\tan\theta}$: the ears are right-hand or left-hand according as $\theta \geq 0$ or $\theta \leq 0$. Since $\widehat{K_{\text{iso}}\left(\frac{\pi}{3}\right)} = \frac{1}{3}(1, -2, 1)$, one can retrieve Δ from $\Delta * K_{\text{iso}}\left(\frac{\pi}{3}\right)$ by constructing $\frac{1}{2}\left(T_{K_{\text{iso}}\left(\frac{\pi}{3}\right)}(\Delta) + T^2_{K_{\text{iso}}\left(\frac{\pi}{3}\right)}(\Delta)\right) = \Delta$: this is Lemoine's problem [21]. With the same idea, one finds $\Delta = \frac{1}{2}\left(T_{K_{\text{iso}}\left(-\frac{\pi}{3}\right)}(\Delta) + T^2_{K_{\text{iso}}\left(-\frac{\pi}{3}\right)}(\Delta)\right)$, $\Delta = 2T^2_{K\left(\frac{1}{2}\right)}(\Delta) - T_{K\left(\frac{1}{2}\right)}(\Delta)$, and $\Delta = T_{K(z)}(\Delta) + \frac{1}{3(z-\xi)(z-\overline{\xi})}\left(T^3_{K(z)}(\Delta) - T_{K(z)}(\Delta)\right)$ for $z \neq \xi, \overline{\xi}$. A triangle Δ and its classical Kiepert triangle $\Delta * K_{\text{iso}}(\theta)$ are always perspective [4, 20] and, if Δ is proper and nonisosceles, the perspectors form the equilateral Kiepert hyperbola of Δ (Figure 5) as θ runs from $-\frac{\pi}{2}$ to $\frac{\pi}{2}$, *i.e.*, the hyperbola through the vertices of Δ, the centroid G, and the orthocenter H (which is the perspector in the limit case $|\theta| = \frac{\pi}{2}$). We now look at this limit case more closely.

The vertices of $\Delta * K_{\text{iso}}(\theta)$ tend for $|\theta| \to \frac{\pi}{2}-$ to the infinite points of the altitudes of Δ on the line at infinity (when Δ has three different vertices). On the other hand, $\lim_{|\theta| \to \frac{\pi}{2}-} \sigma_{K_{\text{iso}}(\theta)} = -1 = \sigma(0, 1, -1)$: the limit shape of $\Delta * K_{\text{iso}}(\theta)$ when $|\theta| \to \frac{\pi}{2}-$ is thus the shape of $\Delta * (0, 1, -1)$ for any nontrivial triangle Δ. This is clear geometrically: with $\Delta = (z_0, z_1, z_2)$, the angles of $\Delta * K_{\text{iso}}(\theta)$ tend for $|\theta| \to \frac{\pi}{2}-$ to the angles of the (quarter-turned) triangle

$$(z_2 - z_1, z_0 - z_2, z_1 - z_0) = \Delta * (0, 1, -1),$$

whose vertices are the tips of the vectors $z_1 \to z_2$, $z_2 \to z_0$, $z_0 \to z_1$ starting from 0 (Figure 6). Convolving Δ with the normalized $(0, 1, -1)$ gives a scaled down and quarter-turned "equally shaped" bounded copy of "Δ with infinite similar isosceles ears". Here is another description of the filter $T_{(0,1,-1)}$: it translates $\Delta = (z_0, z_1, z_2)$ to $\Delta_1 = \Delta - \hat{z}_0 e_0 = (w_0, w_1, w_2)$ with centroid at the origin and then blows up the $\frac{1}{3}$-medial triangle (with cyclically shifted vertices) $\Delta_2 = \Delta_1 * \left(\frac{1}{3}, \frac{2}{3}, 0\right)$ to $3\Delta_2 = (W_0, W_1, W_2) = \Delta * (0, 1, -1)$ (Figure 6). $T^2_{(0,1,-1)}(\Delta)$ is three times the half-turned Δ_1 (enlarged and rotated about the origin). $\Delta * (0, 1, -1)$ is thus directly similar to $\Delta * \left(0, \frac{1}{3}, \frac{2}{3}\right) = \Delta * K\left(\frac{2}{3}\right)$, the $\frac{1}{3}$-medial triangle of Δ, and two triangles have opposite shapes (possibly after multiplying one of the shapes by $\zeta^{\pm 1}$) if and only if they are directly similar to the $\frac{1}{3}$-medial triangle of each other: since the $\frac{1}{3}$-medial triangle is directly similar to the $\frac{2}{3}$-medial triangle and to the median triangle (Figure 6), this proves that two triangles have
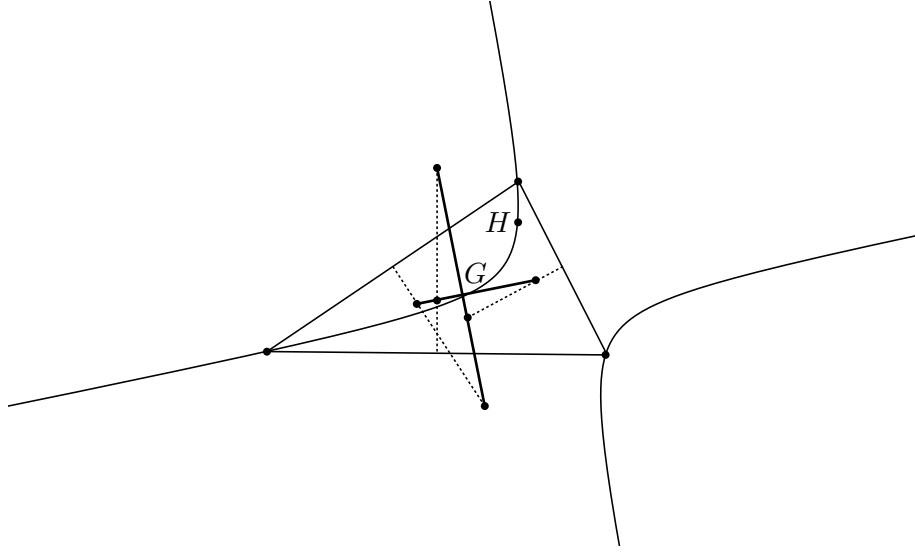
Figure 5. Kiepert hyperbola and both degenerate classical Kiepert triangles with dotted perpendicular bisectors
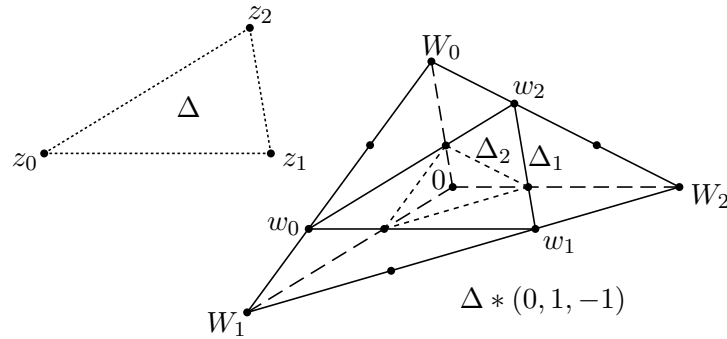
Figure 6

opposite shapes (possibly up to a factor $\zeta^{\pm 1}$) if and only if they are directly similar to the median triangle of each other. The well-known fact that the median triangle of the median triangle is directly similar to the start triangle is equivalent to the fact that the shape of $(0, 1, -1) * (0, 1, -1)$ is 1. If $\Delta'(z)$ is a normalized triangle, remember that $\Delta'(z) * (0, 1, -1)$ and $\Delta'\left(\frac{z-2}{2z-1}\right)$ have the same shape $-\sigma_{\Delta'(z)}$ (Figure 4).

The following theorem is almost immediate.

Theorem 2. (1) *The convolution filter T_Γ is bijective if and only Γ has a full spectrum,* i.e., *if and only if $\Gamma = a(0, 1, -1) + be_0$ with $a, b \neq 0$, or $\Gamma = aK(z) + be_0$ with $z \notin \{\xi, \bar{\xi}\}$, $a \neq 0$, $a + 3b \neq 0$; if $\Gamma = (c_0, c_1, c_2)$, the inverse filter is then the convolution with $\sum_{k=0}^{2} \frac{1}{9\hat{c}_k} e_k$.*

(2) *A pequilateral filter (of shape 0), i.e., a convolution with $aK(\xi) + be_0$, $a \neq 0$, maps nequilateral triangles to trivial triangles and all other nontrivial triangles to pequilateral triangles. A nequilateral filter (of shape ∞), i.e., a convolution with $aK(\overline{\xi}) + be_0$, $a \neq 0$, maps pequilateral triangles to trivial triangles and all other nontrivial triangles to nequilateral triangles.*

(3) *A proper nonequilateral filter T_Γ, i.e., with $|\sigma_\Gamma| \neq 0, 1, \infty$, is smoothing: its action on equilateral triangles is shape-preserving; and according as the filter is positively or negatively oriented, i.e., according as $0 < |\sigma_\Gamma| < 1$ or $1 < |\sigma_\Gamma| < \infty$, the iterates $T_\Gamma^n(\Delta)$ of every mixed Δ are eventually positively or negatively oriented and have a (never reached) pequilateral or nequilateral limit in shape, respectively.*

(4) *A nontrivial filter T_Γ is degenerate (with $|\sigma_\Gamma| = 1$) if and only if $\Gamma = aK + be_0$ for some $a \neq 0$ and some degenerate $K = K(x)$, $x \in \mathbf{R}$, or $K = (0, 1, -1)$.*

(5) *If $\Gamma = a(0, 1, -1) + be_0$, $a \neq 0$, and if $\Delta = (z_0, z_1, z_2)$, one has*

$$T_\Gamma^n(\Delta) = \left(-i\sqrt{3}\,a\right)^n\left(\hat{z}_1 e_1 + (-1)^n \hat{z}_2 e_2\right) + (3b)^n \hat{z}_0 e_0.$$

If Δ is mixed, these iterates $T_\Gamma^n(\Delta)$ are 2-periodic in shape with shape $(-1)^n \sigma_\Delta$ (Figures 6 and 4).

(6) *If $x \in \mathbf{R}$, one has*

$$\widehat{K(x)} = (\hat{c}_0, \hat{c}_1, \overline{\hat{c}_1}) = \tfrac{1}{6}\left(2, -1 + i\sqrt{3}(2x - 1), -1 - i\sqrt{3}(2x - 1)\right) \quad \text{and}$$

$$\sigma_{K(x)} = -e^{i2\arg(\xi - x)} = e^{i2\kappa(x)} \text{ with } \kappa(x) = \arctan\left(\sqrt{3}(2x - 1)\right).$$

If $\Gamma = aK(x) + be_0$ for some $a \neq 0$, one has

$$T_\Gamma^n(\Delta) = \left(-3|\hat{c}_1|e^{-i\kappa(x)}a\right)^n\left(\hat{z}_1 e_1 + e^{i2n\kappa(x)}\hat{z}_2 e_2\right) + (a + 3b)^n \hat{z}_0 e_0 \qquad (5)$$

for every $\Delta = (z_0, z_1, z_2)$, where $3|\hat{c}_1| = \sqrt{3x^2 - 3x + 1}$. When Δ is mixed, these iterates $T_\Gamma^n(\Delta)$ are periodic or nonperiodic in shape (with chaotic behavior) according as $\kappa(x)/\pi$ is rational or irrational, respectively (the period in similarity may be shorter than the period in shape). The period length is $m = 1$ if and only if $\kappa(x) = 0$, i.e., if and only if $K(x) = K(\frac{1}{2})$; $m \geq 2$ is the minimal period length (the same for all mixed Δ) if and only if $\sigma_\Gamma = \sigma_{K(x)} = e^{i2\pi\ell/m}$ for some integer $\ell \in [1, m - 1]$ coprime to m, i.e., if and only $m \geq 3$ and

$$x = \frac{1}{2} + \frac{1}{2\sqrt{3}}\tan\left(\frac{\ell}{m}\pi\right) \qquad (6)$$

for some integer $\ell \in [1, m - 1]$ coprime to m (note that the period 2 corresponds to $K = (0, 1, -1)$ and that $x \in [0, 1]$ exactly when $\frac{\ell}{m} \notin \left]\frac{1}{3}, \frac{2}{3}\right[$); $T_{K(x)}^m(\Delta)$ is then given by the homothety of ratio $(-1)^{m+\min(\ell, m-\ell)}(3|\hat{c}_1|)^m$ about the centroid of Δ.

(7) *When Δ is a mixed triangle and when Γ is degenerate but not trivial, the shapes $(-1)^n \sigma_\Delta$ or $e^{i2n\kappa(x)}\sigma_\Delta$ of the iterates $T_\Gamma^n(\Delta)$ lie on the circle $|s| = |\sigma_\Delta| = R \in {}]0, \infty[$ and correspond to (equibrocardal) normalized triangles $(0, 1, z)$ with vertex z on the Neuberg circle $\mathcal{C}_R$ given by (2) if $R \neq 1$, and to nontrivial degenerate triangles if $R = 1$ (Figures 3 and 4). If m-periodic, $m \geq 1$, these shapes are the vertices (in order) of a regular oriented $\{m/\ell\}$-gon with start at σ_Δ for some*
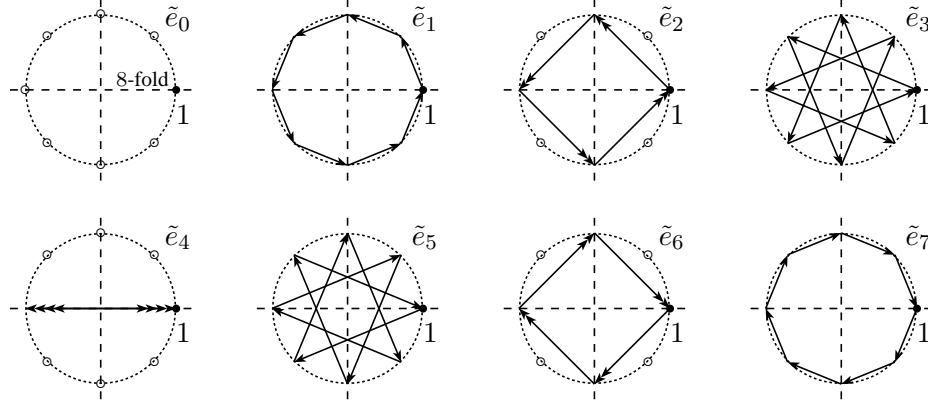
Figure 7. The Fourier base vectors $\tilde{e}_k$ of $\mathbf{C}^8$, $0 \leq k \leq 7$, are the regular $\{8/k\}$-gons $\left(\left(e^{i2\pi/8}\right)^{k \cdot 0}, \left(e^{i2\pi/8}\right)^{k \cdot 1}, \ldots, \left(e^{i2\pi/8}\right)^{k \cdot 7}\right)$.

$\ell \in [0, m-1]$ *coprime to* m *(note that this is the Fourier base polygon* $\tilde{e}_\ell$ *of* $\mathbf{C}^m$ *(Figure 7) multiplied by* σ_Δ *and that the choice of another* ℓ *coprime to* m *only changes the order of the shapes); if nonperiodic,* i.e., *if* $\kappa(x)$ *is an irrational multiple of* π, *these shapes* $T_\Gamma^n(\Delta)$ *are dense on the circle* $|s| = |\sigma_\Delta| = R$, i.e., *the accumulation triangles (in shape) of the sequence* $\left(T_\Gamma^n(\Delta)\right)_{n \geq 0}$ *are the (equibrocardal) normalized triangles* $(0, 1, z)$ *with vertex* z *on the Neuberg circle* $\mathcal{C}_R$ *if* $R \neq 1$ *and the nontrivial degenerate triangles if* $R = 1$.

(8) *When* Δ *is a proper positively oriented mixed triangle with the shape of* $\Delta'(z_0)$ *and when* x *grows on the whole real axis, the shape of* $\Delta * K(x)$ *travels counterclockwise over the whole circle* $|s| = |\sigma_\Delta|$ *starting and ending at* $-\sigma_\Delta$ *excluded, whereas the vertex* z *of the normalized triangle* $\Delta'(z)$ *with the shape of* $\Delta * K(x)$ *turns counterclockwise over the whole Neuberg circle* $\mathcal{C}_{|\sigma_{\Delta'(z_0)}|}$ *of* Figure 4 *starting and ending at* Z_0 *excluded.* $\Delta * (0, 1, -1)$ *fills the holes* $-\sigma_\Delta$ *and* Z_0. *The rotation on the Neuberg circle is clockwise if* Δ *is negatively oriented. In the degenerate case* $|\sigma_\Delta| = 1$, z *runs rightwards over the whole extended real axis starting and ending at* $Z_0 = \frac{z_0 - 2}{2z_0 - 1}$ *excluded.*

Note that the result (6) or an equivalent one can be found in [22, 36, 16, 11] and that the last two parts of Theorem 2 probably furnish the solution that the quite incomprehensible paper [19] aimed at. Note also that the iterates $T_\Gamma^n(\Delta)$ of a mixed Δ are 3-periodic in shape if and only if $\Gamma = aK(1) + b$ or $aK(0) + b$, $a \neq 0$, $K(1)$ and $K(0)$ causing the left and right shifts of Δ's vertices.

The proper nonequilateral triangle Δ is directly similar to its $(1 - t)$-medial triangle $\Delta * K(t)$, $t \in \mathbf{R}$, if and only if $\sigma_{K(t)} = \zeta^k$, $k \in \{0, 1, -1\}$, i.e., if and only if $t = \frac{1}{2}, 1, 0$: $\Delta * K(t)$ is then the medial triangle or a copy of Δ with cyclically shifted vertices. The proper nonequilateral triangle Δ is inversely similar to $\Delta * K(t)$ if and only if $\sigma_{K(t)} = \zeta^k e^{-i2 \arg \sigma_\Delta}$, i.e., if and only if

$$t = \frac{1}{2} + \frac{1}{2\sqrt{3}} \tan(k\tfrac{\pi}{3} - \arg \sigma_\Delta), \ k \in \{0, 1, -1\} : \qquad (7)$$

the solutions t depend only on $\arg\sigma_\Delta \pmod \pi$, *i.e.*, the set of solutions for the nonequilateral normalized triangle $\Delta'(z_0) = (0,1,z_0)$ remains the same for all nonequilateral $\Delta'(z)$ with z on the circle $\mathcal{C}'$ through $e^{i\pi/3}$, $e^{-i\pi/3}$, and z_0 (Figure 4). These solutions t are again $0, \frac{1}{2}, 1$ if Δ is isosceles, they are $\frac{1}{3}, \frac{2}{3}$, and the infinite point of the t-axis if Δ is automedian (then $\sigma_{K(t)} = \zeta^k e^{i\pi/3}$, $k = -1, 0, 1$, and the infinite solution corresponds to $\Delta * (0,1,-1)$), and the solutions are three different real numbers $t \neq 0, \frac{1}{3}, \frac{1}{2}, \frac{2}{3}, 1$ in the other cases. It is clear that $\frac{1}{3}$ and $\frac{2}{3}$ appear only for automedian triangles, because the $\frac{2}{3}$- and $\frac{1}{3}$- medial triangles $\Delta * K(\frac{1}{3})$ and $\Delta * K(\frac{2}{3})$, of shape $e^{\mp i\pi/3}\sigma_\Delta$, are directly similar to the median triangle (Figure 6). If Δ is degenerate and nontrivial, Δ and $\Delta * K(t)$ are similar if and only if t is 0, $\frac{1}{2}$, 1, or a solution of (7). Figure 8 shows the values of t for wich $\Delta'(z_0) * K(t)$ is similar to $\Delta'(z_0)$ as functions of the midpoint M of $\mathcal{C}'$, whose radius is $r = \sqrt{M^2 - M + 1}$: by considering a real point $M \pm r$ of $\mathcal{C}'$ and by plugging $\arg\sigma_{\Delta'(M\pm r)}$ given by (1) into (7), one obtains for $k = 0, 1, -1$ the solutions

$$t_0 = \frac{M-1}{M-2}, \quad t_1 = \frac{1}{M+1}, \quad t_{-1} = \frac{M}{2M-1} \tag{8}$$

given cyclically by $t_{k+1}(M) = t_k\left(1 - \frac{1}{M}\right)$ (plain, dashed, and dotted hyperbolas of Figure 8, respectively); the values of M corresponding to isosceles or automedian triangles are the midpoints of the dotted circles of Figure 2. If Δ is neither trivial, nor isosceles, nor automedian, exactly two of the $(1-t)$-medial triangles $\Delta * K(t)$ inversely similar to Δ are inscribed in Δ, and the sum of these two values of t, on each side of $\frac{1}{2}$, is never 1. The cosine law in $\Delta'(z_0)$ with $z_0 = x_0 + iy_0$ on $\mathcal{C}'$ and sides $a = |z_0 - 1|$, $b = |z_0|$, $c = 1$, and the equation $M^2 - M + 1 = r^2 = (x_0 - M)^2 + (b^2 - x_0^2)$ give $M = \frac{1-b^2}{a^2-b^2}$, and thus by (8)

$$1 - t_0 = \frac{a^2 - b^2}{2a^2 - b^2 - c^2}, \quad 1 - t_1 = \frac{b^2 - c^2}{2b^2 - c^2 - a^2}, \quad 1 - t_{-1} = \frac{c^2 - a^2}{2c^2 - a^2 - b^2}, \tag{9}$$

which are correct by similarity for any nonequilateral and nontrivial triangle ABC with sides a, b, c opposite to the vertices (then $M = \frac{c^2-b^2}{a^2-b^2}c$, $t_0 = \frac{M-c}{M-2c}$, $t_1 = \frac{c}{M+c}$, $t_{-1} = \frac{M}{2M-c}$ if $A = 0$, $B = c > 0$). Since the set $\{t_0, t_1, t_{-1}\}$ is invariant under a cyclic shift of the vertices, each set of solutions t appears for three different M in Figure 8: for $M = \frac{a^2-b^2}{a^2-c^2}$, $M = \frac{b^2-c^2}{b^2-a^2}$, and $M = \frac{c^2-a^2}{c^2-b^2}$ (whose product is -1 in the nonisosceles case) given cyclically by $M \mapsto 1 - \frac{1}{M}$ (once in $\left[\frac{1}{2}, 2\right[$, once in $\left[-1, \frac{1}{2}\right[$, and once in the rest of the extended real axis). Note that (9) already appeared in [18] with another proof.

Start for example from a proper nonequilateral *isosceles* Δ with real shape λ (after a cyclic permutation of its vertices, if necessary); choose $x = \frac{1}{2} + \frac{1}{2\sqrt{3}}\tan(\frac{\ell}{m}\pi)$ for some *odd* $m \geq 3$ and some integer $\ell \in [1, m-1]$ coprime to m: the m-periodic shapes of the equibrocardal $T^n_{K(x)}(\Delta)$ are the vertices in order of $\lambda\tilde{e}_\ell$ in $\mathbf{C}^m$; the cycle contains no automedian triangle; $T^k_{K(x)}(\Delta)$ and $T^{m-k}_{K(x)}(\Delta)$ form a pair of inversely similar triangles for each integer $k \in \left[1, \frac{m-1}{2}\right]$ since their shapes are
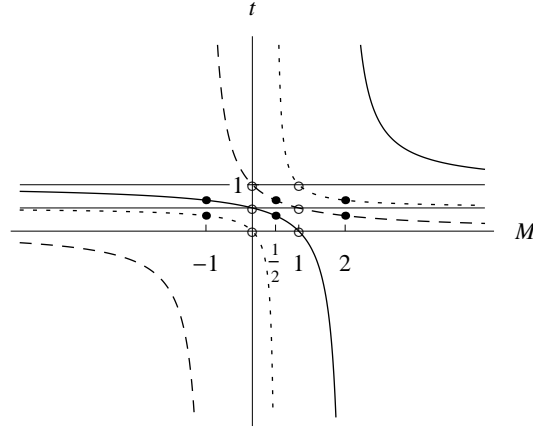
Figure 8. The three or six different values t for which the nonequilateral $\Delta'(z_0)$ and $\Delta'(z_0) * K(t)$ are similar as function of the midpoint M of the circle through $e^{i\pi/3}$, $e^{-i\pi/3}$, and z_0: only $t = 0$, $\frac{1}{2}$, 1 if $\Delta'(z_0)$ is isosceles ($M = 0$, 1, ∞); $t = \frac{1}{3}$, $\frac{2}{3}$, ∞ ($M = -1$, $\frac{1}{2}$, 2) besides $t = 0$, $\frac{1}{2}$, 1 if $\Delta'(z_0)$ is automedian.

complex conjugate; if m is moreover coprime to 3, the cycle contains no two directly similar triangles (hence no other isosceles triangle than Δ) and the minimal period length in similarity is also m; if m is divisible by 3, the first third of the cycle in shape contains no two directly similar triangles, the other thirds are obtained by multiplying the shapes of the first third by $\zeta^{\pm 1}$, and the minimal period length in similarity is $\frac{m}{3}$. (Since similarity does not depend on the order of the vertices, the condition that the isosceles Δ has a real shape can in fact be dropped.)

Start now from a proper nonequilateral *automedian* Δ with, say, purely imaginary shape $i\lambda$ (after a cyclic permutation of its vertices, if necessary); choose x and ℓ as above, but with an *even* $m \geq 2$: the m-periodic shapes of the equibrocardal $T_{K(x)}^n(\Delta)$ are the vertices in order of $i\lambda \tilde{e}_\ell$ in $\mathbf{C}^m$; each triangle in the second half of the cycle is directly similar to the $\frac{1}{3}$-medial triangle of the triangle with the same rank in the first half (and conversely), since they have opposite shapes; $T_{K(x)}^{m/2}(\Delta)$ is thus inversely similar to the automedian Δ; each pair $T_{K(x)}^k(\Delta)$, $T_{K(x)}^{m/2-k}(\Delta)$ of the first half consists of inversely similar triangles (except $T_{K(x)}^{m/4}(\Delta)$ if m is divisible by 4), and this property is inherited by the second half. If m is moreover coprime to 3, the cycle contains no two directly similar triangles and no other automedian triangles than Δ and $T_{K(x)}^{m/2}(\Delta)$; if m is divisible by 3 (hence by 6), there are no two directly similar triangles in the same third of the cycle in shape and the only automedian triangles are the $T_{K(x)}^{km/6}(\Delta)$, which are directly and inversely similar to Δ for $k = 0, 2, 4$ and $k = 1, 3, 5$, respectively. We consider for example the automedian triangle Δ_0 with sides 1, $\sqrt{2}$, $\sqrt{3}$ and $x = \frac{3+\sqrt{6}-\sqrt{3}}{6} \approx 0.61957$ corresponding to $m = 8$, $\ell = 1$ to construct the iterated $(1-x)$-medial triangle
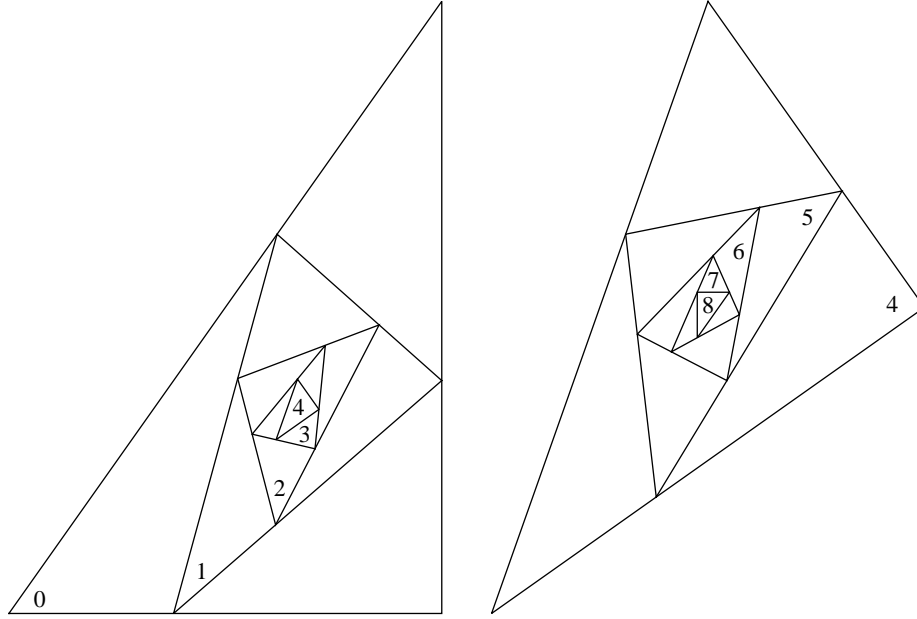
Figure 9

of Δ_0, whose minimal period in shape has length 8: σ_{Δ_0} is $(\sqrt{3} - \sqrt{2})i$ when $\Delta_0 = (0, 1, 1 + \sqrt{2}\,i)$, and $\sigma_{\Delta_{k+1}} = e^{i\pi/4}\sigma_{\Delta_k}$ (Figure 9). Δ_k and Δ_{k+4} are similar to the $\frac{1}{3}$-medial triangle of each other and are thus nonsimilar if not automedian; Δ_0 and Δ_4 are right-angled, automedian and inversely similar; Δ_1 and Δ_3 are inversely similar, as are Δ_5 and Δ_7, and these four triangles are neither isosceles, nor automedian, nor right-angled (Figures 1 and 2); Δ_2 and Δ_6 are isosceles; by (5), Δ_8 is obtained from Δ_0 by a half-turn about the centroid of Δ_0 followed by a homothety of ratio $\frac{17}{4} - 3\sqrt{2} \approx 0.00736$ about this centroid. Figure 10 shows the corresponding normalized triangles with their vertices $f^{-1}\big(e^{ik\pi/4}\sigma_{\Delta_0}\big)$ on the Neuberg circle: note the position of the vertices of the inversely similar and of the isosceles triangles [17, p. 289].

Remark. In [22], the triangle $S_{p,q}(\Delta) = (w_0, w_1, w_2)$ is constructed cyclically from the proper $\Delta = (z_0, z_1, z_2)$ for real p and q with $pq \neq 1$: w_0 is the intersection of the cevian issued from z_1 dividing the side $z_2 \to z_0$ in the ratio $p : (1 - p)$ and of the cevian issued from z_0 dividing the side $z_1 \to z_2$ in the ratio $(1 - q) : q$. $S_{p,1-p}(\Delta)$ is the p-Rooth triangle of [11].
The centroid-preserving transformation $S_{p,q}$ amounts to the convolution of Δ with the degenerate triangle $\frac{1}{1-pq}\big(p(1-q), (1-p)(1-q), q(1-p)\big)$: by Theorem 1, $S_{p,q}(\Delta)$ is thus obtained for $p(2q-3) \neq -1$ by submitting $\Delta * K\big(\frac{q-p}{p(2q-3)+1}\big)$ to a homothety of ratio $\frac{p(2q-3)+1}{1-pq}$ with respect to the centroid of Δ. Remember that $\Delta * K(x) = S_{0,x}(\Delta)$ is the $(1 - x)$-medial triangle of Δ for $x \in \mathbf{R}$. If
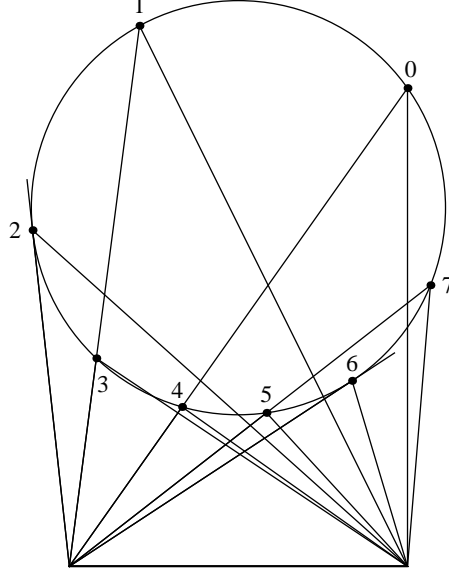
Figure 10

$p(2q - 3) = -1$, $S_{p,q}$ is the convolution with $\frac{1-2q}{3}(0, 1, -1) + \frac{1}{3}e_0$ and $S_{p,q}(\Delta)$ is the $\frac{1}{3}$-medial triangle of Δ transformed by a cyclic left shift of its vertices and by a homothety of ratio $1 - 2q$ with respect to the centroid of Δ; $S_{\frac{1}{2},\frac{1}{2}}$ maps in particular every triangle to its centroid.

For every fixed real $h \neq 0, -1, \pm 2$, the different pairs $(p_1, q_1) = \left(\frac{h-1}{h-2}, \frac{h+1}{h+2}\right)$ and $(p_2, q_2) = \left(\frac{1}{h+2}, \frac{1-h}{2}\right)$ are such that $S_{p_1,q_1}(\Delta)$ and $S_{p_2,q_2}(\Delta)$ have the same vertices: $S_{p_1,q_1}(\Delta)$ is the $\frac{1}{3}$-medial triangle transformed by a homothety of ratio h with respect to its centroid, and $S_{p_2,q_2}(\Delta)$ is the same triangle after a cyclic left shift of the vertices; $h = -3$ corresponds in particular to $S_{\frac{4}{5},2}$ and $S_{-1,2}$.

For $p \in \mathbf{R} \setminus \{\frac{1}{2}\}$, the triangle $\frac{1-p(1-p)}{1-2p} S_{p,1-p}(\Delta) = \Delta * \frac{1}{1-2p}\left(p^2, p(1-p), (1-p)^2\right)$ is a p-median triangle of Δ [11], *i.e.*, a triangle whose sides are parallel to and as long as the cevians connecting the corresponding vertices of Δ and $\Delta * K(1 - p)$. The $\frac{1}{2}$-median or median triangle is for example $\Delta * \left(-\frac{1}{2}, 0, \frac{1}{2}\right)$ with centroid 0.

5. Isosceles ears

The added ears are isosceles if and only if the shape of the convolving triangle is real or ∞ and different from -1. The convolving triangle is then $aK_{\text{iso}}(\theta) + be_0$, $a \neq 0$, for some $K_{\text{iso}}(\theta) = K\left(\frac{1+i\tan\theta}{2}\right)$, $|\theta| < \frac{\pi}{2}$, with shape $\frac{1-\sqrt{3}\tan\theta}{1+\sqrt{3}\tan\theta} = \frac{2}{1+\sqrt{3}\tan\theta} - 1$. Since a product of real shapes is real, a composition of convolutions with $a_1 K_{\text{iso}}(\theta_1) + b_1 e_0$ and $a_2 K_{\text{iso}}(\theta_2) + b_2 e_0$ is again a convolution with some $aK_{\text{iso}}(\theta) + be_0$, or with $a(0, 1, -1) + be_0$, or with a trivial triangle. Since $\sigma_{K_{\text{iso}}(\theta)}$

is real and nonzero for $\theta \neq \pm\frac{\pi}{6}$, the triangles Δ and $\Delta * K_{\mathrm{iso}}(\theta)$, $\theta \neq \pm\frac{\pi}{6}$, are by Figure 2 always simultaneously isosceles or automedian, respectively.

If $\Delta'(z_0)$ is a normalized triangle with finite $z_0 \neq e^{\pm i\pi/3}$, the shapes of the classical Kiepert triangles $\Delta'(z_0) * K_{\mathrm{iso}}(\theta)$, $|\theta| < \frac{\pi}{2}$, and of $\Delta'(z_0)*(0,1,-1)$ form the extended line $\lambda\sigma_{\Delta'(z_0)}$ and are the shapes of the normalized triangles $\Delta'(z)$ with vertex z on the circle $\mathcal{C}'$ through $e^{i\pi/3}$, $e^{-i\pi/3}$, and z_0 (Figure 4). As θ grows on $\left[0, \frac{\pi}{2}\right[$, the vertex z of the triangle $\Delta'(z)$ with the shape of $\Delta'(z_0) * K_{\mathrm{iso}}(\theta)$ moves from z_0 to Z_0 (excepted) on the arc of $\mathcal{C}'$ that contains $e^{i\pi/3}$.

Each proper nonequilateral Δ of shape s has exactly two degenerate classical Kiepert triangles $\Delta * K_{\mathrm{iso}}(\theta)$: for $\theta = \arctan\frac{|s|-1}{\sqrt{3}(1+|s|)}$ and $\theta = \arctan\frac{1+|s|}{\sqrt{3}(|s|-1)}$; these are inward Kiepert triangles, *i.e.*, the ears intersect Δ's interior, their position does not depend on the vertices' order in Δ, they correspond to the real points of the circle $\mathcal{C}'$ and mark the transition between the positively and negatively oriented $\Delta *$ $K_{\mathrm{iso}}(\theta)$. These two perpendicular [20] degenerate triangles intersect at the centroid of Δ (which is their common centroid) and they are parallel to the asymptotes of Δ's Kiepert hyperbola (Figure 5). The degenerate classical Kiepert triangles of a nontrivial degenerate Δ are the medial triangle and the almost Kiepert $\Delta *$ $(0, 1, -1)$.

We determine now the conditions under which the triangles Δ and $\Delta * K_{\mathrm{iso}}(\theta)$ are similar. We suppose that Δ is proper, not equilateral, and positively oriented, and we exclude the evident case $K_{\mathrm{iso}}(0) = K(\frac{1}{2})$. We set $\sigma_\Delta = s$ with $0 < |s| < 1$ and denote the shape $\frac{1-\sqrt{3}\tan\theta}{1+\sqrt{3}\tan\theta}$ of $K_{\mathrm{iso}}(\theta)$ by $\mu \in \mathbf{R} \setminus \{-1, 1\}$. μs is the shape of a triangle inversely similar to Δ if and only if $\mu s = \frac{1}{\bar{s}}$, *i.e.*, if and only if $\mu = \frac{1}{|s|^2}(> 1)$: this corresponds to inward ears. μs is the shape of a triangle directly similar to Δ if and only if $\mu s \in \left\{\frac{1}{s}, \zeta\frac{1}{s}, \zeta^2\frac{1}{s}\right\}$, and this is possible in two cases:

(1) $s = \lambda\zeta^k$, $\lambda \in \,]-1, 1[$, $k = 0, 1, 2$, and $\mu = \frac{1}{|s|^2}(> 1)$: Δ is then isosceles and $K_{\mathrm{iso}}(\theta)$ is the same as in the inversely similar case.

(2) $s = \lambda i\zeta^k$, $\lambda \in \,]-1, 1[$, $k = 0, 1, 2$, and $\mu = \frac{-1}{|s|^2}(< -1)$: Δ is then automedian.

Writing $|s| = R$ and dropping now the condition that Δ is positively oriented, one sees that the proper nonequilateral Δ and $\Delta * K_{\mathrm{iso}}(\theta)$, $\theta \neq 0$, are inversely similar (and inversely oriented) exactly when $\theta = \Theta_1 = \arctan\frac{R^2-1}{\sqrt{3}(R^2+1)}$, and directly similar (and inversely oriented) exactly when Δ is automedian and $\theta = \Theta_2 = \arctan\frac{R^2+1}{\sqrt{3}(R^2-1)}$. Note that $0 < |\Theta_1| < \frac{\pi}{6} < |\Theta_2| < \frac{\pi}{2}$ and that these are inward ears.

By (3), $\Delta * K_{\mathrm{iso}}(\Theta_1) = \Delta * K_{\mathrm{iso}}(\mp\omega)$ is the first Brocard triangle (the base angles of the ears are the Brocard angle of Δ): it is thus immediate that the first Brocard triangle has the centroid of Δ. Figure 11 shows two equibrocardal isosceles triangles with the same base (the apex angle of the right triangle is $30°$), their first Brocard triangles and their Brocard points. Equibrocardal isosceles triangles $\Delta_{1,2}$ with the same orientation have base angles θ_1, θ_2 given by (4), and
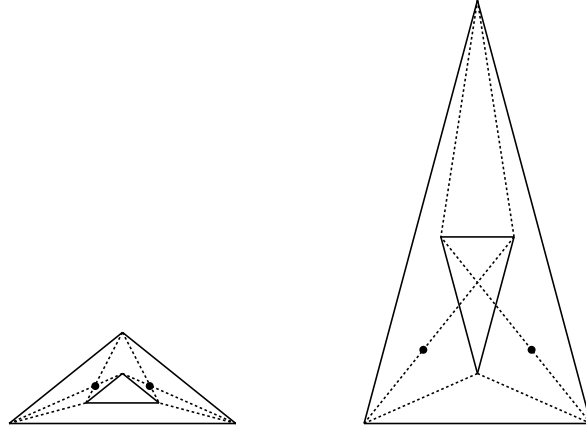
Figure 11

$\tan \Theta_1 = \frac{-2 \tan \theta_{1,2}}{3 + \tan^2 \theta_{1,2}}$; if one neglects the order of the vertices, the first Brocard triangle is obtained from $\Delta_{1,2}$ by a homothety of ratio $-\frac{1}{2} + \frac{3}{3 + \tan^2 \theta_{1,2}} \in \left]-\frac{1}{2}, \frac{1}{2}\right[$ with respect to the centroid of $\Delta_{1,2}$ (the homothety ratio can be computed directly by considering the normalized $\Delta = \left(0, 1, \frac{1 + i \tan \theta_{1,2}}{2}\right)$); the sign of the homothety ratio changes at $\theta = \frac{\pi}{3}$, and the homothety ratios corresponding to θ_1 and to θ_2 differ only by their sign (Figure 11).

Suppose now that Δ is proper and automedian with Brocard angle ω. One has $3 \tan|\Theta_2| = \cot \omega$ by (3). On the other side, $\cot \omega = 3 \cot \gamma$ when γ is the middle angle of any nontrivial automedian triangle [5, p. 17]: thus $|\Theta_2| = \frac{\pi}{2} - \gamma$, the ears' apex angle is 2γ, the apex of the ear over the middle side is the circumcenter of Δ by the inscribed angle theorem, and the sides of $\Delta * K_{\mathrm{iso}}(\Theta_2)$ are perpendicular to the sides of Δ with middle side opposite to the circumcenter. $\Delta * K_{\mathrm{iso}}(\Theta_2)$ is thus obtained from Δ by a quarter-turn about the centroid of Δ followed by a homothety of ratio $\frac{|\cot \varphi|}{2}$ about this centroid, where φ (positive or negative as the orientation of Δ) is the angle between the middle side of Δ and its median (the homothety ratio can be computed directly by considering the normalized automedian triangle $\left(0, 1, \frac{1}{2} + \frac{\sqrt{3}}{2} e^{i\varphi}\right)$). Notice that one has also $\tan \Theta_2 = \frac{-1}{\sqrt{3} \sin \varphi}$, $\tan \Theta_1 = \tan(\mp\omega) = \frac{-1}{\sqrt{3}} \sin \varphi$, and that the similarity ratio of the first Brocard triangle to Δ is $\frac{1}{4} \left|1 + e^{i2\varphi}\right| \in \left[0, \frac{1}{2}\right[$ (0 when Δ is equilateral).

The following theorem is proven.

Theorem 3. (1) *A proper nonequilateral triangle Δ is similar to exactly three or two of its classical Kiepert triangles according as it is automedian or not: it is directly similar to its medial triangle, inversely similar to its first Brocard triangle, and, if automedian, directly similar to the triangle constructed from inward isosceles ears with apex angle twice the middle angle of Δ (the apex of the ear over the middle side is then the circumcenter of Δ and the triangles are perpendicular to*

each other). If Δ is automedian, the two cases $\lim_{\theta \to \frac{\pi}{2}-} \Delta * K_{\mathrm{iso}}(\pm\theta)$ are asymptotically inversely similar to Δ.

(2) A proper nonequilateral triangle Δ is isosceles or automedian if and only if it is directly similar to one of its classical Kiepert triangles other than the medial triangle: the corresponding sides are then parallel in the isosceles and perpendicular in the automedian case.
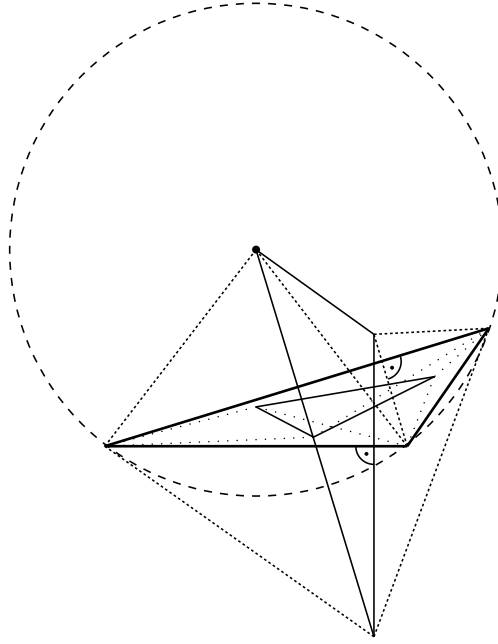
Figure 12. The (up to similarity) only nontrivial triangle with a congruent classical Kiepert triangle, together with its first Brocard triangle

The automedian triangle with sides 1, $\sqrt{1 - \sqrt{\frac{3}{5}}}$ and $\sqrt{1 + \sqrt{\frac{3}{5}}}$ (Figure 12) is up to similarity the only nontrivial triangle with a congruent classical Kiepert triangle: the cotangent of the angle formed by the side 1 and its median is 2. The base angles of the inward ears are $\arctan\sqrt{\frac{5}{3}}$ for the directly congruent classical Kiepert triangle and $\omega = \arctan\frac{1}{\sqrt{15}}$ for the first Brocard triangle, whose similarity ratio to the initial triangle is $\frac{1}{\sqrt{5}}$.

6. Sequences of outward and inward Kiepert triangles

If the triangle $\Delta = (w_0, w_1, w_2)$ is positively oriented or degenerate and if $\mathrm{Im}\, z \geq 0$, the *outward* and *inward* Kiepert triangles of Δ corresponding to outward and inward ears directly similar to the triangle $(0, 1, z)$ are defined by $\Delta^{\mathrm{out}}(z) = \Delta * K(z)$ and $\Delta^{\mathrm{in}}(z) = \Delta * K(1-z)$, respectively. If Δ is negatively oriented and proper, $\Delta^{\mathrm{out}}(z) = \Delta * K(1-z)$ and $\Delta^{\mathrm{in}}(z) = \Delta * K(z)$. The outward ears added to

Δ do not intersect Δ's interior. We set further $\Delta^{\text{out}}(\nabla) = \Delta^{\text{in}}(\nabla) = \Delta * (0, 1, -1)$. Given a sequence $(z_n)_{n \in \mathbf{N}}$ with values in $\{z \in \mathbf{C} \mid \operatorname{Im} z \geq 0\} \cup \{\nabla\}$, and starting from $\Delta = \Delta_0 = \Delta_0^{\text{out}} = \Delta_0^{\text{in}}$, we define inductively $\Delta_{n+1}^{\text{out}} = \Delta_n^{\text{out}}(z_n)$ and $\Delta_{n+1}^{\text{in}} = \Delta_n^{\text{in}}(z_n)$. The centroid remains the centroid of Δ_0 until the first convolution with $(0, 1, -1)$, if any, moves it to the origin.

Theorem 4. *Let $(z_n)_{n \geq 0}$ be a sequence of symbols ∇ and of complex numbers with nonnegative imaginary part; set $\xi = \frac{1}{\sqrt{3}} e^{i\pi/6}$ and $\frac{\nabla - \xi}{\nabla - \bar{\xi}} = -\sigma(0, 1, -1) = 1$. If $z_n \in \mathbf{C}$, denote by $\tilde{z}_n = \frac{1 + i \tan \theta_n}{2}$, with*

$$\theta_n = \arctan \frac{|z_n - \bar{\xi}| - |z_n - \xi|}{\sqrt{3}\big(|z_n - \bar{\xi}| + |z_n - \xi|\big)} \in [0, \tfrac{\pi}{6}],$$

the south pole of the Apollonius circle $\left|\frac{z - \xi}{z - \bar{\xi}}\right| = R$ containing z_n, and set $\theta_n = 0$ if $z_n = \nabla$. Let Δ_0 be a nontrivial and nonequilateral triangle.

The following properties are equivalent.

(1) *The sequence $(\Delta_n^{\text{out}})_{n \geq 0}$ constructed from Δ_0 and (z_n) converges in shape to an equilateral limit.*

(2) $\lim_{n \to \infty} \prod_{k=0}^{n} \frac{z_k - \xi}{z_k - \bar{\xi}} = 0.$

(3) *The sequence of classical Kiepert triangles $(\widetilde{\Delta}_n^{\text{out}})_{n \geq 0}$ constructed from Δ_0 and $(\tilde{z}_n)$ converges in shape to an equilateral limit.*

(4) $\lim_{n \to \infty} \prod_{k=0}^{n} \frac{1 - \sqrt{3} \tan \theta_k}{1 + \sqrt{3} \tan \theta_k} = 0.$

(5) $\theta_n = \frac{\pi}{6}$ *for some n or $\sum_{n=0}^{\infty} \theta_n = \infty$.*

The existence of the equilateral limit does not depend on the choice of the nonequilateral Δ_0.

One can also allow to choose each $\tilde{z}_n$ freely as the north or south pole of the Apollonius circle (in order to always leave $\tilde{z}_n = z_n$ when $\operatorname{Re} z_n = \frac{1}{2}$ for example). One has then to take $\theta_n = \arctan \frac{|z_n - \bar{\xi}| + |z_n - \xi|}{\sqrt{3}(|z_n - \bar{\xi}| - |z_n - \xi|)}$ when $\theta_n \in \left[\frac{\pi}{6}, \frac{\pi}{2}\right[$, and the condition $\sum_{n=0}^{\infty} \theta_n = \infty$ has to be replaced by $\sum_{n=0}^{\infty} \min\big(\theta_n, \frac{\pi}{2} - \theta_n\big) = \infty$, as we showed in [23].

Theorem 4 generalizes [34], where the iterated convolution with a constant triangle $K_{\text{iso}}(\theta)$ is analyzed, and [23], where only classical iterated Kiepert triangles are considered.

Proof. If Δ_0 is positively oriented or degenerate, so are all Δ_n^{out}, and $\sigma_{\Delta_n^{\text{out}}} = \sigma_{\Delta_0} \prod_{k=0}^{n-1} \frac{\xi - z_k}{z_k - \bar{\xi}}$. $\lim_{n \to \infty} \sigma_{\Delta_n^{\text{out}}} = 0$ means $\lim_{n \to \infty} \prod_{k=0}^{n} \left|\frac{z_k - \xi}{z_k - \bar{\xi}}\right| = 0$ since Δ_0 is not equilateral, and each factor in this product is constant on the corresponding Apollonius circle. We proved the equivalence of (4) and (5) in [23].

If Δ_0 is negatively oriented and proper, so are all Δ_n^{out}. Since $\sigma_{K(1-z)} = 1/\sigma_{K(z)}$, one has then $\sigma_{\Delta_n^{\text{out}}} = \sigma_{\Delta_0} \prod_{k=0}^{n-1} \frac{z_k - \bar{\xi}}{\xi - z_k}$: every factor of this product has a modulus ≥ 1, and one has $\lim_{n \to \infty} \sigma_{\Delta_n^{\text{out}}} = \infty$ under the same conditions as in the first case. $\qquad\square$

A nonequilateral limit shape for (Δ_n^{out}) is only possible when $\frac{\xi - z_n}{z_n - \bar\xi}$ converges to 1, *i.e.*, when $\lim_{n\to\infty} z_n = \frac{1}{2}$. But this condition is not sufficient: if $z_n = \frac{1}{2} + \frac{1}{n}$, $n \geq 1$, for example, $\arg\big(\sigma_{\Delta_n^{\text{out}}}\big)$ diverges like the harmonic series.

Suppose that the sequence (Δ_n^{out}) has no equilateral limit shape: the infinite product $\prod_{n=0}^{\infty} \left|\frac{\xi - z_n}{z_n - \bar\xi}\right|$, whose factors lie in $]0, 1]$, has then a limit $L \in]0, 1]$ (and any such L can be obtained by an appropriate choice of the z_n's). The accumulation points of $\big(\sigma_{\Delta_n^{\text{out}}}\big)$ lie on the circle $|s| = L|\sigma_{\Delta_0}|$ $(\leq |\sigma_{\Delta_0}| \leq 1)$ if Δ_0 is positively oriented or degenerate, and on the circle $|s| = \frac{1}{L}|\sigma_{\Delta_0}|$ $(\geq |\sigma_{\Delta_0}| > 1)$ if Δ_0 is negatively oriented and proper: these accumulation shapes correspond to equibrocardal normalized triangles $(0, 1, z)$ with vertex z on the Neuberg circle $\left|\frac{z - e^{i\pi/3}}{z - e^{-i\pi/3}}\right| = L^{\pm 1}|\sigma_{\Delta_0}|$, respectively (Figure 4). The sequence $\big(\sigma_{\Delta_n^{\text{out}}}\big)$ can tend to the accumulation circle with any behavior since the argument of each factor $\frac{\xi - z_n}{z_n - \bar\xi}$ can be changed arbitrarily by replacing z_n by an appropriate number of the Apollonius circle $\left|\frac{z - \xi}{z - \bar\xi}\right| = R$ containing z_n.

Suppose that a sequence of classical iterated Kiepert triangles is given by the successive convolutions with $K_{\text{iso}}(\theta_n)$, $0 \leq \theta_n < \frac{\pi}{2}$, $n \geq 0$, and that this sequence (Δ_n) starts from a positively oriented nonequilateral Δ_0 and has no equilateral limit, *i.e.*, $\sum_{n=0}^{\infty} \min\big(\theta_n, \frac{\pi}{2} - \theta_n\big) < \infty$: the one or two accumulation points of the sequence (θ_n) belong to $\{0, \frac{\pi}{2}\}$, and the corresponding subsequences converge rapidly to the accumulation points, since the sum of the corresponding θ_n or $\frac{\pi}{2} - \theta_n$ is finite; the convolution with $K_{\text{iso}}(\theta_n)$ multiplies the shape by $\lambda_n = \sigma_{K_{\text{iso}}(\theta_n)} = \frac{1 - \sqrt{3}\tan\theta_n}{1 + \sqrt{3}\tan\theta_n} \in]-1, 1]$, and λ_n is about 1 or -1 when θ_n is near to 0 or to $\frac{\pi}{2}$, respectively. As above, $\prod_{n=0}^{\infty}|\lambda_n| = L \in]0, 1]$, but the λ_n are now real: (σ_{Δ_n}) has thus the nonzero limit $\sigma_{\Delta_0} \prod_{n=0}^{\infty} \frac{1 - \sqrt{3}\tan\theta_n}{1 + \sqrt{3}\tan\theta_n}$ $(= \pm L\sigma_{\Delta_0})$ if all λ_n are eventually positive, *i.e.*, if $\lim_{n\to\infty}\theta_n = 0$. Otherwise, the infinite subsequences of the σ_{Δ_n} with positive and negative $\prod_{k=0}^{n-1}\lambda_k$ have nonzero limits $L\sigma_{\Delta_0}$ and $-L\sigma_{\Delta_0}$, respectively, and the sequence (σ_{Δ_n}) has exactly two accumulation points given by $\pm L\sigma_{\Delta_0}$ with $0 < L < 1$. The limit or accumulation shapes and the σ_{Δ_n} are shapes of classical Kiepert triangles of Δ_0 of the form $\Delta_0 * K_{\text{iso}}(\theta)$, $0 \leq \theta < \frac{\pi}{2}$. If existing, the two accumulation shapes $\pm L\sigma_{\Delta_0}$ are also the shapes of two normalized equibrocardal triangles $\Delta'(z_\pm)$ that are directly similar to the median triangle of each other. If the normalized $\Delta'(z_0)$ has the shape of Δ_0, *i.e.*, if $z_0 = \frac{\zeta\sigma_{\Delta_0} - 1}{\zeta - \sigma_{\Delta_0}}$, the vertices $z_\pm$ are given by the intersections of the Neuberg circle $\left|\frac{z - e^{i\pi/3}}{z - e^{-i\pi/3}}\right| = L|\sigma_{\Delta_0}|$ with (the upper half of) the circle $\mathcal{C}'$ through $e^{i\pi/3}$, $e^{-i\pi/3}$, and z_0, on both sides of $e^{i\pi/3}$ (Figure 4): z_+ lies on the arc between $e^{i\pi/3}$ and z_0, z_- between $e^{i\pi/3}$ and $Z_0 = \frac{z_0 - 2}{2z_0 - 1}$, which corresponds to the shape $-\sigma_{\Delta_0}$. z_0 and Z_0 have a strictly positive imaginary part if Δ_0 is proper and are real if Δ_0 is degenerate.

Since Δ and an outward Kiepert triangle of Δ are always simultaneously in the category "positively oriented or degenerate" or in the category "negatively oriented

and proper", an iterated *outward* Kiepert triangle remains unchanged if one modifies the order of the successive convolutions. This is not the case for an iterated inward triangle, because the orientation may change after a convolution, leading to the next convolution with $K(1 - z)$ instead of $K(z)$ for example, and these orientation changes may depend on the order of the convolutions. Note that the inward Kiepert triangle of an outward Kiepert triangle given by the same ears has the shape of the initial triangle or is trivial, since the shapes of $K(z) * K(1 - z)$, $K(1 - z) * K(z)$, and $(0, 1, -1) * (0, 1, -1)$ are all 1 for $z \neq \xi, \overline{\xi}$. A nontrivial outward Kiepert triangle of an inward Kiepert triangle of Δ_0 given by the same ears is in general not even similar to Δ_0: if Δ_0 is proper, nonequilateral, and positively oriented with shape s_0, for example, and if $\sigma_{K(z)} = s$ with $0 < |s| < |s_0|$, $\Delta_0 * K(1 - z)$ is negatively oriented and the end triangle $\Delta_0 * K(1 - z) * K(1 - z)$ is also negatively oriented with shape $\frac{s_0}{s^2}$ of modulus $> \frac{1}{|s_0|}$; this end triangle is never similar to Δ_0.

Except when the sequence has been stopped before by $0 \cdot \infty$ or $\infty \cdot 0$, the shape of $\Delta_{n+1}^{\mathrm{in}}$, $n \geq 0$, is given recursively by $\sigma_{\Delta_{n+1}^{\mathrm{in}}} = \frac{z_n - \overline{\xi}}{\xi - z_n} \cdot \sigma_{\Delta_n^{\mathrm{in}}}$ if $\left| \sigma_{\Delta_n^{\mathrm{in}}} \right| \leq 1$ (then $\left| \sigma_{\Delta_{n+1}^{\mathrm{in}}} \right| \geq \left| \sigma_{\Delta_n^{\mathrm{in}}} \right|$) and by $\sigma_{\Delta_{n+1}^{\mathrm{in}}} = \frac{\xi - z_n}{z_n - \overline{\xi}} \cdot \sigma_{\Delta_n^{\mathrm{in}}}$ if $\left| \sigma_{\Delta_n^{\mathrm{in}}} \right| > 1$ (then $\left| \sigma_{\Delta_{n+1}^{\mathrm{in}}} \right| \leq \left| \sigma_{\Delta_n^{\mathrm{in}}} \right|$). The turning points between stretching factors $\left(\frac{\xi - z_n}{z_n - \overline{\xi}} \right)^{\pm 1}$ of modulus ≤ 1 or ≥ 1, respectively, depend also on Δ_0. By choosing Δ_0 and the z_n appropriately, the sequence (Δ_n^{in}) can thus have any behavior in shape within these constraints. The iterated first Brocard triangles of a proper nonequilateral Δ_0 are for example alternately inversely and directly similar to Δ_0 when Δ_0 is not isosceles, and all directly similar to Δ_0 when Δ_0 is isosceles. If Δ_0 is automedian and if the ears are isosceles with constant apex angle twice the middle angle of Δ_0, the iterated inward Kiepert triangles are all directly similar to Δ_0: the automedian triangle of Figure 12 initiates in particular a 4-periodic sequence given by quarter-turns about the centroid.

References

[1] E. R. Berlekamp, E. N. Gilbert, and F. W. Sinden, A polygon problem, *Amer. Math. Monthly*, 72 (1965) 233–241.

[2] O. Bottema, A triangle transformation, *Elem. Math.*, 29 (1974) 135–138.

[3] G. Darboux, Sur un problème de géométrie élémentaire, *Bull. Sci. Math. Astr., 2e Sér.*, 2 (1878) 298–304.

[4] R. H. Eddy and R. Fritsch, The conics of Ludwig Kiepert: a comprehensive lesson in the geometry of the triangle, *Amer. Math. Monthly*, 67 (1994) 188–205.

[5] A. Emmerich, *Die Brocardschen Gebilde und ihre Beziehungen zu den verwandten merkwürdigen Punkten und Kreisen des Dreiecks*, Reimer, Berlin, 1891.
http://archive.org/details/diebrocardschen00emmegoog

[6] J. Chris Fisher, D. Ruoff, and J. Shilleto, Perpendicular polygons, *Amer. Math. Monthly*, 92 (1985) 23–37.

[7] S. B. Gray, Generalizing the Petr-Douglas-Neumann theorem on n-gons, *Amer. Math. Monthly*, 110 (2003) 210–227.

[8] B. Grünbaum, Lecture notes for a course *Modern Elementary Geometry* given in spring 1997, EPrint Collection, University of Washington, 1999.
`http://hdl.handle.net/1773/15592`

[9] B. Grünbaum, Is Napoleon's theorem really Napoleon's theorem?, *Amer. Math. Monthly*, 119 (2012) 495–501.

[10] M. Hajja, H. Martini, and M. Spirova, On converses of Napoleon's theorem and a modified shape function, *Beitr. Algebra Geom.*, 47 (2006) 363–383.

[11] M. Hajja, On nested sequences of triangles, *Result. Math.*, 54 (2009) 289–299.

[12] M. Hajja, The sequence of generalized median triangles and a new shape function, *J. Geom.*, 96 (2010) 71–79.

[13] M. Hajja, Generalized Napoleon and Torricelli transformations and their iterations, *Beitr. Algebra Geom.*, 51 (2010) 171–190.

[14] R. L. Hitt and X.-M. Zhang, Dynamic geometry of polygons, *Elem. Math.*, 56 (2001) 21–37.

[15] R. Honsberger, *Episodes in Nineteenth and Twentieth Century Euclidean Geometry*, Math. Assoc. Amer., Washington DC, 1995.

[16] D. Ismailescu and J. Jacobs, On sequences of nested triangles, *Period. Math. Hung.*, 53 (2006) 169–184.

[17] R. A. Johnson, *Advanced Euclidean Geometry*, Dover reprint, 2007.

[18] M. S. Klamkin, W. J. Blundon, and D. Sokolowsky, Problem 210, *Crux Math.*, 3 (1977) 10; Solution, *Ibid.*, 3 (1977) 160–164.

[19] P. T. Krasopoulos, Kronecker's approximation theorem and a sequence of triangles, *Forum Geom.*, 8 (2008) 27–37.

[20] F. van Lamoen and P. Yiu, The Kiepert pencil of Kiepert hyperbolas, *Forum Geom.*, 1 (2001) 125–132.

[21] E. Lemoine and L. Kiepert, Question 864, *Nouv. Ann. Math., 2ᵉ Sér.*, 7 (1868) 191; Solution, *Ibid.*, 8 (1869) 40–42.

[22] H. Nakamura and K. Oguiso, Elementary moduli space of triangles and iterative processes, *J. Math. Sci. Univ. Tokyo*, 10 (2003) 209–224.

[23] G. Nicollier and A. Stadler, Limit shape of iterated Kiepert triangles, *Elem. Math.*, 68 (2013) 1–4.

[24] G. Nicollier, Convolution filters for polygons and the Petr-Douglas-Neumann theorem, *Beitr. Algebra Geom.* (online publication 2013). doi:10.1007/s13366-013-0143-9

[25] P. Pech, The harmonic analysis of polygons and Napoleon's theorem, *J. Geom. Graph.*, 5 (2001) 13–22.

[26] F. Schmidt, 200 Jahre französische Revolution – Problem und Satz von Napoleon mit Variationen, *Didaktik der Mathematik*, 19 (1990) 15–29.

[27] I. J. Schoenberg, The finite Fourier series and elementary geometry, *Amer. Math. Monthly*, 57 (1950) 390–404.

[28] D. B. Shapiro, A periodicity problem in plane geometry, *Amer. Math. Monthly*, 91 (1984) 97–108.

[29] R. J. Stroeker, Brocard points, circulant matrices, and Descartes' folium, *Math. Mag.*, 61 (1988) 172–187.

[30] S. Szabó, Affine regular polygons, *Elem. Math.*, 60 (2005) 137–147.

[31] D. Vartziotis and J. Wipper, On the construction of regular polygons and generalized Napoleon vertices, *Forum Geom.*, 9 (2009) 213–223.

[32] D. Vartziotis and J. Wipper, Classification of symmetry generating polygon-transformations and geometric prime algorithms, *Math. Pannon.*, 20 (2009) 167–187.

[33] D. Vartziotis and J. Wipper, Characteristic parameter sets and limits of circulant Hermitian polygon transformations, *Linear Algebra Appl.*, 433 (2010) 945–955.

[34] D. Vartziotis and S. Huggenberger, Iterative geometric triangle transformations, *Elem. Math.*, 67 (2012) 68–83.

[35] J. E. Wetzel, Converses of Napoleon's theorem, *Amer. Math. Monthly*, 99 (1992) 339–351.

[36] B. Ziv, Napoleon-like configurations and sequences of triangles, *Forum Geom.*, 2 (2002) 115–128.

University of Applied Sciences of Western Switzerland, Route du Rawyl 47, CH–1950 Sion, Switzerland

E-mail address: `gregoire.nicollier@hevs.ch`

On the Conic Through the Intercepts of the Three Lines Through the Centroid and the Intercepts of a Given Line

Paul Yiu

Abstract. Let $\mathscr{L}$ be a line intersecting the sidelines of triangle ABC at X, Y, Z respectively. The lines joining these intercepts to the centroid give rise to six more intercepts on the sidelines which lie on a conic $\mathscr{Q}(\mathscr{L}, G)$. We show that this conic (i) degenerates in a pair of lines if $\mathscr{L}$ is tangent to the Steiner inellipse, (ii) is a parabola if $\mathscr{L}$ is tangent to the ellipse containing the trisection points of the sides, (iii) is a rectangular hyperbola if $\mathscr{L}$ is tangent to a circle $\mathscr{C}_G$ with center G. We give a ruler and compass construction of the circle $\mathscr{C}_G$. Finally, we also construct the two lines each with the property that the conic $\mathscr{Q}(\mathscr{L}, G)$ is a circle.

1. Introduction

In the plane of a triangle ABC, consider a line $\mathscr{L}$ intersecting the sidelines BC, CA, AB respectively at X, Y, Z. Consider also three lines, $\mathcal{L}_a$ through X intersecting CA, AB at Y_a, Z_a, $\mathcal{L}_b$ through Y intersecting AB, BC at Z_b, X_b, and $\mathcal{L}_c$ through Z intersecting BC, CA at X_c, Y_c. The six points X_b, X_c, Y_c, Y_a, Z_a, Z_b lie on a conic $\mathscr{Q}$ whose equation can be determined as follows.
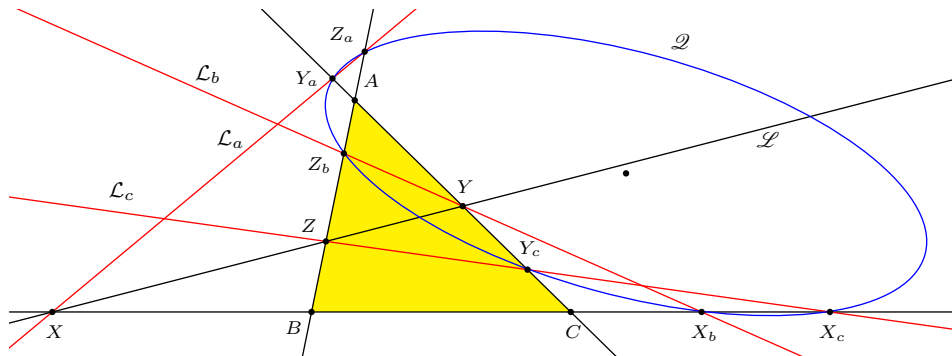
Figure 1

Let $L =: px + qy + rz = 0$ be the equation of $\mathscr{L}$ in homogeneous barycentric coordinates with respect to triangle ABC, so that

$$X = (0 : r : -q), \qquad Y = (-r : 0 : p), \qquad Z = (q : -p : 0).$$

Suppose further that $\mathcal{L}_a$ joins X to a point $P_1 = (f_1 : g_1 : h_1)$, $\mathcal{L}_b$ joins Y to a point $P_2 = (f_2 : g_2 : h_2)$, and $\mathcal{L}_c$ joins Z to a point $P_3 = (f_3 : g_3 : h_3)$,

so that these lines are represented by linear equations $L_a = 0$, $L_b = 0$, $L_c = 0$ respectively. These linear forms are

$$L_a = \begin{vmatrix} x & y & z \\ 0 & r & -q \\ f_1 & g_1 & h_1 \end{vmatrix}$$

$$= (qg_1 + rh_1)x - qf_1y - rf_1z,$$

$$L_b = -pg_2x + (rh_2 + pf_2)y - rg_2z,$$

$$L_c = -ph_3x - qh_3y + (pf_3 + qg_3)z.$$

Proposition 1. *The polynomial $L_aL_bL_c - L(P_1)L(P_2)L(P_3)xyz$ is divisible by $px + qy + rz$.*

Proof. If we put $x = -\frac{qy+rz}{p}$, then

$$L_a = (qg_1 + rh_1)x - f_1(qy + rz) = (qg_1 + rh_1)x + f_1 \cdot px = L(P_1)x,$$

$$L_b = L(P_2)y,$$

$$L_c = L(P_3)z.$$

It follows that, regarded as a polynomial in x, $L_aL_bL_c - L(P_1)L(P_2)L(P_3)xyz$, evaluated at $x = -\frac{qy+rz}{p}$ is equal to 0. Thus, the cubic polynomial is divisible by $px + qy + rz$.   □

Since $L_aL_bL_c - L(P_1)L(P_2)L(P_3)xyz$ is divisible by $px + qy + rz$, the remaining quadratic factor yields a conic $\mathscr{Q}$ containing the six points X_b, X_c, Y_c, Y_a, Z_a, Z_b. For example, if we regard the given line $\mathscr{L}$ as the trilinear polar of $P = (u : v : w)$, and take $\mathscr{L}_a$, $\mathscr{L}_b$, $\mathscr{L}_c$ to be the lines AX, BY, CZ respectively, then $\mathscr{Q}$ is the circumconic $uyz + vzx + wxy = 0$ with perspector P.

2. Preliminaries on conics

We shall make use of the following basic results on conics associated with a triangle. Other preliminary results of triangle geometry can be found in [3]. Consider a conic with barycentric equation

$$\mathscr{C} : \qquad \alpha x^2 + \beta y^2 + \gamma z^2 + 2\lambda yz + 2\mu zx + 2\nu xy = 0.$$

Since this equation can be expressed in the form

$$\begin{pmatrix} x & y & z \end{pmatrix} \begin{pmatrix} \alpha & \nu & \mu \\ \nu & \beta & \lambda \\ \mu & \lambda & \gamma \end{pmatrix} \begin{pmatrix} x \\ y \\ z \end{pmatrix} = 0,$$

we call $M := \begin{pmatrix} \alpha & \nu & \mu \\ \nu & \beta & \lambda \\ \mu & \lambda & \gamma \end{pmatrix}$ the matrix of the conic $\mathscr{C}$. The adjoint matrix of M, namely,

$$M^{\#} = \begin{pmatrix} \beta\gamma - \lambda^2 & \lambda\mu - \gamma\nu & \nu\lambda - \beta\mu \\ \lambda\mu - \gamma\nu & \gamma\alpha - \mu^2 & \mu\nu - \alpha\lambda \\ \nu\lambda - \beta\mu & \mu\nu - \alpha\lambda & \alpha\beta - \nu^2 \end{pmatrix},$$

defines the dual conic of $\mathscr{C}$. It is easy to verify that

$$MM^{\#} = M^{\#}M = (\det M)I_3.$$

Let $G := \begin{pmatrix} 1 & 1 & 1 \end{pmatrix}$. [1] The *characteristic* of M is the number

$$
\begin{aligned}
\chi(M) :=\ & GM^{\#}G^{\mathsf{t}} \\
=\ & 2\mu\nu + 2\nu\lambda + 2\lambda\mu - \lambda^2 - \mu^2 - \nu^2 \\
& - 2(\alpha\lambda + \beta\mu + \gamma\nu) + \beta\gamma + \gamma\alpha + \alpha\beta.
\end{aligned}
$$

Proposition 2. *The conic defined by the symmetric matrix M*
(a) *degenerates into a pair of lines if $\det M = 0$,*
(b) *is a parabola if $\det M \neq 0$ and $\chi(M) = 0$,*
(c) *has center $Q = GM^{\#}$ if $(\det M)\chi(M) \neq 0$.*

Proof. Let $Q = GM^{\#}$. For arbitrary 1×3 matrix P and real number t,

$$
\begin{aligned}
(Q + tP)M(Q + tP)^{\mathsf{t}} =\ & QMQ^{\mathsf{t}} + (PMQ^{\mathsf{t}} + QMP^{\mathsf{t}})t + (PMP^{\mathsf{t}})t^2 \\
=\ & QMQ^{\mathsf{t}} + 2(QMP^{\mathsf{t}})t + (PMP^{\mathsf{t}})t^2 \\
=\ & (GM^{\#})M(GM^{\#})^{\mathsf{t}} + 2((GM^{\#})MP^{\mathsf{t}})t + (PMP^{\mathsf{t}})t^2 \\
=\ & (\det M)(GM^{\#}G^{\mathsf{t}}) + 2(\det M)(GP^{\mathsf{t}})t + (PMP^{\mathsf{t}})t^2 \\
=\ & (\det M)\chi(M) + 2(\det M)(GP^{\mathsf{t}})t + (PMP^{\mathsf{t}})t^2.
\end{aligned}
$$

Consider the following possibilities.

(a) If $\det M = 0$, this equation becomes $(Q + tP)M(Q + tP)^{\mathsf{t}} = (PMP^{\mathsf{t}})t^2$. With $t = 0$, this shows that Q is a point on the conic, and for every point P not on the conic, the line PQ intersects $\mathscr{C}$ only at Q (corresponding to $t = 0$). On the other hand, if P lies on the conic, then every point on the line PQ also lies on the conic. It follows that the conic is a union of two lines, possibly identical. The two lines are parallel (possibly identical) if $\chi(M) = 0$. Otherwise, they intersect at a finite point Q.

(b) If $\det M \neq 0$ and $\chi(M) = 0$, then Q is an infinite point on the conic $\mathscr{C}$, and for every finite point P, there is at most one nonzero t for which $tQ + P$ lies on the conic. This shows that $\mathscr{C}$ is a parabola whose axis has infinite point Q.

(c) Suppose $\det M \neq 0$ and $\chi(M) \neq 0$. In this case, $Q = GM^{\#}$ is a finite point. For every infinite point P (satisfying $PG^{\mathsf{t}} = 0$), we have

$$(Q + tP)M(Q + tP)^{\mathsf{t}} = (\det M)\chi(M) + (PMP^{\mathsf{t}})t^2. \tag{1}$$

There are at most two infinite point P satisfying $PMP^{\mathsf{t}} = 0$ (which are the infinite points of the asymptote when $\mathscr{C}$ is a hyperbola). Apart from these infinite points, if the line through Q with infinite point P intersects $\mathscr{C}$ at two real points, these intersections are symmetric with respect to Q. This shows that Q is the center of the conic. $\qquad\square$

---

[1]The symbol G also denotes the centroid of triangle ABC, which has homogeneous barycentric coordinates $(1 : 1 : 1)$.

The equation of the conic $\mathscr{C}$ can be rewritten in the form

$$\theta yz + \varphi zx + \psi xy + (x + y + z)(\alpha x + \beta y + \gamma z) = 0, \tag{2}$$

where

$$\theta = 2\lambda - (\beta + \gamma), \quad \varphi = 2\mu - (\gamma + \alpha), \quad \psi = 2\nu - (\alpha + \beta). \tag{3}$$

Proposition 3. *Suppose* $(\det M)\chi(M) \neq 0$ *and* $\theta\varphi\psi \neq 0$. *The conic* $\mathscr{C}$ *is homothetic to the circumconic*

$$\mathscr{C}_0 : \qquad\qquad\qquad \theta yz + \varphi zx + \psi xy = 0.$$

The ratio of homothety is the square root of $\frac{4 \det M}{\theta\varphi\psi}$.

Proof. By Proposition 2(c), the center of the conic $\mathscr{C}$ is the point $Q = GM^{\#}$. The circumconic $\mathscr{C}_0$ (with θ, φ, ψ given by (3)) has matrix

$$M_0 = \frac{1}{2} \begin{pmatrix} 0 & \psi & \varphi \\ \psi & 0 & \theta \\ \varphi & \theta & 0 \end{pmatrix}. \tag{4}$$

Its center is the point

$$Q_0 = (\theta(\varphi + \psi - \theta) : \varphi(\psi + \theta - \varphi) : \psi(\theta + \varphi - \psi)). \tag{5}$$

For the matrix M_0 in (4), we have
(i) $\det(M_0) = \frac{\theta\varphi\psi}{4}$,
(ii) $\chi(M_0) = \frac{1}{4}(2\varphi\psi + 2\psi\theta + 2\theta\varphi - \theta^2 - \varphi^2 - \psi^2) = \chi(M)$ by substitutions using (3).

Note that

$$M = M_0 + \frac{1}{2} \begin{pmatrix} \alpha & \beta & \gamma \\ \alpha & \beta & \gamma \\ \alpha & \beta & \gamma \end{pmatrix} + \frac{1}{2} \begin{pmatrix} \alpha & \alpha & \alpha \\ \beta & \beta & \beta \\ \gamma & \gamma & \gamma \end{pmatrix} = M_0 + \frac{1}{2}(G^{\mathsf{t}}L + L^{\mathsf{t}}G),$$

where $L = \begin{pmatrix} \alpha & \beta & \gamma \end{pmatrix}$.

Let $P = (u : v : w)$ be an infinite point. By (1), the point $Q + tP$ lies on the conic $\mathscr{C}$ if and only if

$$(PMP^{\mathsf{t}})t^2 + (\det M)\chi(M) = 0. \tag{6}$$

Now,

$$\begin{aligned}
PMP^{\mathsf{t}} &= P\left(M_0 + \frac{1}{2}\left(G^{\mathsf{t}}L + L^{\mathsf{t}}G\right)\right)P^{\mathsf{t}} \\
&= PM_0P^{\mathsf{t}} + \frac{1}{2}(PG^{\mathsf{t}})(LP^{\mathsf{t}}) + \frac{1}{2}(PL^{\mathsf{t}})(PG^{\mathsf{t}})^{\mathsf{t}} \\
&= PM_0P^{\mathsf{t}}.
\end{aligned}$$

Applying equation (6) to the circumconic $\mathscr{C}_0$, by replacing M by M_0, we conclude that the intersection of $\mathscr{C}_0$ with the line through Q_0 with the same infinite
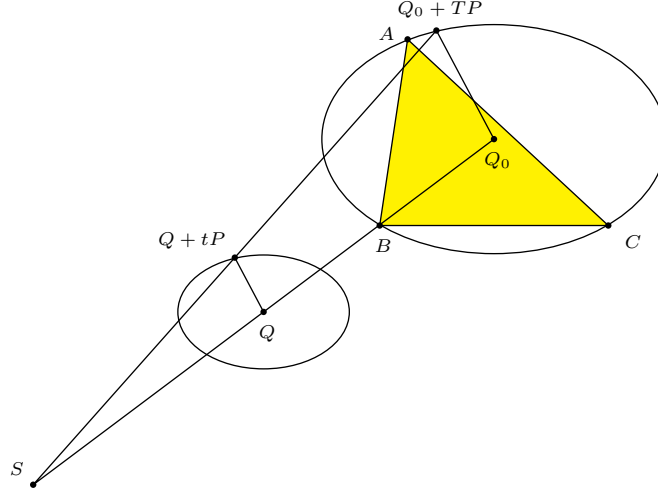
Figure 2.

point P is $Q_0 + TP$ with T given by

$$(PM_0P^t)T^2 + (\det M_0)\chi(M_0) = 0,$$

$$(PMP^t)T^2 + \frac{\theta\varphi\psi\chi(M)}{4} = 0. \tag{7}$$

Comparing equations (6) and (7), we conclude that parallel lines (with infinite point P) through Q and Q_0 intersect the conics $\mathscr{C}$ and $\mathscr{C}_0$ respectively at points $Q + tP$ and $Q_0 + TP$ with

$$\frac{t^2}{T^2} = \frac{4\det M}{\theta\varphi\psi},$$

which is independent of the infinite point P (for which $PMP^t \neq 0$). Furthermore, the line joining $Q_0 + TP$ to $Q + tP$ intersects the line $Q_0 Q$ at a fixed point S such that $\frac{SQ}{SQ_0} = \frac{t}{T}$ (see Figure 2). This shows that the two conics are homothetic at S, with ratio of homothety equal to $\frac{t}{T}$, the square root of $\frac{4\det M}{\theta\varphi\psi}$. □

Remark. The conic $\mathscr{C}$ contains an infinite point if and only if $\chi(M) \leq 0$. [2]

3. The conic $\mathscr{D}(\mathscr{L}, G)$ associated with the centroid

We shall study the special case when $P_1 = P_2 = P_3 = G$, the centroid of triangle ABC. Here,

$$\begin{aligned}
L_a &= (q+r)x - qy - rz, \\
L_b &= -px + (r+p)y - rz, \\
L_c &= -px - qy + (p+q)z,
\end{aligned}$$

---

[2]Proof: Putting $x = -(y+z)$ into the equation of $\mathscr{C}$, we obtain a quadratic in y and z with discriminant $-4\chi(M)$.

and

$$L(P_1) = L(P_2) = L(P_3) = p + q + r.$$

It follows that

$$L_a L_b L_c - (p + q + r)^3 xyz = (px + qy + rz)Q(x, y, z)$$

where

$$Q(x, y, z) = p(q + r)x^2 + q(r + p)y^2 + r(p + q)z^2 - (p(p + q + r) + 2qr)yz$$
$$- (q(p + q + r) + 2rp)zx - (r(p + q + r) + 2pq)xy. \tag{8}$$

The conic $\mathcal{Q}(\mathcal{L}, G)$ in question is defined by the equation $Q(x, y, z) = 0$. The matrix of the conic is

$$M(\mathcal{L}) = \frac{1}{2} \begin{pmatrix} 2p(q + r) & -r(p + q + r) - 2pq & -q(p + q + r) - 2rp \\ -r(p + q + r) - 2pq & 2q(r + p) & -p(p + q + r) - 2qr \\ -q(p + q + r) - 2rp & -p(p + q + r) - 2qr & 2r(p + q) \end{pmatrix}. \tag{9}$$

We shall investigate the possibilities that $\mathcal{Q}(\mathcal{L}, G)$ be (i) degenerate, (ii) a parabola, (iii) a rectangular hyperbola, (iv) a circle.

Lemma 4. *Let $\mathcal{L}$ be the line $px + qy + rz = 0$. The matrix $M(\mathcal{L})$ has*
(a) *determinant* $\det M(\mathcal{L}) = -\frac{1}{4}(p + q + r)^4 (qr + rp + pq)$,
(b) *adjoint matrix*

$$M(\mathcal{L})^\# = \frac{(p + q + r)^2}{4} \begin{pmatrix} -p^2 & 2qr + 2rp + pq & 2qr + rp + 2pq \\ 2qr + 2rp + pq & -q^2 & qr + 2rp + 2pq \\ 2qr + rp + 2pq & qr + 2rp + 2pq & -r^2 \end{pmatrix}, \tag{10}$$

and
(c) *characteristic* $\chi(M(\mathcal{L})) = \frac{(p+q+r)^2}{4}(-p^2 - q^2 - r^2 + 10qr + 10rp + 10pq)$.

4. Degenerate $\mathcal{Q}(\mathcal{L}, G)$

From Proposition 2(a), the conic $\mathcal{Q}(\mathcal{L}, G)$ is degenerate when
(i) $p + q + r = 0$, or
(ii) $pq + qr + rp = 0$.

(i) corresponds to the trivial case when the line $\mathcal{L} : px + qy + rz = 0$ contains the centroid $G = (1 : 1 : 1)$. The conic $\mathcal{Q}(\mathcal{L}, G)$ is simply the line $\mathcal{L}$ counted twice.

In (ii), $(p : q : r)$ being a point on the Steiner circum-ellipse $xy + yz + zx = 0$, the line $px + qy + rz = 0$ is tangent to the dual conic, which is the Steiner in-ellipse. This means that *if $\mathcal{L}$ is tangent to the Steiner in-ellipse, then the conic $\mathcal{Q}(\mathcal{L}, G)$ degenerates into two lines.* Actually, these two lines complete with $\mathcal{L}$ a poristic triangle between the two ellipses (see Figure 3).

We shall henceforth assume $p + q + r \neq 0$ and $qr + rp + pq \neq 0$.

Figure 3.

5. The lines $\mathscr{L}$ for which $\mathscr{Q}(\mathscr{L}, G)$ are parabolas
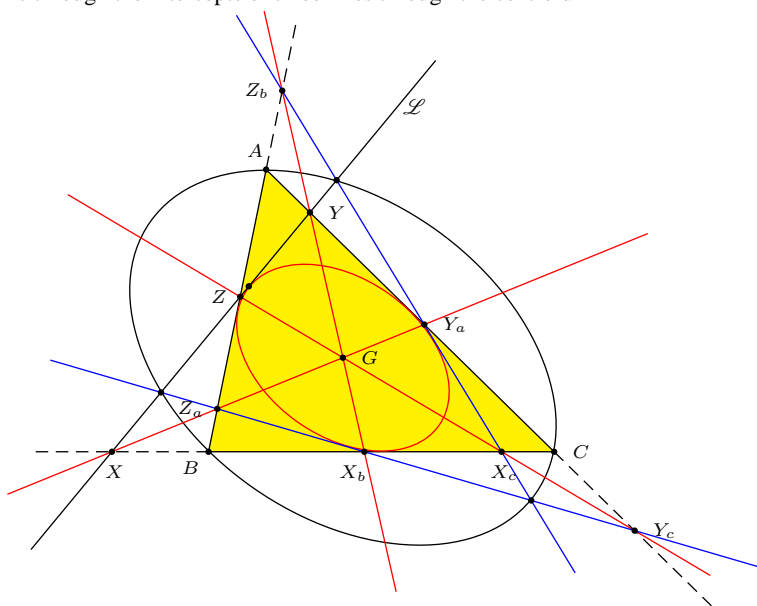
By Proposition 2(b) and Lemma 4(b), we conclude easily that $\mathscr{Q}(\mathscr{L}, G)$ is a parabola if and only if $(p : q : r)$ is a point on the ellipse

$$\mathscr{E}_0 : \qquad\qquad -x^2 - y^2 - z^2 + 10yz + 10zx + 10xy = 0$$

with center G. Equivalently, the line $\mathscr{L}$ is tangent to the conic dual to $\mathscr{E}_0$. This is the ellipse

$$\mathscr{E}_0^* : \qquad\qquad -2x^2 - 2y^2 - 2z^2 + 5yz + 5zx + 5xy = 0,$$

also with center G, and containing the trisection points of the sides of the triangle.

Theorem 5 (Dergiades). *The conic $\mathscr{Q}(\mathscr{L}, G)$ is a parabola if and only if the line $\mathscr{L}$ is tangent to the ellipse $\mathscr{E}_0^*$.*

Proposition 6. *If $\mathscr{L} : \ px + qy + rz = 0$ is the tangent to $\mathscr{E}_0^*$ at P, then the parabola $\mathscr{Q}(\mathscr{L}, G)$ and the ellipse $\mathscr{E}_0^*$ have*
(i) a common tangent parallel to $\mathscr{L}$ at the antipode of P on $\mathscr{E}_0^*$, and
(ii) two remaining common points on the parallel to $\mathscr{L}$ through the centroid G.

Proof. We take the matrices of the dual ellipses $\mathscr{E}_0$ and $\mathscr{E}_0^*$ to be

$$M = \begin{pmatrix} -1 & 5 & 5 \\ 5 & -1 & 5 \\ 5 & 5 & -1 \end{pmatrix} \quad \text{and} \quad M^* = \begin{pmatrix} -4 & 5 & 5 \\ 5 & -4 & 5 \\ 5 & 5 & -4 \end{pmatrix}$$

respectively. The line $\mathscr{L} : \ px + qy + rz = 0$ is tangent to the ellipse $\mathscr{E}_0^*$ at the point

$$P = \begin{pmatrix} p & q & r \end{pmatrix} M = \begin{pmatrix} -p + 5q + 5r & 5p - q + 5r & 5p + 5q - r \end{pmatrix}.$$
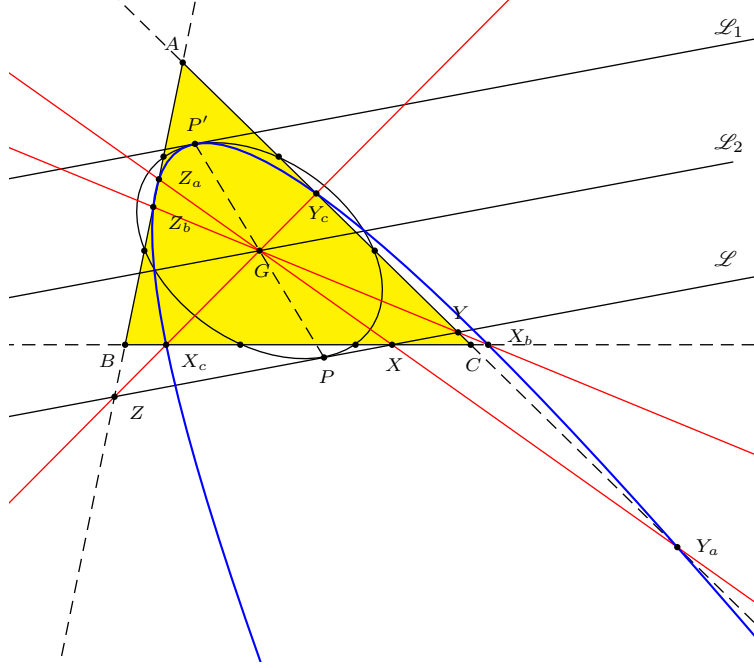
Figure 4

With the matrix $M(\mathscr{L})$ given in (9), and $t = \frac{1}{18}(p + q + r)^2$, it is routine to verify that

$$\begin{pmatrix} x & y & z \end{pmatrix} (M(\mathscr{L}) + tM^*) \begin{pmatrix} x \\ y \\ z \end{pmatrix} = -\frac{1}{9}L_1(x, y, z)L_2(x, y, z),$$

where

$$L_1(x, y, z) = (-p + 2q + 2r)x + (2p - q + 2r)y + (2p + 2q - r)z,$$
$$L_2(x, y, z) = (-2p + q + r)x + (p - 2q + r)y + (p + q - 2r)z.$$

Note that the lines $\mathscr{L}_1 : L_1(x, y, z) = 0$ and $\mathscr{L}_2 : L_2(x, y, z) = 0$ are both parallel to $\mathscr{L}$ (with infinite point $(q - r : r - p : p - q)$). Since the point $(-p + 2q + 2r : 2p - q + 2r : 2p + 2q - r)$ lies on both conics dual to the ellipse $\mathscr{E}_0^*$ and the parabola $\mathscr{Q}(\mathscr{L}, G)$, the line $\mathscr{L}_1$ is a common tangent of the two conics. The point of tangency is

$$\begin{pmatrix} -p + 2q + 2r & 2p - q + 2r & 2p + 2q - r \end{pmatrix} M$$
$$= 3 \begin{pmatrix} 7p + q + r & p + 7q + r & p + q + 7r \end{pmatrix}.$$

This is the antipode of P on the ellipse $\mathscr{E}_0^*$.

The other line $\mathscr{L}_2$ clearly contains the centroid G, and therefore a pair of antipodal points on the ellipse $\mathscr{E}_0^*$. These two points also lies on the parabola $\mathscr{Q}(\mathscr{L}, G)$.

$\square$

6. The lines $\mathscr{L}$ for which $\mathscr{Q}(\mathscr{L}, G)$ are rectangular hyperbolas

Apart from the cases of pairs of lines and parabolas, the type of the conic $\mathscr{Q}(\mathscr{L}, G)$ can be easily determined by an application of Proposition 2(c) and Proposition 3.

Proposition 7. *If $p + q + r \neq 0$ and $qr + rp + pq \neq 0$, the conic $\mathscr{Q}(\mathscr{L}, G)$ has center*

$$Q = (-p^2 + 3p(q + r) + 4qr : -q^2 + 3q(r + p) + 4rp : -r^2 + 3r(p + q) + 4pq).$$

It is homothetic to the circumconic

$$(p + 2q)(p + 2r)yz + (q + 2r)(q + 2p)zx + (r + 2p)(r + 2q)xy = 0, \quad (11)$$

with ratio of homothety τ given by

$$\tau^2 = \frac{(p + q + r)^4(pq + qr + rp)}{(p + 2q)(p + 2r)(q + 2r)(q + 2p)(r + 2p)(r + 2q)}, \quad (12)$$

provided $(p + 2q)(p + 2r)(q + 2r)(q + 2p)(r + 2p)(r + 2q) \neq 0$.

Since the conic $\mathscr{Q}(\mathscr{L}, G)$ is homothetic to the circumconic defined by (11), it is a rectangular hyperbola if and only if this circumconic contains the orthocenter $H = \left(\frac{1}{S_A} : \frac{1}{S_B} : \frac{1}{S_C}\right)$, i.e.,

$$S_A(p + 2q)(p + 2r) + S_B(q + 2r)(q + 2p) + S_C(r + 2p)(r + 2q) = 0.$$

Equivalently, the line $\mathscr{L} : px + qy + rz = 0$ is tangent to the conic dual to

$$\mathscr{E}_1 : \quad S_A(x + 2y)(x + 2z) + S_B(y + 2z)(y + 2x) + S_C(z + 2x)(z + 2y) = 0.$$
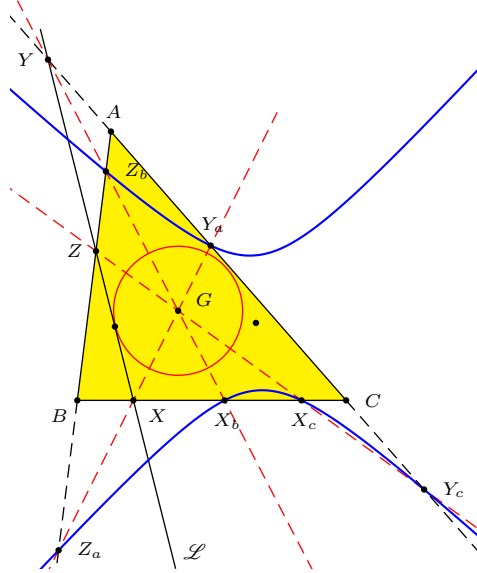
Figure 5

Proposition 8. *The conic $\mathscr{E}_1$ is an ellipse with center G. Its dual conic is a circle also with center G.*

Proof. The matrix of the conic $\mathscr{E}_1$ being

$$M_1 = \begin{pmatrix} S_A & S_A + S_B + 2S_C & S_A + 2S_B + S_C \\ S_A + S_B + 2S_C & S_B & 2S_A + S_B + S_C \\ S_A + 2S_B + S_C & 2S_A + S_B + S_C & S_C \end{pmatrix},$$

with

$$\det M_1 = 9(S_A + S_B + S_C)(S_{BC} + S_{CA} + S_{AB}) = \frac{9}{2}(a^2 + b^2 + c^2)S^2 \neq 0,$$

the conic is nondegenerate. The adjoint matrix is

$$M_1^{\#} = \begin{pmatrix} m_{aa} & m_{ab} & m_{ac} \\ m_{ab} & m_{bb} & m_{bc} \\ m_{ac} & m_{bc} & m_{cc} \end{pmatrix}$$

where

$$\begin{aligned} m_{aa} &= -4S_A(S_A + S_B + S_C) - (S_{BB} + S_{BC} + S_{CC}), \\ m_{ab} &= -S_{CC} + 2S_{BC} + 2S_{AC} + 2S_{AA} + 5S_{AB} + 2S_{BB}, \\ m_{ac} &= -S_{BB} + 2S_{AB} + 2S_{BC} + 2S_{CC} + 5S_{AC} + 2S_{AA}, \\ m_{bc} &= -S_{AA} + 2S_{AB} + 2S_{AC} + 2S_{BB} + 5S_{BC} + 2S_{CC}, \end{aligned}$$

and m_{bb}, m_{cc} are analogously defined. It is easy to check that

$$m_{aa} + m_{ab} + m_{ac} = m_{ab} + m_{bb} + m_{bc} = m_{ac} + m_{bc} + m_{cc}$$
$$= 3(S_{BC} + S_{CA} + S_{AB}) = 3S^2.$$

From this we conclude that the conic $\mathscr{E}_1$ has center G. Also, $\chi(M_1) = 9S^2 > 0$. It follows that $\mathscr{E}_1$ is an ellipse. [3]

The equation of the dual conic can be written in the form

$$\begin{aligned} &9(S_A + S_B + S_C)((S_B + S_C)yz + (S_C + S_A)zx + (S_A + S_B)xy) \\ &+ (x + y + z)(m_{aa}x + m_{bb}y + m_{cc}z) \\ &= 0. \end{aligned}$$

From this it is clear that this dual conic is a circle. The center has coordinates given by $G(M_1^{\#})^{\#}$, which we may simply take as $GM_1 = 3(S_A + S_B + S_C)G$. This is the centroid G. $\square$

We denote this circle by $\mathscr{C}_G$.

Theorem 9. *The conic $\mathscr{Q}(\mathscr{L}, G)$ is a rectangular hyperbola if and only if the line $\mathscr{L}$ is tangent to the circle $\mathscr{C}_G$.*

---

[3]See Remark at the end of §2.

6.1. *Construction of the centroidal circle* $\mathscr{C}_G$. Since

$$\det M_1 = 9(S_A + S_B + S_C)(S_{BC} + S_{CA} + S_{AB}) = 9S^2(S_A + S_B + S_C),$$

we have

$$\det M_1^{\#} = (\det M_1)^2 = 81S^4(S_A + S_B + S_C)^2. \tag{13}$$

Making use of Proposition 3 and (13), we determine the ratio of homothety of $\mathscr{C}_G$ and the circumcircle as the square root of

$$\frac{4\det M_1^{\#}}{(9(S_A + S_B + S_C))^3(S_B + S_C)(S_C + S_A)(S_A + S_B)} = \frac{8S^4}{9a^2b^2c^2(a^2 + b^2 + c^2)}.$$

This means that the square of the radius of the circle $\mathscr{C}_G$ is

$$\frac{8S^4}{9a^2b^2c^2(a^2 + b^2 + c^2)} \cdot \frac{a^2b^2c^2}{4S^2} = \frac{2S^2}{9(a^2 + b^2 + c^2)} = \frac{S}{3a} \cdot \left(\frac{2}{3} \cdot \frac{a^2}{a^2 + b^2 + c^2} \cdot \frac{S}{a} \right).$$

In the last expression, the first factor is the height of the centroid G above the line BC. The second factor is $\frac{2}{3}$ of the height of the symmedian point K above the same line. This leads to the following construction of the circle.

Figure 6

Construction 10. *Given triangle ABC with centroid G and symmedian point K, construct*
(1) the pedals X and Y of G and K on the line BC,
(2) a point X' on the extension of XG such that $GX' = \frac{2}{3}YK$,
(3) the circle with diameter XX',
(4) the perpendicular through G to the line XX' to intersect the circle in (3) at Z and Z'.
The circle with center G and diameter ZZ' is the circle $\mathscr{C}_G$.

7. The lines $\mathscr{L}$ for which $\mathscr{Q}(\mathscr{L}, G)$ are circles

The conic $\mathscr{Q}(\mathscr{L}, G)$ is a circle if and only if

$$(p + 2q)(p + 2r) \ : \ (q + 2r)(q + 2p) \ : \ (r + 2p)(r + 2q) \ = \ a^2 : b^2 : c^2. \quad (14)$$

We may regard $(p : q : r)$ as a common point of conics defined by

$$\frac{(x + 2y)(x + 2z)}{a^2} = \frac{(y + 2z)(y + 2x)}{b^2} = \frac{(z + 2x)(z + 2y)}{c^2},$$

or equivalently,

$$\frac{(x + y + z)^2 - (y - z)^2}{a^2} = \frac{(x + y + z)^2 - (z - x)^2}{b^2} = \frac{(x + y + z)^2 - (x - y)^2}{c^2}.$$

The equation of the second and third expression can be rewritten as

$$(b^2 - c^2)(x + y + z)^2 = b^2(x - y)^2 - c^2(z - x)^2; \quad (15)$$

similarly for the other two equations. Thus, $(p : q : r)$ is a common point of the conics

$$F_a := \ c^2 y^2 - b^2 z^2 - 2(b^2 - c^2)yz - 2(b^2 - 2c^2)zx - 2(2b^2 - c^2)xy = 0,$$
$$F_b := \ a^2 z^2 - c^2 x^2 - 2(c^2 - a^2)zx - 2(c^2 - 2a^2)xy - 2(2c^2 - a^2)yz = 0,$$
$$F_c := \ b^2 x^2 - a^2 y^2 - 2(a^2 - b^2)xy - 2(a^2 - 2b^2)yz - 2(2a^2 - b^2)zx = 0.$$

We easily determine, by Proposition 2(c), that these conics all have center G. Since

$$\begin{aligned} F_a + F_b + F_c = \ & 3((b^2 - c^2)yz + (c^2 - a^2)zx + (a^2 - b^2)xy) \\ & + (x + y + z)((b^2 - c^2)x + (c^2 - a^2)y + (a^2 - b^2)z) = 0 \end{aligned}$$

is degenerate, this represents the two asymptotes of a hyperbola with center G, homothetic to the Kiepert hyperbola. These asymptotes, as is well known, are parallel to the axes of the Steiner circum-ellipse. We therefore conclude that the common points of the conics $F_a = F_b = F_c = 0$ are on an axis of the Steiner ellipse, which turns out to be the minor axis. Each of these two points leads to a conic $\mathscr{Q}(\mathscr{L}, G)$ which is a circle.

We shall make use of the following notations:

$$\mathsf{P} := \ a^2 + b^2 + c^2;$$
$$\mathsf{P}_a := \ b^2 + c^2 - 2a^2, \quad \mathsf{P}_b := c^2 + a^2 - 2b^2, \quad \mathsf{P}_c := a^2 + b^2 - 2c^2;$$
$$\mathsf{Q} := \ a^4 + b^4 + c^4 - b^2 c^2 - c^2 a^2 - a^2 b^2.$$

Lemma 11. *The infinite points of the Kiepert hyperbola are*

$$((b^2 - c^2)(\mathsf{P}_a + \varepsilon\sqrt{\mathsf{Q})} \ : \ (c^2 - a^2)(\mathsf{P}_b + \varepsilon\sqrt{\mathsf{Q})} \ : \ (a^2 - b^2)(\mathsf{P}_c + \varepsilon\sqrt{\mathsf{Q})})$$

for $\varepsilon = \pm 1$.

The point for $\varepsilon = -1$ is the infinite point of the minor axis of the Steiner ellipse. It is the point X_{3414} of [2]. The infinite point corresponding to $\varepsilon = +1$ is X_{3413}.
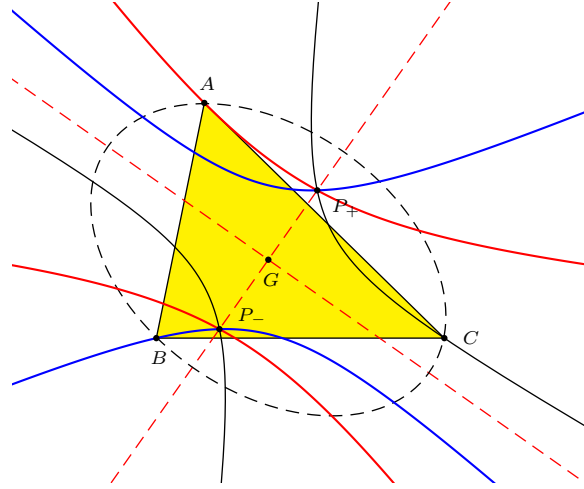
Figure 7

Proposition 12. *The two real common points of the conics $F_a = 0$, $F_b = 0$, $F_c = 0$ are*

$$P_\varepsilon = (\varepsilon t + (b^2 - c^2)(\mathsf{P}_a - \sqrt{\mathsf{Q}}) : \cdots : \cdots) \qquad (16)$$

for $\varepsilon = \pm 1$, where t is the square root of

$$\frac{1}{9}(\mathsf{P} + 2\sqrt{\mathsf{Q}})(\mathsf{P}_a - \sqrt{\mathsf{Q}})(\mathsf{P}_b - \sqrt{\mathsf{Q}})(\mathsf{P}_c - \sqrt{\mathsf{Q}}). \qquad (17)$$

Proof. A point on the minor axis of the Steiner ellipse is of the form (16) for some t. Substituting into the equation $F_a = 0$, or equivalently (15), and solving, we obtain

$$t^2 = \frac{1}{9}(\lambda + \mu\sqrt{\mathsf{Q}}),$$

where

$$\lambda = 4\mathsf{Q}^2 + \mathsf{P}\mathsf{P}_a\mathsf{P}_b\mathsf{P}_c, \qquad (18)$$
$$\mu = 2(\mathsf{P}_a\mathsf{P}_b\mathsf{P}_c + \mathsf{P}\mathsf{Q}). \qquad (19)$$

Since $\mathsf{P}_a + \mathsf{P}_b + \mathsf{P}_c = 0$ and $\mathsf{P}_a\mathsf{P}_b + \mathsf{P}_b\mathsf{P}_c + \mathsf{P}_c\mathsf{P}_a = -3\mathsf{Q}$, we have

$$\begin{aligned}
\lambda + \mu\sqrt{\mathsf{Q}} &= 2\mathsf{Q}\sqrt{\mathsf{Q}}(\mathsf{P} + 2\sqrt{\mathsf{Q}}) + \mathsf{P}_a\mathsf{P}_b\mathsf{P}_c(\mathsf{P} + 2\sqrt{\mathsf{Q}}) \\
&= (\mathsf{P} + 2\sqrt{\mathsf{Q}})(2\mathsf{Q}\sqrt{\mathsf{Q}} + \mathsf{P}_a\mathsf{P}_b\mathsf{P}_c) \\
&= (\mathsf{P} + 2\sqrt{\mathsf{Q}})(-\sqrt{\mathsf{Q}}^3 + (\mathsf{P}_a + \mathsf{P}_b + \mathsf{P}_c)\mathsf{Q} \\
&\qquad - (\mathsf{P}_a\mathsf{P}_b + \mathsf{P}_b\mathsf{P}_c + \mathsf{P}_c\mathsf{P}_a)\sqrt{\mathsf{Q}} + \mathsf{P}_a\mathsf{P}_b\mathsf{P}_c) \\
&= (\mathsf{P} + 2\sqrt{\mathsf{Q}})(\mathsf{P}_a - \sqrt{\mathsf{Q}})(\mathsf{P}_b - \sqrt{\mathsf{Q}})(\mathsf{P}_c - \sqrt{\mathsf{Q}})
\end{aligned}$$

leading to the factorization of t^2 given in (17) above. $\qquad\square$

Figure 8.

The points P_ε, $\varepsilon = \pm 1$, correspond to two lines $\mathscr{L}_\varepsilon$ which are common tangents to the conics dual to $F_a = 0$, $F_b = 0$, and $F_c = 0$ (see Figure 8). For t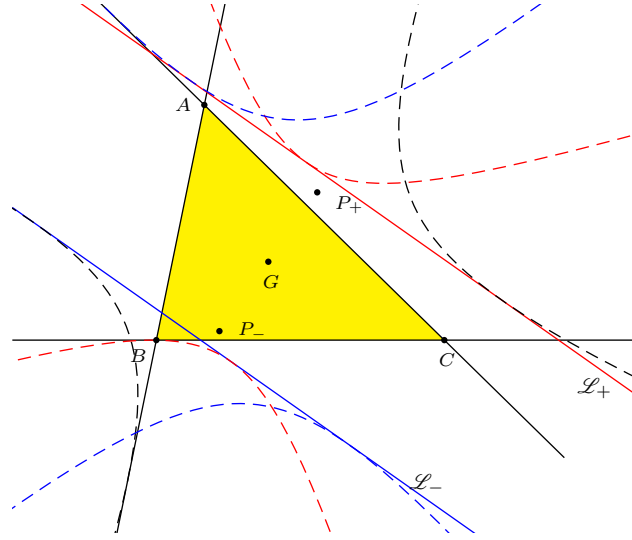hese two lines, the conics $\mathscr{Q}(\mathscr{L}_\varepsilon, G)$ are circles, which we simply denote by $\mathscr{C}_\varepsilon$ (see Figure 9).
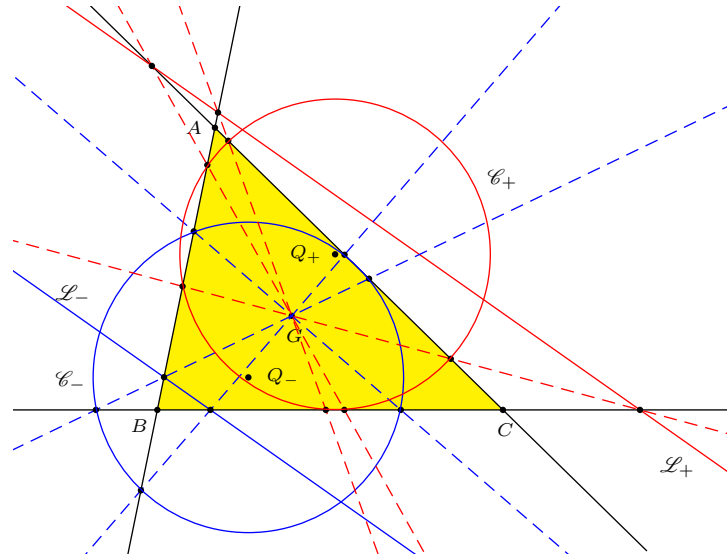
Figure 9.

Proposition 13. *The two circles $\mathscr{C}_\varepsilon$, $\varepsilon = \pm 1$, have centers*

$$Q_\varepsilon = \left(\frac{f + g\sqrt{Q}}{\varepsilon \cdot 3t} + (b^2 - c^2)(P_a - \sqrt{Q}) : \cdots : \cdots \right), \tag{20}$$

where

$$f = 4Q^2 - PP_aP_bP_c = 8Q^2 - \lambda, \tag{21}$$
$$g = 2(P_aP_bP_c - PQ) = 4P_aP_bP_c - \mu. \tag{22}$$

They are congruent and have radius

$$\rho = \frac{P + 2\sqrt{Q}}{18S} \cdot \sqrt{P - \sqrt{Q}}.$$

Proof. With (p, q, r) given by (14), and λ, μ by (18), (19), we have

$$(p + 2q)(p + 2r) = a^2W, \quad (q + 2r)(q + 2p) = b^2W, \quad (r + 2p)(r + 2q) = c^2W$$

for

$$\begin{aligned}
W &= \frac{(p - q)^2 - (r - p)^2}{b^2 - c^2} = 3(P_a - \sqrt{Q})(P_a^2 - P_a\sqrt{Q} - 2Q) \\
&= 3(P_a - \sqrt{Q})^2(P_a + 2\sqrt{Q}) \\
&= 3(P_b - \sqrt{Q})^2(P_b + 2\sqrt{Q}) \\
&= 3(P_c - \sqrt{Q})^2(P_c + 2\sqrt{Q}).
\end{aligned}$$

Note that

$$\begin{aligned}
p + q + r &= \varepsilon \cdot 3t, \\
pq + qr + rp &= 3t^2 - 2Q^2 - P_aP_bP_c\sqrt{Q} \\
&= \frac{1}{3}\left(\lambda + \mu\sqrt{Q} - 6Q^2 - 3P_aP_bP_c\sqrt{Q} \right) \\
&= \frac{1}{3}\left(2PQ\sqrt{Q} - 2Q^2 + PP_aP_bP_c - P_aP_bP_c\sqrt{Q} \right) \\
&= \frac{1}{3}\left(2Q\sqrt{Q}(P - \sqrt{Q}) + P_aP_bP_c(P - \sqrt{Q}) \right) \\
&= \frac{1}{3}(P - \sqrt{Q})\left(8Q\sqrt{Q} + 4(P_a + P_b + P_c)Q \right. \\
&\qquad\qquad \left. + 2(P_aP_b + P_bP_c + P_cP_a)\sqrt{Q} + P_aP_bP_c \right) \\
&= \frac{1}{3}(P - \sqrt{Q})(P_a + 2\sqrt{Q})(P_b + 2\sqrt{Q})(P_c + 2\sqrt{Q}).
\end{aligned}$$

From these,

$$
\begin{aligned}
&-p^2 + 3p(q+r) + 4qr \\
&= 4(pq + qr + rp) - p(p+q+r) \\
&= 4(3t^2 - 2\mathsf{Q}^2 - \mathsf{P}_a\mathsf{P}_b\mathsf{P}_c\sqrt{\mathsf{Q}}) - (\varepsilon t + (b^2 - c^2)(\mathsf{P}_a - \sqrt{\mathsf{Q}}))\varepsilon \cdot 3t \\
&= 9t^2 - 8\mathsf{Q}^2 - 4\mathsf{P}_a\mathsf{P}_b\mathsf{P}_c\sqrt{\mathsf{Q}} - 3\varepsilon(b^2 - c^2)(\mathsf{P}_a - \sqrt{\mathsf{Q}})t \\
&= \lambda - 8\mathsf{Q}^2 + (\mu - 4\mathsf{P}_a\mathsf{P}_b\mathsf{P}_c)\sqrt{\mathsf{Q}} - 3\varepsilon(b^2 - c^2)(\mathsf{P}_a - \sqrt{\mathsf{Q}})t \\
&= -f - g\sqrt{\mathsf{Q}} - 3\varepsilon(b^2 - c^2)(\mathsf{P}_a - \sqrt{\mathsf{Q}})t \\
&= -\varepsilon \cdot 3t\left(\frac{f + g\sqrt{\mathsf{Q}}}{\varepsilon \cdot 3t} + (b^2 - c^2)(\mathsf{P}_a - \sqrt{\mathsf{Q}}) \right),
\end{aligned}
$$

where f and g are given in (21) and (22) above. Similarly,

$$
-q^2 + 3q(r+p) + 4rp = -\varepsilon \cdot 3t\left(\frac{f + g\sqrt{\mathsf{Q}}}{\varepsilon \cdot 3t} + (c^2 - a^2)(\mathsf{P}_b - \sqrt{\mathsf{Q}}) \right),
$$

$$
-r^2 + 3r(p+q) + 4pq = -\varepsilon \cdot 3t\left(\frac{f + g\sqrt{\mathsf{Q}}}{\varepsilon \cdot 3t} + (a^2 - b^2)(\mathsf{P}_c - \sqrt{\mathsf{Q}}) \right).
$$

By Proposition 2(c), the center of the circle $\mathscr{C}_\varepsilon$ is the point Q_ε given by (20) above. Furthermore, the homothetic ratio of $\mathscr{C}_\varepsilon$ and the circumcircle is the square root of

$$
\frac{(p+q+r)^4(pq+qr+rp)}{(p+2q)(p+2r)(q+2r)(q+2p)(r+2p)(r+2q)} = \frac{(\mathsf{P} + 2\sqrt{\mathsf{Q}})^2(\mathsf{P} - \sqrt{\mathsf{Q}})}{3 \cdot 27a^2b^2c^2}.
$$

From these, it follows that the common radius of the circles $\mathscr{C}_\varepsilon$ is

$$
\frac{\mathsf{P} + 2\sqrt{\mathsf{Q}}}{9abc}\sqrt{\mathsf{P} - \sqrt{\mathsf{Q}}} \cdot \frac{abc}{2S} = \frac{\mathsf{P} + 2\sqrt{\mathsf{Q}}}{18S}\sqrt{\mathsf{P} - \sqrt{\mathsf{Q}}}.
$$

$\square$

References

[1] M. Bataille, On the foci of circumparabolas, *Forum Geom.*, 11 (2011) 57–63.
[2] C. Kimberling, *Encyclopedia of Triangle Centers*, available at
   `http://faculty.evansville.edu/ck6/encyclopedia/ETC.html`.
[3] P. Yiu, *Introduction to the Geometry of the Triangle*, Florida Atlantic University Lecture Notes, 2001; revised, 2013, available at `http://math.fau.edu/Yiu/Geometry.html`

   Paul Yiu: Department of Mathematical Sciences, Florida Atlantic University, 777 Glades Road, Boca Raton, Florida 33431-0991, USA
   E-mail address: `yiu@fau.edu`

The f-belos

Antonio M. Oller-Marcén

Abstract. The *arbelos* is the shape bounded by three mutually tangent semicircles with collinear diameters. Recently, Sondow introduced the parabolic analog, the *parbelos* and proved several properties of the parbelos similar to properties of the arbelos. In this paper we give one step further and generalize the situation considering the figure bounded by (quite) arbitrary similar curves, the f-*belos*. We prove analog properties to those of the arbelos and parbelos and, moreover, we characterize the parbelos and the arbelos as the f-beloses satisfying certain conditions.

1. Introduction

The *arbelos* ($\acute{\alpha}\rho\beta\eta\lambda o\varsigma$, literally "shoemaker's knife") was introduced in Proposition 4 of Archimedes' Book of Lemmas [1, p. 304]. It is the plane figure bounded by three pairwise tangent semicircles with diameters lying on the same line (see the left-hand side of Figure 1). In addition to the properties proved by Archimedes himself, there is a long list of properties satisfied by this figure. Boas's paper [3] presents some of them and is a good source for references.

It is quite surprising to discover that for 23 centuries no generalizations of this figure were introduced. Recently, Sondow [4] has extended the original construction considering latus rectum arcs of parabolas instead of semicircles (see right-hand side of Figure 1). In his paper, Sondows proves several interesting properties of his construction (named *parbelos*) that are, in some sense, counterparts of properties of the arbelos.
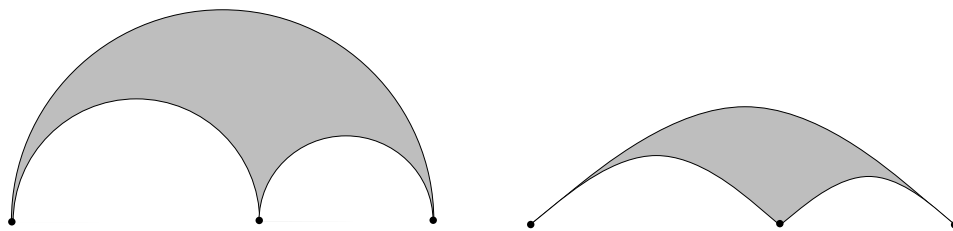

Figure 1. An arbelos (left) and a parbelos (right).

The motivation for considering latus rectum arcs of parabolas instead of semicircles is clear. Just like all circles are similar, so too all parabolas are similar. Of course this is a very special property of these curves which is not shared even by other conics. Nevertheless, it gives the clue for a further generalization of both

the arbelos and the parbelos. In a suitable generalization, the three considered arcs must be similar curves.

In Section 2 we present our construction and the resulting family of figures that we shall call *f-belos*. Subsequent sections are mainly devoted to extend and give analogs of some of the properties found in [4]. In passing we will see how arbelos and parbelos appear as particular cases of our construction imposing certain seemingly unrelated conditions.

2. The f-belos

Let $f : [0, 1] \longrightarrow \mathbb{R}$ be a function such that $f(x) > 0$ except for $f(0) = f(1) = 0$. We will assume that f is continuous in $[0, 1]$ and differentiable in $(0, 1)$. Given $p \in (0, 1)$ we define functions $g : [0, p] \longrightarrow \mathbb{R}$ and $h : [p, 1] \longrightarrow \mathbb{R}$ given by:

$$g(x) = pf(x/p),$$

$$h(x) = (1 - p)f \left(\frac{x - p}{1 - p} \right).$$

Observe that both g and h are similar to f (g is obtained by a homothety centered at the origin and h is obtained by a homothety followed by a translation). In what follows we will consider the case when the graphs of g and h are below the graph of f so that a situation like the one in Figure 2 makes sense.
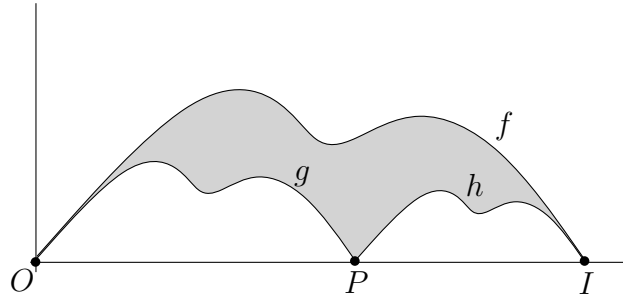
Figure 2.   The f-belos.

Given the function f we will call the figure obtained in the previous construction an f-belos. The point $P = (p, 0)$ will be called the cusp of the f-belos. We will denote $O = (0, 0)$ and $I = (1, 0)$ (see Figure 2).

Observe that if $f(x) = \sqrt{x - x^2}$ we recover the original arbelos, while if $f(x) = x - x^2$ we obtain Sondow's parbelos.

3. Elementary properties of the f-belos

In spite of the generality of the latter construction, the f-belos satisfy several interesting properties which, in some sense, extend those of the arbelos and the parbelos. These properties are analogs of Properties 1 and 2 in [4].

Proposition 1. *The upper and lower boundaries of an f-belos have the same length.*

Proof. If L_f is the length of the upper boundary, L_g is the length of the lower arc corresponding to the graph of g and L_h in the length of the lower arc corresponding to the graph of h it follows by their similarity that $L_g = pL_f$ and $L_h = (1-p)L_f$. Hence, the result. $\square$

The following lemma is easy to prove and it is closely related to Plato's analogy of the line [2].

Lemma 2. *Consider a segment $\overline{AB}$ and choose any point $C \in \overline{AB}$ except the endpoints. Now, let $D \in \overline{AC}$ and $E \in \overline{CB}$ be points such that*

$$\frac{|AC|}{|CB|} = \frac{|AD|}{|DC|} = \frac{|CE|}{|EB|}.$$

Then,

$$|DC| = |CE| = \frac{|AC| \cdot |CB|}{|AB|}.$$

As a consequence we obtain the following property.

Proposition 3. *Under each lower arc of an f-belos, construct a new f-belos similar to the original. Of the four lower arcs, the middle two are congruent, and their common length equals one half the harmonic mean of the lengths of the original lower arcs.*

Proof. It is enough to apply the previous lemma noting that the lengths of the considered arcs are proportional to the length of the horizontal segment that they determine. $\square$

4. The parallelogram associated to a point

Let $x_0 \in (0,1)$ and consider the point $P_1 = (x_0, f(x_0))$. This point lies on the graph of f and hence, by similarity, it has corresponding points P_2 and P_3 in the graphs of g and h, respectively. Namely $P_2 = (px_0, pf(x_0))$ and $P_3 = ((1-p)x_0 + p, (1-p)f(x_0))$ (see Figure 3). Observe that $\overrightarrow{P_2P_1} = \overrightarrow{PP_3} = (1-p)(x_0, f(x_0))$. Hence, $P_1P_2PP_3$ is a parallelogram. Since it depends on the choice of x_0, we will denote this parallelogram $\mathcal{P}(x_0)$.

It is interesting to study when $\mathcal{P}(x_0)$ is a rectangle. This leads to a surprising characterization of the arbelos.

Proposition 4. *Given an f-belos, the parallelogram $\mathcal{P}(x_0)$ is a rectangle if and only if $f(x_0)^2 = x_0 - x_0^2$. Consequently, $\mathcal{P}(x_0)$ is a rectangle for every $x_0 \in (0,1)$ if and only if f describes a semicircle (i.e., the figure is an arbelos).*

Proof. We have that $\overrightarrow{P_2P} = (p - px_0, -pf(x_0))$. Then, $\mathcal{P}(x_0)$ is a rectangle if and only if $\overrightarrow{P_2P_1} \perp \overrightarrow{P_2P}$; *i.e.*, if and only if

$$0 = \overrightarrow{P_2P} \cdot \overrightarrow{P_2P_1} = p(1-p)[x_0(1-x_0) - f(x_0)^2].$$

$\square$
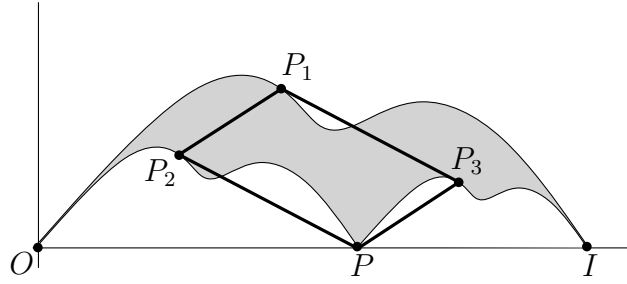
Figure 3.   The parallelogram associated to the point P_1.

The area of the parallelogram $\mathcal{P}(x_0)$ can be easy computed by:

$$\mathrm{area}(\mathcal{P}(x_0)) = ||\overrightarrow{P_2P_1} \times \overrightarrow{P_2P}|| = ||(0,0,-p(1-p)f(x_0))|| = p(1-p)f(x_0).$$

This fact leads to the following property.

Proposition 5. *Given an f-belos, let $c \in (0,1)$ be such that $f(c)$ is the mean value of f on $[0,1]$ and let $\mathcal{P}(c)$ be the parallelogram associated to c (see Figure 4) . Then:*

$$\mathrm{area}(f\text{-}belos) = 2\mathrm{area}(\mathcal{P}(c)).$$
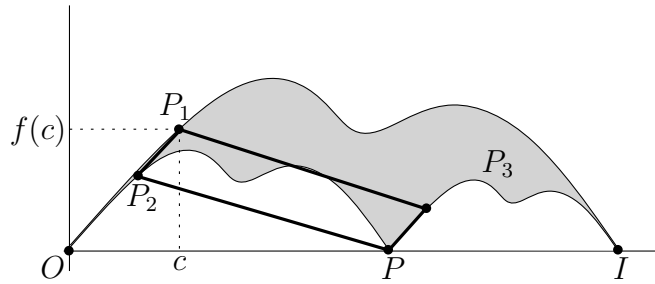
Figure 4.   The parallelogram associated to the point $(c, f(c))$.

Proof. Let us denote by A the area below the upper arc of the f-belos; *i.e.*,

$$A = \int_0^1 f(x) \, dx.$$

By similarity, the area below the lower arc corresponding to the graph of g is p^2A, while the area below the lower arc corresponding to the arc of h is $(1-p)^2A$. Hence the area of the f-belos is:

$$A - p^2A - (1-p)^2A = 2p(1-p)A.$$

Moreover, the mean value theorem for integration states that there exists $c \in (0,1)$ such that $A = \int_0^1 f(x) \, dx = f(c)$. Consequently, the area of the f-belos is

$$2p(1-p)f(c),$$

where $f(c)$ is the mean value of f on $[0, 1]$.

Since, by the above consideration, area$(\mathcal{P}(c)) = p(1-p)f(c)$, the result follows. □

We will see how this property in fact generalizes Property 3 in [4].

Remark. Consider a parbelos; *i.e.*, an f-belos with $f(x) = x - x^2$. In this context Property 3 in [4] states that

$$\text{area(parbelos)} = \frac{4}{3}\text{area}(\mathcal{P}(1/2)).$$

Let us see how this follows from Property 4 above.

The mean value of f in $(0, 1)$ is $1/6$. Consequently, area$(\mathcal{P}(c)) = \dfrac{p(1-p)}{6}$.

On the other hand, while $f(1/2) = 1/4$, we have that area$(\mathcal{P}(1/2)) = \dfrac{p(1-p)}{4}$.

Hence:

$$\text{area(parbelos)} = 2\text{area}(\mathcal{P}(c)) = \frac{4}{3}\text{area}(\mathcal{P}(1/2))$$

as claimed.

5. The tangent parallelogram

Throughout this section we will consider an f-belos such that f is also differentiable in $x = 0$ and $x = 1$. Hence, we consider the tangents to f in $x = 0$ and in $x = 1$ and the tangents in $x = p$ to g and h and a situation like Figure 5 makes sense.
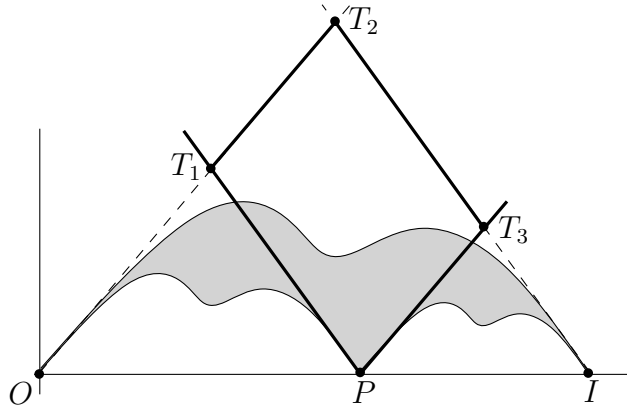

Figure 5.   The tangent parallelogram of an f-belos.

The fact that $T_1T_2T_3P$ is a parallelogram (that we will denote by $\mathcal{T}$) follows readily from the similarity of f, g and h (observe that $g'(p) = h'(0)$ and that $g'(1) = f'(1)$). In the following property we compute its area.

Proposition 6. *The area of $\mathcal{T}$ is given by:*

$$\text{area}(\mathcal{T}) = p(1-p)\left|\frac{f'(0)f'(1)}{f'(0) - f'(1)}\right|.$$

Proof. Since the sides of the parallelogram are given by the equations

$$\overline{T_1T_2}:\ y = f'(0)x,$$
$$\overline{PT_3}:\ y = f'(0)(x - p),$$
$$\overline{T_1P}:\ y = f'(1)(x - p),$$
$$\overline{T_2T_3}:\ y = f'(1)(x - 1),$$

it is easy to find the coordinates of T_i for $i = 1, 2, 3$ and obtain

$$\overrightarrow{T_1T_2} = \frac{(1-p)f'(1)}{f'(1) - f'(0)}(1, f'(0)) \quad \text{and} \quad \overrightarrow{T_1P} = \frac{-pf'(0)}{f'(1) - f'(0)}(1, f'(1)).$$

With these, we have that

$$\text{area}(\mathcal{T}) = \|\overrightarrow{T_1T_2} \times \overrightarrow{T_1P}\| = \left\|\frac{p(1-p)f'(0)f'(1)}{(f'(1) - f'(0))^2}(0, 0, f'(0) - f'(1))\right\|$$

and the result follows. $\qquad\square$

In the parbelos , $\mathcal{T}$ is in fact a rectangle [4, Property 4]. The general situation is as follows.

Proposition 7. *The tangent parallelogram $\mathcal{T}$ is a rectangle if and only if $f'(0)f'(1) = -1$. In such case we have that*

$$\text{area}(\mathcal{T}) = p(1-p)\frac{f'(0)}{1 + f'(0)^2}.$$

Proof. The first part is straightforward recalling that two lines of slopes m_1 and m_2 are perpendicular if and only if $m_1m_2 = -1$. For the second statement it is enough to put $f'(1) = -1/f'(0)$ in the previous property. $\qquad\square$

Since we have that $2f'(0) \leq 1 + f'(0)^2$, the following property follows (recall the notation from the previous section).

Proposition 8. *Given an f-belos, let $f(c)$ be the mean value of f on $[0, 1]$. Let also $\mathcal{P}(c)$ be the parallelogram associated to c and $\mathcal{T}$ the tangent parallelogram. If $f'(0)f'(1) = -1$; i.e., if $\mathcal{T}$ is a rectangle, then:*

$$\text{area}(\mathcal{P}(c)) \geq 2f(c)\text{area}(\mathcal{T});$$

and equality holds if and only if $f'(0) = -f'(1) = 1$.

Proof. Properties 4 and 6 imply that

$$\text{area}(\mathcal{P}(c)) = f(c)p(1-p) = f(c)\frac{\text{area}(\mathcal{T})}{\frac{f'(0)}{1+f'(0)^2}} \geq 2f(c)\text{area}(\mathcal{T}).$$

And equality holds if and only if $2f'(0) = 1 + f'(0)^2$; *i.e.*, if and only if $f'(0) = 1$. $\qquad\square$

Remark. In the parbelos $f(x) = x - x^2$, so we have $f'(0) = 1 = -f'(1)$ and equality holds in Property 7. Moreover (recall the remark after Property 4), $f(c) = 1/6$. Hence:

$$\text{area}(\mathcal{T}) = \frac{\text{area}(\mathcal{P}(c))}{2f(c)} = \frac{3}{2}\text{area}(\text{parbelos}),$$

as was already proved in [4, Property 4].

Now, if $f'(0)f'(1) = -1$, $\mathcal{T}$ is a rectangle, so it makes sense to consider its circumcircle Γ. In [4, Property 6] it was proved that, in the parbelos case (*i.e.*, when $f(x) = x - x^2$) the circumcircle of the tangent rectangle passes through the focus of the upper parabola (*i.e.*, through the point $(1/2, 0)$). This property can be generalized in the following way.

Proposition 9. *Given an f-belos such that its tangent parallelogram $\mathcal{T}$ is a rectangle;* i.e., *such that $f'(0)f'(1) = -1$, the circumcircle Γ of $\mathcal{T}$ intersects the axis OX at the point $(p, 0)$ and $\left(\dfrac{1}{1 + f'(0)^2}, 0\right)$* (see Figure 6)*. Consequently:*

- Γ *is tangent to OX if and only if $p = \dfrac{1}{1 + f'(0)^2}$.*
- Γ *intersects OX at $x = 1/2$ if and only if $f'(0) = 1$.*

Proof. The center of this circle is the midpoint of $\overline{T_1T_3}$; *i.e.*,

$$C_\Gamma = \left(\frac{p + 1 + pf'(0)^2}{2(1 + f'(0)^2)}, \frac{f'(0)}{2(1 + f'(0)^2)}\right).$$

This circle clearly intersects OX at P but, of course, it will intersect the axis OX in another point (unless Γ is tangent to OX). Hence we are looking for $p \neq \alpha \in (0, 1)$ such that $(\alpha, 0) \in \Gamma$. This condition leads to:

$$\left(\frac{p + 1 + pf'(0)^2}{2(1 + f'(0))^2} - \alpha\right)^2 + \left(\frac{f'(0)}{2(1 + f'(0))^2}\right)^2 = \left(\frac{p + 1 + pf'(0)^2}{2(1 + f'(0))^2} - p\right)^2 + \left(\frac{f'(0)}{2(1 + f'(0))^2}\right)^2.$$

Consequently

$$(\alpha^2 - p^2) - (\alpha - p)\frac{p + 1 + pf'(0)^2}{2(1 + f'(0)^2)} = 0$$

and, since $p \neq \alpha$,

$$\alpha = \frac{p + 1 + pf'(0)^2}{2(1 + f'(0)^2)} - p = \frac{1}{1 + f'(0)^2}$$

as claimed. $\square$

Now, we turn again to the general case, when $\mathcal{T}$ is "only" a parallelogram. The equation of the line passing through T_1 and T_3 is:

$$\overline{T_1T_3}: \ [(1 - 2p)f'(0)f'(1)]x + [pf'(0) - (1 - p)f'(1)]y + p^2 f'(0)f'(1) = 0.$$

We are interested in studying when this line is tangent to the graph of f at $(p, f(p))$. This interest is motivated by [4, Property 5], where it was proved that, in a parbelos, the diagonal of the tangent rectangle opposite to the cusp is tangent to the upper parabola at the point $(p, f(p))$. In fact we will see how this property characterizes parbeloses.
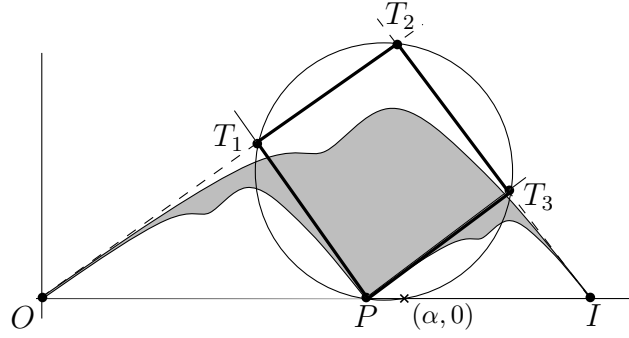
Figure 6.   The circumcircle of $\mathcal{T}$.

Proposition 10. *The point* $(p, f(p))$ *lies on* $\overline{T_1T_3}$ *(see Figure 7) if and only if*

$$f(p) = \frac{p(p-1)f'(0)f'(1)}{pf'(0) - (1-p)f'(1)}.$$

In addition, the line $\overline{T_1T_3}$ *is tangent to the graph of* f *at the point* $(p, f(p))$ *if and only if*

$$f'(p) = \frac{(2p-1)f'(0)f'(1)}{pf'(0) - (1-p)f'(1)}.$$

Proof. For the first part it is enough to substitute $(p, f(p))$ in the equation of $\overline{T_1T_3}$. For the second part, the slope of $\overline{T_1T_3}$ must coincide with $f'(p)$.   □
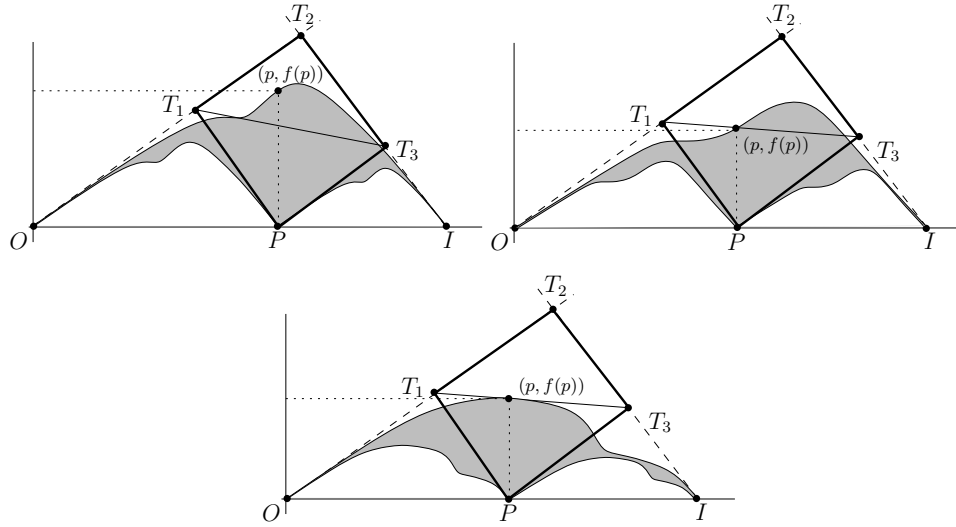
Figure 7.   Different relative positions of f and $\overline{T_1T_3}$ at $(p, f(p))$.

We will close the paper with a property that surprisingly characterizes the parbelos among all possible f-beloses. Parbeloses are the only f-beloses such that the diagonal of $\mathcal{T}$ opposite to the cusp is tangent to f at $(p, f(p))$ for every $p \in (0, 1)$.

Proposition 11. *Given an f-belos, let $\mathcal{T}$ be its tangent parallelogram. Then the diagonal of $\mathcal{T}$ opposite to the cusp is tangent to f at $(p, f(p))$ for every $p \in (0, 1)$ if and only if f is a parabola $f(x) = k(x - x^2)$. Moreover, in this case $\mathcal{T}$ is a rectangle if and only if $k = 1$.*

Proof. The first part of the previous property leads to

$$f(x) = \frac{x(x - 1)f'(0)f'(1)}{xf'(0) - (1 - x)f'(1)}$$

for every $x \in [0, 1]$. In this case we have that

$$f'(x) = \frac{f'(0)f'(1)[x^2 f'(0) + (1 - x)^2 f'(1)]}{[xf'(0) - (1 - x)f'(1)]^2}.$$

Hence, if f is tangent to $\overline{T_1 T_3}$ at $(p, f(p))$ for every $p \in (0, 1)$, the second part of the previous property implies that:

$$f'(x) = \frac{f'(0)f'(1)[x^2 f'(0) + (1 - x)^2 f'(1)]}{[xf'(0) - (1 - x)f'(1)]^2} = \frac{(2x - 1)f'(0)f'(1)}{xf'(0) - (1 - x)f'(1)}$$

for every $x \in (0, 1)$. Some computations lead to

$$(f'(0) + f'(1))(x - x^2) = 0$$

for every $x \in [0, 1]$ and hence $f'(0) = -f'(1)$ so

$$f(x) = \frac{-x(x - 1)f'(0)^2}{xf'(0) + (1 - x)f'(0)} = f'(0)(x - x^2),$$

and the result follows. $\square$

References

[1] Archimedes, *The works of Archimedes*, Dover Publications Inc., Mineola, NY, 2002; reprint of the 1897 edition and the 1912 supplement, edited by T. L. Heath.

[2] Y. Balashov, Should plato's line be divided in the mean and extreme ratio?, *Ancient Philosophy*, 14 (1994) 283–295.

[3] H. P. Boas, Reflections on the arbelos, *Amer. Math. Monthly*, 113 (2006) 236–249.

[4] J. Sondow, The parbelos, a parabolic analog of the arbelos, to appear in *Amer. Math. Monthly*; available at arXiv:1210.2279[math.HO].

Antonio M. Oller-Marcén: Centro Universitario de la Defensa, Academia General Militar, Ctra. de Huesca, s/n, 50090 Zaragoza, Spain

E-mail address: oller@unizar.es

FORUM GEOM

Why Are the Side Lengths of the Squares Inscribed in a Triangle so Close to Each Other?

Victor Oxman and Moshe Stupel

Abstract. We compare the side lengths of the squares inscribed in a non-obtuse triangle.

Given non-obtuse triangle ABC we consider an inscribed square. The construction is well known (see, for instance, [1] and [2, Problem 9, pp.16,64]). One can easily note that the side lengths of the squares based on the various sides of the triangle are almost equal to each other (Figure 1). Why does it happen? In this note we will give the answer to this question.
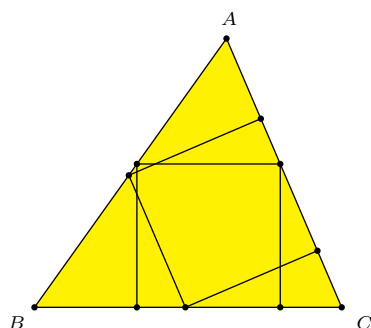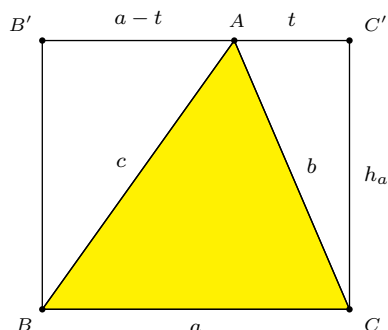
Figure 1   Figure 2

Let $BC = a$, $AC = b$, $AB = c$, and h_a, h_b, h_c the corresponding altitudes of triangle ABC. Denote the side lengths of the squares based on BC and AC by x_a and x_b respectively. One can easily verify that $x_a = \frac{ah_a}{a+h_a}$. Given a and $h_a > 0$, consider a non-obtuse triangle ABC with $BC = a$ and altitude h_a on the side BC. The vertex A lies on the side $B'C'$ of the rectangle $BB'C'C$ with $BB' = h_a$ (see Figure 2).

Let $AC' = t$. We have $b^2 = t^2 + h_a^2$ and $c^2 = (a-t)^2 + h_a^2$. Note that

$$x_b = \frac{bh_b}{b+h_b} = \frac{ah_a}{\sqrt{t^2+h_a^2} + \frac{ah_a}{\sqrt{t^2+h_a^2}}} = \frac{ah_a\sqrt{t^2+h_a^2}}{t^2 + h_a(a+h_a)}.$$

We shall assume $a \geq b$. This requires $h_a \leq a$ and $t \in [0, t_0]$, where $t_0 = \sqrt{a^2 - h_a^2}$. Since we require triangle ABC to be non-obtuse, $b^2 + c^2 \geq a^2$. This implies $t^2 - at + h_a^2 \geq 0$. This is always the case when $h_a \geq \frac{a}{2}$. When $h_a < \frac{a}{2}$,

---

we must further restrict $t \in [0, t_1] \cup [t_2, t_0]$, where

$$t_1 = \frac{a - \sqrt{a^2 - 4h_a^2}}{2}, \qquad t_2 = \frac{a + \sqrt{a^2 - 4h_a^2}}{2}.$$

Note that $t_0^2 - t_2^2 = \frac{a(a - \sqrt{a^2 - 4h_a^2})}{2} \geq 0$.

Now consider the function

$$f(t) := \frac{x_a}{x_b} = \frac{t^2 + h_a(a + h_a)}{(a + h_a)\sqrt{t^2 + h_a^2}}$$

defined on

$$\mathcal{D} := \begin{cases} [0, t_0], & \text{if } \frac{a}{2} \leq h_a \leq a, \\ [0, t_1] \cup [t_2, t_0] & \text{if } 0 < h_a < \frac{a}{2} \end{cases}.$$

This is a restriction of the function

$$F(t) = \frac{t^2 + h_a(a + h_a)}{(a + h_a)\sqrt{t^2 + h_a^2}}$$

defined on $[0, a]$. It has derivative

$$F'(t) = \frac{1}{a + h_a} \cdot \frac{t(t^2 - h_a(a - h_a))}{(t^2 + h_a^2)^{\frac{3}{2}}}.$$

From this it is clear that the only interior critical point is $t^* = \sqrt{h_a(a - h_a)}$, and that $F(t)$ is decreasing on $[0, t^*]$ and increasing on $[t^*, a]$. Therefore, $F(t) \geq F(t^*) = \frac{2\sqrt{ah_a}}{a + h_a}$ for every $t \in [0, a]$.

Note that $F(0) = F(t_0) = 1$. This means $f(t) \leq 1$ for $t \in \mathcal{D}$, and $x_a \leq x_b$.

(1) For $h_a \geq \frac{a}{2}$, comparing $f(t^*) = \frac{2\sqrt{ah_a}}{a + h_a}$ with the boundary values $f(0) = 1$ and $f(t_0) = 1$, we conclude that

$$\min\{f(t) : t \in \mathcal{D}\} = \frac{2\sqrt{ah_a}}{a + h_a}.$$

As a function of $h_a \in \left[\frac{a}{2}, a\right]$, $\frac{2\sqrt{ah_a}}{a + h_a}$ is increasing. Therefore, for $t \in \mathcal{D} = [0, t_0]$,

$$\frac{x_a}{x_b} = f(t) \geq \frac{2\sqrt{ah_a}}{a + h_a} \geq \frac{2\sqrt{a \cdot \frac{a}{2}}}{a + \frac{a}{2}} = \frac{2\sqrt{2}}{3}.$$

(2) If $h_a < \frac{a}{2}$, then

$$t^{*2} - t_1^2 = \frac{a(\sqrt{a^2 - 4h_a^2} - (a - 2h_a))}{2} = \frac{a\sqrt{a - 2h_a}(\sqrt{a + 2h_a} - \sqrt{a - 2h_a})}{2} > 0,$$

$$t_2^2 - t^{*2} = \frac{a(\sqrt{a^2 - 4h_a^2} + (a - 2h_a))}{2} > 0.$$

It follows that the critical point t^* is not in the interior of $\mathcal{D} = [0, t_1] \cup [t_2, t_0]$. Comparing boundary values, we have

$$\min\{f(t) : t \in \mathcal{D}\} = \min\{f(t_1), f(t_2)\}.$$

Note that $f(t_1) = f(t_2)$ because when $t = t_1$ or t_2, $\angle BAC = 90°$. In fact, for $j = 1, 2$,

$$f(t_j) = \frac{a(t_j + h_a)}{(a + h_a)\sqrt{at_j}} = \frac{\sqrt{a}}{a + h_a} \cdot \sqrt{\frac{(t_j + h_a)^2}{t_j}} = \frac{\sqrt{a(a + 2h_a)}}{a + h_a}.$$

As a function of $h_a \in \left(0, \frac{a}{2}\right]$, $\frac{\sqrt{a(a+2h_a)}}{a+h_a}$ is decreasing. Therefore, for $t \in \mathcal{D} = [0, t_1] \cup [t_2, t_0]$,

$$\frac{x_a}{x_b} = f(t) \geq \frac{\sqrt{a(a + 2h_a)}}{a + h_a} \geq \frac{\sqrt{a(a + 2 \cdot \frac{a}{2})}}{a + \frac{a}{2}} = \frac{2\sqrt{2}}{3}.$$

We conclude that in all cases,

$$1 \geq \frac{x_a}{x_b} \geq \frac{2\sqrt{2}}{3} = 0.94\ldots.$$

The difference between x_a and x_b is less than 6% of x_b. This explains why the lengths of the sides of the inscribed squares are very close to each other.

Note that from the above reasoning the smallest inscribed square in a non-obtuse triangle is based on the longest side.

References

[1] F. M. van Lamoen, Inscribed squares, *Forum Geom.*, 207–214.
[2] I. M. Yaglom, *Geometric Transformations*, II, Random Hon muse, New York, 1968.

Victor Oxman: Western Galilee College, P.O.B. 2125, Acre 24121 Israel
E-mail address: victor.oxman@gmail.com

Moshe Stupel: Shaanan College, P.O.B. 906, Kiryat Shmuel, Haifa 26109 Israel
E-mail address: stupel@bezeqint.net

Pairings of Circles and Sawayama's Theorem

Paris Pamfilos

Abstract. In this article we study pairs of projectively related circles, tangent to a fixed circle, and point out properties, which in a class of particular cases specialize to Sawayama's theorem.

1. Introduction

The well known Sawayama-Thebault theorem ([6]) states that the centers O_1, O_2 of the two circles k_1, k_2 defined by a cevian AW of the triangle ABC are collinear
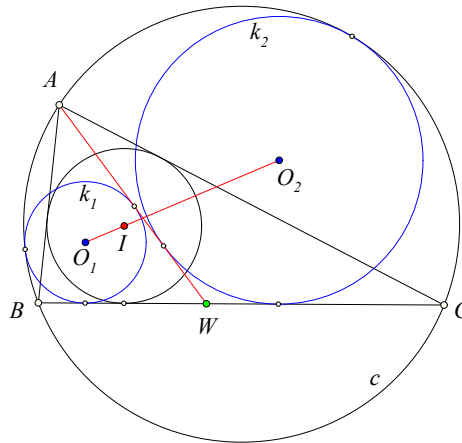
Figure 1. Sawayama-Thebault theorem: O_1, I, O_2 are collinear

with the incenter I of ABC (See Figure 1). The circles k_1, k_2 are, by definition, tangent to AW, BC and the circumcircle c of the triangle. For the history of the problem and a synthetic proof I refer to Ayme's article [1].

In this article we study pairs of projectively related circles (k_1, k_2) called *pairings of circles* and reveal properties, that in some particular cases, called *Sawayama pairings*, lead to Sawayama's theorem.

The general pairings of circles, considered here, result by fixing a triple (c, h, P) of a circle, a line h intersecting c at two non-diametral points B, C and a point inside the circle c but $P \neq O$ and $P \notin h$.

Then we consider all lines through the point P. The intersection points (X, X') of a line through P with the circle, define a pair of circles (k_1, k_2), which are correspondingly tangent to c at X and X' and also tangent to h at points (Z, Z') (See Figure 2). These circles have their centers Y, Y' correspondingly on lines
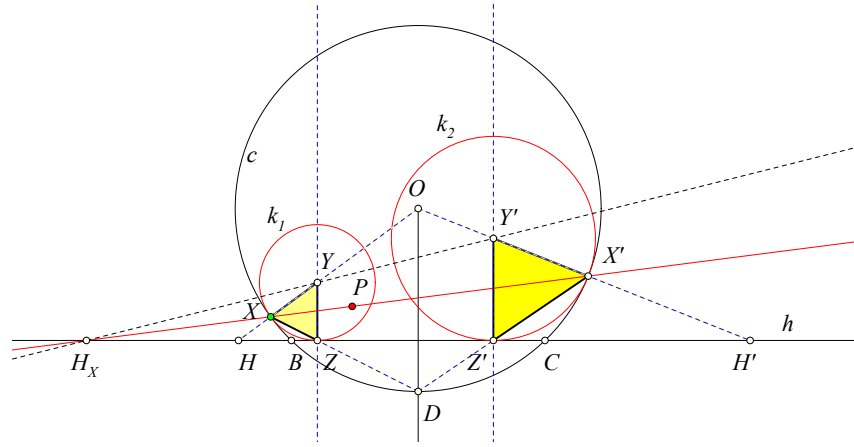
Figure 2. Circle pairing defined by the triple (c, h, P)

OX, OX', and it is easy to see that their respective chords $XZ, X'Z'$ pass always through the middle D of the smaller arc BC, defined on c by h. In fact, using this property, and considering a variable line through P intersecting the circle c at X, X', one can define Z, Z' by correspondingly intersecting DX, DX' with h and defining the two isosceles triangles $XYZ, X'Y'Z'$. The resulting triangles are line perspective, since corresponding sides intersect along line OD. Hence they are also point perspective and define a point H_X on line h, which is collinear with the centers Y, Y', as well as with the contact points X, X' of the circles k_1, k_2. This construct is called in the sequel the *basic configuration*.

In §2 we discuss a fundamental property of the basic configuration coming from the projective geometry aspect. In §3 we deduce that the line of centers YY' always passes through a fixed point I and locate its position. In addition we show a property of the map $Z' = f(Z)$, defined on line h (Theorem 5). In §4 we investigate two pencils of circles, naturally connected to the basic configuration and giving the geometric meaning and consequences of the calculations of the preceding section. In §5 we establish the existence of a certain variable line, associated to pairing and pivoting about a fixed point (Theorem 13). This line, called *pivoting line*, specializes in Sawayama's theorem to the cevian AW from the vertex of the triangle of reference ABC. In §6 we characterize the Sawayama pairings and note a resulting proof of Sawayama's theorem. Finally in §7 we supply a few details concerning the case of Sawayama's theorem.

2. The projective aspect

In the sequel (AB, CD) denotes the intersection of the lines AB and CD, $D = C(A, B)$ denotes the harmonic conjugate of C with respect to (A, B), and $(ABCD) = \frac{CA}{CB} : \frac{DA}{DB}$ denotes the cross ratio of the four points. Next construction is a typical one of the definition of a homology of the projective plane [3, p.9]. Given two
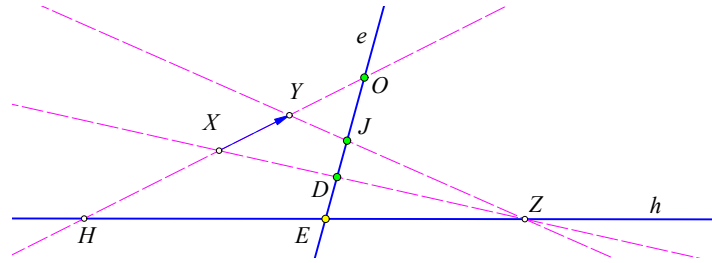
Figure 3. A typical homology $Y = f(X)$

lines e, h, intersecting at point E, and three points D, J, O on e, define the transformation f as follows: For each point X of the plane, let Z be the intersection $Z = (XD, h)$ and set $Y = f(X) = (XO, ZJ)$. Defining $H = (h, XO)$, the equality of cross ratios $(OHXY) = (OEDJ)$ proves next lemma.

Lemma 1. *The map f is a homology with center O, axis h and homology coefficient equal to the cross ratio $k = (OEDJ)$.*

Of particular interest for our subject is the case in which point J goes to infinity,
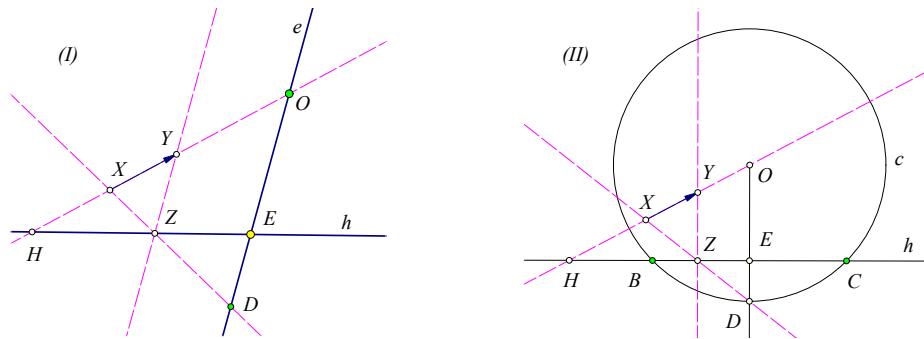
Figure 4. Specializing twice the previous homology

then the configuration becomes like the one of figure $4(I)$ and the cross ratio has the value $k = \frac{DO}{DE}$. A further specialization of the previous figure to $4(\text{II})$, in which points D, E, O are defined by a circle $c(O, r)$ and a line h, intersecting the circle at two non-diametral points B, C, leads to the projective aspect of our basic configuration. In this case E is the projection of the center O on h and D is the intersection of the half-line OE with c. Using these notations and conventions the following lemma is valid.

Lemma 2. *For each point X of the circle c the triangle XYZ is isosceles and the circle $k_1(Y, |XY|)$ is tangent to the circle c at X and to line h at Z. As X varies on the circle c the center Y of k_1 describes a parabola.*

In fact, the first claim follows from an easy angle chasing argument (See Figure 5). From this, or considering the locus as the image $f(c)$ of the circle via the
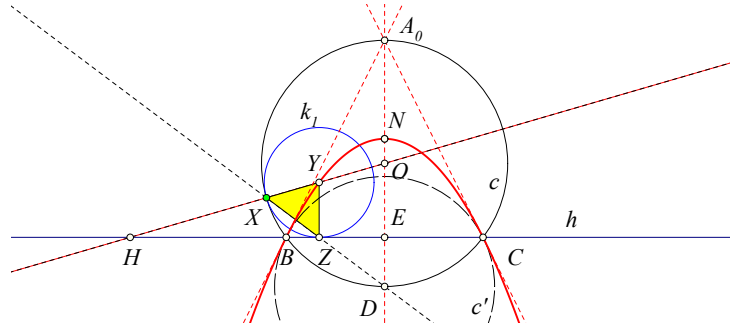
Figure 5. Tangent circles and parabola of centers

homology, follows also easily that the geometric locus of the centers Y of the circles k_1 is a parabola tangent to the triangle A_0BC at B, C and point A_0 being the diametral of D. The parabola passes through the middle N of A_0E and is also tangent to the circle $c'(D, |DB|)$.

3. Pairs of circles

The *circle pairing* of our basic configuration results by considering all lines through the fixed point P. Joining each point X of the circle c with P and considering the second intersection point X' with c one defines an involution ([7, I p.221]) of the points of c denoted by g_P. Point X on the circle and the corresponding
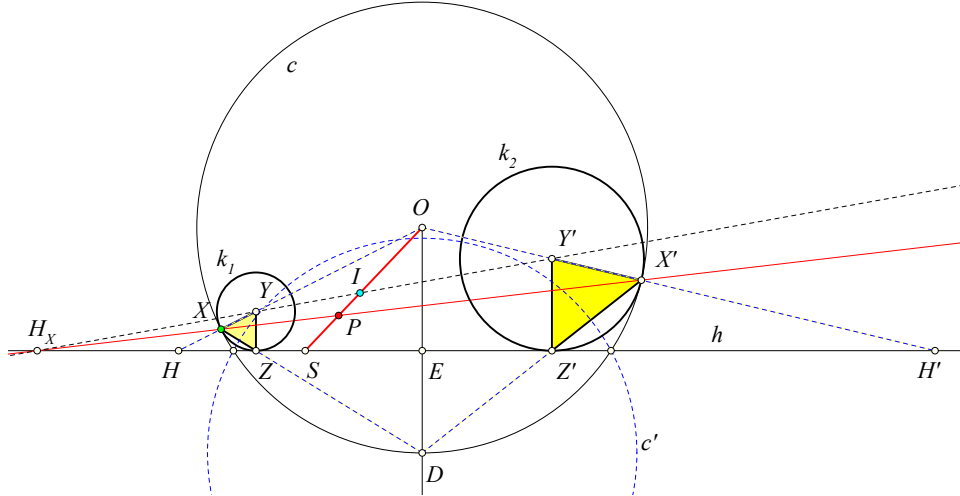
Figure 6. Pairing of circles for the triple (c, h, P)

point $X' = g_P(X)$ define, by the recipe of the previous section, two triangles $XYZ, X'Y'Z'$ and their corresponding circumcircles k_1, k_2 (See Figure 6).

Lemma 3. *Circle c' is orthogonal to circles k_1 and k_2 and points $X, Z, X'Z'$ are concyclic.*

This follows by considering the inversion with respect to circle c'. It is easily seen that this interchanges circle c and line h and fixes, as a whole, circles k_1 and k_2. Hence these two circles are orthogonal to c'. The second claim is a consequence of the first one.

As noticed in the introduction, the two triangles are perspective and their perspectivity center H_X is on line h. With the notations adopted so far the following is true.

Lemma 4. *The lines YY', joining the centers of the circles k_1, k_2, pass through a fixed point I lying on line OP. The points P, I are related by the homology f defined by the triple (c, h, P):*

$$\frac{PO}{PS} = \frac{IO}{IS} \cdot \frac{DO}{DE}.$$

In fact, lines YY' are images $YY' = f(XX')$ of lines XX' under the homology f, hence they pass all through $I = f(P)$. As a result, I lies on OP and taking the intersection $S = (OP, h)$ we have $(OSPI) = \frac{DO}{DE}$. The formula results by expanding the cross ratio $(OSPI) = \frac{PO}{PS} : \frac{IO}{IS}$.

Theorem 5. *With the previous notations the map $Z' = f(Z)$ on line h is an involution, which in line coordinates with origin at the projection Q of I on h obtains the form, for a constant w:*

$$z' = \frac{-w^2}{z}.$$

Figure 7. The involution $Z' = g(Z)$

In fact, using the involution $X' = g_P(X)$ on the circle and intersecting h with the rays of the pencil through D one defines a corresponding involution $Z' = g(Z)$

on line h. This, taking coordinates z, z' with origin at Q, is described by a Moebius transformation ([7, I,p.157]) of the kind (See Figure 7).

$$z' = \frac{az + b}{cz - a}.$$

The rest of the theorem, on the form of this involution (vanishing of a), follows immediately from the collinearity of D, P, Q, which is a consequence of Lemma 4. In fact, if the line XX' passing through P, obtains the position of PD, then points X', D become coincident and the corresponding circle k_2 becomes the tangent to c at D, the line of centers YY' becomes orthogonal to h and passes through I (See Figure 7). For this particula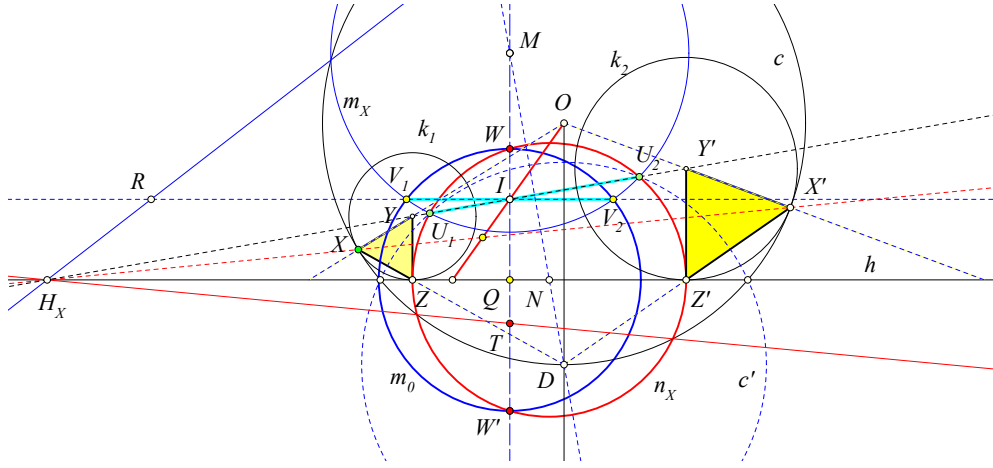r position of XX' we see also that as point X' converges to D, the corresponding Z' goes to infinity. Thus for $z = 0$ the value of $f(z)$ must be infinity, hence $a = 0$, thereby proving the theorem by setting the constant $w^2 = -b/c$. The value of the constant can be easily calculated by

Figure 8. The value of the constant

letting X take the place of the intersection point of the line OP with c. Then XX' becomes a diameter of c and $DZZ', DX'X$ become similar right angled triangles. Setting for D the coordinates $D(e, d)$ and denoting the coordinates of all other points by corresponding small letters, we obtain

$$(z - e)(z' - e) = -d^2 \qquad \text{and} \qquad (z - s)(z' - s) = \delta,$$

where $\delta = -|SX||SX'|$ is the power of S with respect to the circle c. The second equation follows from the concyclicity of points Z, X, Z', X' (Lemma 3). From these we obtain the value

$$-w^2 = zz' = \frac{s(d^2 + e^2) + e(\delta - s^2)}{e - s}.$$

Figure 9. Involution $Z' = g(Z)$ by orthogonals through W

Interpreting geometrically the theorem, we deduce that there is a fixed point $W(0, w)$ on the axis QI, such that the involution $Z' = g(Z)$ is defined by means of the intersections of line h by two orthogonal lines rotating about W ([5, Involution, p.3]), this is formulated in the following.

Corollary 6. *The circle pairing induces an involution $Z' = g(Z)$ on line h, which coincides with the one defined by means of pairs of orthogonal lines rotating about a fixed point W lying on line IQ.*

4. Two auxiliary pencils of circles

Here we continue the exploration of the basic configuration using the notation and conventions of the previous sections.

Theorem 7. *The following properties of the basic configuration are true.*
(1) The radical axis DN of circles k_1 and k_2 passes through D and the middle N of ZZ'.
(2) If $M = (DN, IQ)$, then the circle m_X centered at M and orthogonal to k_1 and k_2, intersects the parallel h' to h from I at two fixed points V_1 and V_2.
(3) The circles m_X are members of a pencil with base points V_1 and V_2.

Property (1) immediately follows from Lemma 3, since then D is on the radical axis of the two circles, and because of the tangency to line h, the middle N of ZZ' is also on the radical axis of k_1 and k_2 (See Figure 10).

Property (2) follows from the fact that both circles c' and m_X being orthogonal to k_1 and k_2, their radical axis coincides with YY', which passes through I. The power of I with respect to c' and m_X is constant and equal in absolute value to $|IV_1|^2$, as claimed.

Property (3) is an immediate consequence of (2).

Figure 10. The pencil of circles m_X with base points V_1, V_2

Corollary 8. *The radical axis of circle m_X and c passes through a fixed point R on $V_1 V_2$ and passes also through H_X.*

The first claim is a well known property for the radical axis of members of a pencil and a fixed circle ([2, p.210]). The second claim follows from the fact that H_X is the radical center of circles c', c and m_X.

Next theorem deals with the circles having diameter ZZ'. Since by Theorem 5 the map $Z' = g(Z)$ is an involution, we know that this is a pencil of circles ([4, vol.II,p.27]). Here we make precise the kind of the pencil and the location of its base points. Note that this pencil and the one of the preceding theorem have a common member m_0 carrying the base points of both pencils.

Theorem 9. *The following properties are valid.*
(1) *The circle n_X with diameter ZZ' is orthogonal to k_1 and k_2.*
(2) *The circle n_X intersects the circle m_0 centered at Q and passing through V_1 and V_2, at its diametral points W and W'.*
(3) *The circles n_X are members of a pencil with base points W and W'.*

Property (1) follows from the fact that n_X has its center at the middle N of ZZ', from which the tangents to k_1, k_2 are equal (See Figure 11).

Property (2) results from Theorem 5. Another proof results from the fact that circle n_X belongs to the pencil of orthogonal circles to k_1 and k_2. From this it follows that circles m_X, c' and n_X pass through the two base points U_1, U_2 lying on line YY', which passes through I. Let W and W' be the diametral points of circle m_0 on the diameter passing through I. Then $|IW||IW'| = |IV_1||IV_2|$ but also, since V_1V_2, U_1U_2 are chords of the circle m_X it is $|IV_1||IV_2| = |IU_1||IU_2|$. This implies that I is on the radical axis of m_0, n_X, which, since both circles have their center on h, is orthogonal to h. Thus it coincides with IQ or equivalently with WW'.

Figure 11. The pencil of circles n_X with base points W, W'

Property (3) is an immediate consequence of (2). Note that point W coincides with the one defined in Corollary 6.

Corollary 10. *The radical axis of circle n_X and c passes through a fixed point T on WW', and passes also through point H_X.*

The first claim is a well known property for the radical axis of members of a pencil and a fixed circle ([2, p.210]). The second claim follows from the fact that H_X is the radical center of circles c, m_X and n_X.

5. The pivoting line of the pairing of circles

Next figure results by drawing orthogonals respectively to lines WZ and WZ' from the centers Y and Y' of the circles k_1 and k_2. These intersect at right angles at point W_X and intersect also the parallel h' to h from I at points W_1, W_2.

Theorem 11. *Lines ZW_1 and $Z'W_2$ are parallel and W_X varies on a fixed line h'' parallel to h at distance equal to $|WI|$.*

To prove the theorem a short calculation seems unavoidable. For this, we use coordinates along line h and its orthogonal through Q, as in §3. Denoting coordinates with respective small letters and by r, r', r_1, r_2 respectively the radii of circles c, c', k_1, k_2, we find easily the relations

$$zz' = -w^2, \qquad r'^2 = -2rd, \qquad w^2 = 2d(i-r) - d^2 - e^2,$$

$$r_1 = \frac{1}{2d}(2rd + (z-e)^2 + d^2), \qquad r_2 = \frac{1}{2d}(2rd + (z'-e)^2 + d^2),$$

$$w_1 = \frac{wz + (r_1 - i)z'}{w}, \qquad w_2 = \frac{wz' + (r_2 - i)z}{w}.$$

From these, by a short calculation, we see that

$$w_2 - w_1 = (z' - z).$$

Figure 12. Pair of parallels $ZW_1, Z'W_2$

This means that W_1W_2 is equal in length to ZZ', thus lines ZW_1 and $Z'W_2$ are parallel, as claimed. The other claims are consequences of this property, since then $W_1W_2W_X$ and $Z'ZW$ are equal right angled triangles and projecting W_X on IW to T, we get $|QT| = |WI|$ (See Figure 12).

Next theorem states a property of the tangents to k_1, k_2 at points K, K', resulting by intersecting these circles respectively with lines WZ and WZ'. These tangents are the reflections of line h on lines W_XW_1 and W_XW_2 respectively. The theorem rests upon a simple criterion recognizing the passing of a variable line through a fixed point. Its proof is a simple calculation which I omit.

Figure 13. Lines passing through a fixed point A

Lemma 12. *If a variable line intersects the* $x-$*axis* e *and a parallel to it* e' *at distance* q*, so that the coordinates* x, x' *of the intersection points satisfy an equation of the form*

$$ax + bx' + c = 0,$$

then the variable line passes through the fixed point with coordinates

$$A = \frac{1}{a+b}(-c, qb).$$

Theorem 13. *The tangents to circles* k_1, k_2*, which are reflections of* h*, respectively, on* W_XW_1*,* W_XW_2 *are parallel and equidistant to the median* W_XM *of the right angled triangle* $W_XW_1W_2$*. This median passes through a fixed point* A*, independent of the position of* X *on the circle* c*.*

Figure 14. The pivoting line $W_X M$ and the parallel tangents at K, K'

That the tangents are parallel follows easily by measuring the angles at their intersection points with h. Similarly follows their parallelity to the median $W_X M$ (See Figure 14). ?

To show that line $W_X M$ passes through a fixed point it suffices, according to the previous lemma, to show that the x-coordinates of points M and W_X satisfy a linear relation. In fact, a somewhat extended calculation shows that $(W_X)_x$ and M_x satisfy the equation

$$(w - d)(W_X)_x + (2d - w)M_x - ew = 0.$$

From this and the previous lemma follows that line $W_X M$ passes through the fixed point

$$A = \frac{1}{d}\left(ew, i(2d - w)\right).$$

In the sequel line $W_X M$ is called the *pivoting line* of the circle pairing.

6. Sawayama pairings

I call the pairing of circles k_1, k_2 defined by the basic configuration (c, h, P) a *Sawayama pairing*, when the corresponding point I of the configuration is on the arc of circle c' lying inside c (See Figure 15). The formulas of the preceding section imply then that points W and I coincide $(i = w)$ and consequently that W_X lies on line h. This implies in turn that the three parallels coincide with the pivoting line of the pairing, which is also the median of triangle $W_X W_1 W_2$ and which becomes simultaneously tangent to the two circles k_1, k_2 while passing also through the fixed point A. A short calculation shows also that in these circumstances point A lies on circle c, thus producing the figure of Sawayama's theorem. In fact, the last ingredient of the figure is the collinearity of points A, I and D, which, in view of the previous conventions for the coordinates reduces to an easy check of the vanishing of a determinant. By a well known property of the incenter ([2, p.76]),
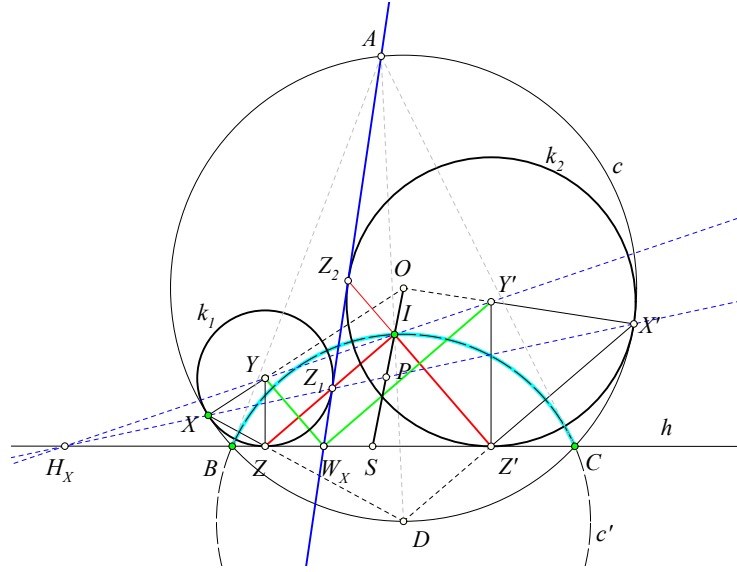
Figure 15. Sawayama pairing characterized by $Q \in c'$

point I coincides with the incenter of triangle ABC, thereby proving the next theorem.

Theorem 14. *Each Sawayama pairing* k_1, k_2 *corresponds to a triangle* ABC *with incenter* I *and cevians* AW_X, *such that the two circles are tangent to the circumcircle* c *of the triangle and also tangent to the cevian* AW_X *and side* BC. *The centers* Y, Y' *of the circles and the incenter are collinear.*

Fixing the basic configuration (c, h, P), so that the corresponding point I lies on the arc of c' contained in c, we obtain another proof of Sawayama's theorem, once we can show, that point I can obtain every possible position on the aforementioned arc of c' and, for each position of I, the corresponding pivoting lines AW_X can obtain all positions of the cevians through A of triangle ABC. That I can take every position on the claimed arc of c', is a simple consequence of the homographic relation of I to P described in §3. Next lemma makes this point clear and shows that the whole arc BC on c is obtained from a proper arc of an ellipse via the homography f, defined in §2. The somewhat more interesting verification that the pivoting line AW_X obtains all positions of cevians from A is handled in the next section.

Lemma 15. *For* I *varying on circle* c' *the corresponding point* P *varies on an ellipse, which is tangent to circle* c *at points* B *and* C.

In fact, since $I = f(P)$ is a homology, the claimed relation is given through the inverse homology $P = f^{-1}(I)$, which has the same center and axis and ratio $k' = \frac{DE}{DO}$. Hence the curve $c'' = f^{-1}(c')$ is a conic and the other claims result from simple geometric considerations.

Figure 16. The locus c'' of P as Q varies on c'

7. The cevians
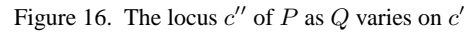
Using the notation of the previous sections, we deduce here various properties of the Sawayama pairings, appearing to be of interest and leading to the proof that, for a fixed point I on the arc of c' lying inside c, the corresponding pivoting lines AW_X, for variable X, obtain all positions of the cevians through A.

Lemma 16. *The circle c'' with diameter Z_1Z_2 is orthogonal to circles k_1, k_2 and the diametral point I' defines line II' which is parallel to BC. Also the triples of points (Z_1, I', V) and (Z_2, I', V') are collinear.*

Figure 17. The parallel to h line II' and the radical axis of $c_x, c_{X'}$

The proof of parallelity follows from the equality of angles $W_X Z' Z_2$, $W_X Z_2 Z'$, TIZ_2 (See Figure 17). The collinearity of Z_1, I', V follows from the equality of angles $W_X Z' I$, $ZW_X Y$ and the parallelity of VZ_1 to YW_X.

Corollary 17. *Line YY' passes through the intersection points I, I'' of the circles c' and c''.*
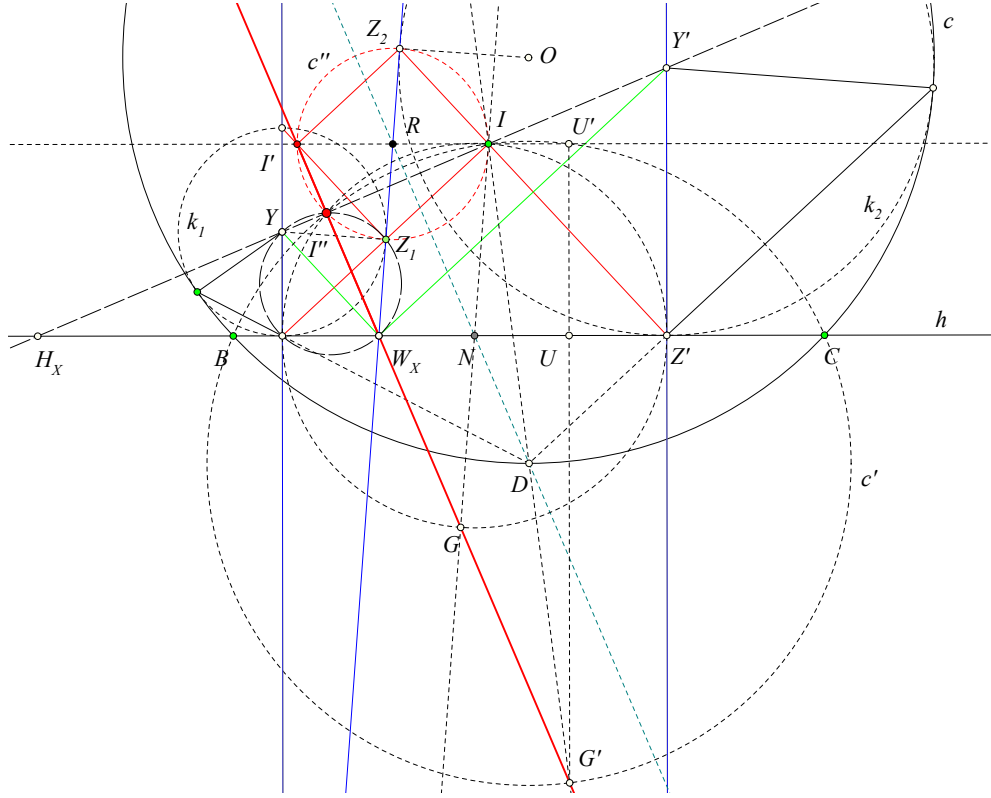
Figure 18. Line $I'W_X$

Lemma 18. *Line $I'I''$ is orthogonal to II'' and passes through point W_X and also through points G, G', which are correspondingly diametrals of I with respect to the circle with diameter ZZ' and the circle c'.*

In fact, by the previous lemma, angle $I'I''I$ is a right one (See Figure 18). Also I'' is on the circle with diameter YW_X, which passes through Z, Z_1. Thus I', I'', W_X are collinear. The center N of the circle with diameter ZZ' is on line RD, which is the radical axis of circles k_1, k_2 and is orthogonal to II' at its middle. Hence $I'W_X$ is parallel to RD. This implies the two other statements of the lemma.

Corollary 19. *The cross ratio $\kappa = (BCW_XH_X)$ is constant and equal to $\frac{UB}{UC}$. Here U is the projection of G' on BC.*

This follows by considering the pencil $I''(B, C, W, H_X)$ of lines through I''. The lines of the pencil pass through fixed points of the circle c'. Thus their cross ratio is independent of the position of I'' on this circle. Its value is easily calculated

by letting I'' take the place of U', which is the projection of G' on II'. Then H_X goes to infinity and κ becomes equal to the stated value.

Corollary 20. *Fixing point I, which becomes the incenter of triangle ABC, the pivoting lines AW_X of the Sawayama pairing take the positions of all cevians through A and Sawayama's theorem is true.*

In fact, by the previous corollary, the constancy of cross ratio implies that for variable X on c points H_X obtain all positions on line BC and consequently W_X, being related to H_X by a line-homography, obtains also all possible positions on this line.

References

[1] J.-L. Ayme, Sawayama and Thebault's theorem, *Forum Geom.*, 3 (2003) 225–229.
[2] N. A. Court, *College Geometry*, Dover reprint, 2007.
[3] L. Cremona, *Elements of Projective Geometry*, Clarendon Press, Oxford, 1893.
[4] S. L. Loney, *The Elements of Coordinate Geometry*, 2 volumes, MacMillan and Co., London, 1934.
[5] G. Papelier, *Exercices de Geometrie Moderne*, Editions Jacques Gabay, 1996.
[6] Y. Sawayama, A new geometrical proposition, *Amer. Math. Monthly*, 12 (1905) 222–224.
[7] O. Veblen and J. Young, *Projective Geometry*, vol. I, II, Ginn and Company, New York, 1910.

Paris Pamfilos: Department of Mathematics, University of Crete, Crete, Greece
E-mail address: pamfilos@math.uoc.gr

Derivation of the Law of Cosines via the Incircle

Larry Hoehn

Abstract. The law of cosines can be derived without using special cases and without using the Pythagorean theorem.

Most trigonometry textbooks treat the derivation of the law of cosines as three separate cases depending on whether the triangle is acute, obtuse, or right. In this note we derive a proof using an arbitrary general triangle and we do not use the Pythagorean theorem.

We let ABC be any triangle whose incircle is tangent at D, E, and F as shown in Figure 1. Let $a = BC$, $b = CA$, $c = AB$, and r be the radius of the incircle with incenter I. We derive our formula by equating independent expressions for r.
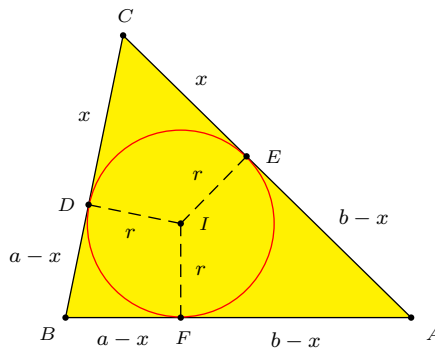
Figure 1.

If $x = CD = CE$, then $c = (a - x) + (b - x)$ so that $x = \frac{1}{2}(a + b - c)$. In the right triangle CEI, $x = r \cot \frac{C}{2}$. Solving $\frac{1}{2}(a + b - c) = r \cot \frac{C}{2}$ for r yields

$$r = \frac{a + b - c}{2 \cot \frac{C}{2}}. \tag{1}$$

By computing the area of triangle ABC in two ways we obtain

$$\frac{1}{2}ab \sin C = \frac{1}{2}ar + \frac{1}{2}br + \frac{1}{2}cr,$$

and

$$r = \frac{ab \sin C}{a + b + c}. \tag{2}$$

From (1) and (2), we have $\frac{a+b-c}{2\cot\frac{C}{2}} = \frac{ab\sin C}{a+b+c}$. Cross multiplying and making use of some well known trigonometric identities we obtain the following.

$$
\begin{aligned}
(a+b)^2 - c^2 &= 2ab\sin C\cot\frac{C}{2} \\
&= 2ab\left(2\sin\frac{C}{2}\cos\frac{C}{2}\right)\cdot\frac{\cos\frac{C}{2}}{\sin\frac{C}{2}} \\
&= 4ab\cos^2\frac{C}{2}.
\end{aligned}
$$

Therefore,

$$
\begin{aligned}
c^2 &= (a+b)^2 - 4ab\cos^2\frac{C}{2} \\
&= a^2 + b^2 - 2ab\left(2\cos^2\frac{C}{2} - 1\right) \\
&= a^2 + b^2 - 2ab\cos C.
\end{aligned}
$$

Since the identity $\sin^2 x + \cos^2 x = 1$ (and hence $\cos 2x = 2\cos^2 x - 1$) can be derived independently [2] without the Pythagorean theorem, we have derived the law of cosines without the use of the Pythagorean theorem. This also answers a question in a footnote in [1, p. 135] whether this is possible.

References

[1] O. Byer, F. Lazebnik, and D. L. Smeltzer, *Methods for Euclidean Geometry*, MAA, 2010.
[2] J. Zimba, On the possibility of trigonometric proofs of the Pythagorean theorem, *Forum Geom.*, 9 (2009) 275–278.

Larry Hoehn: Austin Peay State University, Clarksville, Tennessee 37044, USA
E-mail address: hoehnl@apsu.edu

On the Fermat Geometric Problem

Zvonko Čerin

Abstract. We consider the Fermat configuration generated by a point on a circle over the side of a rectangle. When the ratio of the rectangle's sides is $\sqrt{2}$, then many properties do not depend on a position of the point. Some properties hold for all ratios and other ratios can also have interesting geometric consequences. Our proofs use analytic geometry but some parts include also synthetic arguments.

1. Introduction

Among the numerous questions that Pierre Fermat formulated, the following geometric problem is our main concern (see Figure 1).
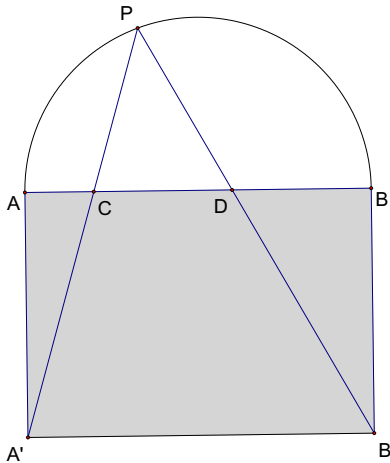
Figure 1. The configuration of the Fermat problem.

Fermat Problem. Let P be a point on the semicircle that has the top side AB of the rectangle $ABB'A'$ as a diameter. Let $\frac{|AB|}{|AA'|} = \sqrt{2}$. Let the segments PA' and PB' intersect the side AB in the points C and D, respectively. Then $|AD|^2 + |BC|^2 = |AB|^2$.

The great Leonard Euler in [6] has provided the first rather long proof, which is old fashioned (for his time), and avoids the analytic geometry (which offers rather simple proofs as we shall see later). Several more concise synthetic proofs are now known (see [10], [7, pp. 602, 603], [1, pp. 168, 169] and [8, pp. 181, 264]). A very nice description of Euler's proof is available on the Internet (see [11]).

The analytic proof was recently recalled in [9] where it was observed that the above relation holds for all points on the circle with the segment AB as a diameter.

For a circle, we shall consider a slightly more general situation where the quotient $\frac{|AB|}{|AA'|}$ is a positive real number m (see Figure 2.).

Figure 2. The extended Fermat configuration for a circle.

For given different points A and B and any points P_1, P_2, P_3, P_4 in the plane, let

$$\varphi(P_1 P_2, P_3 P_4) := \frac{|P_1 P_2|^2 + |P_3 P_4|^2}{|AB|^2}.$$

In this notation, the above Fermat Problem for the circle is the implication $(a) \Rightarrow (b)$ in Theorem 1 below.

Theorem 1. *Let $U_b = \varphi(AD, BC)$. The following statements are equivalent.*
(a) $m = \sqrt{2}$, and
(b) $U_b = 1$.

Proof. We shall use analytic geometry, which offers a simple proof. Let the origin of the rectangular coordinate system be the midpoint O of the side AB so that the points A and B have coordinates $(-r, 0)$ and $(r, 0)$ for some positive real number r (the radius of the circle). The equation of the circle is a standard $x^2 + y^2 = r^2$.

The coordinates of the points A' and B' are $\left(-r, -\frac{2r}{m}\right)$ and $\left(r, -\frac{2r}{m}\right)$. For any real number t, let $u = 1 - t^2$, $v = 1 + t^2$, $z = mt$, $\eta = v - z$ and $\vartheta = v + z$. An arbitrary point P on the circle has coordinates $\left(\frac{ru}{v}, \frac{2rt}{v}\right)$. From similar right-angled triangles PVC and PQA' and $s = \frac{2r}{m}$, we easily find that $C\left(\frac{r(u-z)}{\vartheta}, 0\right)$

and $D\left(\frac{r(u+z)}{\vartheta}, 0\right)$. The equivalence of the statements (a) and (b) follows from the identity $U_b - 1 = \frac{t^2(m^2-2)}{\vartheta^2}$. $\qquad\square$

The fact that $(a) \implies (b)$ can be proved more simply by synthetic methods. Here is an adaptation of Lionnet's proof from [7, p. 602], which works for any point on the circle (see Figure 2).

Let the directed lengths $\overrightarrow{AC}, \overrightarrow{CD}, \overrightarrow{DB}$ be a, b, c. Then

$$\begin{aligned} AD^2 + BC^2 - AB^2 &= (a+b)^2 + (b+c)^2 - (a+b+c)^2 \\ &= b^2 - 2\,a\,c, \end{aligned}$$

so that

$$AD^2 + BC^2 = AB^2 \qquad \Longleftrightarrow \qquad b^2 = 2\,a\,c. \qquad (1)$$

Now draw CY and DZ perpendicular to AB, with Y on PA and Z on PB. Using pairs of similar triangles, we have

$$\frac{YC}{AA'} = \frac{PC}{PA'} = \frac{CD}{A'B'} = \frac{PD}{PB'} = \frac{ZD}{BB'}.$$

Hence $YCDZ$ is a rectangle similar to $AA'B'B$. The triangles YCA, BDZ are equiangular, so $\frac{YC}{a} = \frac{c}{DZ}$. But $YC = DZ = \frac{CD}{\sqrt{2}} = \frac{b}{\sqrt{2}}$. Thus $b^2 - 2\,a\,c$ vanishes, hence $AD^2 + BC^2 = AB^2$.
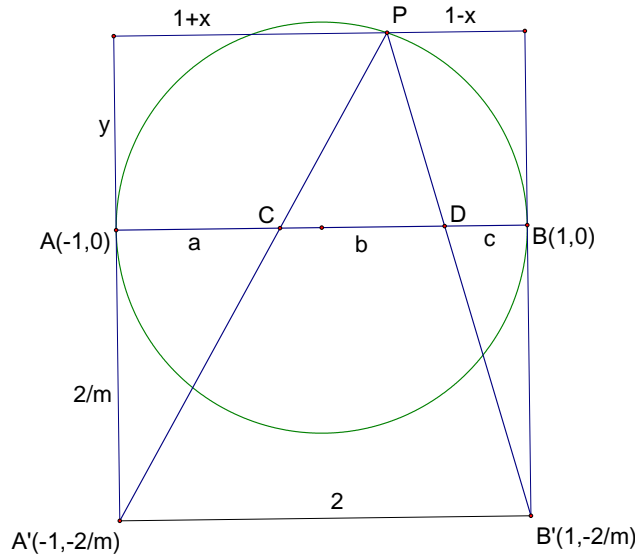
Figure 3. Simple analytic proof.

We can also use the equivalence (1) to obtain a simple analytic proof (see Figure 3). There is no loss of generality in taking the radius of the circle as the unit of

length. By similar triangles,

$$\frac{a}{\frac{2}{m}} = \frac{1+x}{\frac{2}{m}+y}, \quad \frac{b}{y} = \frac{2}{\frac{2}{m}+y} \quad \text{and} \quad \frac{c}{\frac{2}{m}} = \frac{1-x}{\frac{2}{m}+y}.$$

Simplifying $b^2 - 2\,a\,c$ and putting $x^2 = 1 - y^2$ we find that this difference is $\frac{4\,y^2\,(m^2-2)}{(2+m\,y)^2}$.

Let A'', B'', P' be the reflections of the points A', B', P in the line AB. We close this introduction with a remark that most of our results come in related pairs. The second version, which requires no extra proof, comes (for example in Theorem 1) by replacing the points C and D with the points C' and D', which are the intersections of the line AB with the lines PA'' (or $P'A'$) and PB'' (or $P'B'$). In other words, if $V_b = \varphi(AD', BC')$, then (a) and

(b') $\quad V_b = 1$

are also equivalent. Moreover, (a) and

(b'') $\quad U_b = V_b$

are equivalent as well.

2. Invariants of the Fermat configuration

Our primary goal is to present several statements similar to (b), (b') and (b'') that could replace it in Theorem 1. In other words, we explore what other relationships in the Fermat configuration remain invariant as the point P changes position on the circle.

We begin with the diagonals of the trapezium $A'B'DC$ (see Figure 2).

Theorem 2. *Let* $U_c = \varphi(A'D, B'C)$ *and* $V_c = \varphi(A'D', B'C')$.
Consider the statements
(c) $\quad U_c = 2, \quad$ *(c')* $\quad V_c = 2, \quad$ *(c'')* $\quad U_c = V_c.$
The following are true.
$(a) \Leftrightarrow (c'')$,
(a) *implies each of the statements* (c) *and* (c').

Proof. With straightforward computations one can easily check that

$$V_c - U_c = \frac{2(m^2 - 2)v\,t^3}{\vartheta^2\,\eta^2},$$

$$2 - U_c = \frac{(m^2 - 2)v(2\,z + v)}{m^2\,\vartheta^2},$$

$$V_c - 2 = \frac{(m^2 - 2)v(2\,z - v)}{m^2\,\eta^2}.$$

Of course, Pythagoras' theorem might be useful in computing the function φ. For instance, for U_c we have

$$A'D^2 + B'C^2 = AA'^2 + BB'^2 + AD^2 + BC^2.$$

But $AA'^2 + BB'^2 = AB^2$ and $AD^2 + BC^2 = AB^2$. Hence $U_c = 2$.

This method will also yield generalizations. Take points A_*, B_*, C_*, D_* with $\mathbf{AA}_* = \lambda \mathbf{AA'}$, $\mathbf{BB}_* = \lambda \mathbf{BB'}$, $\mathbf{BC}_* = \mu \mathbf{BC}$, $\mathbf{AD}_* = \mu \mathbf{AD}$. Then it follows easily that $\varphi(A_* D_*, B_* C_*) = \lambda^2 + \mu^2$. $\qquad\square$

For points X and Y, let $X \oplus Y$ be the center of the square built on the segment XY such that the triangle $X(X \oplus Y)Y$ has the positive orientation (counterclockwise). When the point $X \oplus Y$ is shortened to M, then M^* denotes $Y \oplus X$.

The midpoints G, H, G', H' of the segments AC, BD, AC', BD' and the top N of the semicircle over AB are used in the next theorem. In other words, $N = B \oplus A$. The center O of the circle (i. e., the midpoint of the segment AB; the origin of the rectangular coordinate system) appears also.

Theorem 3. *Let* $U_d = \varphi(NG, NH)$, $V_d = \varphi(NG', NH')$, $U_e = \varphi(OG, OH)$ *and* $V_e = \varphi(OG', OH')$ *(see Figure 4).*
The following statements are equivalent.
(a) $m = \sqrt{2}$,
(d) $U_d = \frac{3}{4}$, (d') $V_d = \frac{3}{4}$, (d'') $U_d = V_d$, (d*) $U_d = 3\,U_e$,
(e) $U_e = \frac{1}{4}$, (e') $V_e = \frac{1}{4}$, (e'') $U_e = V_e$, (e*) $V_d = 3\,V_e$.

Proof. This time the differences $U_d - \frac{3}{4}$ and $U_e - \frac{1}{4}$ both simplify to $\frac{t^2(m^2-2)}{4\,\vartheta^2}$, which has the factor $m^2 - 2$ again. Similarly, $V_d - U_d$ and $V_e - U_e$ both are equal $\frac{m\,v\,t^3(m^2-2)}{\eta^2\,\vartheta^2}$. Finally, $3\,U_e - U_d$ is $\frac{t^2(m^2-2)}{2\,\vartheta^2}$. The other differences are analogous quotients that have η instead of ϑ.

The following synthetic proof shows that the statements (a) and (b) together imply (d) and (e).

A dilatation with center A and scale factor 2 maps GO on to CB, thus $GO = \frac{CB}{2}$; similarly $OH = \frac{AD}{2}$. Consequently for U_e we have

$$OG^2 + OH^2 = \tfrac{BC^2}{4} + \tfrac{AD^2}{4} = \tfrac{1}{4}AB^2.$$

Similarly, for U_d we have $NG^2 = NO^2 + OG^2$ and $NH^2 = NO^2 + OH^2$ so that

$$NG^2 + NH^2 = 2\,NO^2 + \frac{BC^2 + AD^2}{4} = \frac{AB^2}{2} + \frac{AB^2}{4} = \frac{3}{4}AB^2.$$

$\qquad\square$

Let G_s, H_s, G'_s, H'_s be the points that divide the segments NG, NH, NG', NH' in the same ratio $s \neq -1$ (i. e., $NG_s : G_s G = s : 1$, etc.).

Theorem 4. *Let* $m_s = \frac{s^2+2}{4(s+1)^2}$, $n_s = \frac{3\,s^2}{4(s+1)^2}$,
$U_f = \varphi(OG_s, OH_s)$, $V_f = \varphi(OG'_s, OH'_s)$,
$U_g = \varphi(NG_s, NH_s)$, $V_g = \varphi(NG'_s, NH'_s)$.
If $s \neq 0$, *then the following statements are equivalent.*
(a) $m = \sqrt{2}$,
(f) $U_f = m_s$, (f') $V_f = m_s$, (f'') $U_f = V_f$,
(g) $U_g = n_s$, (g') $V_g = n_s$, (g'') $U_g = V_g$.

Proof. Since $G_s = \left(\frac{-r\,s\,t(m+t)}{(s+1)\vartheta}, \frac{r}{s+1}\right)$ and $H_s = \left(\frac{r\,s(1+z)}{(s+1)\vartheta}, \frac{r}{s+1}\right)$, the difference $U_f - m_s$ is $\frac{s^2 t^2 (m^2-2)}{4(s+1)^2 \vartheta^2}$. The other parts are proved with analogous arguments. □

Theorem 5. *Let* $\lambda = \frac{3\,s^2}{s^2+2}$. *If* $s \neq 0$, 1, *then the following statements are equivalent.*

(a) $m = \sqrt{2}$,
(f*) $U_g = \lambda\,U_f$,
(g*) $V_g = \lambda\,V_f$.

Proof. For $s \neq 0$, 1, the equivalence of (a) and (f^*) is a consequence of the equality $\lambda\,U_f - U_g = \frac{s^2\,t^2(s-1)(m^2-2)}{2\,(s+1)(s^2+2)\,\vartheta^2}$. □
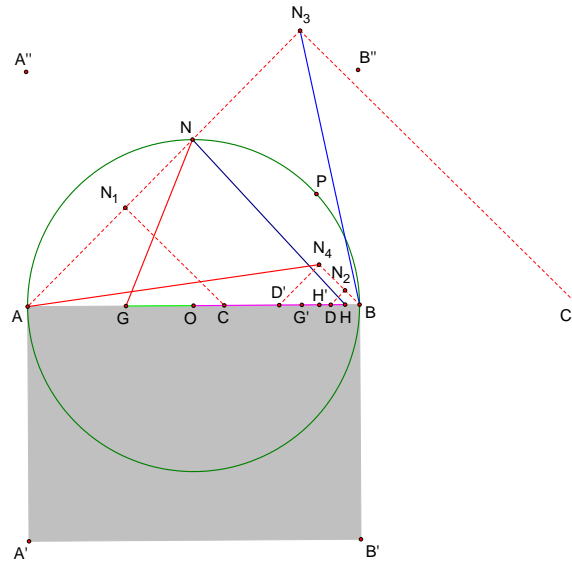
Figure 4. Points O, N, $N_1, \ldots N_4$ in Theorems 3 and 6.

Let N_1, N_2, N_3, N_4 denote the highest points on the semicircles built on the segments AC, BD, AC', BD' above the line AB. In other words, $N_1 = C \oplus A$, $N_2 = B \oplus D$, $N_3 = C' \oplus A$, $N_4 = B \oplus D'$.

Theorem 6. *Let* $U_h = \varphi(BN_1, AN_2)$, $V_h = \varphi(BN_3, AN_4)$,
$U_i = \varphi(NN_1, NN_2)$, $V_i = \varphi(NN_3, NN_4)$ (see Figure 4).
The following statements are equivalent.

(a) $m = \sqrt{2}$,
(h) $U_h = \frac{3}{2}$,   (h′) $V_h = \frac{3}{2}$,   (h″) $U_h = V_h$,   (h*) $3\,U_i = U_h$,
(i) $U_i = \frac{1}{2}$,   (i′) $V_i = \frac{1}{2}$,   (i″) $U_i = V_i$,   (i*) $3\,V_i = V_h$.

Proof. Since $N_1 = \left(\frac{-r\,t(m+t)}{\vartheta}, \frac{r}{\vartheta} \right)$ and $N_2 = \left(\frac{r(1+z)}{\vartheta}, \frac{r\,t^2}{\vartheta} \right)$, we get

$$U_h - \tfrac{3}{2} = U_i - \tfrac{1}{2} = \frac{t^2\left(m^2-2\right)}{2\,\vartheta^2}.$$

This proves the equivalence of (a) with (h) and (i). The proofs of the other equivalences are similar.

The synthetic proof of the implication $(a) \Rightarrow (h)$ uses the right-angled triangles AHN_2 and BGN_1 to get $AN_2^2 = (a+b+\frac{c}{2})^2 + \frac{c^2}{4}$ and $BN_1^2 = (\frac{a}{2}+b+c)^2 + \frac{a^2}{4}$. But $b^2 = 2\,a\,c$ implies $AN_2^2 + BN_1^2 = \frac{3}{2}AB^2$.

Let $a' = \frac{a}{\sqrt{2}}$, etc. For the implication $(a) \Rightarrow (i)$, from the isosceles right-angled triangles ABN, ACN_1, BDN_2 we get $NN_1^2 = (b'+c')^2$ and $NN_2^2 = (a'+b')^2$. But $b^2 = 2\,a\,c$ implies $NN_1^2 + NN_2^2 = \frac{1}{2}AB^2$. $\square$

In the following theorem we also use the points N_1, N_2, N_3 and N_4. However, we do not use the function φ.

Theorem 7. *The following statements are equivalent.*
(a) $m = \sqrt{2}$,
(j) $|N_1N_2| = |AN|$,   (j') $|N_3N_4| = |AN|$,   (j'') $|N_1N_2| = |N_3N_4|$,
(k) $|N_1N_2|^2 + |N_2N_3|^2 + |N_3N_4|^2 + |N_4N_1|^2 = 2\,|AB|^2$.

Proof. For $(a) \Leftrightarrow (j)$, we easily get $|N_1N_2|^2 - |AN|^2 = \frac{2\,r^2t^2\left(m^2-2\right)}{\vartheta^2}$.

Since the coordinates of N_3 and N_4 are $\left(\frac{r\,t(m-t)}{\eta}, \frac{r}{\eta} \right)$ and $\left(\frac{r(1-z)}{\eta}, \frac{r\,t^2}{\eta} \right)$,

$$|N_1N_2|^2 + |N_2N_3|^2 + |N_3N_4|^2 + |N_4N_1|^2 - 2\,|AB|^2 = \frac{8\,r^2\,t^2(m^2-2)(v^2+z^2)}{\eta^2\,\vartheta^2}.$$

This shows that $(a) \Leftrightarrow (k)$.

Note that by projecting BC orthogonally on to AN, we obtain NN_1, and its length is $\frac{BC}{\sqrt{2}}$. Similarly, $|NN_2| = \frac{AD}{\sqrt{2}}$. The fourth vertex of the rectangle with sides NN_1, NN_2 is the point M_1 used later in the paper. Hence $|NM_1| = |N_1N_2| = |AN|$, proving $(a) \Rightarrow (o)$ in Theorem 9 below. $\square$

Notice that $|N_1N_2^*|^2 + |N_2^*N_3^*|^2 + |N_3^*N_4|^2 + |N_4N_1|^2 = 2\,|AB|^2$ if and only if $m = 1$.

Let $N_5 = A \oplus D$, $N_6 = C \oplus B$, $N_7 = A \oplus D'$ and $N_8 = C' \oplus B$.

Theorem 8. *Let $U_\ell = \varphi(AN_5, BN_6)$, $V_\ell = \varphi(AN_7, BN_8)$,*
$U_m = \varphi(GN_6, HN_5)$, $V_m = \varphi(G'N_8, H'N_7)$ and
$U_n = \varphi(NN_5, NN_6)$, $V_n = \varphi(NN_7, NN_8)$.
The following ten statements are equivalent:
(a) $m = \sqrt{2}$,
(ℓ) $U_\ell = \frac{1}{2}$,   (ℓ') $V_\ell = \frac{1}{2}$,   (ℓ'') $U_\ell = V_\ell$,
(m) $U_m = \frac{3}{4}$,   (m') $V_m = \frac{3}{4}$,   (m'') $U_m = V_m$,
(n) $U_n = \frac{3}{2}$,   (n') $V_n = \frac{3}{2}$,   (n'') $U_n = V_n$.

Proof. Since $N_5 = \left(\frac{-r\,t^2}{\vartheta}, \frac{-r(1+z)}{\vartheta}\right)$ and $N_6 = \left(\frac{r}{\vartheta}, \frac{-r\,t(m+t)}{\vartheta}\right)$, we obtain $U_\ell - \frac{1}{2} = \frac{t^2\left(m^2-2\right)}{2\,\vartheta^2}$. This shows the equivalence of (a) and (ℓ). The other equivalences have similar proofs.

In order to prove the implication $(a) \Rightarrow (\ell)$ in synthetic fashion, from the isosceles right-angled triangles ADN_5 and BCN_6, we get $AN_5^2 + BN_6^2 = \frac{AD^2}{2} + \frac{BC^2}{2} = \frac{1}{2}AB^2$. $\qquad\square$

Let $\lambda_s = \frac{3((s+1)^2+1)}{4(s+1)^2}$. The equality $\varphi(G_s N_6, H_s N_5) = \lambda_s$ is true if and only if $m = \sqrt{2}$. In fact, this is the first equivalence from another similar group that involve points G_s and H_s.
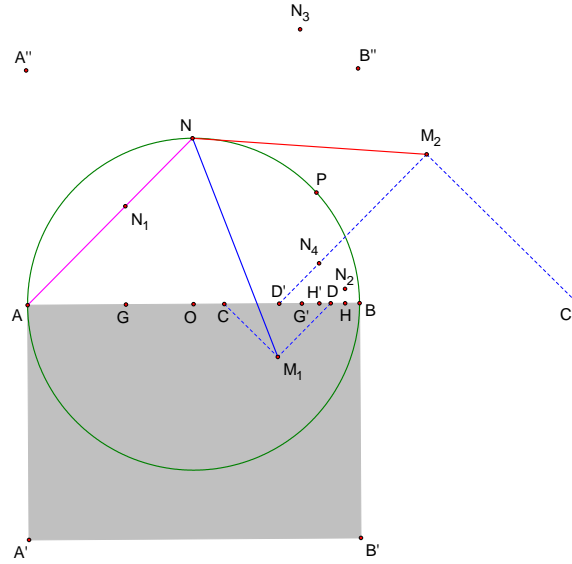
Figure 5. Points M_1 and M_2 in Theorem 9.

The next theorem uses the centers of squares on the segments CD and $C'D'$. Let $M_1 = C \oplus D$ and $M_2 = C' \oplus D'$.

Theorem 9. *Let* $U_o = |N\,M_1| - |A\,N|$, $V_o = |N\,M_2| - |A\,N|$,
$U_p = \varphi(M_1 N_1, M_1 N_2)$ *and* $V_p = \varphi(M_2 N_3, M_2 N_4)$ (see Figure 5).
The following statements are equivalent:
(a) $m = \sqrt{2}$,
(o) $U_o = 0$,   (o$'$) $V_o = 0$,   (o$''$) $U_o = V_o$,
(p) $U_p = \frac{1}{2}$,   (p$'$) $V_p = \frac{1}{2}$,   (p$''$) $U_p = V_p$.

Proof. Since $M_1 = \left(\frac{r\,u}{\vartheta}, -\frac{r\,z}{\vartheta}\right)$, the difference $|M_1 N|^2 - |AN|^2$ is $\frac{2\,r^2\,t^2(m^2-2)}{\vartheta^2}$. Similarly, $|M_2 N|^2 - |M_1 N|^2 = \frac{8\,r^2\,t^2\,v\,z(m^2-2)}{\eta^2\vartheta^2}$. This shows that $(a) \Leftrightarrow (o)$ and $(a) \Leftrightarrow (o'')$. The $(a) \Rightarrow (o)$ is proved also as follows.

From the right-angled triangle NN_1M_1, since $\frac{b^2}{2} = ac$, we get $NM_1^2 = (a'+b')^2 + (b'+c')^2 = a'^2 + b^2 + c'^2 + ab + bc = (a'+b'+c')^2 = NA^2$. $\square$

For any point X in the plane, let G_1, G_2, G_3, G_4, G_5 and G_6 denote the centroids of the triangles $ACX, CDX, DBX, AC'X, C'D'X$ and $BD'X$.

Theorem 10. *Let* $U_q = \varphi(G_2G_1, G_2G_3)$ *and* $V_q = \varphi(G_5G_4, G_5G_6)$.
The following statements are equivalent:
(a) $m = \sqrt{2}$,
(q) $U_q = \frac{1}{9}$, (q') $V_q = \frac{1}{9}$, (q'') $U_q = V_q$.

Proof. If $X = (x, y)$, then the points G_1, G_2 and G_3 have the same ordinate $\frac{y}{3}$ while their abscissae are $\frac{x}{3} - \frac{2rt(m+t)}{3\vartheta}$, $\frac{x}{3} + \frac{2ru}{3\vartheta}$ and $\frac{x}{3} + \frac{2r(z+1)}{3\vartheta}$. It follows that $U_q - \frac{1}{9} = \frac{t^2(m^2-2)}{9\vartheta^2}$ that proves $(a) \Leftrightarrow (q)$.

The implication $(b) \Rightarrow (q)$ could be proved as follows. Let I denote the midpoint of the segment CD. A dilatation with center C and scale factor 2 maps GI on to AD, thus $GI = \frac{AD}{2}$; similarly $HI = \frac{BC}{2}$. Hence $\varphi(GI, HI) = \frac{1}{4}$. On the other hand, a dilatation with center X and scale factor $\frac{3}{2}$ maps G_1G_2 on to GI, thus $G_1G_2 = \frac{2}{3}GI$; similarly $G_3G_2 = \frac{2}{3}HI$. Hence $U_q = \frac{1}{9}$. $\square$

Let U and V be the midpoints of the segments CC' and DD'.

Theorem 11. *Let* $U_s = \varphi(NU, NV)$, $U_t = \varphi(OU, OV)$ *and* $V_t = \varphi(N_6U, N_5V)$.
The following statements are equivalent:
(a) $m = \sqrt{2}$,
(s) $U_s = 1$,
(t) $U_t = \frac{1}{2}$, (t') $V_t = \frac{1}{2}$, (t'') $U_t = V_t$.

Proof. Since abscissae of U and V are $\frac{r(uv+z^2)}{\eta\vartheta}$ and $\frac{r(uv-z^2)}{\eta\vartheta}$, we get $U_s - 1 = U_t - \frac{1}{2} = \frac{t^2v^2(m^2-2)}{\eta^2\vartheta^2}$. This proves $(a) \Leftrightarrow (s)$ and $(a) \Leftrightarrow (t)$. $\square$

Theorem 12. *Let* $W = U \oplus V$, $U_u = |WO| - \frac{|AB|}{2}$,
$U_{v(i,j)} = \varphi(WN_i, WN_j)$ *for* $i \in \{1,3\}$ *and* $j \in \{2,4\}$ *and* $U_w = \varphi(W^*N, WN)$.
The following statements are equivalent:
(a) $m = \sqrt{2}$,
(u) $U_u = 0$,
(w) $U_w = 1$,
(x) *the lines* WN_1 *and* WN_2 *are perpendicular,*
(y) *the lines* WN_3 *and* WN_4 *are perpendicular,*
($v_{i,j}$) $U_{v(i,j)} = \frac{1}{2}$ *for* $i \in \{1,3\}$ *and* $j \in \{2,4\}$.

Proof. Since the coordinates of the point W is the pair $\left(\frac{ruv}{\eta\vartheta}, \frac{rz^2}{\eta\vartheta} \right)$, we get that $|WO|^2 - r^2 = \frac{2r^2t^2v^2(m^2-2)}{\eta^2\vartheta^2}$. This proves $(a) \Leftrightarrow (u)$.

For the equivalence $(a) \Leftrightarrow (x)$, note that the lines WN_1 and WN_2 have equations

$$(z^2 - \eta)x + (z^2 - \vartheta)y = \lambda \quad \text{and} \quad (m^2 - \eta)x - (m^2 - \vartheta)y = \mu,$$

where λ and μ are real numbers. These lines are perpendicular if and only if $2\,v\,z(m^2-2)$ is zero. $\qquad\square$

Let $K_1 = B \oplus N_1$, $K_2 = N_2 \oplus A$, $K_3 = B \oplus N_3$, $K_4 = N_4 \oplus A$. These points can be defined more simply. They all are at the same hight as N and vertically above the points N_6, N_5, N_8, N_7, respectively.

Theorem 13. *Let $\lambda = \frac{7}{4} + \sqrt{2}$, $U_z = \varphi(A'K_2, B'K_1)$ and $V_z = \varphi(A'K_4, B'K_3)$. For the statements*
(a) $m = \sqrt{2}$,
(z) $U_z = \lambda$,   (z') $V_z = \lambda$,
we have (a)$\Rightarrow$(z) *and* (a)$\Rightarrow$(z').

Proof. Since K_2 and K_1 have abscissae $-\frac{r\,t^2}{\vartheta}$ and $\frac{r}{\vartheta}$, we conclude that $\lambda - U_z = \frac{[(4(m+1)\vartheta^2 - z^2)\sqrt{2} + m(z+2\,v)(3\,z+2\,v)](m-\sqrt{2})}{4\,m^2\,\vartheta^2}$. When (a) is true, then this difference is zero. The proof of $(a) \Rightarrow (z')$ is similar. $\qquad\square$

Let $K = P \oplus A'$, $L = P \oplus B'$, $S = P \oplus A''$, $T = P \oplus B''$.

Theorem 14. *Let $\lambda = 1 + \frac{\sqrt{2}}{2}$, $U_\alpha = \varphi(AK^*, BL)$ and $V_\alpha = \varphi(AS, BT^*)$. The following statements are equivalent:*
(a) $m = \sqrt{2}$,
(α) $U_\alpha = \lambda$,   (α') $V_\alpha = \lambda$.

Proof. Since $\left(\frac{r(\vartheta - t\,z)}{m\,v}, -\frac{r(m+\eta)}{m\,v}\right)$ and $\left(\frac{r(m-\vartheta)}{m\,v}, -\frac{r(t\,z+\eta)}{m\,v}\right)$ are the coordinates of the points K^* and L, we get that $\lambda - U_\alpha$ is equal to $\frac{(1+\sqrt{2})(m-\sqrt{2})(m+2-\sqrt{2})}{2\,m^2}$. It follows from Theorem 18 that the same holds for V_α. $\qquad\square$

Let S_1, T_1, S_2 and T_2 denote the midpoints of the segments $A'C$, $B'D$, $A'C'$ and $B'D'$. Note that (a) implies that

$$\varphi(G_s S_1, H_s T_1) = \varphi(G'_s S_2, H'_s T_2) = \frac{(s+1+\sqrt{2})^2 + 1}{4(s+1)^2}.$$

Theorem 15. *Let $\lambda_\pm = 1 \pm \frac{\sqrt{2}}{2}$,*
$U_\beta = \varphi(NS_1, NT_1)$, $V_\beta = \varphi(NS_2, NT_2)$,
$U_\gamma = \varphi(N^*S_1, N^*T_1)$, $V_\gamma = \varphi(N^*S_2, N^*T_2)$,
$U_\delta = \varphi(OS_1, OT_1)$ *and* $V_\delta = \varphi(OS_2, OT_2)$.
Consider the statements
(a) $m = \sqrt{2}$,
(β) $U_\beta = \lambda_+$,   (β') $V_\beta = \lambda_+$,   (β'') $U_\beta = V_\beta$,
(γ) $U_\gamma = \lambda_-$,   (γ') $V_\gamma = \lambda_-$,   (γ'') $U_\gamma = V_\gamma$,
(δ) $U_\delta = \frac{1}{2}$,   (δ') $V_\delta = \frac{1}{2}$,   (δ'') $U_\delta = V_\delta$.
The following are true:
(i) *The statements* (a), (β''), (γ'') *and* (δ'') *are equivalent.*
(ii) (a) *implies each of the statements* (β), (β'), (γ), (γ'), (δ) *and* (δ').

Proof. For the implication $(a) \Rightarrow (\delta)$, from the right-angled triangles OGS_1 and OHT_1 and Theorem 3, we get that the sum $OS_1^2 + OT_1^2$ is equal to $(OG^2 + GS_1^2) + (OH^2 + HT_1^2)$, i. e., to $(OG^2 + OH^2) + \frac{AB^2}{4} = \frac{1}{2}AB^2$. $\qquad\square$

For points X and Y, let ϱ_X^Y be the reflection of the point X in the point Y. Let $Q = \varrho_A^D$, $R = \varrho_B^C$, $Q' = \varrho_A^{D'}$, $R' = \varrho_B^{C'}$.

Theorem 16. *Let $U_\varepsilon = \varphi(A'Q, B'R)$ and $V_\varepsilon = \varphi(A'Q', B'R')$.*
Consider the statements
(a) $\quad m = \sqrt{2}$,
$(\varepsilon) \quad U_\varepsilon = 5$, $\quad (\varepsilon') \quad V_\varepsilon = 5$, $\quad (\varepsilon'') \quad U_\varepsilon = V_\varepsilon$.
The following are true:
(i) *The statements* (a), (ε'') *are equivalent.*
(ii) (a) *implies each of the statements* (ε) *and* (ε').

Proof. Since $Q = \left(\frac{r(u+3\,z+2)}{\vartheta}, 0\right)$ and $R = \left(\frac{r(3\,u-3\,z-2)}{\vartheta}, 0\right)$, we get that $5 - U_\varepsilon$ is equal to $\frac{\eta(m^2-2)(\vartheta+2\,z)}{m^2\,\vartheta^2}$. From this we conclude that $(a) \Rightarrow (\varepsilon)$.

From the right-angled triangles $AA'Q$ and $BB'R$, we get that $A'Q^2$ and $B'R^2$ are $4(a+b)^2 + A'A^2$ and $4(b+c)^2 + B'B^2$. By adding we conclude from (1) that $U_\varepsilon = 5$. Also, we have $\varphi(N_5 Q, N_6 R) = \frac{5}{2}$ and $\varphi(AQ, BR) = 4$. $\qquad\square$

3. Common properties for all ratios

Of course, there are many properties that hold for all ratios m. The following are two examples of such properties.
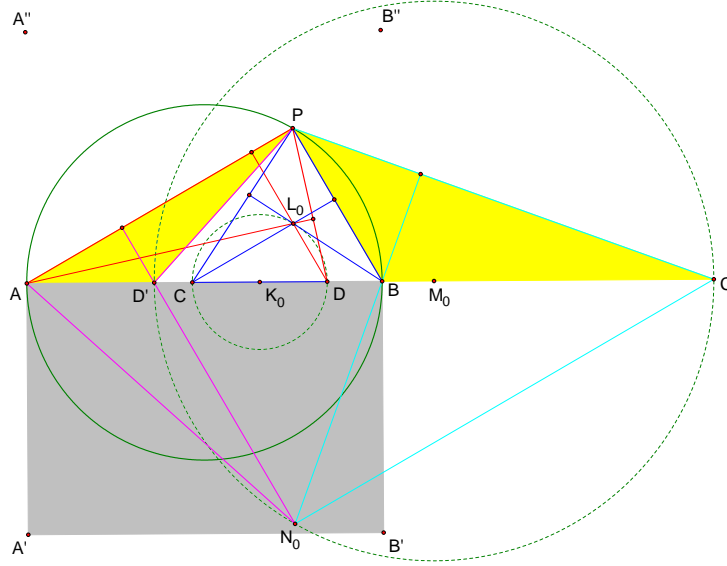
Figure 6. Common orthocenters in Theorem 17.

Theorem 17. (i) *The triangles ADP and BCP have the same orthocenter that lies on a circle with the segment CD as a diameter.*

(ii) *The triangles $AD'P$ and $BC'P$ have a common orthocenter. It lies on a circle with the segment $C'D'$ as a diameter.*

Proof. The orthocenters of the triangles ADP and BCP both have coordinates $\left(\frac{r\,u}{v}, \frac{2\,m\,r\,t^2}{\vartheta\,v}\right)$.

If K_0 is the midpoint of the segment CD and L_0 is the orthocenter of the triangle ADP, then $|CK_0|^2 - |K_0L_0|^2 = 0$ so that L_0 lies on the circle with the segment CD as a diameter. $\square$

Theorem 18. *The equalities*

$$\varphi(AK, BL^*) = \varphi(AS^*, BT) \quad and \quad \varphi(AK^*, BL) = \varphi(AS, BT^*)$$

hold for all points P on the circle and every ratio m.

Proof. Both $\varphi(AK, BL^*)$ and $\varphi(AS^*, BT)$ have the value $\frac{(m-1)^2+1}{2\,m^2}$ while both $\varphi(AK^*, BL)$ and $\varphi(AS, BT^*)$ have the value $\frac{(m+1)^2+1}{2\,m^2}$. $\square$

4. Some other interesting ratios

Our last result is different because in it some other ratios besides $\sqrt{2}$ appear. This has happened already in a comment following the proof of Theorem 9. Let $\lambda = 1 - \frac{\sqrt{2}}{2}$.

Theorem 19. *The ratio m is either $\sqrt{2}$ or $2 + \sqrt{2}$ if and only if for every point P on the circle the equalities $\varphi(AK, BL^*) = \lambda$ and/or $\varphi(AS^*, BT) = \lambda$ hold.*

Proof. Since $\left(-\frac{r(\vartheta+t\,z)}{m\,v}, \frac{r(m-\eta)}{m\,v}\right)$ and $\left(\frac{r(m+\vartheta)}{m\,v}, \frac{r(t\,z-\eta)}{m\,v}\right)$ are the coordinates of the points K and L^*, we get that $\lambda - \varphi(AK, BL^*)$ will factor out as the quotient $\frac{\left(1-\sqrt{2}\right)\left(m-\sqrt{2}\right)\left(m-2-\sqrt{2}\right)}{2\,m^2}$. The same is true for $\varphi(AS^*, BT)$ by Theorem 18. $\square$

Conclusion. Fermat conjectured that $(a) \Rightarrow (b)$ and Euler proved this. We added (b'), (b''), $(c), \ldots, (\varepsilon'')$ and discovered here that many are equivalent. Also, in related papers, we consider how to replace the circle with an arbitrary conic and propose the space versions for the sphere and some other surfaces (see [2], [3], [4] and [5]).

References

[1] E. C. Catalan, *Théorèmes et problèmes de Géométrie*, 6e ed., Paris, 1879.

[2] Z. Čerin, Fermat bases of conics, to appear in *J. Geom.*.

[3] Z. Čerin, On the modified Fermat problem, to appear in *Missouri J. Math. Sci.*

[4] Z. Čerin, Rectangular hexahedrons as Fermat bases of quadrics, to appear in *Sarajevo J. Math.*

[5] Z. Čerin, Generalization of a geometry problem posed by Fermat, *J. Geom. Graphics*, 17 (2013) 1–5.

[6] L. Euler, Various geometric demonstrations, New Commentaries of the Petropolitan Academy of Sciences I, (1747/48), 1750, 49–66 (English translation prepared in 2005 by Adam Glover).

[7] F. G. -M., *Exercices de Géométrie (6e ed.)*, Éditions Jacques Gabay, Paris 1991. (Reprint of the 6th edition published by Mame and De Gigord, Paris 1920.)

[8] M. L. Hacken, Sur un théorème de Fermat, *Mathesis*, 27 (1907), 181, 264.

[9] Ž. Hanjš and V. P. Volenec, O jednom (davno riješenom) Fermatovom problemu, *Matematičko-fizički*, list LXI 4 (2010–2011) 225 (in croatian).

[10] E. Lionnet, Solutions des questions proposées, *Nouvelles Annales de Mathématiques*, Series 2, 9 (1870) 189–191.

[11] E. Sandifer, *A forgotten Fermat problem*, How Euler Did It, MAA, Washington, DC, 2007, available at www.maa.org/ed-sandifers-how-euler-did-it.

Zvonko Čerin: Kopernikova 7, 10010 Zagreb, CROATIA, Europe
E-mail address: cerin@math.hr

Jigsawing a Quadrangle from a Triangle

Floor van Lamoen

Abstract. For an acute-angled triangle ABC, we construct two isotomic points P and Q on BC and P' and Q' on AB and AC respectively, such that BPP' and CQQ' are right triangles which, when rotated about P' and Q' respectively through appropriate angles fit with $AP'Q'$ to a quadrangle with a new fourth vertex A'. We show that AA' passes trough the circumcenter O.

Given an acute-angled triangle ABC consider the construction of a pair of isotomic points P and Q on the side BC (with $BP = QC < \frac{1}{2} \cdot BC$) such that the perpendiculars to BC at P and Q intersect AB and AC at P' and Q' satisfying $P'Q' = PP' + QQ'$.
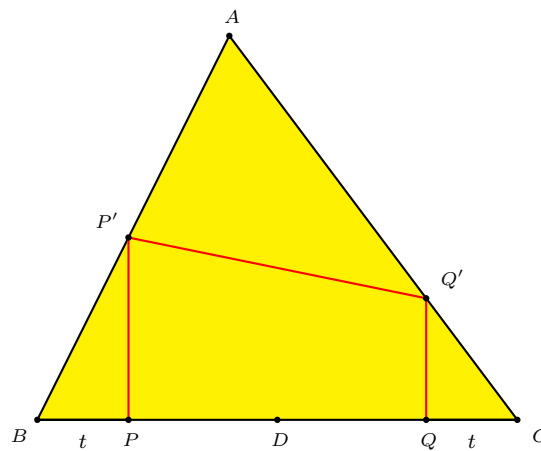
Figure 1

If we put $BP = QC = t$, then $PP' = t \cdot \tan B$, $QQ' = t \cdot \tan C$, and $P'Q' = t(\tan B + \tan C) = \frac{t \sin A}{\cos B \cos C}$. Applying the law of cosines to triangle $AP'Q'$, we have

$$\left(c - \frac{t}{\cos B}\right)^2 + \left(b - \frac{t}{\cos C}\right)^2 - 2\left(c - \frac{t}{\cos B}\right)\left(b - \frac{t}{\cos C}\right)\cos A = t^2 \cdot \frac{1 - \cos^2 A}{\cos^2 B \cos^2 C}.$$

Clearing denominators and rearranging terms, we have

$$(1 - \cos^2 A - \cos^2 B - \cos^2 C + 2\cos A \cos B \cos C)t^2$$
$$+ 2\cos B \cos C(b\cos B + c\cos C - a\cos A)t - a^2 \cos^2 B \cos^2 C = 0. \quad (1)$$

Making use of the following identities

$$b \cos B + c \cos C - a \cos A = 2a \cos B \cos C,$$
$$1 - \cos^2 A - \cos^2 B - \cos^2 C = 2 \cos A \cos B \cos C,$$

we rewrite (1) as

$$4t^2 \cos A + 4at \cos B \cos C - a^2 \cos B \cos C = 0 \qquad (2)$$

after cancelling a common factor $\cos B \cos C$. Writing $x = \frac{a}{2} - t$, or $2t = a - 2x$, we have

$$(a - 2x)^2 \cos A + 2a(a - 2x) \cos B \cos C - a^2 \cos B \cos C = 0$$
$$4x^2 \cos A - 4ax(\cos A + \cos B \cos C) + a^2(\cos A + \cos B \cos C) = 0$$
$$4x^2 \cos A - 4ax \sin B \sin C + a^2 \sin B \sin C = 0. \qquad (3)$$

From this,

$$x = \frac{a \sin B \sin C - a\sqrt{\sin B \sin C(\sin B \sin C - \cos A)}}{2 \cos A}$$
$$= \frac{a \sin B \sin C - a\sqrt{\sin B \cos B \cdot \sin C \cos C}}{2 \cos A} \qquad (4)$$

Applying the law of sines to triangle ABC, with $b = 2R \sin B$ and $c = 2R \sin C$ for the circumradius R, we have

$$\frac{2x}{a} = \frac{2R \sin B \sin C - 2R\sqrt{\sin B \sin C \cdot \cos B \cos C}}{2R \cos A}$$
$$= \frac{b \sin C - \sqrt{b \cos B \cdot c \cos C}}{2R \cos A}$$
$$= \frac{AX - \sqrt{BX \cdot XC}}{2R \cos A} = \frac{AX - X_1 X}{AH} = \frac{AX_1}{AH},$$

where H is the orthocenter of triangle ABC, and the altitude AX intersects the semicircle with diameter BC at X_1 (see Figure 2). This leads to the following construction of the trapezoid $PQQ'P'$.

Let O and G be the circumcenter and centroid of triangle ABC, and D the midpoint of BC.

(1) Construct the semicircle with diameter BC (on the same side of A) to intersect the A-altitude at X_1.

(2) Construct the line $X_1 G$ to intersect OD at X_2.

(3) Construct the parallels to OB and OC through X_2 to meet AC in P and Q respectively.

(4) Construct the perpendiculars to BC at P and Q to intersect AB and AC at P' and Q' respectively.

These points satisfy $PP' + QQ' = P'Q'$.

Proof. In Figure 2,

$$\frac{X_2 D}{OD} = \frac{PD}{BD} = \frac{2x}{a} = \frac{AX_1}{AH}.$$
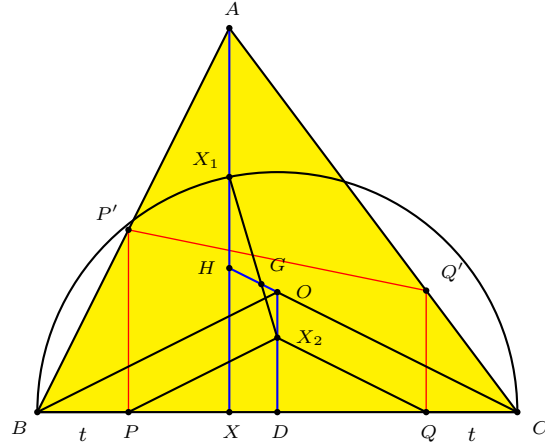
Figure 2.

Since $AH = 2 \cdot OD$, we have $AX_1 = 2 \cdot X_2D$, and $HX_1 = AH - AX_1 = 2 \cdot OD - 2 \cdot X_2D = 2 \cdot OX_2$. From this it is clear that X_1X_2 passes through the centroid G which divides HO in the ratio $HG : GO = 2 : 1$. □

We rotate triangle BPP' about P' and triangle CQQ' about C so that the images of P and Q coincide at a point on $P'Q'$. Then the images of B and C coincide at a point A'.
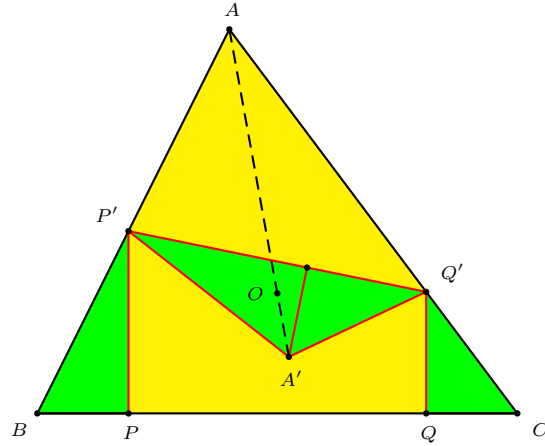
Figure 3.

Consider the quadrilateral $AP'A'Q'$. Note that $\angle Q'A'P' = \angle B + \angle C$, so that the quadrilateral is cyclic. Hence,

$$\angle Q'AA' = \angle Q'P'A' = \angle PP'B = \frac{\pi}{2} - B.$$

This means that AA' passes through the circumcenter O of triangle ABC.

By symmetry, if we perform similar constructions on the sides CA and AB, and obtain points B', C' corresponding to A', the lines BB' and CC' also pass through the circumcenter O, as does AA'.

References

[1] F. M. van Lamoen, ADGEOM messages 110, 113, 121 May 23, 2013;
http://tech.groups.yahoo.com/group/AdvancedPlaneGeometry/message/110.

[2] P. Yiu, ADGEOM messages 111, 112, May 23, 2013;
http://tech.groups.yahoo.com/group/AdvancedPlaneGeometry/message/111.

Floor van Lamoen: Ostrea Lyceum, Bergweg 4, 4461 NB Goes, The Netherlands
E-mail address: fvanlamoen@planet.nl

FORUM GEOM

Pedal Polygons

Daniela Ferrarello, Maria Flavia Mammana, and Mario Pennisi

Abstract. We study the pedal polygon $H_1 H_2 \cdots H_n$ of a point P with respect to a polygon **P**, where the points H_i are the feet of the perpendiculars drawn from P to the sides of **P**. In particular we prove that if **P** is a quadrilateral which is not a parallelogram, there exists one and only one point P for which the points H_i are collinear.

1. Introduction

Consider a polygon $A_1 A_2 \cdots A_n$ and call it **P**. Let P be a point and let H_i be the foot of the perpendicular from P to the line $A_i A_{i+1}$, $i = 1, 2, \ldots, n$ (with indices i taken modulo n). The points H_i usually form a polygon $H_1 H_2 \cdots H_n$, which we call the *pedal polygon* of P with respect to **P**, and denote by **H** (see Figure 1). We call P the *pedal point*. See ([2, p.22]) for the notion of pedal triangle.
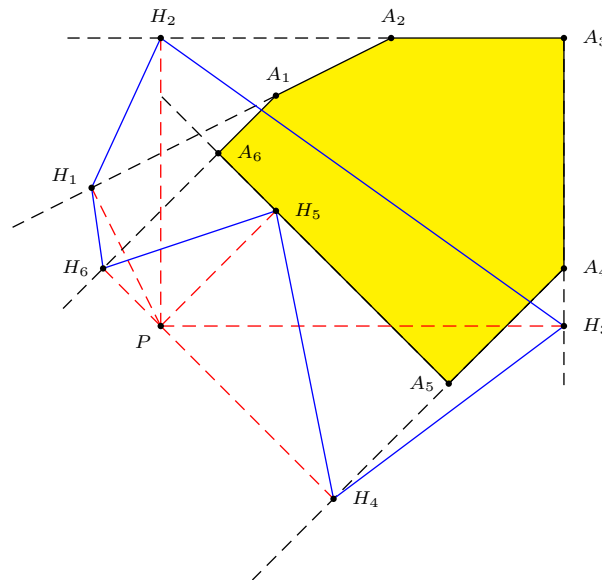
Figure 1

In this article we find some properties of the pedal polygon **H** of a point P with respect to **P**. In particular, when **P** is a triangle we find the points P such that the pedal triangle **H** is a right, obtuse or acute triangle. When **P** is a quadrilateral which is not a parallelogram, we prove that there exists one and only one point P for which the points H_i are collinear. Moreover, we find the points P for which

the pedal quadrilateral **H** of P has at least one pair of parallel sides. We also prove that, in general, there exists one and only one pedal point with respect to which **H** is a parallelogram. In the last part of the paper, we find some properties of the pedal polygon **H** in the general case of a polygon **P** with n sides.

2. Properties of the pedal triangle

Let **P** be a triangle. The pedal triangle of the circumcenter of **P** is the medial triangle of **P**; the one of the orthocenter is the orthic triangle of **P**; the one of the incenter is the Gergonne triangle of **P** (*i.e.*, the triangle whose vertices are the points in which the incircle of **P** touches the sides of **P**).

Theorem 1. [2, p.41] *If* **P** *is a triangle, the points* H_i *are collinear if and only if* P *lies on the circumcircle of* **P**.

The line containing the points H_i is called *Simson line* of the point P with respect to **P** (see Figure 2).
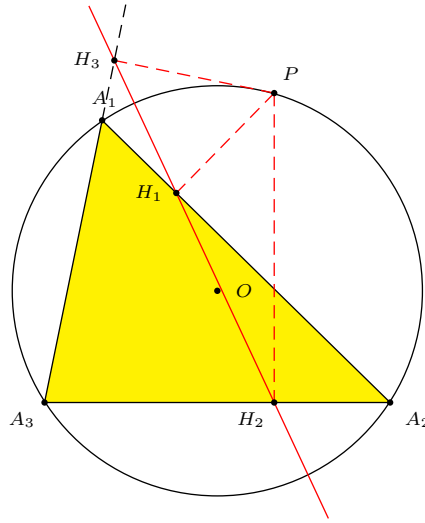
Figure 2.

Theorem 2. [1, p.108] *The points* **P** *for which the pedal triangle* **H** *is isosceles are all and only the points that lie on at least one of the Apollonius circles associated to the vertices of* **P**.

The Apollonius circle associated to the vertex A_i is the locus of points P such that $PA_{i+1} : PA_{i+2} = A_iA_{i+2} : A_iA_{i+1}$. The three Apollonius circles are coaxial and they intersect in the two isodynamic points of the triangle **P**, I_1 and I_2. Therefore, *the isodynamic points of* **P** *are the only points whose pedal triangles with respect to* **P** *are equilateral* (see Figure 3).
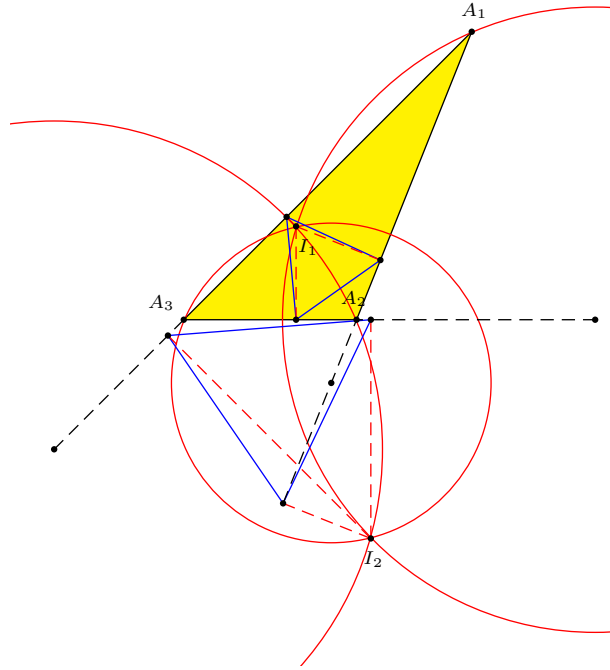
Figure 3

We will find now the points P whose pedal triangle is a right, acute, obtuse triangle. Let P be a point (see Figure 4) and let $A_i A_{i+1} = a_{i+2}$, $PA_i = x_i$, $H_i H_{i+1} = h_{i+2}$. Since the quadrilateral $A_i H_i P H_{i+2}$ is cyclic, $h_i = x_i \sin A_i$ ([2, p.2]).
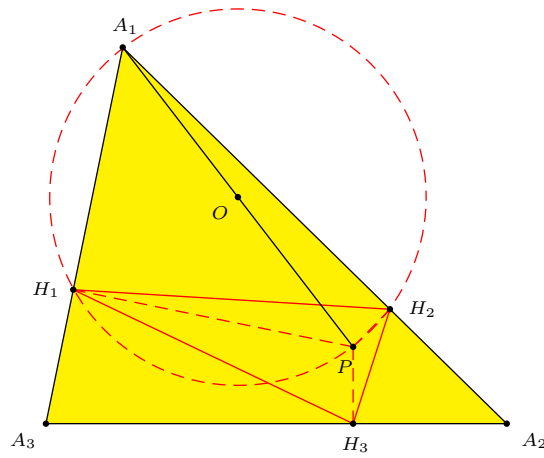
Figure 4

By the Pythagorean theorem and its converse, the pedal triangle of P is right in H_i if and only if

$$x_i^2 \sin^2 A_i \;=\; x_{i+1}^2 \sin^2 A_{i+1} \;+\; x_{i+2}^2 \sin^2 A_{i+2}.$$

By the law of sines, this is equivalent to

$$a_i^2 x_i^2 \;=\; a_{i+1}^2 x_{i+1}^2 \;+\; a_{i+2}^2 x_{i+2}^2. \tag{1}$$

This relation represents the locus γ_i of points P for which the triangle $\mathbf{H}$ is right in H_i. Therefore, the locus of points P whose pedal triangle is a right triangle is $\gamma_1 \cup \gamma_2 \cup \gamma_3$. Observe that γ_i contains the points A_{i+1} and A_{i+2}; moreover, γ_i and γ_{i+1} intersect only in the point A_{i+2}.

We verify now that γ_1 is a circle. Set up an orthogonal coordinate system such that $A_2 \equiv (1,0)$ and $A_3 \equiv (-1,0)$; let $A_1 \equiv (a,b)$ and $P \equiv (x,y)$. The relation (1) becomes:

$$4((x-a)^2+(y-b)^2) = ((a+1)^2+b^2)((x-1)^2+y^2)+((a-1)^2+b^2)((x+1)^2+y^2).$$

Simplifying, we obtain the equation of a circle:

$$(a^2 + b^2 - 1)(x^2 + y^2) + 4by - (a^2 + b^2 - 1) = 0.$$

Moreover, it is not hard to verify that the tangents to the circumcircle of $\mathbf{P}$ in the points A_2 and A_3 pass through the center of γ_1.

Analogously the same holds for γ_2 and γ_3. We can then state that γ_i is a circle passing through the points A_{i+1} and A_{i+2}; the tangents to the circumcircle of $\mathbf{P}$ in the points A_{i+1} and A_{i+2} pass through the center C_i of γ_i; moreover, γ_i and γ_{i+1} are tangent in A_{i+2}. Then, if $C_1 C_2 C_3$ is the tangential triangle of $A_1 A_2 A_3$, γ_i is the circle with center C_i passing through A_{i-1} and A_{i+1} (see Figure 5).
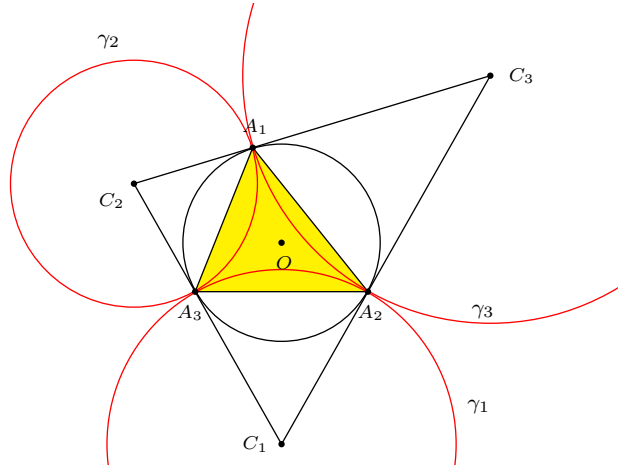
Figure 5

Observe that, by the law of cosines, the angle in H_i of the pedal triangle of P is obtuse if and only if:

$$a_i^2 x_i^2 > a_{i+1}^2 x_{i+1}^2 + a_{i+2}^2 x_{i+2}^2,$$

i.e., the point P lies inside the circle γ_i. Thus, we have established the following theorem.

Theorem 3. *The pedal triangle of a point P is*
(a) *a right triangle if and only if P lies on one of the circles γ_i,*
(b) *an obtuse triangle if and only if P is inside one of the circles γ_i,*
(c) *an acute triangle if and only if P is external to all the circles γ_i.*

3. Properties of the pedal quadrilateral

Let $\mathbf{P}$ be a cyclic quadrilateral. The pedal quadrilateral of the circumcenter of $\mathbf{P}$ is the Varignon parallelogram of $\mathbf{P}$, and the one of the anticenter ([6, p.152]) is the principal orthic quadrilateral of $\mathbf{P}$ ([5, p.80]).

Let $\mathbf{P}$ be a tangential quadrilateral. The pedal quadrilateral of the incenter of $\mathbf{P}$ is the contact quadrilateral of $\mathbf{P}$, *i.e.*, the quadrilateral whose vertices are the points in which the incircle of $\mathbf{P}$ touches the sides of $\mathbf{P}$.

For a generic quadrilateral, we consider the problem of finding the pedal points for which the points H_i are collinear.

It is easy to verify that if $\mathbf{P}$ has only one pair of parallel sides, there is only one pedal point P for which the points H_i are collinear. P is the common point to the lines containing opposite and non parallel sides of $\mathbf{P}$, and the points H_i lie on the perpendicular from P to the parallel sides of $\mathbf{P}$. On the other hand, if $\mathbf{P}$ is a parallelogram, there is no point with respect to which the points H_i are collinear.
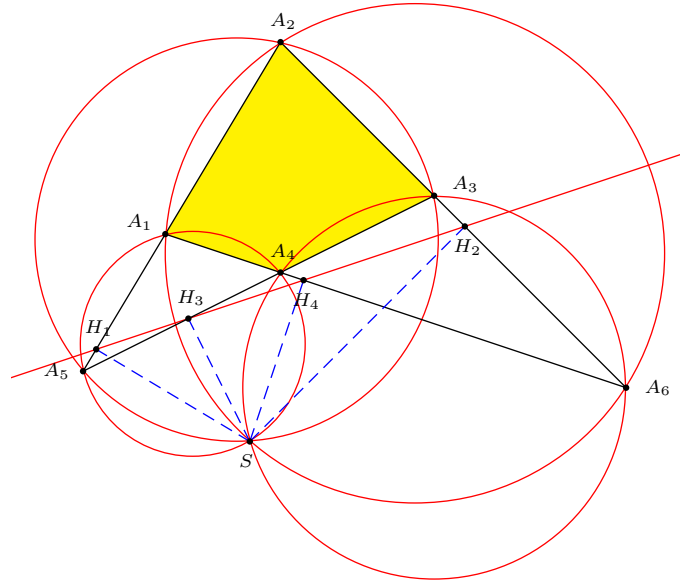
Figure 6

Suppose now that $\mathbf{P}$ is a quadrilateral without parallel sides (see Figure 6). Let A_5 be the common point to the lines $A_1 A_2$ and $A_3 A_4$, and A_6 the common point

to A_2A_3 and A_1A_4. Consider the four triangles $A_1A_2A_6$, $A_2A_3A_5$, $A_3A_4A_6$, $A_1A_4A_5$, and let $\mathcal{C}_1, \mathcal{C}_2, \mathcal{C}_3, \mathcal{C}_4$ be their circumcircles, respectively.

If the pedal point P lies on one of the circles $\mathcal{C}_i$, then, by Theorem 1, at least three of the points H_i are collinear. It follows that the four points H_i are collinear if and only if P lies in every $\mathcal{C}_i$. The four circles are concurrent in the Miquel point of the quartet of lines containing the sides of $\mathbf{P}$ ([3, p.82]). Thus, we have established the following theorem.

Theorem 4. *If $\mathbf{P}$ is a quadrilateral, that is not a parallelogram, there exists one and only one pedal point with respect to which the points H_i are collinear.*

We call this point the *Simson point* of the quadrilateral $\mathbf{P}$, and denote it by S. We call the *Simson line* of $\mathbf{P}$ the line containing the points H_i. Observe that the points H_i determine a quadrilateral if and only if $P \notin \mathcal{C}_1 \cup \mathcal{C}_2 \cup \mathcal{C}_3 \cup \mathcal{C}_4$.

Theorem 5. *If $\mathbf{P}$ is a quadrilateral which is not a parallelogram, the reflections of the Simson point with respect to the lines containing the sides of $\mathbf{P}$ are collinear and the line ℓ containing them is parallel to the Simson line.*
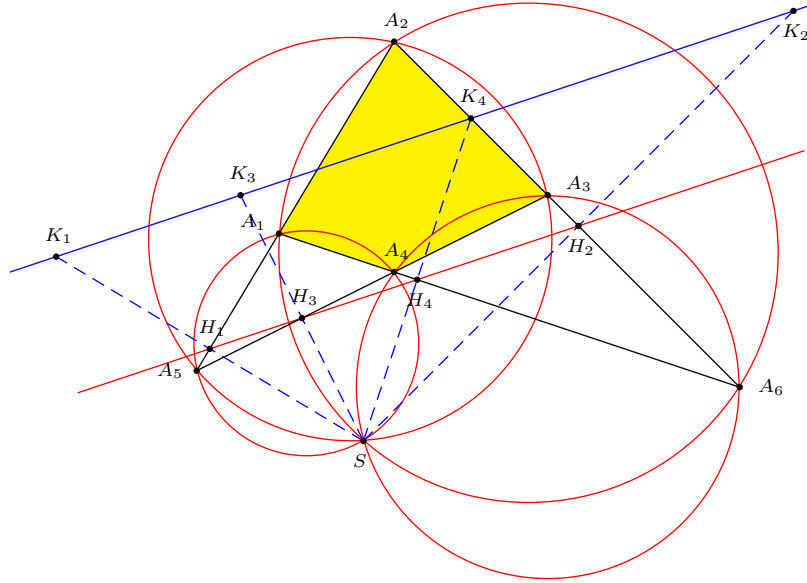
Figure 7

Proof. The theorem is trivially true if $\mathbf{P}$ has one pair of parallel sides. Suppose that $\mathbf{P}$ is without parallel sides (see Figure 7). Let K_i, $i = 1, 2, 3, 4$, be the reflection of S with respect to the line A_iA_{i+1}. The points S, H_i and K_i are collinear and $SH_i = H_iK_i$, then K_i is the image of H_i under the homothety $\mathsf{h}(S, 2)$. Then, since the points H_i are collinear (Theorem 4), the points K_i are also collinear. Moreover, the line ℓ containing the points K_i is parallel to the Simson line of $\mathbf{P}$. $\square$

Conjecture. If **P** is a cyclic quadrilateral without parallel sides, the line ℓ passes through the anticenter H of **P**, and the Simson line bisects the segment SH.

Figure 8

The conjecture was suggested by using a dynamic geometry software (see Figure 8). However, we have been unable to prove it.

If **P** is a cyclic quadrilateral with a pair of parallel sides, then **P** is an isosceles trapezoid. The line ℓ coincides with the Simson line, *i.e.*, the line joining the midpoints of the bases of **P**, and passes through the anticenter of **P**. In this case the Simson line contains the segment SH.

We now find the points P whose pedal quadrilaterals have at least on pair of parallel sides.

If **P** is a parallelogram, then the points P whose pedal quadrilaterals have at least one pair of parallel sides are all and only the points of the diagonals of **P**.

Suppose now that **P** is not a parallelogram. We prove that the locus of *the point P whose pedal quadrilateral has the sides H_1H_4 and H_2H_3 parallel is the circle A_1A_3S* (see Figure 9).

First observe that S is a point with respect to whom H_1H_4 and H_2H_3 are parallel because the points H_i are collinear. Set up now an orthogonal coordinate system such that $A_1 \equiv (-1, 0)$ and $A_3 \equiv (1, 0)$; let $A_2 \equiv (a, b)$, $A_4 \equiv (c, d)$ and

$P \equiv (x, y)$. If $H_1 H_4$ and $H_2 H_3$ are parallel, then P lies on the circle γ of equation:

$$(hd + kb)x^2 + (hd + kb)y^2 - (hk - 4bd)y = hd + kb,$$

where $h = a^2 + b^2 - 1$ and $k = c^2 + d^2 - 1$.

Note that the points A_1 and A_3 are on γ, and γ is the circle $A_1 A_3 S$.
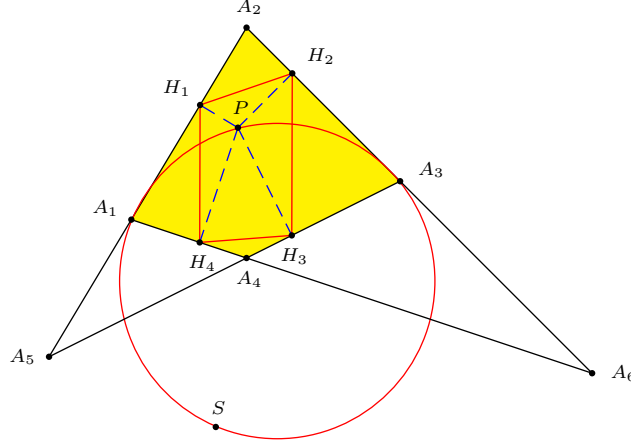
Figure 9

Analogously we can prove that *the points P whose pedal quadrilateral has the sides $H_1 H_2$ and $H_3 H_4$ parallel is the circle $A_2 A_4 S$.* Therefore we have established the following theorem.

Theorem 6. *The points P whose pedal quadrilaterals have at least one pair of parallel sides are precisely those on the circles $A_1 A_3 S$ and $A_2 A_4 S$.*
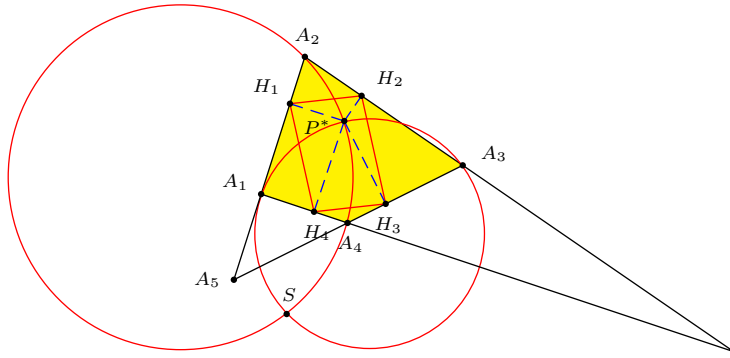
Figure 10

In general, the circles $A_1 A_3 S$ and $A_2 A_4 S$ intersect at two points, the Simson point S and one other point P^* (see Figure 10). The pedal quadrilateral of P^* is

a parallelogram. We call P^* the *parallelogram point* of $\mathbf{P}$. Observe that if $\mathbf{P}$ is a parallelogram the parallelogram point is the intersection of the diagonals of $\mathbf{P}$.

If $\mathbf{P}$ is cyclic, the pedal quadrilateral of the circumcenter O of $\mathbf{P}$ is the Varignon parallelogram of $\mathbf{P}$. Therefore, the parallelogram point of $\mathbf{P}$ is O. It follows that *if $\mathbf{P}$ is cyclic, the Simson point is the intersection point of the circles A_1A_3O and A_2A_4O, other than O.*

4. Some properties of the pedal polygon

Let $\mathbf{P}$ be a polygon with n sides. Consider the pedal polygon $\mathbf{H}$ of a point P with respect to $\mathbf{P}$. We denote by $\mathbf{Q}_i$ the quadrilateral $PH_iA_{i+1}H_{i+1}$, for $i = 1, 2, \ldots, n$. Since the angles in H_i and in H_{i+1} are right, $\mathbf{Q}_i$ cannot be concave.

Lemma 7. *If $ABCD$ is a convex or a crossed quadrilateral such that ABC and CDA are right angles, then it is cyclic. Moreover, its circumcenter is the midpoint of AC and its anticenter is the midpoint of BD.*
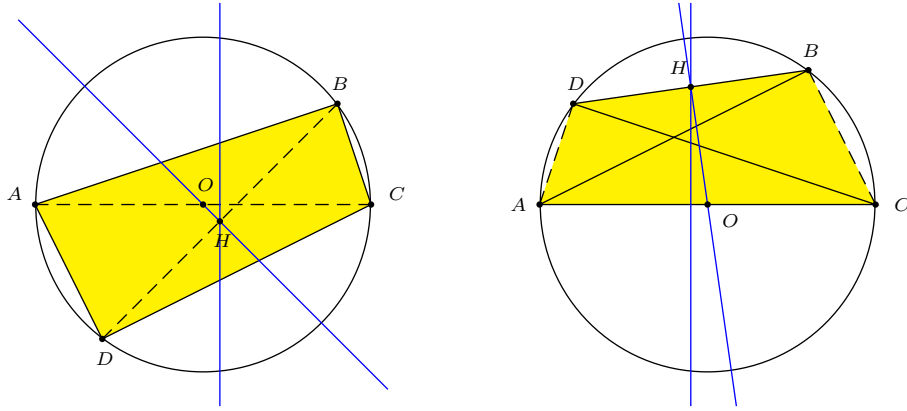
Figure 11

Proof. Let $ABCD$ be a convex or a crossed quadrilateral with ABC and CDA right angles (see Figure 11). Then, it is cyclic with the diagonal AC as diameter. (When it is a crossed quadrilateral it is inscribed in the semicircle with diameter AC). Then its circumcenter O is the midpoint of AC.

Consider the maltitudes with respect to the diagonals AC and BD. The maltitude through O is perpendicular to the chord BD of the circumcircle, then it passes through the midpoint H of BD. But also the maltitude relative to AC passes through H. Then, the anticenter of the quadrilateral is H. Note that the maltitudes of a crossed quadrilateral $ABCD$ are concurrent because they are also the maltitudes of the cyclic convex quadrilateral $ACBD$. $\qquad\square$

By Lemma 7, the quadrilaterals $\mathbf{Q}_i$ are cyclic. Denote by O_i and A_i' the circumcenter and the anticenter of $\mathbf{Q}_i$ respectively. We call $O_1 O_2 \ldots O_n$ the *polygon of the circumcenters* of $\mathbf{P}$ with respect to P and denote it by $\mathbf{P}_c(P)$. We call $A_1' A_2' \ldots A_n'$ the *polygon of the anticenters* of $\mathbf{P}$ with respect to P and we denote it with $\mathbf{P}_a(P)$.

Theorem 8. *The polygon $\mathbf{P}_c(P)$ is the image of $\mathbf{P}$ under the homothety* $\mathsf{h}\left(P, \frac{1}{2}\right)$.

Proof. By Lemma 7, the circumcenter O_i of $\mathbf{Q}_i$ is the midpoint of $A_i P$ (see Figure 12 for a pentagon $\mathbf{P}$). $\qquad\square$
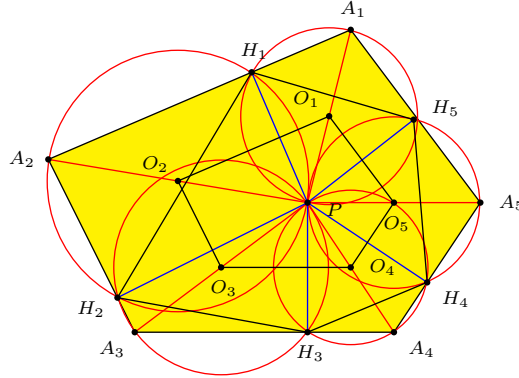
Figure 12

Note that by varying P the polygons $\mathbf{P}_c(P)$ are all congruent to each other (by translation).

Theorem 9. *The polygon $\mathbf{P}_a(P)$ is the medial polygon of $\mathbf{H}$, with vertices the midpoints of the segments $H_i H_{i+1}$ for $i = 1, 2, \ldots, n$.*
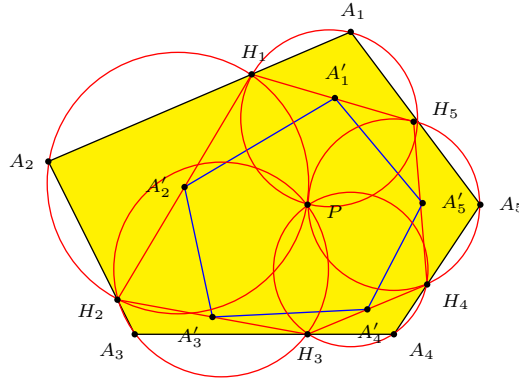
Figure 13

Proof. By Lemma 7, the anticenter A'_i of $\mathbf{Q}_i$ is the midpoint of H_iH_{i+3} (see Figure 13 for a pentagon).   □

Corollary 10. (a) *If* $\mathbf{P}$ *is a triangle,* $\mathbf{P}_a(P)$ *is the medial triangle of* $\mathbf{H}$.
(b) *If* $\mathbf{P}$ *is a quadrilateral,* $\mathbf{P}_a(P)$ *is the Varignon parallelogram of* $\mathbf{H}$.

Theorem 11. *If* $\mathbf{H}$ *is cyclic, the Euler lines of the quadrilaterals* $\mathbf{Q}_i$ *are concurrent at the circumcenter of* $\mathbf{H}$.

Proof. The Euler line of the quadrilateral $\mathbf{Q}_i$ passes through the circumcenter O_i of $\mathbf{Q}_i$ and through the anticenter A'_i of $\mathbf{Q}_i$, that is the midpoint of H_iH_{i+3}, then it is the perpendicular bisector of a side of $\mathbf{H}$ (see Figure 14 for a quadrilateral).   □
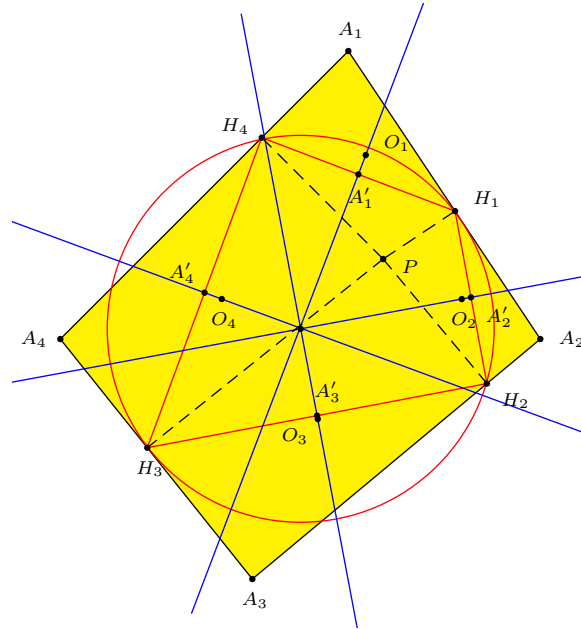
Figure 14

Corollary 12. *If* $\mathbf{P}$ *is a triangle, the Euler lines of the quadrilaterals* $\mathbf{Q}_i$ *are concurrent at the circumcenter of* $\mathbf{H}$ *(see Figure 15).*

Remark. If $\mathbf{P}$ is a quadrilateral and $\mathbf{H}$ is not cyclic, the Euler lines of the quadrilaterals $\mathbf{Q}_i$ bound a quadrilateral affine to $\mathbf{H}$ ([4, p.471]).

References

[1] O. Bottega, *Topics in Elementary Geometry*, second edition, Springer, 2008.
[2] H.S.M. Coxeter and S.L. Greitzer, *Geometry revisited*, Math. Assoc. America, 1967.
[3] R. Honsberger, *Episodes in nineteenth and twentieth century Euclidean geometry*, Math. Assoc. America, 1995.
[4] M. F. Mammana and B. Micale, Quadrilaterals of Triangle Centres, *The Mathematical Gazette*, 92 (2008) 466-475.

Figure 15
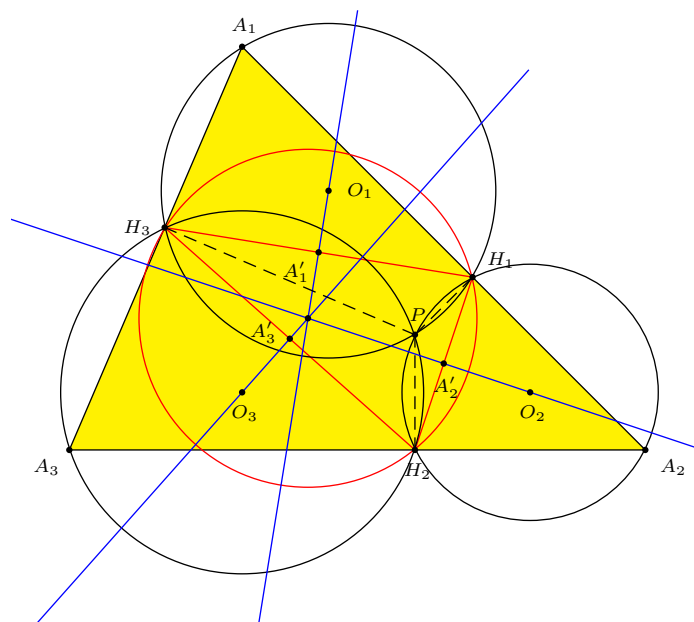
[5] M. F. Mammana, B. Micale and M. Pennisi, Orthic Quadrilaterals of a Convex Quadrilateral,
    Forum Geom., 10 (2010) 79-91.
[6] P. Yiu, *Notes on Euclidean Geometry*, Florida Atlantic University Lecture Notes, 1998; avail-
    able at `math.fau.edu/Yiu/Geometry.html`.

Daniela Ferrarello: Department of Mathematics and Computer Science, University of Catania,
Viale A. Doria 6, 95125, Catania, Italy
    E-mail address: `ferrarello@dmi.unict.it`

Maria Flavia Mammana: Department of Mathematics and Computer Science, University of Cata-
nia, Viale A. Doria 6, 95125, Catania, Italy
    E-mail address: `fmammana@dmi.unict.it`

Mario Pennisi: Department of Mathematics and Computer Science, University of Catania, Viale
A. Doria 6, 95125, Catania, Italy
    E-mail address: `pennisi@dmi.unict.it`

Special Inscribed Trapezoids in a Triangle

Nikolaos Dergiades

Abstract. We give a generalization Floor van Lamoen's recent result on jigsawing a quadrangle in a triangle.

1. Construction of an inscribed trapezoid

This note is a generalization of a recent result of Floor van Lamoen [1].

For an arbitrary point A' on the side BC of a given triangle ABC, we want to find on BC two points P, P' isotomic with respect to B and C such that the parallels from P, P' to AA' meet their closest sides AB, AC at the points Q, Q' and we have in the trapezoid $QPP'Q'$,

$$QQ' = PQ + P'Q'. \tag{1}$$
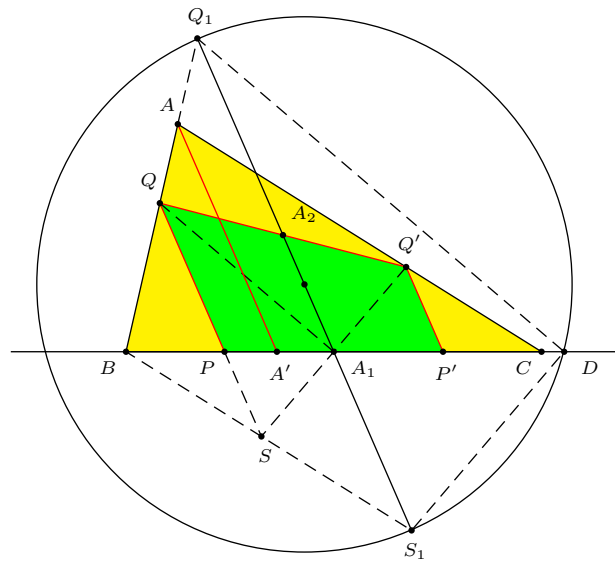
Figure 1.

Let A_1 be the midpoint of BC. The parallel from A_1 to AA' meets QQ' at its midpoint A_2, the line AB at Q_1, and the parallel from B to AC at a point S_1. The symmetric of Q' in A_1 is the point S, the intersection of BS_1 and QP. Since $A_1A_2 = \frac{PQ+P'Q'}{2} = \frac{QQ'}{2}$, the triangle A_1QQ' is right angled, and the same holds for the triangle A_1QS. The parallel from Q_1 to QA_1 meets the line BC at a point

D and from $\frac{BS}{BS_1} = \frac{BQ}{BQ_1} = \frac{BA_1}{BD}$, we conclude that DS_1 is parallel to A_1S. Hence angle Q_1DS_1 is a right angle and the point D lies on the circle with diameter S_1Q_1. This leads to the following construction.

Figure 2.

Construct
(1) the parallel from A_1 to AA' to intersect the line AB at Q_1 and the parallel from B to AC at S_1,
(2) the circle with diameter Q_1S_1 to intersect BC at the point D such that A_1 is between B, D,
(3) the parallels from A_1 to DQ_1 and DS_1 to intersect AB at Q and AC at Q' respectively,
(4) the parallels to AA' from Q and Q' to intersect BC at P and P' respectively.

The points P, P' are isotomic with respect to BC, and the trapezoid $QPP'Q'$ satisfies (1) (see Figure 2).

2. An intersting property

Rotate triangle QBP about Q to $QA''P''$ with P'' on QQ'. Since $Q'P'' = Q'P'$ and $P'C = BP$, a rotation about Q' will bring triangle $Q'CP'$ to $Q'A''P''$. The lines QP'' and QA'' are the reflections of QB and QP in the bisector of angle Q of triangle AQQ'. Since QP is parallel to AA', the line QA'' contains the isogonal conjugate of the infinite point of AA' in triangle AQQ'. For the same reason, the line $Q'A''$ also contains the isogonal conjugate of the same infinite point. It follows that A'' is this isogonal conjugate, and it lies on the circumcircle of AQQ' (see Figure 3).

Figure 3.

In particular, if AA' is an altitude of triangle ABC, then the line AA'' passes through the circumcenter of the triangle.

Reference

[1] F. M. van Lamoen, Jigsawing a quadrangle from a triangle, *Forum Geom.*, 13 (2013) 149–152.

Nikolaos Dergiades: I. Zanna 27, Thessaloniki 54643, Greece
E-mail address: ndergiades@yahoo.gr

FORUM GEOM

Gossard's Perspector and Projective Consequences

Wladimir G. Boskoff, Laurenţiu Homentcovschi, and Bogdan D. Suceavă

Abstract. Considering as starting point a geometric configuration studied, among others, by Gossard, we pursue the projective study of a triangle in the Euclidean plane, its Euler line and its nine-point circle, and we relate Pappus' Theorem to the nine-point circle and Euler line.

1. Introduction

The relative position of Euler's line with respect to the sides of a triangle has raised the geometers' interest since the very first paper on this topic, Leonhard Euler's classical work [10].

In 1997, problem A1 from the W. L. Putnam competition explored the case when Euler's line is parallel to one of the sides of a triangle. *Amer. Math. Monthly* published Problem 10980 proposed by Ye Zhong Hao and Wu Wei Chao, whose statement is the following. *Consider four distinct straight lines in the same plane, with the property that no two of them are parallel, no three are concurrent, and no three form an equilateral triangle. Prove that, if one of the lines is parallel to the Euler line of the triangle formed by the other three, then each of the four given lines is parallel to the Euler line of the triangle formed by the other three.* In the Editorial Comment following the solution of problem 10980 (see vol. 111 (2004), pp.824), the editors have pointed out the meaningful contributions to the history of this problem, especially Gossard's presentation at an A. M. S. conference in 1915. A generalization from 1999, given by Paul Yiu, is mentioned in [13].

In the *Bulletin of the A. M. S.* from 1916, we find O. D. Kellogg's report on Gossard's 1915 talk at the AMS Southwestern Section Conference (see [15]). As far as we know, Gossard's paper has not been published, although we know from the report what he proved and what methods he used. The summary, as published by the *Bulletin*, is the following: *"Euler proved that orthocenter, circumcenter, and centroid of a triangle are collinear, and the line through them has received the name Euler line. He also proved that the Euler line of a given triangle together with two of its sides forms a triangle whose Euler line is parallel with the third side of the given triangle. By the use of vector coordinates or ordinary projective coordinates, Professor Gossard proves the following theorem: the three Euler lines of*

---

*the triangles formed by the Euler line and the sides, taken by twos, of a given trian-
gle, form a triangle triply perspective with the given triangle and having the same
Euler line. The orthocenters, circumcenters and centroids of these two triangles
are symmetrically placed as to the center of perspective."*

Our goal in the present note goes beyond providing elementary proofs for these
facts, and aims to explore the deeper geometric meaning of a phenomenon seen in
the above mentioned results. Application 1 is Ye and Wu's problem. Applications
3 and 4, proved below, are just particular cases of Application 1. Proposition 1 is
Gossard result from 1916, with a different proof. Furthermore, the original tools
in Gossard's work were ordinary projective coordinates. That's why tt would be
natural to explore from a projective viewpoint the geometric structure inspired by
Euler's original contribution, which made the substance in Gossard's work. In the
last part of our paper, we discuss the projective viewpoint on the relative position
of the Euler line and the three lines forming a given triangle. We will show how
Euler's line can be regarded as the axis of a projectivity between two sides of a
triangle. This result was also proved by D. Barbilian (see [4]), and it appears in
a note unpublished during Barbilian's life. The result is presented below in our
Proposition 4. We have been able to reconstruct the context of Barbilian's work
and we have obtained incidence results that complete the discussion on Ye and
Wu's problem.

Finally, with Propositions 3 and 4, which as far as we know appear for the first
time here, we extend the projective analysis on this geometric structure (*i.e.*, a
triangle, its Euler line and its nine-point circle) and will relate Pappus' Theorem to
the nine-point circle and Euler line. We also study the parallelism of Euler's line
with one of the sides of the triangle from the projective viewpoint. In conclusion,
one of the most important consequences of our investigation is that we are able
to better understand the geometric connections between Euler's line and the nine-
point circle using projective methods. Our geometric motivation was the belief
that beyond the synthetic and analytic methods, one can fathom the entire depth
of a geometry problem by understanding the projective background of a certain
geometric structure.

2. Synthetic and analytic viewpoint

First, we prove a Lemma which will become our main tool of investigation. This
Lemma was inspired by Ye and Wu's problem. Consider the Euclidean plane and
a Cartesian frame. Let A, B, C be three arbitrary points in the Eulcidean plane.

Lemma 1. *Denote by m_E the slope of Euler's line in ΔABC and by m_1, m_2, m_3
the slopes of the lines BC, AC, and AB, respectively. Then*

$$m_E = -\frac{m_1 m_2 + m_3 m_1 + m_2 m_3 + 3}{m_1 + m_2 + m_3 + 3 m_1 m_2 m_3}.$$

Proof. Measuring the slope of the angle between BC and the Euler's line of ΔABC,
we have (see Figure 1):
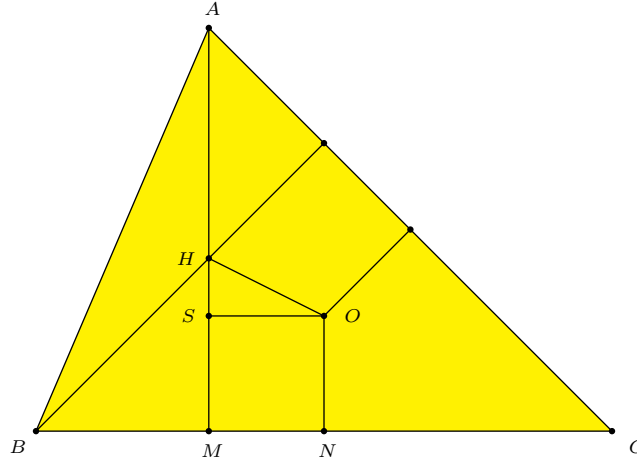
Figure 1

$$\frac{m_1 - m_E}{1 + m_1 m_E} = \tan\angle(HOS) = \frac{HS}{MN} = \frac{AM - AH - ON}{BN - BM}$$

$$= \frac{2R\sin B\sin C - 2R\cos A - R\cos A}{R\sin A - 2R\sin C\cos B}$$

$$= \frac{2\sin B\sin C + 3\cos(B+C)}{\sin(B+C) - 2\sin C\cos B}$$

$$= \frac{3\cos B\cos C - \sin B\sin C}{\sin B\cos C - \sin C\cos B}$$

$$= \frac{3 - \tan B\tan C}{\tan B - \tan C}.$$

Replacing in the last relation the following expressions

$$\tan B = \frac{m_3 - m_1}{1 + m_1 m_3}, \qquad \tan C = \frac{m_1 - m_2}{1 + m_1 m_2},$$

we get the equality

$$\frac{m_1 - m_E}{1 + m_1 m_E} = \frac{3 - \frac{m_3 - m_1}{1 + m_1 m_3} \cdot \frac{m_1 - m_2}{1 + m_1 m_2}}{\frac{m_3 - m_1}{1 + m_1 m_3} - \frac{m_1 - m_2}{1 + m_1 m_2}}.$$

Cross-multiplying and collecting the like-terms, we obtain:

$$m_1 m_2 + m_1 m_3 + m_1 m_E + m_2 m_3 + m_2 m_E + m_3 m_E + 3m_E m_1 m_2 m_3 + 3 = 0.$$

Solving for m_E in this relation immediately yields the relation from the statement of our lemma.   □

We should remark here that any other relative positions of the points A, B, C yield the same result. Now, we present several applications of this lemma.

Application 1. (Problem 10980, *American Mathematical Monthly*, proposed by Ye Zhong Hao and Wu Wei Chao, 109 (2002) 921, solution, 110 (2004) 823–824.) Consider four distinct straight lines in the same plane, with the property that no two of them are parallel, no three are concurrent, and no three form an equilateral triangle. Prove that, if one of the lines is parallel to the Euler line of the triangle formed by the other three, then each of the four given lines is parallel to the Euler line of the triangle formed by the other three.

   Solution: Denote by m_1, m_2, m_3, and m_4 the slopes of the four lines d_1, d_2, d_3, d_4, respectively. Suppose that Euler's line of the triangle formed by the lines d_1, d_2, d_3 is parallel to d_4 and has slope m_E. Then $m_E = m_4$ and we get

$$m_1m_2 + m_1m_3 + m_1m_4 + m_2m_3 + m_2m_4 + m_3m_4 + 3m_4m_1m_2m_3 + 3 = 0.$$

This relation is symmetric in any one of the slopes and the conclusion follows immediately. $\square$

Application 2. Consider ΔABC and $\Delta A'B'C'$ such that the measure of the oriented angles between the straight lines AB and $A'B'$, AC and $A'C'$, and BC and $B'C'$, respectively, are equal to α. Then the measure of the angle between Euler's line of ΔABC and Euler's line of $\Delta A'B'C'$ is also α.

   Solution: We consider the following construction (see Figure 2). On the circumcircle of ΔABC, we consider the points A'', B'' and C'' such that $A''B'' \| A'B'$, $A''C'' \| A'C'$ and $B''C'' \| B'C'$. More precisely, we choose A'' such that the angle $(\widehat{AOA''})$ is α.
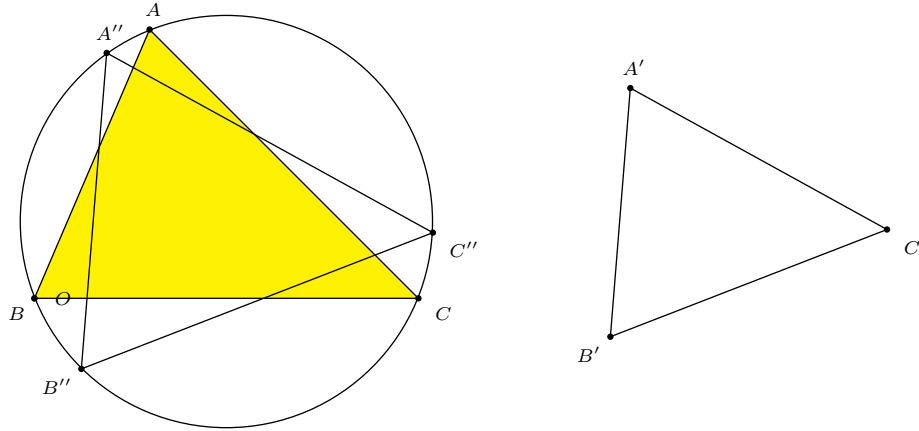
Figure 2

   Let us consider now the rotation R_O^α of center O (O is the circumcenter of ΔABC) and oriented angle α. Then $m(\angle(AB, A''B'')) = m(\angle(AC, A''C'')) = m(\angle(BC, B''C''))$ yields $A'' = R_O^\alpha(A), B'' = R_O^\alpha(B), C'' = R_O^\alpha(C)$. We denote by e, e' and e'' Euler's lines of ΔABC, $\Delta A'B'C'$, and respectively $\Delta A''B''C''$. Then $\Delta A''B''C''$ is obtained by rotating ΔABC about O by α. Thus, all the elements of ΔABC rotate about O. This means $e'' = R_O^\alpha(e)$, or $m(\angle(e, e'')) = \alpha$. Since the slopes satisfy the following equalities $m_{A''B''} = m_{A'B'}$, $m_{A''C''} = $

$m_{A'C''}$, and $m_{B''C''} = m_{B'C'}$, then $m_{e''} = m_{e'}$, which actually means $m(\angle(e, e')) = \alpha$. □

Remark. Let ΔABC and $\Delta A'B'C'$ be two triangles with the property $AB \perp A'B'$, $AC \perp A'C'$, $BC \perp B'C'$. Then the Euler lines of the two triangles are perpendicular.

We can prove this Remark directly from Lemma 1. However, we can also provide a direct argument for its proof. Denote by m_1', m_2', m_3' the slopes of the side and by m_E' the slope of Euler's line of $\Delta A'B'C'$. Then

$$
\begin{aligned}
m_E' &= -\frac{m_1'm_2' + m_3'm_1' + m_2'm_3' + 3}{m_1' + m_2' + m_3' + 3m_1'm_2'm_3'} \\
&= -\frac{\left(-\frac{1}{m_1}\right)\left(-\frac{1}{m_2}\right) + \left(-\frac{1}{m_3}\right)\left(-\frac{1}{m_1}\right) + \left(-\frac{1}{m_2}\right)\left(-\frac{1}{m_3}\right) + 3}{\left(-\frac{1}{m_1}\right) + \left(-\frac{1}{m_2}\right) + \left(-\frac{1}{m_3}\right) + 3\left(-\frac{1}{m_1}\right)\left(-\frac{1}{m_2}\right)\left(-\frac{1}{m_3}\right)} \\
&= \frac{m_1 + m_2 + m_3 + 3m_1m_2m_3}{m_1m_2 + m_3m_1 + m_2m_3 + 3} \\
&= -\frac{1}{m_E}.
\end{aligned}
$$

This proves that the two lines are perpendicular.

Application 3. In the acute triangle ABC, Euler's line is parallel to BC if and only if $\tan B \tan C = 3$.

Note: In [17], it is mentioned that this problem was proposed by Dan Brânzei. We have discussed this application in [6]. The solution uses a direct trigonometric argument. We present here the analytic argument based on Lemma 1.

Solution: Choose a coordinate system so that the x-axis is parallel to BC. If we denote by m_1 the slope of the straight line BC, then $m_1 = 0$. Denoting m_2, m_3, m_e the slopes of the straight lines AC, AB, and Euler's line e, respectively, we get from Lemma 1:

$$
m_e = -\frac{m_2m_3 + 3}{m_2 + m_3}.
$$

Thus, Euler's line e of ΔABC is parallel to BC if and only if $m_e = 0$, which is equivalent to $m_2m_3 = -3$. Now we take into account that $m_2 = -\tan C$ and $m_3 = \tan B$ (or, depending on the position of ΔABC, we could have $m_2 = \tan C$ and $m_3 = -\tan B$). Consequently, $\tan B \tan C = 3$. □

For an interesting connection between the formula obtained here for m_e and Tzitzeica surfaces, a topic studied in depth in affine differential geometry, see [2]. For a graphical study of Tzitzeica surfaces by using Mathematica, see [3]. For the importance of Tzitzeica's surfaces in the development of differential geometry at the beginning of the 20th century, see [1].

Application 4. (W. L. Putnam Competition, 1997) A rectangle, $HOMF$, has sides $HO = 11$ and $OM = 5$. A triangle ABC has H as the intersection of the altitudes, O the center of the circumscribed circle, M the midpoint of BC, and F the foot of the altitude from A. What is the length of BC ?

Solution: Since Euler's line is parallel to BC, by the previous application, we have $\tan B \tan C = 3$. This is just a consequence of the previous application. We can continue our argument as in [14], pg.233, or [6]. Expressing $\tan B$ and $\tan C$ from triangles ABF and AFC, respectively, we get

$$\frac{h_a}{BF} \cdot \frac{h_a}{FC} = 3.$$

Since $HG \| BC$, we have $h_a = AF = 3FH = 3 \cdot 5 = 15$. Therefore, $BF \cdot FC = \frac{15 \cdot 15}{3} = 75$. Namely, we express $BC^2 = (BF+FC)^2 = (FC-BF)^2 + 4BF \cdot FC$. To compute the first term in the last expression we write $FC - BF = FM + MC - (BM - FM) = 2FM = 2OH = 22$. Therefore, $BC^2 = 22^2 + 4 \cdot 75 = 784$, thus $BC = 28$. $\qquad\qquad\qquad\qquad\qquad\qquad\qquad\qquad\qquad\qquad\qquad\square$

Lemma 2. *Euler's line of $\triangle ABC$ intersects the lines AB and AC in M, respectively N. Then Euler's line of $\triangle AMN$ is parallel to BC.*
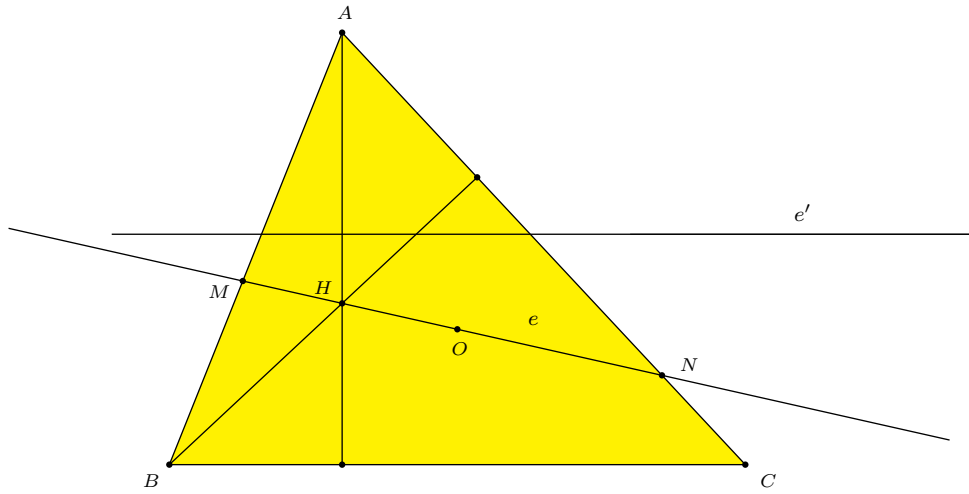
Figure 3

Proof. Choose a coordinate system so that the x-axis is parallel to BC, as in Application 3 (see Figure 3). If we denote by m_1 the slope of the straight line BC, then $m_1 = 0$. Denoting m_2, m_3, m_e the slopes of the straight lines AC, AB, and respectively Euler's line e. By Lemma 1:

$$m_e = -\frac{m_2 m_3 + 3}{m_2 + m_3},$$

and the slope of Euler's line of $\triangle AMN$ is

$$m_{e'} = -\frac{m_e m_2 + m_e m_3 + m_2 m_3 + 3}{m_e + m_2 + m_3 + 3m_e m_2 m_3}.$$

In fact, the numerator of the last expression is

$$m_e m_2 + m_e m_3 + m_2 m_3 + 3$$
$$= m_e(m_2 + m_3) + m_2 m_3 + 3$$
$$= \left(-\frac{m_2 m_3 + 3}{m_2 + m_3}\right)(m_2 + m_3) + m_2 m_3 + 3 = 0.$$

In fact, we proved that $m_{e'} = 0$, which means that $e' \| BC$. $\qquad\square$

Application 5. Consider two triangles such that $\Delta ABC \equiv \Delta A'B'C'$ and they have the same Euler's line. Then $\Delta A'B'C'$ is obtained from ΔABC either by a translation, or by a central symmetry. $\qquad\square$

    Example 1. Problem 244 in [19] states the following. Let H be the orthocenter of ΔABC, and O_a, O_b, O_c the circumcenters of triangles BHC, CHA, AHB. Then $\Delta ABC \equiv \Delta O_a O_b O_c$ have the same nine-point circle and the same Euler's line. This provides us an example of two triangles that have the same Euler's line (see Figure 4).
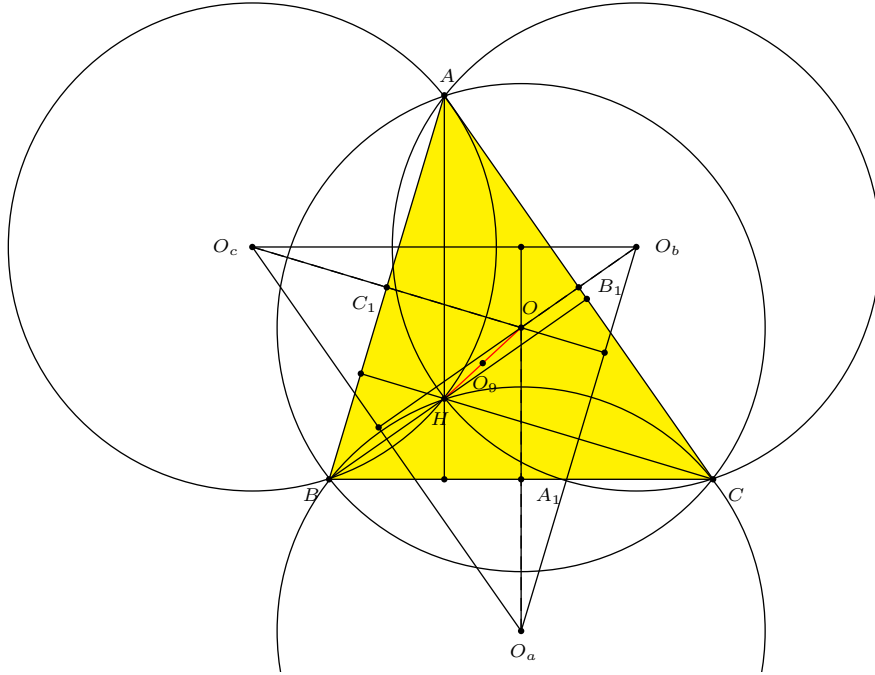
Figure 4.

    Example 2. Now we describe two triangles of interest that have the same Euler's line. Consider ΔABC and its circumcircle $\mathcal{C}$. Consider also the incircle tangent to BC, AC and AB respectively in D, E, and F. On the straight lines AI, BI, CI we consider the excenters (*i.e.*, the centers of the excircles) I_a, I_b, and I_c. Remark that

the circumcircle of ΔABC is the nine-point circle of $\Delta I_a I_b I_c$, because A, B, C are the feet of the altitudes (e.g. $AI_a \perp I_b I_c$).
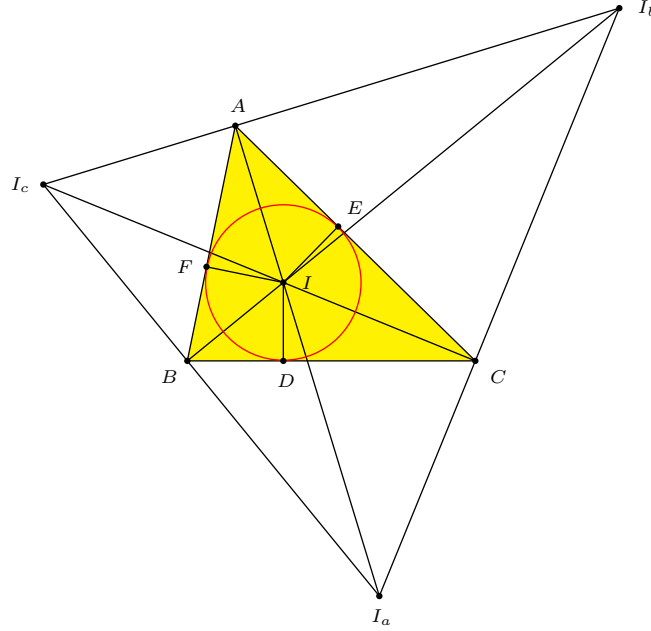
Figure 5.

Thus, I is the orthocenter in $\Delta I_a I_b I_c$, and O is the center of the nine-point circle in $\Delta I_a I_b I_c$. Therefore, OI is Euler's line in $\Delta I_a I_b I_C$. Remark that ΔDEF and $\Delta I_a I_b I_c$ have parallel sides. Therefore their Euler's lines must be parallel (we may say that this is a consequence of Application 2). But the circumcenter of ΔDEF is the point I. This means that the Euler's line of ΔDEF passes through I and, being parallel to OI, must be OI.   □

3. Gossard's perspector

In this section we present an elementary proof of Gossard's result cited in [15].

Proposition 3 (Gossard, [15]). *Denote by e the Euler line of an arbitrary ΔABC in the Euclidean plane. Suppose that e intersects BC, AB, AC in M, N, and respectively P. Denote by e_1, e_2, e_3 Euler's lines of $\Delta ANP, \Delta BMN$, and ΔCPM, respectively. Denote A', B', C' the intersection of the following pair of lines: $e_2 \cap e_3, e_1 \cap e_3$, and $e_1 \cap e_2$, respectively. Then $\Delta A'B'C' \equiv \Delta ABC$, and $\Delta A'B'C'$ has the same Euler line e, and there exists a point I_G (called Gossard's perspector) on the line e such that $\Delta A'B'C'$ is the symmetric of ΔABC by the symmetry centered in I_G.*

The proof presented below is based on Lemma 1. Thus, we claim that it may be more elementary than Gossard's original proof, as it is presented by Kellogg in [15]. An important rôle in the proof is played by the conditions $e_1 \| BC$, $e_2 \| AC$, $e_3 \| AB$.
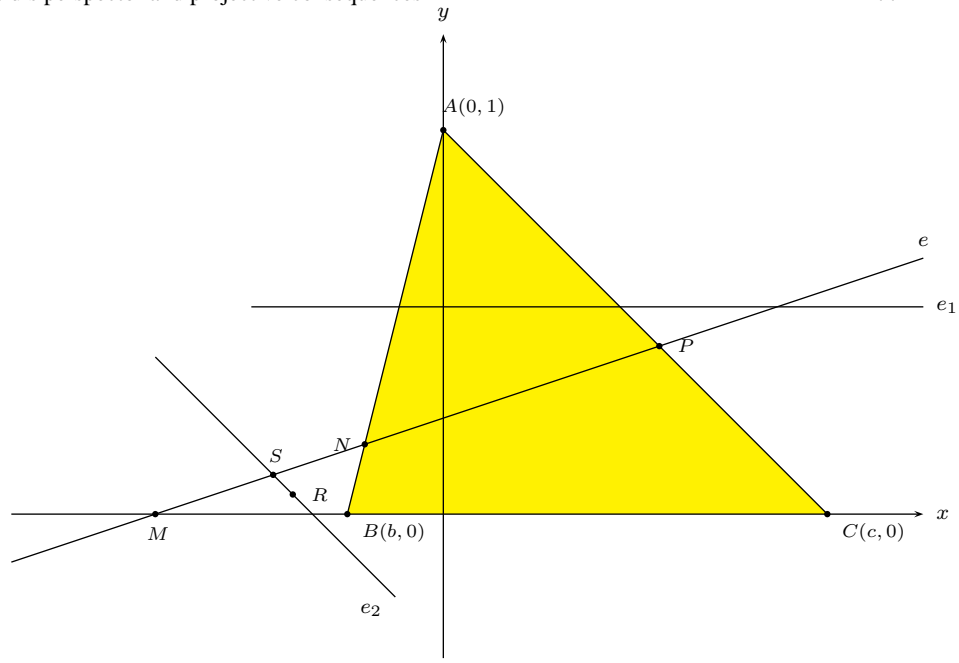
Figure 6

Proof. We choose coordinate axis such that the vertices of $\triangle ABC$ have the co-ordinates $A(0,1), B(b,0), C(c,0)$ (see Figure 4). Let G be the gravity center of $\triangle ABC$; then $G(\frac{b+c}{3}, \frac{1}{3})$. The slope of Euler's line in $\triangle ABC$ is given by

$$m_e = -\frac{m_2 m_3 + 3}{m_2 + m_3} = -\frac{\left(-\frac{1}{c}\right)\left(-\frac{1}{b}\right) + 3}{-\frac{1}{c} - \frac{1}{b}} = \frac{3bc + 1}{b + c}.$$

Thus, the equation of Euler's line is $y = \frac{3bc+1}{b+c} x - bc$. The coordinates of the points $M, N,$ and P are:

$$M\left(\frac{bc(b+c)}{3bc+1}, 0\right),$$

$$N\left(\frac{b(b+c)(bc+1)}{3b^2c + 2b + c}, \frac{2b^2c - bc^2 + b}{3b^2c + 2b + c}\right),$$

$$P\left(\frac{c(b+c)(bc+1)}{3bc^2 + 2c + b}, \frac{2bc^2 - b^2c + c}{3bc^2 + 2c + b}\right).$$

The line e_1 passes through the center of gravity of $\triangle ANP$ and is parallel to BC, therefore it has the equation

$$(e_1): \qquad\qquad y = \frac{y_N + y_P + y_A}{3}.$$

At the intersection of lines e and e_1 we have the point Q whose coordinates are

$$Q\left(\frac{b+c}{3bc+1} \cdot \frac{1}{3}(E + 3bc), \frac{1}{3}E\right),$$

where we have denoted by

$$E = \frac{2b^2c - bc^2 + b}{3b^2c + 2b + c} + \frac{2bc^2 - b^2c + c}{3bc^2 + 2c + b} + 1.$$

The center of gravity of ΔBMN, denoted R, has the coordinates

$$(x_R, y_R) = \left(\frac{1}{3} \left(\frac{bc(b+c)}{3bc+1} + b + \frac{b(b+c)(bc+1)}{3b^2c + 2b + c} \right), \frac{1}{3} \cdot \frac{2b^2c - bc^2 + b}{3b^2c + 2b + c} \right).$$

Euler's line in ΔBMN passes through R and is parallel to AC, thus it has the equation

$$(e_2): \qquad\qquad\qquad y - y_R = -\frac{1}{c}(x - x_R).$$

Denote by S the intersection of the lines e and e_2. We get

$$y_S = \frac{(3bc + 1)(x_R + cy_R) - bc(b+c)}{3bc^2 + 2c + b}.$$

To emphasize the transformation by symmetry (as described in [15]), we claim that $y_S + y_p = y_Q + y_M$. This is equivalent to

$$\frac{(3bc + 1)(x_R + cy_R) - bc(b+c)}{3bc^2 + 2c + b} + \frac{2bc^2 - b^2c + c}{3bc^2 + 2c + b}$$
$$= \frac{1}{3} \left(\frac{2b^2c - bc^2 + b}{3b^2c + 2b + c} + \frac{2bc^2 - b^2c + c}{3bc^2 + 2c + b} + 1 \right).$$

By replacing x_R and y_R and simplifying the relation, we obtain the desired equality. Therefore, the segments $[PS]$ and $[QM]$ have the same midpoint. (It is not necessary to check also that $x_P + x_S = x_Q + x_M$, since P, S, Q and M are collinear.)

Denote by I_G the common midpoint of those two segments. As above, one can prove that I_G is the midpoint of the segment $[NT]$, where $\{T\} = e_3 \cap e$. The analogy of the computation can be further seen since the coordinates of I_G are symmetric in b and c. Thus, with the above notation for E, I_G has the coordinates

$$(x_{I_G}, y_{I_G}) = \left(= \frac{1}{2} \left(\frac{bc(b+c)}{3bc+1} + \frac{b+c}{3bc+1} \cdot \frac{1}{3}(E + 3bc) \right), \frac{1}{6}E \right).$$

We can write the coordinates in the form

$$I_G \left(\frac{1}{6} \cdot \frac{b+c}{3bc+1}(E + 6bc), \frac{1}{6}E \right).$$

This is the point called *the Gossard perspector.* Denote S_{I_G} the symmetry of center I_G in the Euclidean plane. Since $e_1 \| BC, Q \in e_1\ M \in BC$, and I_G is the midpoint of $[QM]$, we have $e_1 = S_{I_G}(BC)$. Similarly $e_2 = S_{I_G}(AC)$, $e_3 = S_{I_G}(AB)$.

Then, we have obtained the following:

$$\{A'\} = e_2 \cap e_3 = S_{I_G}(AC) \cap S_{I_G}(AB) = S_{I_G}(AC \cap AB) = S_{I_G}(\{A\}).$$

Similarly, $\{B'\} = S_{I_G}(\{B\})$, and $\{C'\} = S_{I_G}(C)$.

Consequently, $\Delta A'B'C' \equiv \Delta ABC$, and $\Delta A'B'C' = S_{I_G}(\Delta ABC)$.

Denoting G and G' the gravity centers of ΔABC and $\Delta A'B'C'$, we have $\{G'\} = S_{I_G}(\{G\})$. For the orthocenters we get a similar correspondence: $\{H'\} = S_{I_G}(\{H\})$. Thus, $e' = S_{I_G}(e)$, where e' is Euler's line of $\Delta A'B'C'$. But $I_G \in e$. Thus, Euler's line e passes through the center of symmetry. We deduce that $S_{I_G}(e) = e$, or $e' = e$. Finally, we proved that ΔABC and $\Delta A'B'C'$ have the same Euler's line. This completes the analytic proof of Gossard's prospector theorem, as mentioned in our introduction (see [15]). $\qquad\square$

Example 3. We have seen in Example 1 (see [19], 244) that if H is the orthocenter of ΔABC, and O_a, O_b, O_c are the circumcenters of triangles BHC, CHA, AHB, then ΔABC and $\Delta O_aO_bO_c$ have the same Euler's line (see Figure 4). In fact, O_a, O_b, and O_c are the symmetric points of O with respect to the sides BC, AC and, respectively, AB. Denote by A_1, B_1, and C_1 the midpoints of the sides BC, AC and, respectively, AB.

Then H is the circumcenter of $\Delta O_aO_bO_c$. Actually, $\Delta O_aO_bO_c$ is the homothetic of $\Delta A_1B_1C_1$ by homothety of center O and ratio 2. Thus, $\Delta O_aO_bO_c$ has the sides parallel and congruent to the sides of ΔABC, and, furthermore, $OO_a \perp BC$, and also $OO_a \perp O_bO_c$, (and the similar relations). This proves that O is the orthocenter of $\Delta O_aO_bO_c$. Therefore ΔABC and $\Delta O_aO_bO_c$ interchanged among them the orthocenters and the circumcenters. This is the argument to see that the Euler's lines in the two triangles are the same and the two triangles have the same center of the nine-point circle, since O_9 is the midpoint of OH. Further, ΔABC and $\Delta O_aO_bO_c$ are symmetric with respect to O_9. Therefore, Gossard's perspector in $\Delta O_aO_bO_c$ is the symmetric of Gossard perspector in ΔABC with respect to O_9, the center of the nine-point circle.

4. Projective viewpoint

Consider now a projectivity $f : d_1 \to d_2$. (See also [7, pp.39 ff], [8, pp.9-11]) The geometric locus of the points from which the the projectivity is seen as an involution of pencils of lines is called axis of the projectivity.
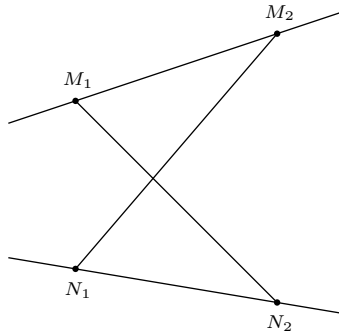
Figure 7.

More precisely (see Figure 7), any projectivity relating ranges on two distinct lines determines another special line, the axis of projectivity, which contains the

intersection of the cross-joints of any pairs of corresponding points (see [8, pp.36-37]). This result is known as *the axis theorem.* To illustrate it, if $M_1 \to N_1$ and $M_2 \to N_2$, then the point $\{P\} = M_1 N_2 \cap M_2 N_1$ lies on the axis of the projectivity, since we have the mapping $r_1 = PM_1 \to PN_1 = r_2$ and $r_2 = PM_2 \to PN_1 = r_1$. Thus, $r_1 \to r_2$ and $r_2 \to r_1$, which means that the projectivity $f : d_1 \to d_2$ is seen as an involution. As a consequence, we remind here the well-known geometric structure called *Pappus' line*.
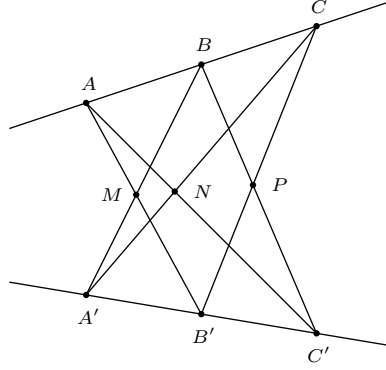
Figure 8.

Let $A, B, C \in d_1$ and $A', B', C' \in d_2$. Then the points $\{M\} = AB' \cap BA'$, $\{N\} = AC' \cap AC' \cap CA'$, $\{P\} = BC' \cap CB'$, are collinear (see Figure 8). This result can be viewed as an immediate consequence of the axis theorem. Indeed, consider the projectivity $f : d_1 \to d_2$ uniquely determined by $A \to A'$, $B \to B'$, $C \to C'$. By the axis theorem, we get immediately that the points $\{M\} = AB' \cap BA'$, $\{N\} = AC' \cap AC' \cap CA'$, $\{P\} = BC' \cap CB'$ are collinear. With this preparation, we are able to show that *the Euler's line of a triangle ABC can be regarded as the axis of projectivity for three suitable projectivities between the sides of* $\triangle ABC$ (see Figure 9).
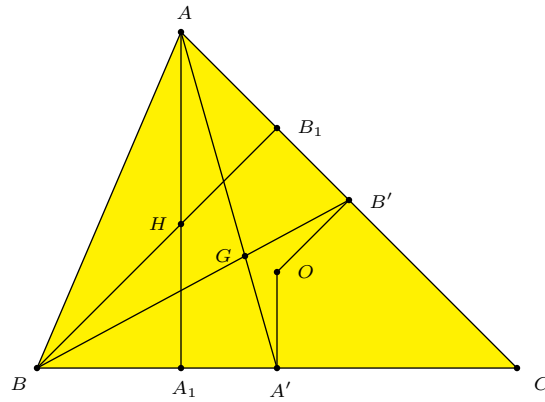
Figure 9.

Denote by A', B', C' the midpoints of the sides BC, AC, and respectively AB. Denote by A_1, B_1, C_1 the feet of altitudes from A, B, C. We use the standard notations for O, the circumcircle, G the center of gravity, and H the orthocenter of $\triangle ABC$. There are three projectivities, each one between two sides of $\triangle ABC$. One of them is $f_C : BC \to AC$, the projectivity determined by $B \to A$, $A_1 \to B_1$, $A' \to B'$. Since H and G appear as cross-joints points, they lie on the axis of projectivity of f_C. Specifically, $\{H\} = AA_1 \cap BB_1$, $\{G\} = BB' \cap AA'$. Since two points determine uniquely a line, and since G and H determine Euler's line, this means that *the Euler's line is identified with the axis of projectivity f_C.* Furthermore, on the Euler's line we get a new point: $\{\Omega_{AB}\} = A_1 B' \cap A' B_1$. We can also emphasize the pair of homologous points that determine O, the circumcenter, in this projectivity. Extend the line determined by the vertex A and by O and denote $\{X\} = AO \cap BC$. Similarly, $\{Y\} = BO \cap AC$. Since in our projectivity $B \to A$, then $X \to Y$. Thus, on the axis of projectivity we obtain $\{O\} = AX \cap BY$.

Considering similar constructions for the projectivities f_A and f_B, we obtain the following fact.

Proposition 4 (Barbilian [4]). *In $\triangle ABC$, let A', B', C' be the midpoints of the sides BC, AC, and respectively AB. Denote by A_1, B_1, C_1 the feet of altitudes from A, B, C. Then the points $\{\Omega_{AB}\} = A_1 B' \cap A' B_1$, $\{\Omega_{CB}\} = C_1 B' \cap C' B_1$, $\{\Omega_{AC}\} = A_1 C' \cap A' C_1$ are collinear and they lie on Euler's line of $\triangle ABC$.*
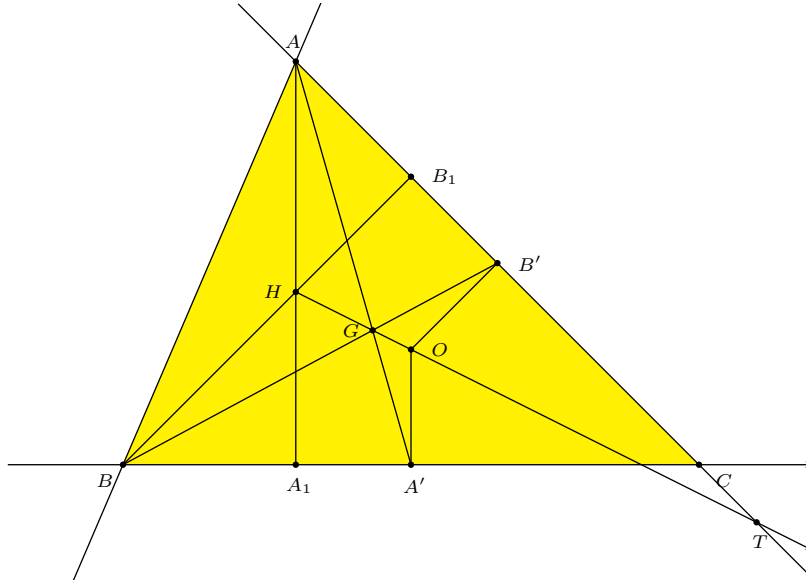
Figure 10.

In the first part, we have presented Applications 3 and 4, where we give synthetic and trigonometric characterizations of the fact that Euler's line is parallel to a side of the triangle. We study here the following question: What is projective condition that the projectivity $f_C : BC \to AC$ must satisfy such that Euler's

line is parallel to BC? Denote by (e) Euler's line in ΔABC. (See Figure 10.) Let $\{T\} = AC \cap (e)$, $\{U\} = BC \cap (e)$. We need to determine the pairs of straight lines that characterize in a projectivity the points T and U. Recall that the projectivity f_C has as homologous points $B \to A$. To get T, consider the pair $C \to (e) \cap AC$. Similarly, we get U by the pair $(e) \cap BC \to C$. Therefore we have obtained the projective characterization of the fact that the Euler line is parallel to a side of the triangle. Thus, we are able to state the projective counterpart of Application 3, which is the trigonometric characterization of this parallelism.

Proposition 5. *In ΔABC, let (e) be the Euler's line. The sufficient condition that $(e) \| BC$, is that the projectivity f_C has $\infty \to C$ as pair of homologous points. Similarly, to have $(e) \| AC$, it is sufficient that f_C has $C \to \infty$ as pairs of homologous points.*

Four our next step, we need to recall here Pappus' Theorem on the circle. Let A, B, C and A', B', C' six points on the circle C. Then the intersection points $AB' \cap A'B$, $AC' \cap A'C$ and $BC' \cap B'C$ are collinear. To recall the idea of the most direct proof, consider the projectivity $f : C \to C$ uniquely determined by $A \to A'$, $B \to B'$, $C \to C'$. Then, the intersection points mentioned in the statement lie precisely on the axis of the projectivity. With this observation, we obtain that Euler's line is the axis of projectivity of a certain projectivity within the nine-point circle. The result is the following.

Proposition 6. *Consider A', B', C' the midpoints of the sides BC, AC and respectively AB. Let A_1, B_1 and C_1 the feet of the altitudes. Consider the projectivity ϕ uniquely determined by $A_1 \to B_1$, $A' \to B'$, $B_2 \to A_2$. Then the points $A_1 A_2 \cap B_1 B_2 = \{H\}$ (the orthocenter of ΔABC), $A_1 B' \cap A' B_1 = \{\Omega_{AB}\}$ and $A'A_2 \cap B'B_2 = \{O_9\}$ (the center of the nine-point circle) are collinear on the axis of projectivity of ϕ.*
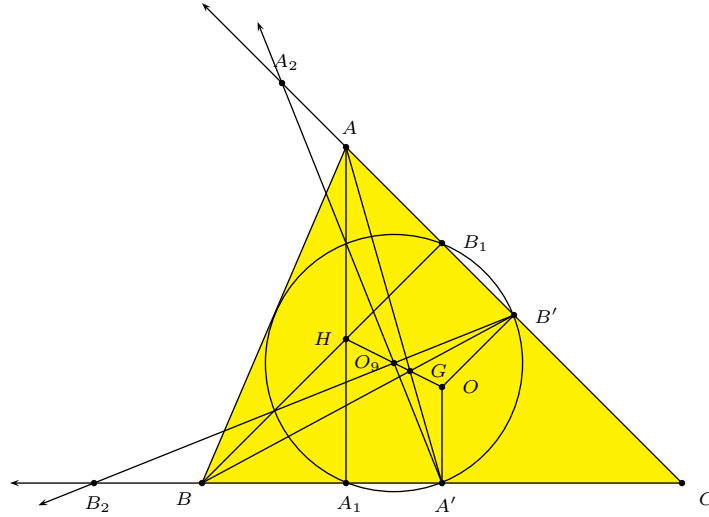
Figure 11.

The proof is just a direct application of Pappus' Theorem on the circle, for the geometric structure described in the statement. Since H and Ω_{AB} are on Euler's line, the axis of projectivity and Euler's line must be the same straight line. As a consequence, the third point, O_9, the center of the nine-point circle, must be on the axis of projectivity, thus on Euler's line.

Proposition 4 appears in [4, pp. 40]. Actually, Dan Barbilian collected in an undated note, published in the cited collection of posthumuous works, several projective properties of the nine-point circle and its connection with Euler's line. He focused mainly on the projective properties, which represent, as we can see, an important part of the more complex phenomenon whose overall picture we tried to present here.

References

[1] A. F. Agnew, A. Bobe, W. G. Boskoff, and B. D. Suceavă, Gheorghe Țiţeica and the origins of affine differential geometry, *Hist. Math.*, 36 (2009) 161–170.

[2] A. F. Agnew, A. Bobe, W. G. Boskoff, L. Homentcovschi, and B. D. Suceavă, The equation of Euler's line yields a Tzitzeica surface, *Elemente der Mathematik*, 64 (2009) 71–80.

[3] A. F. Agnew, A. Bobe, W. G. Boskoff, and B. D. Suceavă, Tzitzeica Curves and surfaces , *The Mathematica Journal*, 12 (2010) 1–18.

[4] D. Barbilian, *Pagini inedite,* vol. II, editors G. Barbilian and V. Gh. Vodă, Ed. Albatros, 1984.

[5] L. M. Blumenthal and K. Menger, *Studies in Geometry,* W. H. Freeman Co., San Francisco, 1970.

[6] W. G. Boskoff and B. D. Suceavă, When Is Euler's Line Parallel to a Side of a Triangle?, *College Math. J.*, 35 (2004) 292–296.

[7] H. S. M. Coxeter, *The Real Projective Plane,* Third Edition, Springer-Verlag, 1992.

[8] H. S. M. Coxeter, *Projective Geometry*, 2nd edition, Springer-Verlag, 1987, 2003.

[9] L. Euler, Variae demonstrationes geometriae, *Novii comm. acad. sci. Petropolitanae*, 1 (1747/8), 1750, 49–66, also *Opera omnia*, series 1, vol. 26, pp.15–32.

[10] L. Euler, Solutio facilis problematum quorundam geometricorum difficillimorum, *Novii comm. acad. sci. Petropolitanae*, 11 (1765), 1765, 103–123, also *Opera omnia*, series 1, vol. 26, pp.139–157.

[11] F. G.-M., *Éxercices de géometrie,* sixiéme édition,Vuibert, Paris, 1920.

[12] M. J. Greenberg, *Euclidean and Non-Euclidean Geometries,* Freeman & Co., Third Edition, 1993.

[13] C. Kimberling - Web resource: Gossard Perspector, http://faculty.evansville.edu/ck6/tcenters/recent/gosspersp.html

[14] K. S. Kedlaya, B. Poonen, R. Vakil - *The William Lowell Putnam Mathematical Competition 1985-2000,* Mathematical Association of America, 2002.

[15] O. D. Kellogg, The Ninth Regular Meeting of the Southwestern Section, *Bull. Amer. Math. Soc.*, 1916 () 215–219.

[16] T. Lalescu, *La Géométrie du Triangle,* Éditions Jacques Gabay, sixiéme édition, 1987.

[17] D. Sachelarie and V. Sachelarie, *The Most Beautiful Problems in Mathematics* (in Romanian), Editura Teora, Bucharest, 1996.

[18] A. Seidenberg, *Lectures in Projective Geometry*, D. Van Nostrand Co. Inc., 1962.

[19] G. Țiţeica, *Problems of Geometry*, (in Romanian), Sixth Edition, Editura Tehnică, 1962, reprinted 1981.

Wladimir G. Boskoff: Department of Mathematics and Computer Science, University Ovidius, Constantza, Romania

E-mail address: `boskoff@univ-ovidius.ro`

Laurenţiu Homentcovschi: Department of Mathematics and Computer Science, University Ovidius, Constantza, Romania

E-mail address: `lhomentcovschi@univ-ovidius.ro`

Bogdan D. Suceavă: California State University Fullerton, Department of Mathematics, P.O. Box 6850, Fullerton, CA 92834-6850

E-mail address: `bsuceava@fullerton.edu`

A Sangaku-Type Problem with Regular Polygons, Triangles, and Congruent Incircles

Naoharu Ito and Harald K. Wimmer

Abstract. We consider a dissection problem of a regular n-sided polygon that generalizes Suzuki's problem of four congruent incircles in an equilateral triangle.

1. Introduction

The geometrical problem that is the starting point of our note is due to Denzaburo Suzuki. It was engraved on a wooden tablet and dedicated 1886 to the Miwatari Shrine in Fukushima prefecture [4, p. 6], [1, p. 24]. Referring to Figure 1 below we state the problem in the following equivalent form.
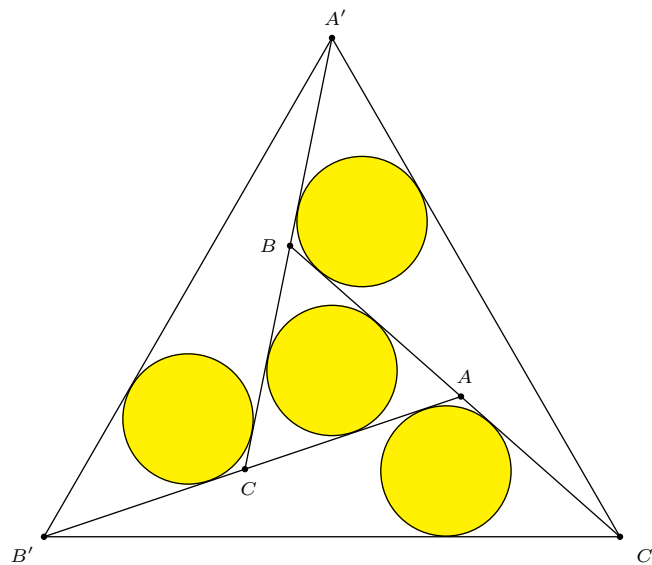
Figure 1. Four incircles in an equilateral triangle

Suzuki's problem of four congruent incircles in an equilateral triangle. Let ABC be an equilateral triangle. The side AC is extended to the point B', the side BA is extended to C', and CB to A', such that the triangles $AB'C'$, $BC'A'$, $CA'B'$ and ABC have congruent incircles. Find the length of $A'B'$ of the exterior equilateral triangle in terms of the length of AB.

_____

Suzuki's problem is an example of a unique brand of mathematics that flourished in Japan in the 18th and 19th century. Amateur mathematicians crafted geometric theorems on wooden tablets (called sangaku), which were displayed in the precincts of a shrine or temple. Remarkably, some of those theorems predate work of Western mathematicians (see [5]). In addition to [1] we also mention the monographs [2] and [3] as sources of sangaku problems. An excellent survey of Japanese temple geometry is Rothman's article [6] in the Scientific American.

In this note we generalize Suzuki's four-congruent-incircles problem. Instead of an equilateral triangle we now consider a regular n-sided polygon. To illustrate the general case we choose $n = 5$. Figure 2 shows the configuration of six congruent incircles in a regular pentagon.
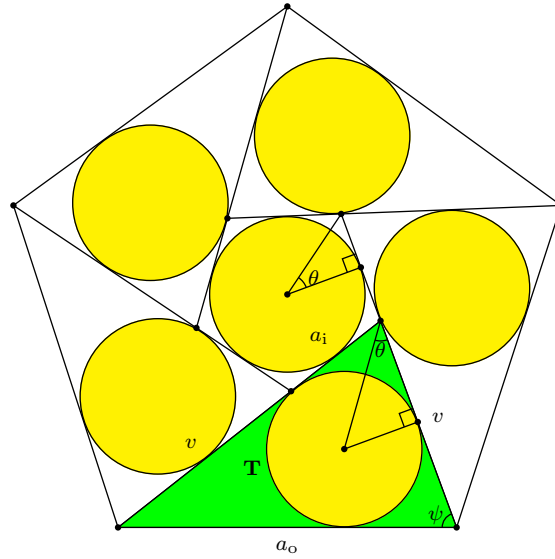
Figure 2. Six congruent incircles in a regular pentagon

Let $\mathbf{P}_o$ be the regular n-sided polygon that forms the exterior boundary of Figure 2 and let $\mathbf{P}_i$ be the regular n-sided polygon in the interior. Our main result is the following.

Theorem 1. *If a_o and a_i are the lengths of the sides of $\mathbf{P}_o$ and $\mathbf{P}_i$ respectively, then*

$$a_o = a_i \left(1 + \sqrt{1 + \left(\sin \frac{\pi}{n} \right)^{-2}} \right). \tag{1}$$

The proof of Theorem 1 will be given in Section 2. In Section 4 we assume that the exterior polygon $\mathbf{P}_o$ is given. We derive a result that leads to a simple construction of the interior polygon $\mathbf{P}_i$. The special cases with $3 \leq n \leq 6$ will be considered in Section 5.

2. Incircles

The proof of Theorem 1 is based on a relation between inradius and area of a triangle.
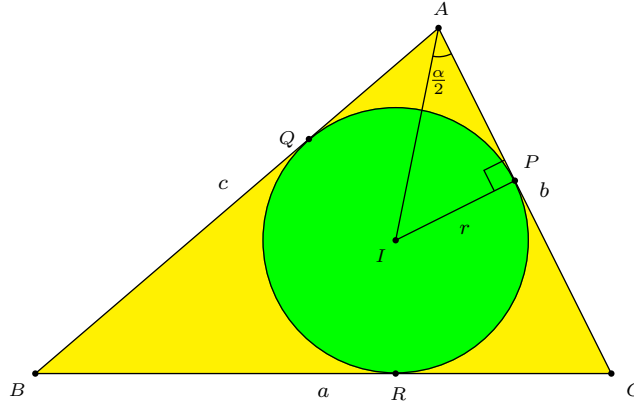
Figure 3. A triangle and its incircle

Consider a triangle ABC in Figure 3 with sides $a = BC$, $b = CA$, $c = AB$, and $\angle BAC = \alpha$. We denote the area, the incenter, and the inradius of the triangle by Δ, I, and r, respectively. Then

$$\Delta = r^2 \cot \frac{\alpha}{2} + ra. \tag{2}$$

This can be seen as follows.

Suppose the incircle touches CA, AB and BC at P, Q and R, respectively. Since $AP = r \cot \frac{\alpha}{2}$, the area of the kite $AQIP$ is given by $r \cdot AP = r^2 \cot \frac{\alpha}{2}$. The area of the triangle BIC is equal to $\frac{1}{2}ra$. Thus the area of the polygon $QBCPIQ$ is ra. Combining the areas of the kite and the polygon, we obtain (2).

The following notation refers to Figure 2. Let $\mathbf{T}$ be one of the n triangles that bound the interior polygon $\mathbf{P}_i$. Then $\mathbf{T}$ has sides a_o, v, $v + a_i$. Let ψ be the angle between v and a_o. We set $\theta = \frac{\pi}{n}$. Then the angle opposite to a_o is equal to $2\theta = \frac{2\pi}{n}$.

3. Proof of Theorem 1

If r_i is the radius of the incircle of $\mathbf{P}_i$, then $r_i = \frac{1}{2}a_i \cot \theta$. Let F_o, F_i and F be the areas of $\mathbf{P}_o$, $\mathbf{P}_i$ and $\mathbf{T}$ respectively. Then

$$F_o = \frac{n\,a_o^2}{4} \cot \theta \quad \text{and} \quad F_i = \frac{n\,a_i^2}{4} \cot \theta,$$

and $nF + F_i = F_o$. Therefore,

$$F = \frac{1}{n}(F_o - F_i) = \frac{1}{4}(a_o^2 - a_i^2) \cot \theta.$$

Let ρ be the inradius of $\mathbf{T}$. Then (2) implies $F = \rho^2 \cot\theta + a_{\mathrm{o}}\rho$. Hence,

$$\frac{a_{\mathrm{o}}^2 - a_{\mathrm{i}}^2}{4} \cot\theta = \rho^2 \cot\theta + a_{\mathrm{o}}\rho.$$

Now assume that the incircles of $\mathbf{P}_{\mathrm{i}}$ and $\mathbf{T}$ are equal, i.e.,

$$r_{\mathrm{i}} = \rho = \frac{1}{2} a_{\mathrm{i}} \cot\theta.$$

We obtain $a_{\mathrm{o}}^2 - a_{\mathrm{i}}^2 = a_{\mathrm{i}}^2 \cot^2\theta + 2a_{\mathrm{o}}a_{\mathrm{i}}$. This yields the quadratic equation

$$a_{\mathrm{o}}^2 - 2a_{\mathrm{i}}a_{\mathrm{o}} = a_{\mathrm{i}}^2(1 + \cot^2\theta) = a_{\mathrm{i}}^2(\sin\theta)^{-2}.$$

Then $a_{\mathrm{o}} > 0$ implies (1).

4. The triangle T

Suppose the exterior polygon $\mathbf{P}_{\mathrm{o}}$ is given. How can one construct the triangle $\mathbf{T}$ and subsequently the interior polygon $\mathbf{P}_{\mathrm{i}}$? The angle opposite to a_{o} is equal to $\frac{2\pi}{n}$. Hence it suffices to know how to obtain the angle ψ between a_{o} and v. For that purpose we derive the following result due to P. Yiu.

Theorem 2. *The angle ψ between a_{o} and v is given by*

$$\cos\psi = \sin^2\frac{\pi}{n}. \tag{3}$$

Proof. It follows from (2) that the area of the triangle $\mathbf{T}$ is given by

$$F = \rho^2 \cot\frac{\psi}{2} + \rho(v + a_{\mathrm{i}}) \tag{4}$$

and

$$F = \rho^2 \cot\frac{\pi - (2\theta + \psi)}{2} + \rho v.$$

Substituting $a_{\mathrm{i}} = 2\rho\tan\theta$ in (4) leads to

$$\cot\frac{\psi}{2} + 2\tan\theta = \tan(\theta + \frac{\psi}{2}) = \frac{\tan\theta + \tan\frac{\psi}{2}}{1 - \tan\theta\tan\frac{\psi}{2}},$$

which is equivalent to

$$\cot\frac{\psi}{2} - 2\tan^2\theta\tan\frac{\psi}{2} = \tan\frac{\psi}{2},$$

and

$$\tan^2\frac{\psi}{2} = \frac{1}{1 + 2\tan^2\theta}. \tag{5}$$

From this,

$$\cos\psi = \frac{1 - \tan^2\frac{\psi}{2}}{1 + \tan^2\frac{\psi}{2}} = \frac{1 - \frac{1}{1+2\tan^2\theta}}{1 + \frac{1}{1+2\tan^2\theta}} = \frac{\tan^2\theta}{1 + \tan^2\theta} = \sin^2\theta.$$

$\square$

5. Special cases

We apply Theorem 1 and Theorem 2 to numbers $n \leq 6$. Note that the righthand side of (1) becomes infinitely large as n goes to infinity. In the case $n = 6$ (and also in a less conspicuous form with $n = 5$) we encounter the golden ratio $\phi = \frac{1}{2}(1 + \sqrt{5})$. To check the case $n = 5$ we recall

$$\cos \frac{2\pi}{5} = \frac{\sqrt{5} - 1}{4} \quad \text{and} \quad \sin \frac{2\pi}{5} = \frac{\sqrt{10 + 2\sqrt{5}}}{4}.$$

In the case $n = 3$ we obtain the known solution of Suzuki's 4-congruent-incircles problem of Section 1. The following table summarizes the data for $n = 3, 4, 5, 6$.

n	$\cos \psi$	$\frac{a_\mathrm{o}}{a_\mathrm{i}}$
3	$\frac{3}{4}$	$\frac{3 + \sqrt{21}}{3}$
4	$\frac{1}{2}$	$1 + \sqrt{3}$
5	$\frac{5 - \sqrt{5}}{8} = \frac{\sqrt{5}}{4\phi}$	$1 + \sqrt{3 + \frac{2}{\sqrt{5}}}$
6	$\frac{1}{4}$	$1 + \sqrt{5} = 2\phi$
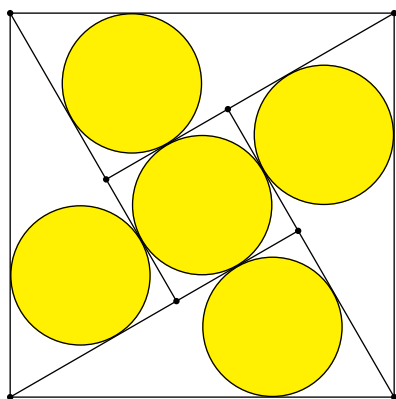
Figure 4. Five congruent incircles in a square
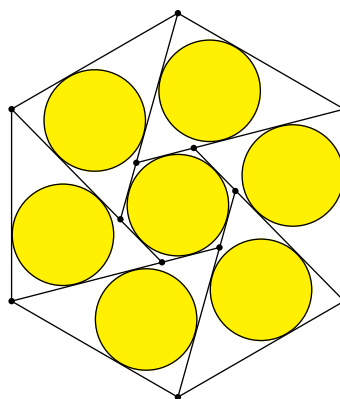
Figure 5. Seven congruent incircles in a regular hexagon

References

[1] H. Fukagawa and D. Pedoe, *Japanese Temple Geometry Problems*, Charles Babbage Research Foundation, Winnipeg, 1989.
[2] H. Fukagawa and J. F. Rigby, *Traditional Japanese Mathematics Problems from the 18th and 19th Centuries*, Science Culture Technology Press, Singapore, 2002.
[3] H. Fukagawa and T. Rothman, *Sacred Mathematics: Japanese Temple Geometry*, Princeton University Press, Princeton, 2008.
[4] A. Hirayama and H. Norii, Fukushima no Sangaku (in Japanese), vol. 4, 1969, self-published.

[5] D. Normile, "Amateur" proofs blend religion and scholarship in ancient Japan, *Science*, 307, no. 5716 (2005) 1715–1716.

[6] T. Rothman, Japanese temple geometry, *Scientific American*, 278 (1998) May issue, 84–91.

Naoharu Ito: Department of Mathematical Education, Nara University of Education, Nara 630-8528, Japan
E-mail address: naoharu@nara-edu.ac.jp

Harald K. Wimmer: Mathematisches Institut, Universität Würzburg 97074 Würzburg, Germany
E-mail address: wimmer@mathematik.uni-wuerzburg.de

A Generalization of the Conway Circle

Francisco Javier García Capitán

Abstract. For any point in the plane of the triangle we show a conic that becomes the Conway circle in the case of the incenter. We give some properties of the conic and of the configuration of the six points that define it.

Let ABC be a triangle and I its incenter. Call B_a the point on line CA in the opposite direction to AC such that $AB_a = BC = a$ and C_a the point on line BA in the opposite direction to AB such that $AC_a = a$. Define C_b, A_b and A_c, B_c cyclically. The six points A_b, A_c, B_c, B_a, C_a, C_b lie in a circle called the *Conway circle* with I as center and squared radius $r^2 + s^2$ as indicated in Figure 1. This configuration also appeared in Problem 6 in the 1992 Iberoamerican Mathematical Olympiad. The problem asks to establish that the area of the hexagon $C_a B_a A_b C_b B_c A_c$ is at least $13\Delta(ABC)$ (see [4]).
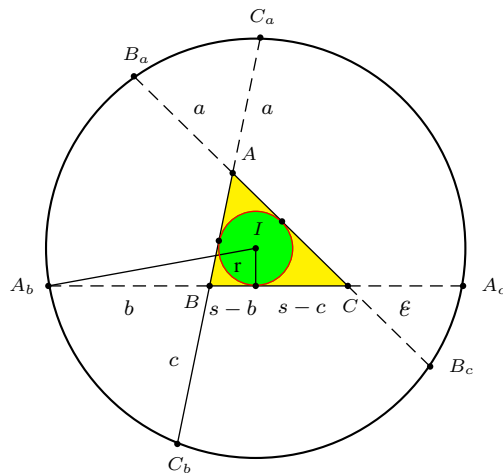
Figure 1. The Conway circle
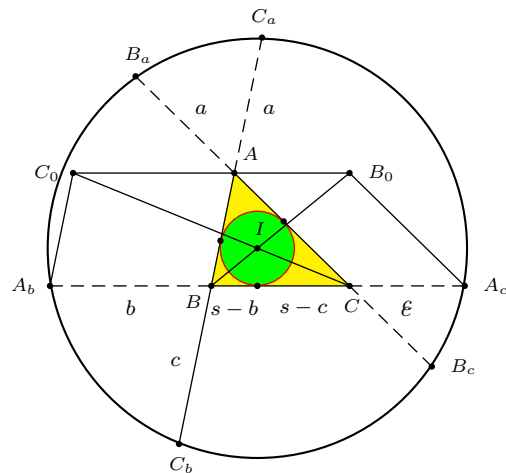
Figure 2

Figure 2 shows a construction of these points which can be readily generalized. The lines BI and CI intersect the parallel of BC through A at B_0 and C_0. The points A_b and A_c are obtained by completing the parallelograms BAC_0A_b and CAB_0A_c. If we take an arbitrary point $P = (u : v : w)$ instead of I, then $B_0 = (u : -w : w)$ and $C_0 = (u : v : -v)$. From these, we determine the points

A_b, A_c, and analogously the other four points (see Figure 3). In homogeneous barycentric coordinates, these are

$$A_b = (0 : u + v : -v), \quad A_c = (0 : -w : w + u);$$
$$B_c = (-w : 0 : v + w), \quad B_a = (u + v : 0 : -u);$$
$$C_a = (w + u : -u : 0), \quad C_b = (-v : v + w : 0).$$

Proposition 1. *The area of ABC is the geometric mean of the areas of the triangles AB_aC_a, BC_bA_b, CA_cB_c.*

Proof. From the coordinates of these points, we have

$$\frac{\Delta(AB_aC_a)}{\Delta(ABC)} = \frac{u^2}{vw}, \quad \frac{\Delta(BC_bA_b)}{\Delta(ABC)} = \frac{u^2}{vw}, \quad \frac{\Delta(CA_cB_c)}{\Delta(ABC)} = \frac{u^2}{vw}.$$

Therefore, $\Delta(ABC)^3 = \Delta(AB_aC_a) \cdot \Delta(BC_bA_b) \cdot \Delta(CA_cB_c)$. $\qquad \square$

Theorem 2. *For any point P, the six points A_b, A_c, B_c, B_a, C_a, C_b always lie on a conic.*
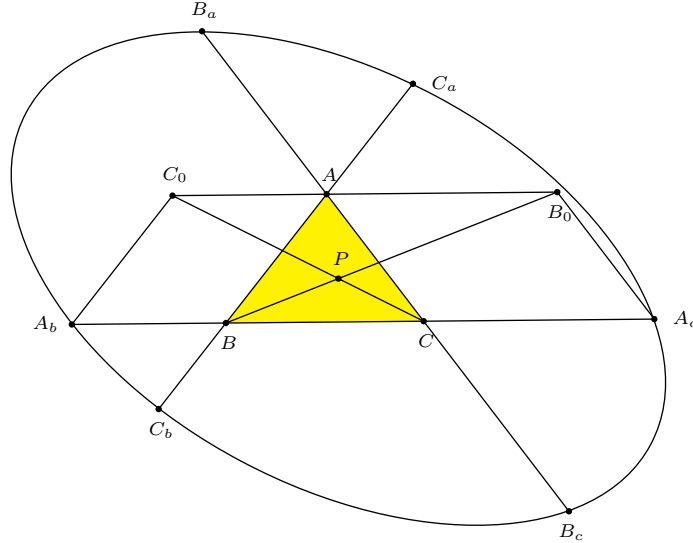
Figure 3

Proof. They all lie on the conic $\Gamma(P)$ with equation

$$u(v + w)x^2 + v(w + u)y^2 + w(u + v)z^2 + (vw + (u + v)(u + w))yz$$
$$+(wu + (v + w)(v + u))zx + (uv + (w + u)(w + v))xy$$
$$= 0.$$

$\qquad \square$

From the matrix form $XMX^t = 0$ for $\Gamma(P)$ where

$$M = \begin{pmatrix} 2u(v+w) & (u+w)(v+w)+uv & (u+v)(v+w)+uw \\ (u+w)(v+w)+uv & 2v(u+w) & (u+v)(u+w)+vw \\ (u+v)(v+w)+uw & (u+v)(u+w)+vw & 2w(u+v) \end{pmatrix}$$

we have

$$|M| = 2(v+w-u)(u+v-w)(u-v+w)(uvw+u^2v+uv^2+u^2w+v^2w+uw^2+vw^2),$$

and $\Gamma(P)$ has discriminant

$$\delta(P) = -\frac{1}{4}(v+w-u)(u+v-w)(u-v+w)(u+v+w).$$

Therefore we can get the following results:

Proposition 3. (a) *The conic $\Gamma(P)$ is degenerate when P lies on the sides of the medial triangle or in the cubic K327.*

(b) *If the conic $\Gamma(P)$ is nondegenerate, it is homothetic to the circumconic with perspector $(u^2 : v^2 : w^2)$ and has center P.*

Proof. (b) follows from rewriting the equation of the conic $\Gamma(P)$ in the form

$$(u^2yz + v^2zx + w^2xy) + (x+y+z)(u(v+w)x + v(w+u)y + w(u+v)z) = 0.$$

$\square$

Proposition 4. *The conic $\Gamma(P)$ and the circumconic with perspector P^2 have the same infinite points.*

If $P = (u : v : w)$ and $u = v + w$, then $\Gamma(P)$ factors as

$$(vx + wx + vy + 2wy + wz)(vx + wx + vy + 2vz + wz) = 0,$$

two parallel lines to the cevian AP. If P lies on $K327$, then $\Gamma(P)$ factors as two lines through P in the directions of the asymptotes of the circumconic with perspector P^2.

If P lies outside the sidelines of the medial triangle and the cubic $K327$, the conic $\Gamma(P)$ is an ellipse when P is interior to the medial triangle and a hyperbola otherwise.

Corollary 5. *The conic $\Gamma(P)$ is*
(a) *a circle if and only if P is the incenter or an excenter of the triangle,*
(b) *a rectangular hyperbola if and only if P lies on the polar circle.*

Remarks. (1) If $P = I_a$, the center of the excircle on the side BC, then $\Gamma(I_a)$ is a circle with squared radius $r_a^2 + (s-a)^2$

(2) The polar circle $S_A x^2 + S_B y^2 + S_C z^2 = 0$ contains real points only if triangle ABC has an obtuse angle.

Proposition 6. (a) *If A', B', C' are the midpoints of B_aC_a, C_bA_b, A_cB_c respectively, the lines AA', BB', CC' concur at P.*

(b) *If A'', B'', C'' are the midpoints of B_cC_b, C_aA_c, A_bB_a respectively, the lines AA'', BB'', CC'' concur at P.*
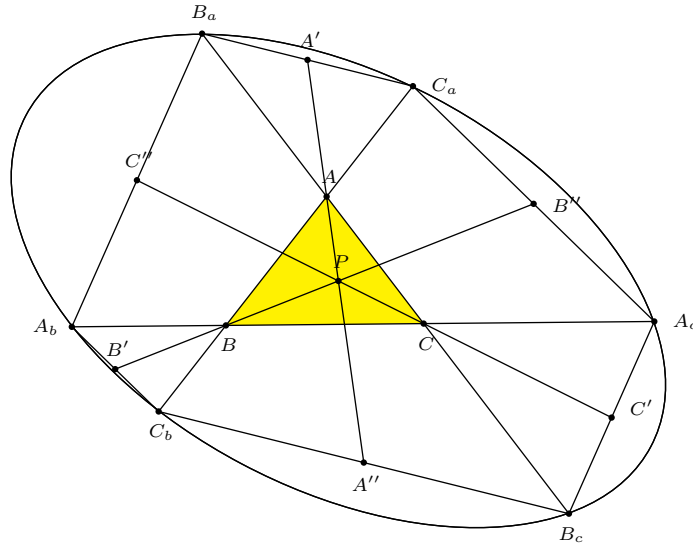
Figure 4

Proof. In homogeneous barycentric coordinates,

$$A' = (2vw + wu + uv : -uv : -uw),$$
$$A'' = (-(v^2 + w^2) : v(v + w) : w(v + w).$$

These points clearly lie on the line AP: $wy - vz = 0$. Similarly, B', B'' lie on BP and C', C'' lie on CP. $\qquad\square$

Proposition 7. *If $P = (u : v : w)$, both of the triangles formed by the lines B_aC_a, C_bA_b, A_cB_c and the lines B_cC_b, C_aA_c, A_bB_a are perspective with ABC at the isotomic conjugate of the anticomplement of P,* i.e.,

$$Q = \left(\frac{1}{v + w - u} : \frac{1}{w + u - v} : \frac{1}{u + v - w} \right).$$

Proof. (a) The lines B_aC_a, C_bA_b, A_cB_c have equations

$$
\begin{array}{ccccccc}
ux & + & (w+u)y & + & (u+v)z & = & 0, \\
(v+w)x & + & vy & + & (u+v)z & = & 0, \\
(v+w)x & + & (w+u)y & + & wz & = & 0.
\end{array}
$$

They bound a triangle with vertices

$$X = (-u(u + v + w) : (v + w)(u + v - w) : (v + w)(w + u - v)),$$
$$Y = ((w + u)(v + w - u) : -v(u + v + w) : (w + u)(v + w - u)),$$
$$Z = ((u + v)(w + u - v) : (u + v)(w + u - v) : -w(u + v + w)).$$
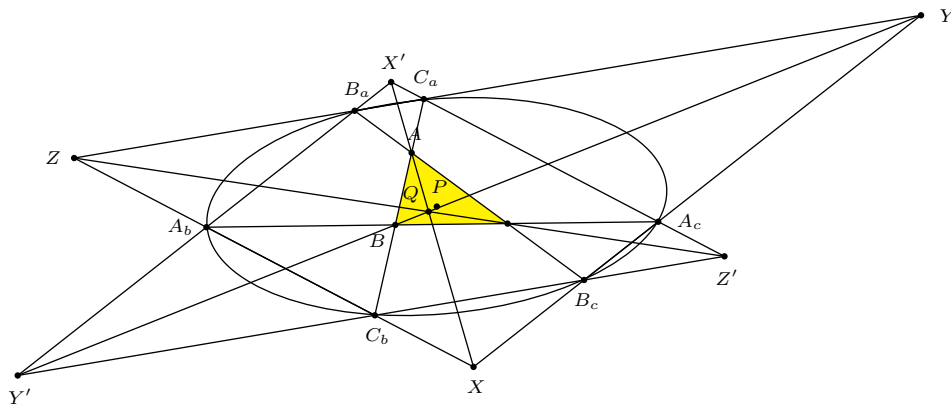
Figure 5

See Figure 5. This is perspective with ABC at

$$Q = \left(\frac{1}{v+w-u} : \frac{1}{w+u-v} : \frac{1}{u+v-w} \right).$$

(b) The lines B_cC_b, C_aA_c, A_bB_a have equations

$$
\begin{array}{rcrcrcl}
(v+w)x & + & vy & + & wz & = & 0, \\
ux & + & (w+u)y & + & wz & = & 0, \\
ux & + & vy & + & (u+v)z & = & 0.
\end{array}
$$

They bound a triangle with vertices

$$
\begin{aligned}
X' &= (-(u+v+w) : u+v-w : w+u-v), \\
Y' &= (v+w-u : -(u+v+w) : v+w-u), \\
Z' &= (w+u-v : w+u-v : -(u+v+w)).
\end{aligned}
$$

The triangle $X'Y'Z'$ is clearly perspective at the same point Q.   □

In the case of the Conway configuration, this is the Gergonne point.

References

[1] A. Bogomolny, Conway's Circle: What is it? `http://www.cut-the-knot.org/Curriculum/Geometry/ConwaysCircle.shtml`
[2] Q. Castellsaguer, The Triangles Web, `http://www.xtec.cat/~qcastell/ttw/`
[3] D. Grinberg and E. W. Weisstein, Conway Circle, MathWorld–A Wolfram Web Resource, `http://mathworld.wolfram.com/ConwayCircle.html`
[4] The Art of Problem Solving: `http://www.artofproblemsolving.com/Forum/resources.php?c=1&cid=29&year=1992&sid=7e0e85e6aef918d5dfa674aadfe60e70`

Francisco Javier García Capitán: Departamento de Matemáticas, I.E.S. Alvarez Cubero, Avda. Presidente Alcalá-Zamora, s/n, 14800 Priego de Córdoba, Córdoba, Spain
E-mail address: `garciacapitan@gmail.com`

On Polygons Admitting a Simson Line
as Discrete Analogs of Parabolas

Emmanuel Tsukerman

Abstract. We call a polygon which admits a Simson line a *Simson polygon*. In this paper, we show that there is a strong connection between Simson polygons and the seemingly unrelated parabola. We begin by proving a few general facts about Simson polygons. We use an inductive argument to show that no convex n-gon, $n \geq 5$, admits a Simson line. We then determine a property which characterizes Simson n-gons and show that one can be constructed for every $n \geq 3$. We proceed to show that a parabola can be viewed as a limit of special Simson polygons, which we call *equidistant Simson polygons*, and that these polygons provide the best piecewise linear continuous approximation to the parabola. Finally, we show that equidistant Simson polygons can be viewed as discrete analogs of parabolas and that they satisfy a number of results analogous to the pedal property, optical property, properties of Archimedes triangles and Lambert's Theorem of parabolas. The corresponding results for parabolas are easily obtained by applying a limit process to the equidistant Simson polygons.

1. Introduction

The Simson-Wallace Theorem (see, e.g., [5]) is a classical result in plane geometry. It states that

Theorem 1. *(Simson-Wallace Theorem[1]). Given a triangle ABC and a point P in the plane, the pedal points of P (That is, the feet of the perpendiculars dropped from P to the sides of the triangle) are collinear if and only if P is on the circumcircle of triangle ABC.*

Such a line is called a Simson line of P with respect to triangle ABC.

A natural question is whether an n-gon with $n \geq 4$ can admit a Simson line. In [3, pp.137–144] and [4], it is shown that every quadrilateral possesses a unique

[1]One remark concerning the theorem is that the Simson-Wallace Theorem is most commonly known as "Simson's Theorem", even though "Wallace is known to have published the theorem in 1799 while no evidence exists to support Simson's having studied or discovered the lines that now bear his name" [5]. This is perhaps one of the many examples of Stigler's law of eponymy.

Simson Line, called "the Simson Line of a complete[2] quadrilateral". We call a polygon which admits a Simson line a *Simson polygon*. In this paper, we show that there is a strong connection between Simson polygons and the seemingly unrelated parabola.

We begin by proving a few general facts about Simson polygons. We use an inductive argument to show that no convex n-gon, $n \geq 5$, admits a Simson Line. We then determine a property which characterizes Simson n-gons and show that one can be constructed for every $n \geq 3$. We proceed to show that a parabola can be viewed as a limit of special Simson polygons, called *equidistant Simson polygons*, and that these polygons provide the best piecewise linear continuous approximation to the parabola. Finally, we show that equidistant Simson polygons can be viewed as discrete analogs of parabolas and that they satisfy a number of results analogous to the pedal property, optical property, properties of Archimedes triangles and Lambert's Theorem of parabolas. The corresponding results for parabolas are easily obtained by applying a limit process to the equidistant Simson polygons.

2. General Properties of Simson Polygons

We begin with an easy Lemma. Throughout, we will use the notation that (XYZ) is the circle through points X, Y, Z.

Lemma 2. *Let S be a point in the interior of two rays AB and AC. Suppose that $ABSC$ is cyclic, and let X be a point on ray AB such that $|AX| < |AB|$. Let $Y = (AXS) \cap AC$. Then $|AY| > |AC|$.*
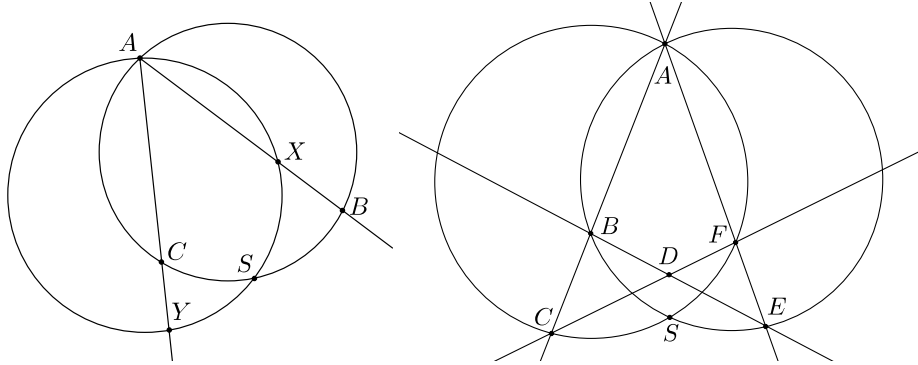
Figure 1. Lemma 2 and Lemma 3

Proof. Since $|AX| < |AB|$, $\angle AXS > \angle ABS$. Since $ABSC$ and $AXSY$ are cyclic, $\angle ACS = \pi - \angle ABS$ and $\angle AYS = \pi - \angle AXS$. Therefore $\angle AYS < \angle ABS$ so that $|AY| > |AC|$.   □

---

[2]A complete quadrilateral is the configuration formed by 4 lines in general position and their 6 intersections. When it comes to pedals, we are only concerned with the sides making up the polygon. Since we extend these, the pedal of a quadrilateral is equivalent to that of its complete counterpart. For this reason, we will refer to a polygon simply by the number of sides it has.

As mentioned in the introduction, in the case of a quadrilateral there is always a unique Simson point defined as a point from which the projections into the sides are collinear. Let A, B, C, D, E, F denote the vertices of the complete quadrilateral, as in fig. 1. It is shown in [3] that the Simson point is the unique intersection of $(AFC) \cap (ABE) \cap (BCD) \cap (DEF)$, also known as the *Miquel point of a complete quadrilateral*. Using Lemma 2, we can conclude the following:

Lemma 3. *Let $ABCDEF$ be a complete quadrilateral where points in each of the triples $A, B, C;$ $B, D, E,$ etc. as in fig. 1 are collinear and angle $\angle CDE$ is obtuse. Denote the Miquel point of $ABCDEF$ by S. There exist no two points X and Y on rays AF, AB respectively with $|AX| < |AF|$, $|AY| < |AB|$ such that (AXY) passes through S.*

Proof. The Miquel point S lies on (AFC) and (ABE). By Lemma 2, no such X and Y exist. □

We call a polygon for which no three vertices lie on a line nondegenerate. In Lemma 4 and Theorems 5 and 6 we will assume that the polygon is nondegenerate.

Lemma 4. *If $\Pi = V_1 \cdots V_n$, $n \geq 5$ is a convex Simson polygon, then Π has no pair of parallel sides.*

Proof. By the nondegeneracy assumption, it is clear that no two consecutive sides can be parallel. So suppose that $V_1 V_2 \parallel V_i V_{i+1}$, $i \notin \{1, 2, n\}$. Then S lies on the Simson line L orthogonal to $V_1 V_2$ and $V_i V_{i+1}$. The projection of S into each other side $V_j V_{j+1}$ must also lie on L, so that either $V_j V_{j+1}$ is parallel to $V_1 V_2$ or it passes through S. By the nondegeneracy assumption, no two consecutive sides can pass through S. Therefore the sides of Π must alternate between being parallel to $V_1 V_2$ and passing through S. It is easy to see that no such polygon can be convex. □

It is worth noting that both the convexity hypothesis and the restriction to $n \geq 5$ in the last result are necessary, for one can construct a non-convex n-gon, $n \geq 5$ having pairs of parallel sides and the trapezoid (if not a parallelogram) is a convex Simson polygon with $n = 4$ having a pair of parallel sides. Using the above result, we can prove:

Theorem 5. *A convex pentagon does not admit a Simson point.*

Proof. Let $\Pi = ABCDE$ be a nondegenerate convex pentagon. Suppose that S is a point for which the pedal in Π is a line. Then in particular the pedal is a line for every 4 sides of the pentagon. Therefore if $BC \cap DE = F$, then S must be a Simson point for $ABFE$, so that S is the Miquel point of $ABFE$. This implies that

$$S = (GAB) \cap (GFE) \cap (HAE) \cap (HBF),$$

where $BC \cap AE = G$ and $AB \cap DE = H$. By the same reasoning applied to quadrilateral $CGED$, S must be the Miquel point of $CGED$. Therefore S lies on (FCD). Because Π is convex, $|FC| < |FB|$ and $|FD| < |FE|$. We can now apply corollary 3 with C and D playing the role of points X and Y to conclude that S cannot lie on (FCD) - a contradiction. □

Consider a convex polygon Π as the boundary of the intersection of half planes $H_1, H_2, \ldots, H_n$. Then the polygon formed from the boundary of $\overset{n}{\underset{\substack{i \neq k \\ i=1}}{\cap}} H_i$ for $k \in \{1, 2, \ldots, n\}$ is also convex.

We are now ready to prove the following result by induction:

Theorem 6. *A convex n-gon with $n \geq 5$ does not admit a Simson point.*

Proof. The base case has been established. Assume the hypothesis for $n \geq 5$, and consider the case for an $(n+1)$-gon Π with vertices $V_1, \ldots, V_{n+1}$. Suppose that Π admits a Simson point. Let $V_{n-1}V_n \cap V_{n+1}V_1 = V'$. This intersection exists by Lemma 4. Since Π admits a Simson point, $\Pi' = V_1 \ldots V_{n-1}V'$ must also admit one. By the preceding remark, Π' is convex, and since it has n sides, the hypothesis is contradicted. Therefore Π cannot admit a Simson line, completing the induction. $\square$

Now that we have established that no convex n-gon (with $n \geq 5$) admits a Simson line, we will proceed to find a necessary and sufficient condition for an n-gon $\Pi = V_1V_2 \ldots V_n$ to have a Simson point. Let $W_i = V_{i-1}V_i \cap V_{i+1}V_{i+2}$ for each i, with $V_{n+k} = V_k$. In case that $V_{i-1}V_i$ and $V_{i+1}V_{i+2}$ are parallel, view W_i as a point at infinity and $(V_iW_iV_{i+1})$ as the line V_iV_{i+1}. For example, in a right-angled trapezoid with $AB \perp BC$ and $AB \perp AD$, S will necessarily lie on the line AB (in fact $S = AB \cap CD$).

Theorem 7. *An n-gon $\Pi = V_1 \cdots V_n$ admits a Simson point S if and only if all circles $(V_iW_iV_{i+1})$ have a common intersection.*

Proof. Assume first that S is a Simson point for Π. The projections of S into $V_{i-1}V_i$, V_iV_{i+1} and $V_{i+1}V_{i+2}$ are collinear. By the Simson-Wallace Theorem (Theorem 1), S is on the circumcircle of $V_iW_iV_{i+1}$.

Conversely, let $S = \underset{i}{\cap}(V_iW_iV_{i+1})$. For each i, this implies that the projections of S into $V_{i-1}V_i$ and $V_{i+1}V_{i+2}$ are collinear. As i ranges from 1 to n we see that all projections of S into the sides are collinear. $\square$

To construct an n-gon with a given Simson point S and Simson line L, let X_1, $X_2, \ldots, X_n$ be n points on L. The n lines the ith of which is perpendicular to SX_i and passing through X_i, $i = 1, \ldots, n$ are the sides of an n-gon with Simson point S and Simson line L. The X_i are the projections of S into the sides of the n-gon and the vertices V_i are the intersections of consecutive pairs of sides.

3. Simson Polygons and Parabolas

In this section we will show that there is a strong connection between Simson polygons and parabolas. In particular, we may view a special type of Simson polygons, which we call equidistant Simson polygons, as discrete analogs of the parabola.
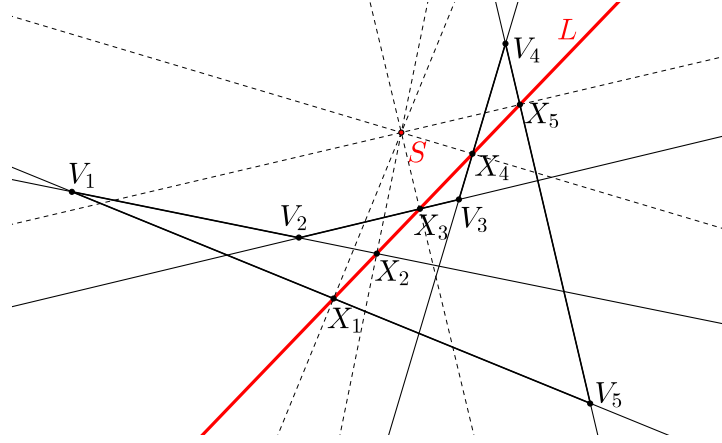
Figure 2. A construction of a pentagon $V_1 V_2 V_3 V_4 V_5$ with Simson point S and Simson line L. The points $X_1, \ldots, X_5$ on L are the projections of S into the sides of the pentagon.

Definition. Let $\Pi = V_1 \cdots V_n$ be a Simson polygon with Simson point S and projections $X_1, \ldots, X_n$ of S into its sides. In the special case that $|X_i X_{i+1}| = \Delta$ for each $i = 1, \ldots, n-1$, we call such a polygon Π an *equidistant Simson polygon*.

The following result shows that all but one of the vertices of an equidistant Simson polygon lie on a parabola. Moreover, the parabola is independent of the position of X_1 (but depends on Δ).

Theorem 8. *Let S be a point and L a line not passing through S. Suppose that $X_1, \ldots, X_n$ are points on L such that $|X_i X_{i+1}| = \Delta$ for all $i = 1, \ldots, n - 1$ and let $\Pi = V_1 \cdots V_n$ be the equidistant Simson polygon with Simson point S and projections $X_1, \ldots, X_n$ of S into its sides. Then $V_1, \ldots, V_{n-1}$ lie on a parabola C. Moreover, C is independent of the position of X_1 on L.*

Proof. Without loss of generality, let $S = (0, s)$, L be the x-axis, $X_i = (X + (i - 1)\Delta, 0)$ and $X_{i+1} = (X + i\Delta, 0)$. A calculation shows that the perpendiculars at X_i and X_{i+1} to the segments SX_i and SX_{i+1}, respectively, intersect at the point $(2X + (2i - 1)\Delta, \frac{(X + (i-1)\Delta)(X + i\Delta)}{s})$. Therefore the coordinates of the intersection satisfy $y = \frac{x^2 - \Delta^2}{4s}$ independently of X. It follows that $V_1, \ldots, V_{n-1}$ lie on the parabola $y = \frac{x^2 - \Delta^2}{4s}$. $\qquad\square$

The fact that C is independent of the position of X_1 on L can be illustrated on figure 3 by supposing that $X_1, X_2, \ldots, X_8$ are being translated on L as a rigid body. Then the independence of C from X_1 implies that C remains fixed and $V_1, \ldots, V_7$ slide together about C.

Corollary 9. *Let C be a parabola with focus F. The locus of projections of F into the lines tangent to C is the tangent to C at its vertex.*
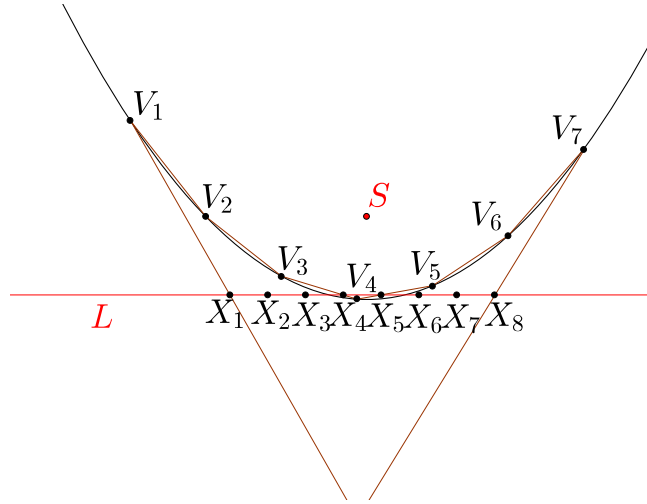
Figure 3. Points $V_1, \ldots, V_8$ are the vertices of an equidistant Simson octagon with a Simson point S, Simson line L and projections $X_1, \ldots, X_8$. By Theorem 8, $V_1, \ldots, V_7$ lie on a parabola.
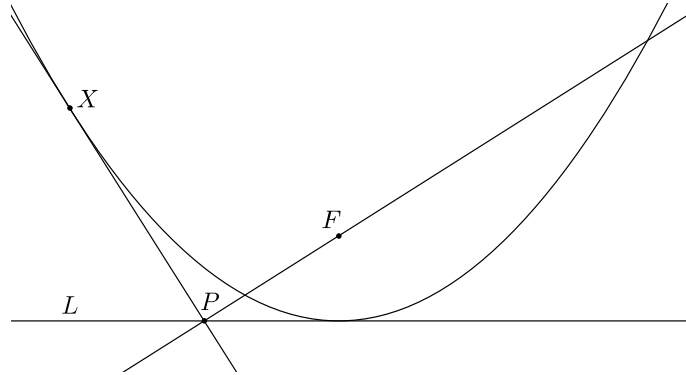
Figure 4. Corollary 9: X is a variable point of C, F is the focus, P is the projection of F into the tangent at X and L is the tangent to C at its vertex.

Proof. As seen in the proof of Theorem 8, the coordinates of the V_i, $i = 1, \ldots, n$ are continuous functions of Δ. Therefore as $n \to \infty$ and $\Delta \to 0$ in Theorem 8, the limit of the polygon is a parabola with focus S and tangent line at the vertex equal to L. $\qquad\qquad\square$

This property can be equivalently stated as: "the pedal curve of the focus of a parabola with respect to the parabola is the line tangent to it at its vertex". This property is by no means new, but its derivation does give a nice connection between the pedal of a polygon and the pedal of the parabola. Specifically, we can view the focus F as the Simson point of a parabola (considered as a polygon with infinitely many points) and the tangent at the vertex as the Simson line of the parabola.

Let $V_1 \cdots V_{n+2}$ be an equidistant Simson polygon. We will now prove that the sides connecting the vertices $V_1, V_2, \ldots, V_{n+1}$ form an optimal piecewise linear continuous approximation of the parabola. To be precise, we show that it is a solution to the following problem:

Problem. Consider a continuous piecewise linear approximation $l(x)$ of a parabola $f(x)$, $x \in [a, b]$ obtained by connecting several points on the parabola. That is, let

$$l(x) = \frac{f(x_{i+1}) - f(x_i)}{x_{i+1} - x_i}(x - x_{i+1}) + f(x_{i+1}) \text{ for } x \in [x_i, x_{i+1}]$$

where $a = x_0 < x_1 < \ldots < x_{n-1} < x_n = b$. Find $x_1, x_2, \ldots, x_{n-1} \in (a, b)$ such that the error

$$\int_a^b |f(x) - l(x)| dx$$

is minimal.

The points $(x_i, f(x_i))$, $i = 0, \ldots, n$ are called knot points and a continuous piecewise linear approximation which solves the problem is called optimal. Since all parabolas are similar, it suffices to consider $f(x) = \frac{x^2 - \Delta^2}{4s}$.

Theorem 10. *The optimal piecewise-continuous linear approximation to $f(x)$ with the setup above is given by the sides $V_1 V_2, V_2 V_3, \ldots, V_n V_{n+1}$ of an equidistant Simson $(n+2)$-gon with $X_1 = \frac{a}{2}$, $\Delta = \frac{b-a}{n}$ and $V_i = (a + (i-1)\Delta, f(a + (i-1)\Delta))$. The knot points $(x_0, f(x_0)), \ldots, (x_n, f(x_n))$ are the vertices $V_1, V_2, \ldots, V_{n+1}$.*

Proof. The equation of the ith line segment simplifies to

$$l(x) = \frac{x(x_{i+1} + x_i) - x_i x_{i+1} - \Delta^2}{4s}, \text{ for } x \in [x_i, x_{i+1}].$$

Therefore $f(x) - l(x) = \frac{(x - x_{i+1})(x - x_i)}{4s}$ for $x \in [x_i, x_{i+1}]$. Integrating $|f(x) - l(x)|$ from x_i to x_{i+1} we get

$$\int_{x_i}^{x_{i+1}} |f(x) - l_i(x)| dx = \frac{(x_{i+1} - x_i)^3}{24|s|}.$$

It is enough to minimize

$$S(x_1, \ldots, x_{n-1}) = 24|s| \int_a^b |f(x) - l(x)| dx = \sum_{i=0}^{n-1} (x_{i+1} - x_i)^3.$$

Taking the partial derivative with respect to x_i for $1 \leq i \leq n-1$ and setting to zero, we get

$$\frac{\partial}{\partial x_i} S(x_1, \ldots, x_{n-1}) = 3(x_i - x_{i-1})^2 - 3(x_{i+1} - x_i)^2 = 0$$
$$\iff (x_i - x_{i-1})^2 = (x_{i+1} - x_i)^2.$$

Since the points are ordered and distinct, $x_i = \frac{x_{i+1}+x_{i-1}}{2}$, so that the x_i's form an arithmetic progression. The x-coordinates of the vertices V_i satisfy this relation, and by uniqueness, the theorem is proved.

$\square$

By similar reasoning, one can see that the same sides of the $(n+2)$-gon are also optimal if the problem is modified to solving the least-squares problem

$$\min_{x_1,\ldots,x_{n-1}} \int_a^b (f(x) - l(x))^2 dx.$$

From the proof of Theorem 10, we have the following interesting result about parabolas.

Corollary 11. *Let $f(x)$ be the equation of parabola, Δ be a real number and let $l(x)$ be the line segment with end points $(y, f(y)), (y + \Delta, f(y + \Delta))$. Then the area*

$$\int_y^{y+\Delta} |f(x) - l(x)| dx$$

bounded by $f(x)$ and $l(x)$ is independent of y.

This property also explains why the x-coordinates of the knot points of the optimal piecewise linear continuous approximation of the parabola are at equal intervals.

We now list some of the properties of equidistant Simson polygons:

Theorem 12. *An equidistant Simson polygon $V_1 V_2 \ldots V_n$ with projections $X_1, X_2, \ldots, X_n$ has the following properties:*

(1) *If $j - i > 0$ is odd, the segments $V_i V_j$, $V_{i+1} V_{j-1}$, $\ldots, V_{\frac{j+i+1}{2}} V_{\frac{j+i-1}{2}}$ are parallel for every $i, j \in \{1, 2, \ldots, n-1\}$.*
(2) *If $j - i > 0$ is even, the segments $V_i V_j$, $V_{i+1} V_{j-1}$, $\ldots, V_{\frac{j+i}{2}-1} V_{\frac{j+i}{2}+1}$ and the tangent to the parabola at $V_{\frac{j+i}{2}}$ are parallel for every $i, j \in \{1, 2, \ldots, n-1\}$.*
(3) *The midpoints of the parallel segments in (1) (respectively (2)) lie on a line orthogonal to the Simson line L.*

Proof. (1). The slope between V_i and V_j is easily calculated to be $\frac{2X+(i+j-1)\Delta}{2s}$.

(2). Recall that the parabola is given by $y = \frac{x^2 - \Delta^2}{4s}$ so that its slope at $V_{\frac{j+i}{2}}$ is $\frac{2X+(2(\frac{j+i}{2})-1)\Delta}{2} = \frac{2X+(j+i-1)\Delta}{2}$.

(3). The x-coordinate of the midpoint of $V_i V_j$ is $2X + (i + j - 1)\Delta$. $\square$

The following property of Simson polygons can be viewed as a discrete analog of the isogonal property of the parabola.
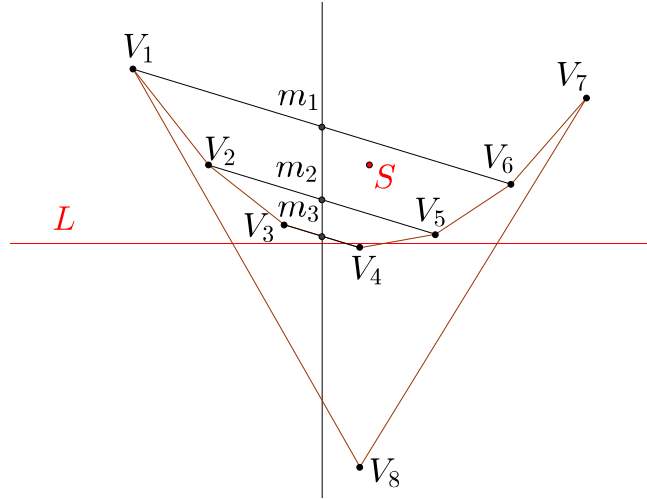
Figure 5. Points $V_1, \ldots, V_8$ are the vertices of an equidistant Simson octagon with Simson point S and Simson line L. By Theorem 12, the segments $V_1 V_6$, $V_2 V_5$ and $V_3 V_4$ are parallel, and their midpoints m_1, m_2 and m_3 all lie on a line perpendicular to L.

Property 1. *Let S and L be the Simson point and Simon line of a Simson polygon (not necessarily equidistant) with vertices $V_1, \ldots, V_n$ and define $X_1, \ldots, X_n$ as before. Let V_i' be the reflection of V_i in L. Then the lines $V_i X_i$ and $V_i X_{i+1}$ are isogonal with respect to the lines $V_i V_i'$ and $V_i S$ (i.e. $\angle V_i' V_i X_i = \angle X_{i+1} V_i S$) for $i = 1, \ldots, n$.*

Proof. The proof is by a straightforward angle count. ☐

In the case when the Simson polygon in Proposition 1 is equidistant, we can take limits to obtain the isogonal property of the parabola:

Corollary 13. *Let C be a parabola with focus F and tangent line L at its vertex. Let X be any point on C and K the tangent at X. Furthermore, let X' be the reflection of X in L. Then K forms equal angles with $X'X$ and FX.*
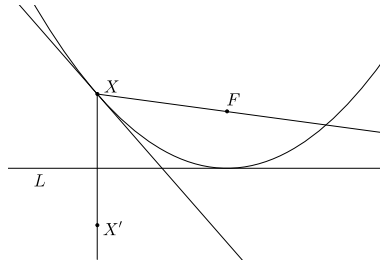
Figure 6. Corollary 13: X is a variable point of the parabola C, F is the focus, L is the tangent to C at its vertex and X' is the reflection of X in L. The lines XF and XX' form equal angles with the tangent at X.

Using the same setup as in Theorem 8 for an equidistant Simson polygon,

Theorem 14. *Let M_i be the midpoint of V_iV_{i+1}, $i = 1, \ldots, n-2$. Then the midpoints M_i lie on a parabola C' with focus S and tangent line at its vertex L.*

Proof. Since $V_i = (2X + (2i-1)\Delta, \frac{(x+(i-1)\Delta)(x+i\Delta)}{s})$,

$$M_i = (2(X + i\Delta), \frac{(X+i\Delta)^2}{s}).$$

Therefore the M_i lie on the parabola $p(x) = \frac{x^2}{4s}$ with focus S. The slope of V_iV_{i+1} is $\frac{X+i\Delta}{s}$, which is the same as that of $p(x)$ at M_i.

□

In a coordinate system where S lies above L, the parabolas C and C' form sharp upper and lower bounds to the piecewise linear curve $f(x)$ formed by the sides connecting $V_1, \ldots, V_{n-1}$ (discussed in Theorem 10). Informally, one can think of C and C' as "sandwiching" $f(x)$, and in the limit $n \to \infty$ and $\Delta \to 0$, the two curves coincide and equal the limit of the polygon.

The following result is a discrete analog of the famous optical reflection property of the parabola.

Corollary 15. *Let M_i be the midpoints of V_iV_{i+1} as in Theorem 14 and p_i be the line passing through M_i orthogonal to L for $i = 1, 2, \ldots, n-2$. Then the reflection p_i' of p_i in V_iV_{i+1} passes through S for each $i = 1, 2, \ldots, n-2$.*
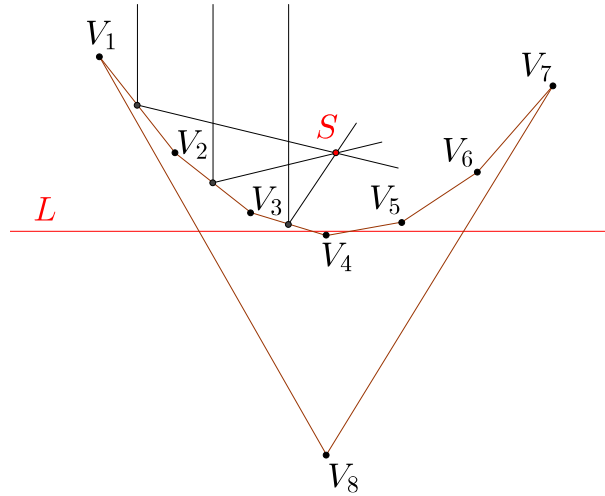
Figure 7. Corollary 15: $\Pi = V_1 \cdots V_8$ is an equidistant Simson polygon. The reflections at the midpoints of the sides of Π of rays orthogonal to L pass through S.

Let X and Y be two points on a parabola C. The triangle formed by the two tangents at X and Y and the chord connecting X and Y is called an *Archimedes Triangle* [2]. The chord of the parabola is called the triangle's base. One of the

results stated in Archimedes' Lemma is that if Z is the vertex opposite to the base of an Archimedes triangle and M is the midpoint of the base, then the median MZ is parallel to the axis of the parabola. The following result yields a discrete analog to Archimedes' Lemma. Let $V_1 \cdots V_n$ be an equidistant Simson polygon.

Theorem 16. *Let $W_{i,j} = V_i V_{i+1} \cap V_j V_{j+1}$ for each $i, j \in \{1, 2, \ldots, n-2\}$ and $i \neq j$. Let $M_{i,j+1}$ and $M_{i+1,j}$ be the respective midpoints of chords $V_i V_{j+1}$ and $V_{i+1} V_j$. Then $W_{i,j} M_{i,j+1}$ and $W_{i,j} M_{i+1,j}$ are orthogonal to L.*

Proof. As shown in the proof of Theorem 12, the x-coordinate of $M_{i,j+1}$ is $2X + (i+j)\Delta$ and that of $M_{i+1,j}$ is the same. The point $W_{i,j}$ is the intersection of the line $V_i V_{i+1}$ given by $y = \frac{X+i\Delta}{s}x - \frac{(X+i\Delta)^2}{s}$ and the line $V_j V_{j+1}$ given by $y = \frac{X+j\Delta}{s}x - \frac{(X+j\Delta)^2}{s}$, so that $W_{i,j} = (2X + (i+j)\Delta, \frac{(X+i\Delta)(X+j\Delta)}{s})$. $\square$

Corollary 17. *The points $W_{i,j+1}, W_{i+1,j}, W_{i+2,j-1}$, etc. and the points $M_{i,j+1}, M_{i+1,j}, M_{i+2,j-1}$, are collinear. The line on which they lie is orthogonal to L.*

Taking limits, we get the following Corollary which includes the part of Archimedes' Lemma stated previously:

Corollary 18. *The vertices opposite to the bases of all Archimedes triangles with parallel bases lie on a single line parallel to the axis of the parabola and passing through the midpoints of the bases.*
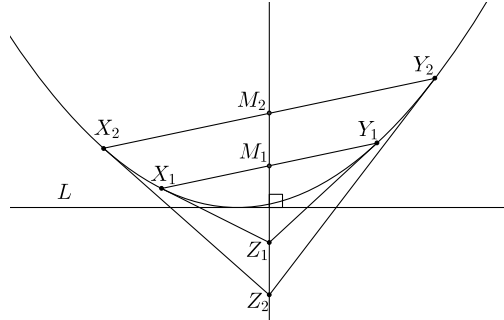
Figure 8. Corollary 18: Triangles $X_1 Y_1 Z_1$ and $X_2 Y_2 Z_2$ are two Archimedes triangles with parallel bases $X_1 Y_1$, $X_2 Y_2$. Points Z_1, Z_2 and the midpoints of the bases M_1, M_2 all lie on a line parallel to the axis of the parabola.

The final theorem to which we give generalization is *Lambert's Theorem*, which states that the circumcircle of a triangle formed by three tangents to a parabola passes through the focus of the parabola [2]. We can prove it using the Simson-Wallace Theorem.

Theorem 19. *Let $V_1 \cdots V_n$ be a Simson polygon (not necessarily equidistant) with Simson point S. Let $i, j, k \in \{1, 2, \ldots, n\}$, be distinct. Then the circumcircle of the triangle T formed from lines $V_i V_{i+1}$, $V_j V_{j+1}$ and $V_k V_{k+1}$ passes through S.*

Proof. Since the projections of S into V_iV_{i+1}, V_jV_{j+1} and V_kV_{k+1} are collinear, S is a Simson point of the triangle T. Therefore by the Simson-Wallace Theorem (Theorem 1), S lies on the circumcircle of T. $\qquad\square$
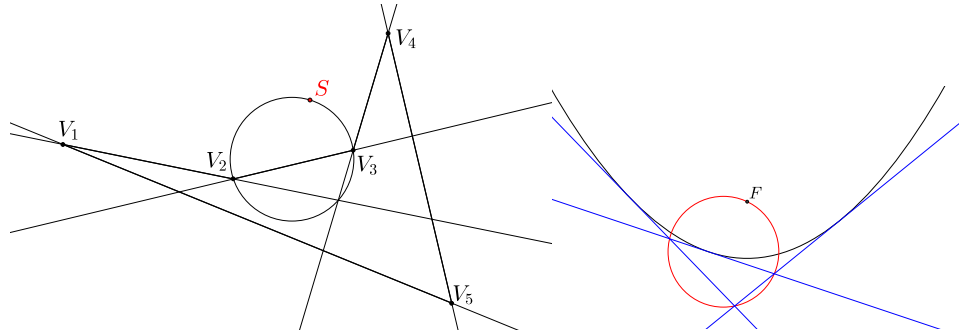
Figure 9. Theorem 19 and Corollary 20.

Corollary 20. *(Lambert's Theorem). The focus of a parabola lies on the circumcircle of a triangle formed by any three tangents to the parabola.*

Proof. Taking the limit of a sequence of equidistant Simson polygons gives Lambert's Theorem for a parabola, since the lines V_iV_{i+1}, V_jV_{j+1}, V_kV_{k+1} become tangents in the limit. $\qquad\square$

References

[1] A. Bogomolny, The Complete Quadrilateral - What Do We Know from Interactive Mathematics Miscellany and Puzzles,
    `http://www.cut-the-knot.org/ctk/CompleteQuadrilateral.shtml`.
[2] A. Bogomolny, The Parabola from Interactive Mathematics Miscellany and Puzzles,
    `http://www.cut-the-knot.org/ctk/Parabola.shtml`.
[3] R. A. Johnson, *Advanced Euclidean Geometry*, Dover Publications, Mineola, NY, 2007.
[4] O. Radko and E. Tsukerman, The Perpendicular Bisector Construction, the Isoptic Point and the Simson Line of a Quadrilateral, *Forum Geom.*, 12 (2012) 161–189.
[5] M. Riegel, Simson's Theorem, `http://www.whitman.edu/mathematics/Senior ProjectArchive/2006/riegelmj.pdf`.

Emmanuel Tsukerman: Department of Mathematics, University of California, Berkeley, CA 94720-3840
E-mail address: `e.tsukerman@berkeley.edu`

Three Natural Homoteties of The Nine-Point Circle

Mehmet Efe Akengin, Zeyd Yusuf Köroğlu, and Yiğit Yargiç

Abstract. Given a triangle with the reflections of its vertices in the opposite sides, we prove that the pedal circles of these reflections are the images of nine-point circle under specific homoteties, and that their centers form the anticevian triangle of the nine-point center. We also construct two concentric circles associated with the pedals of these reflections on the sidelines, and study the triangle bounded by the radical axes of these pedal circles with the nine-point circle.

1. Three pedal circles

Given a triangle ABC with angles α, β, γ, circumcenter O, orthocenter H, and nine-point center N, we let M_a, M_b, M_c be the midpoints of the sides BC, CA, AB, H_a, H_b, H_c the pedals of A on BC, B on CA, C on AB respectively. Consider also the reflections A' of A in BC, B' of B in CA, and C' of C in AB. Our first result (Theorem 3 below) is about the pedal circles of A', B', C' with respect to triangle ABC.

Construct the circle through O, B, C, and let O_a be the second intersection of this circle with the line AO.

Proposition 1. O_a and A' are the isogonal conjugates in triangle ABC.
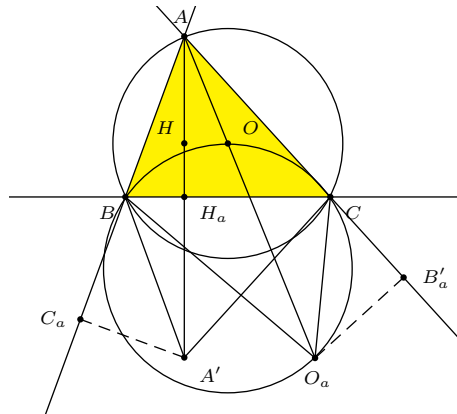
Figure 1

Proof. Clearly the lines AO_a and AH are isogonal with respect to angle A, since O and H are isogonal conjugates. Also,

$$\angle A'BC_a = 2\angle A'AC_a = 2\angle HAB = 2\angle OAC = \angle O^aOC = \angle O^aBC.$$

Therefore, the lines $A'B$ and $O^a B$ are symmetric in the external bisector of angle B, and so are isogonal with respect to angle B. Similarly, $A'C$ and $O^a B$ are isogonal with respect to angle C. This shows that A' and O^a are isogonal conjugates.   □

The points A' and O_a have a common pedal circle, with center at the midpoint N^a of $A'O_a$.

Proposition 2. $O_a A'$ *is parallel to* OH.
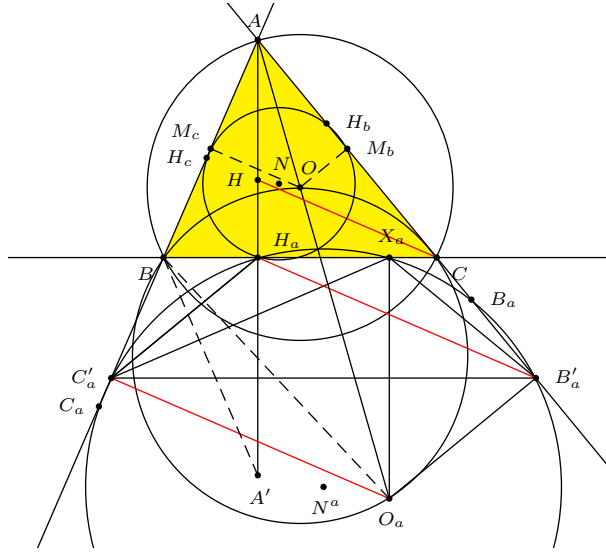
Figure 2

Proof. Let X_a, B'_a, C'_a be the pedals of O_a on BC, CA, AB respectively. From

$$\frac{AM_b}{AB'_a} = \frac{AO}{AO_a} = \frac{AM_c}{AC'_a},$$

we have $B'_a C'_a // M_b M_c // BC$. Therefore the cyclic quadrilateral $B'_a C'_a H_a X_a$, having a pair of parallel sides, must be a symmetric trapezoid. Now,

$$\angle C'_a X_a O_a = \angle C'_a B O_a = \angle CBA' = \beta = \angle C'_a O_a X_a.$$

The second equality is valid because $O_a B$ and $A'B$ are isogonal with respect to B, and the last one because B, X_a, O_a, C'_a are concyclic. It follows that $C'_a O_a = C'_a X_a = B'_a H_a$. Similarly, $B'_a O_a = C'_a H_a$. Therefore, $C'_a O_a B'_a H_a$ is a parallelogram, and $B'_a H_a$ is parallel to $O_a C'_a$, and also to CH, being all perpendicular to AB.

Since M_b and M_c are the midpoints of AC and AB, we have

$$\frac{AO}{AO_a} = \frac{AM_b}{AB'_a} = \frac{AC}{2 \cdot AB'_a} = \frac{AH}{2 \cdot AH_a} = \frac{AH}{AA'}.$$

Therefore, $O_a A'$ is parallel to OH.   □

Theorem 3. *The pedal circle of A' (and O_a) is the image of the nine-point circle of ABC under the homothety* $\mathsf{h}(A, t_a)$, *where* $t_a = \frac{2\sin\beta\sin\gamma}{\cos\alpha}$.

Proof. The circle $B_a B_a' C_a'$ is homothetic to the nine-point circle $H_b M_b M_c$ at A since

$$\frac{AB_a}{AH_b} = \frac{AA'}{AH} = \frac{AO_a}{AO} = \frac{AB_a'}{AM_b} = \frac{AC_a'}{AM_c}.$$

The ratio of homothety is

$$t_a = \frac{AA'}{AH} = \frac{2 \cdot AH_a}{2 \cdot OM_a} = \frac{2R\sin\beta\sin\gamma}{2R\cos\alpha} = \frac{\sin\beta\sin\gamma}{\cos\alpha}.$$

.

Since the center N^a of the pedal circle of A' and O_a is the midpoint of $O_a A'$, the line AN^a intersects OH at its midpoint N, the nine-point center of ABC. □

Analogously let O_b, O_c be the second intersections of the circles OCA, OAB with the lines BO, CO respectively. The common pedal circle of B' and O_b has center N^b the midpoint of $O_b B'$ and that of C' and O_c has center N^c the midpoint of $O_c C'$. These pedal circles are images of the nine-point circle under the homotheties $\mathsf{h}(B, t_b)$ and $\mathsf{h}(C, t_c)$ with $t_b = \frac{\sin\gamma\sin\alpha}{\cos\beta}$ and $t_c = \frac{\sin\alpha\sin\beta}{\cos\gamma}$ respectively.

Theorem 4. $N^a N^b N^c$ *is the anticevian triangle of the nine-point N.*
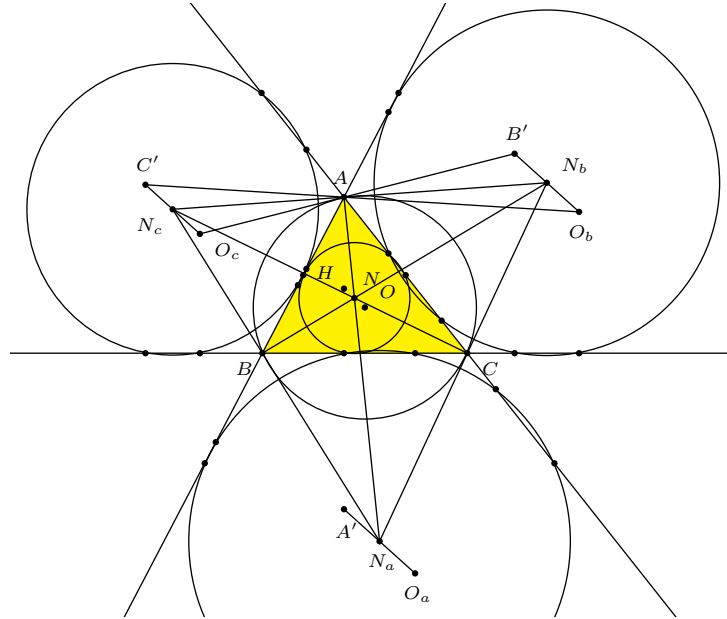
Figure 3

Proof. Since N^a is the midpoint of $O_a A'$ and the nine-point center N is the midpoint of OH, by Proposition 2, A, N, N_a are collinear. Similarly, N^b and N^c are on the cevians BN and CN respectively. We show that the line $N^b N^c$, $N^c N^a$,

$N^a N^b$ contain A, B, C respectively. From this the result follows. It is enough to show that $N^b N^c$ contains A. For this, note that B', A, O_c are collinear because

$$\begin{aligned}
\angle B'AB + \angle BAO_c &= 2\angle B'AC + \angle BOO_c \\
&= 2\alpha + (180° - \angle BOC) \\
&= 2\alpha + (180° - 2\alpha) \\
&= 180°.
\end{aligned}$$

Similarly, O_b, A, and C' are collinear. Therefore, the midpoints of $O_b B'$ and $O_c C'$, namely, N^b and N^c, are collinear with A. □

2. Two concentric circles associated with six pedals

Let $A'' B'' C''$ be the triangle bounded by the lines $B_a C_a$, $C_b A_b$, and $A_c B_c$.

Theorem 5. *The incenter of triangle $A'' B'' C''$ is the orthocenter of the orthic triangle $H_a H_b H_c$, and the incircle touches the sides at the midpoints P_a, P_b, P_c of the segments $B_a C_a$, $C_b A_b$, $A_c B_c$ respectively.*
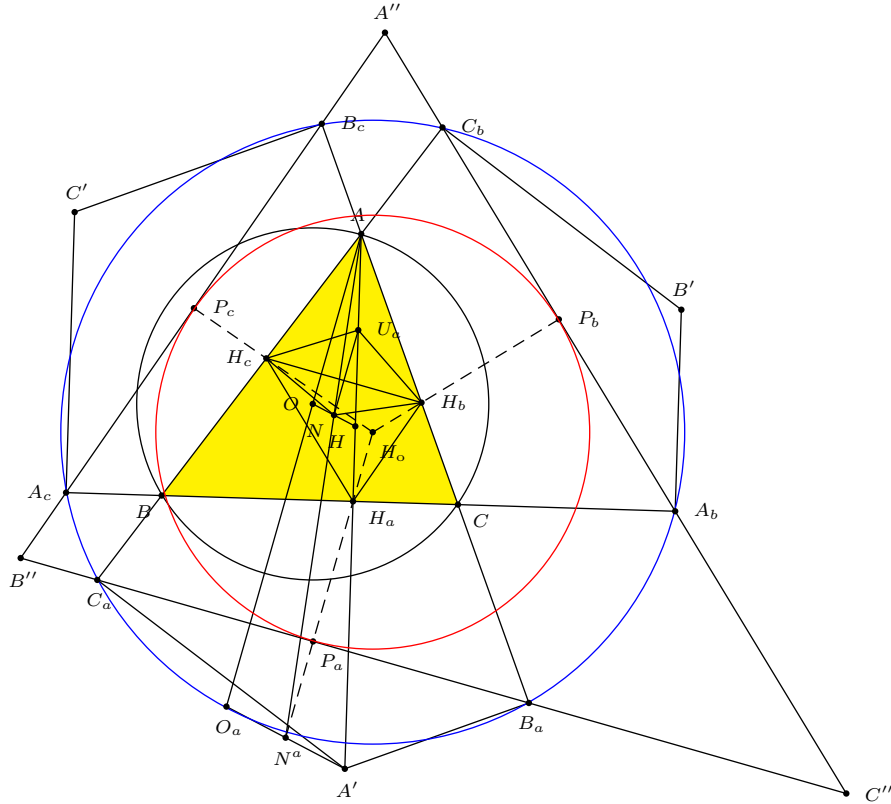
Figure 4.

Proof. We first claim that the segments B_aC_a, C_bA_b, A_cB_c have equal lengths. Note that the homothety $\mathsf{h}(A, t_a)$ maps H_b, H_c to B_a, C_a respectively. Hence,

$$B_aC_a = t_a \cdot H_bH_c = \frac{\sin\beta\sin\gamma}{\cos\alpha} \cdot 2R\sin\alpha\cos\alpha = 4R\sin\alpha\sin\beta\sin\gamma.$$

Since this expression is symmetric in α, β, γ, it also gives the lengths of C_bA_b and A_cB_c.

Note that the corresponding sidelines of triangles $A''B''C''$ and the orthic triangle $H_aH_bH_c$ are parallel. The two triangles are homothetic. By parallelism,

$$\angle A''A_bA_c = \angle H_cH_aA = \angle CH_aH_b = \angle A_bA_cC''.$$

Therefore, $A''A_cA_b$ is an isosceles triangle with $A''A_b = A''A_c$. Since $A_bC_b = A_cB_c$, we deduce that $A''P_b = A''P_c$. Similarly, $B''P_c = B''P_a$ and $C''P_a = C''P_b$. Hence, P_a, P_b, P_c are the points of tangency of the incircle of triangle $A''B''C''$ with its sides.

Next we claim that H_a, N_a and P_a all lie on a line perpendicular to B_aC_a. Let U_a be the midpoint of AH. Since NU_a is parallel to OA, it is perpendicular to B_bH_c. As $NH_b = NH_c$, the line NU_a is the perpendicular bisector of H_bH_c. The homothety $\mathsf{h}(A, t_a)$ maps $U_aH_bNH_c$ into $H_aB_aN^aC_a$, and H_aN^a is the perpendicular bisector of B_aC_a. Therefore, it passes through the midpoint P_a of B_aC_a. Since H_aN^a is perpendicular to H_bH_c, it passes through the orthocenter of the orthic triangle $H_aH_bH_c$. The same is true for the other two lines H_bN^b and H_cN^c, which are the perpendiculars to the sides $C''A''$ and $A''B''$ at the points P_b and P_c respectively. Therefore, the incenter of $A''B''C''$ is the orthocenter of the orthic triangle. $\square$

Remarks. (1) The common length of B_aC_a, C_bA_b, A_cB_c is also the perimeter of the orthic triangle, being $4R\sin\alpha\sin\beta\sin\gamma = R(\sin 2\alpha + \sin 2\beta + \sin 2\gamma)$.

(2) The orthocenter of the orthic triangle is the triangle center $X(52)$ in [3].

Corollary 6. *The lines N^aH_a, N^bH_b, N^cH_c are concurrent at H_o.*

Theorem 7. *The six pedals A_b, A_c, B_c, B_a, C_a, C_b lie on a circle with center H_o.*

Proof. From Theorem 5, we have $H_\mathrm{o}P_a = H_\mathrm{o}P_b = H_\mathrm{o}P_c$. Also recall from the proof of the same theorem, the segments B_aC_a, C_bA_b, A_cB_c have equal lengths. Therefore, $H_\mathrm{o}B_aC_a$, $H_\mathrm{o}C_bA_b$, and $H_\mathrm{o}A_cB_c$ are congruent isosceles triangles, and H_o is the center of a circle containing these six pedals (see Figure 4). $\square$

Theorem 8. *The triangles ABC, $A''B''C''$, and $P_aP_bP_c$ are perspective at the symmedian point of triangle ABC*

Proof. (1) Since AA_cA_b and AB_cC_b are isosceles triangles, B_cC_b and A_cA_b are parallel, and the triangles AC_bB_c and ABC are homothetic (see Figure 5). Now,

$$\angle A''B_cC_b = \angle A''A_cA_b = \angle H_bH_aC = \alpha = \angle B_cAC_b.$$

Similarly, $\angle A''C_bB_c = \angle B_cAC_b$. Therefore, $A''B_c$ and $A''C_b$ are tangents from A'' to the circumcircle of triangle AC_bB_c. The line $A''A$ is a symmedian of triangle AC_bB_c. Since ABC and AC_bB_c are homothetic at A, the same line $A''A$ is a
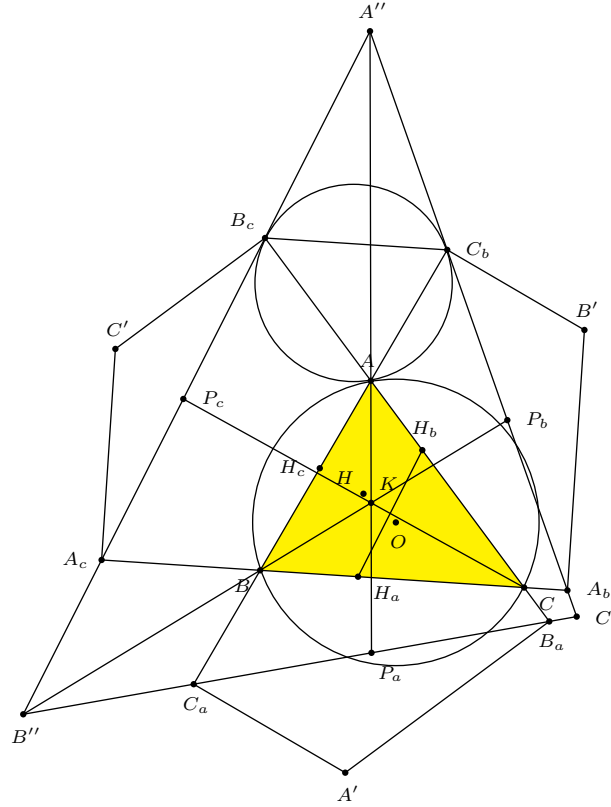
Figure 5.

symmedian of triangle ABC, and it contains the symmedian point K of triangle ABC. The same reasoning shows that $B''B$ and $C''C$ also contain K. Therefore, triangles $A''B''C''$ and ABC are perspective at K.

(2) In triangle ABC, B_aC_a is antiparallel to BC since

$$\angle C_aB_aA = \angle C_aC_bC = \angle BH_aH_b$$

The the reflection of triangles AC_aB_a in the bisector of angle A is homothetic to ABC. Therefore, the median AP_a of triangle AC_aB_a is the same as the symmedian AK; similarly for BP_b and CP_c. The three lines are concurrent at the symmedian point K. □

3. A triangle bounded by three radical axes

Let $\mathscr{L}_a$, $\mathscr{L}_b$, $\mathscr{L}_c$ be the radical axes of the nine-point circle with the pedal circles of A', B', C' respectively. These lines bound a triangle $Q_aQ_bQ_c$. The vertex Q_a is the radical center of the nine-point circle and the pedal circles of B' and C'; similarly for the vertices Q_b and Q_c.
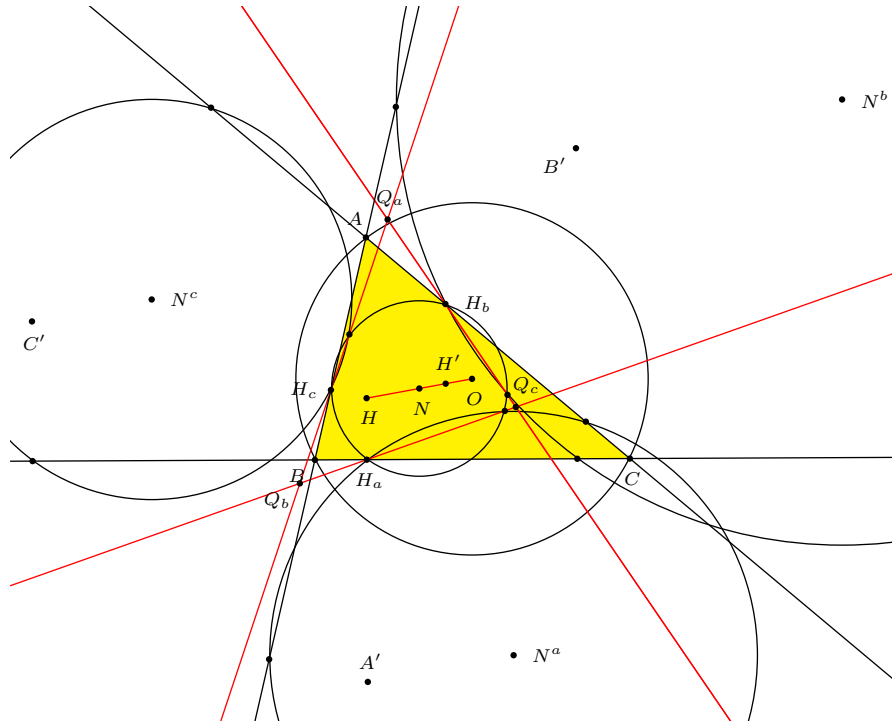
Figure 6

Lemma 9. *Let J_a be the midpoint of OA. The line J_aM_a is perpendicular to Q_bQ_c and contains the midpoint of ON.*
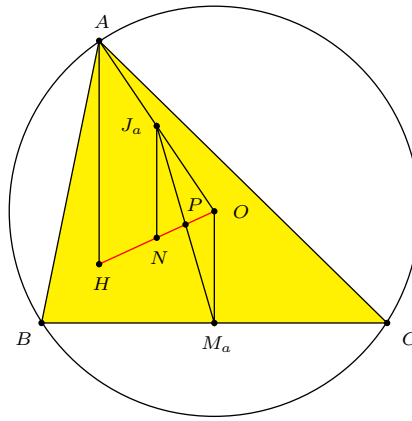
Figure 7.

Proof. Since N is the midpoint of OH, the segment J_aN is parallel to AH and therefore to OM_a. Furthermore, $J_aN = \frac{1}{2}AH = OM_a$. It follows that J_aM_a intersects ON at its midpoint. $\square$

Proposition 10. *Given triangle ABC with incentral triangle DEF, extend AB and AC to P and Q such that $BP = BC = CQ$. Let T be the midpoint PQ, and M the midpoint of the arc BAC of the circumcircle.*

(a) *The line TM is perpendicular EF.*

(b) BT *and* CT *are parallel to* DF *and* DE *respectively.*
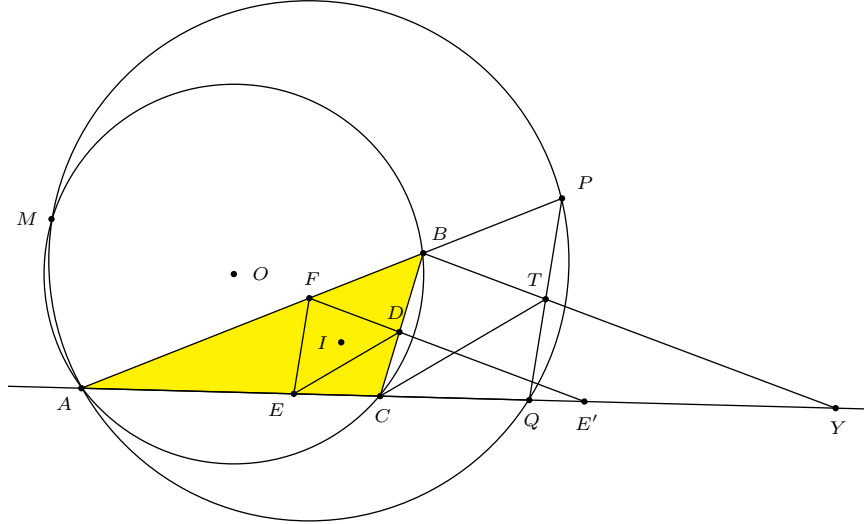
Figure 8.

Proof. (a) By the angle bisector theorem, $AE = \frac{bc}{a+b}$, $AF = \frac{bc}{a+c}$. Therefore, $\frac{AE}{AF} = \frac{a+c}{a+b} = \frac{AQ}{AP}$, showing that PQ is parallel to EF (see Figure 8). On the other hand, the circumcircles of ABC and APQ intersect at A and M, which is the center of the rotation taking the oriented segments BP and CQ into each other (see [4, p.5]). Since $MB = MC$, M is the center of this rotation. Hence, MT is the perpendicular bisector of PQ. We conclude that MT and EF are perpendicular to each other.

(b) We show that BT is parallel to DF.

Let Y be the intersection of the lines BT and AC. Applying Menelaus' theorem to triangle APQ with transversal BTY, we have

$$\frac{AY}{YQ} \cdot \frac{QT}{TP} \cdot \frac{PB}{BA} = -1 \implies \frac{AY}{YQ} = -\frac{AB}{BP} = -\frac{c}{a} \implies \frac{AY}{AQ} = \frac{c}{c-a}.$$

Therefore, $AY = \frac{c(a+b)}{c-a}$. Now, DF intersects AC at E' such that BE' is the external bisector of angle E. $\frac{AE'}{E'C} = -\frac{c}{a} \implies \frac{AE'}{AC} = \frac{c}{c-a}$. It follows that $AE' = \frac{c}{c-a} \cdot b$. From these, $\frac{AE'}{AY} = \frac{b}{a+b} = \frac{AF}{AB}$. Therefore, BT is parallel to DF.

The same reasoning shows that CT is parallel to DE. $\qquad\square$

Remark. Proposition 10 remains valid if P and Q are chosen on the rays BA and CA instead, and BE, BF are external bisectors.

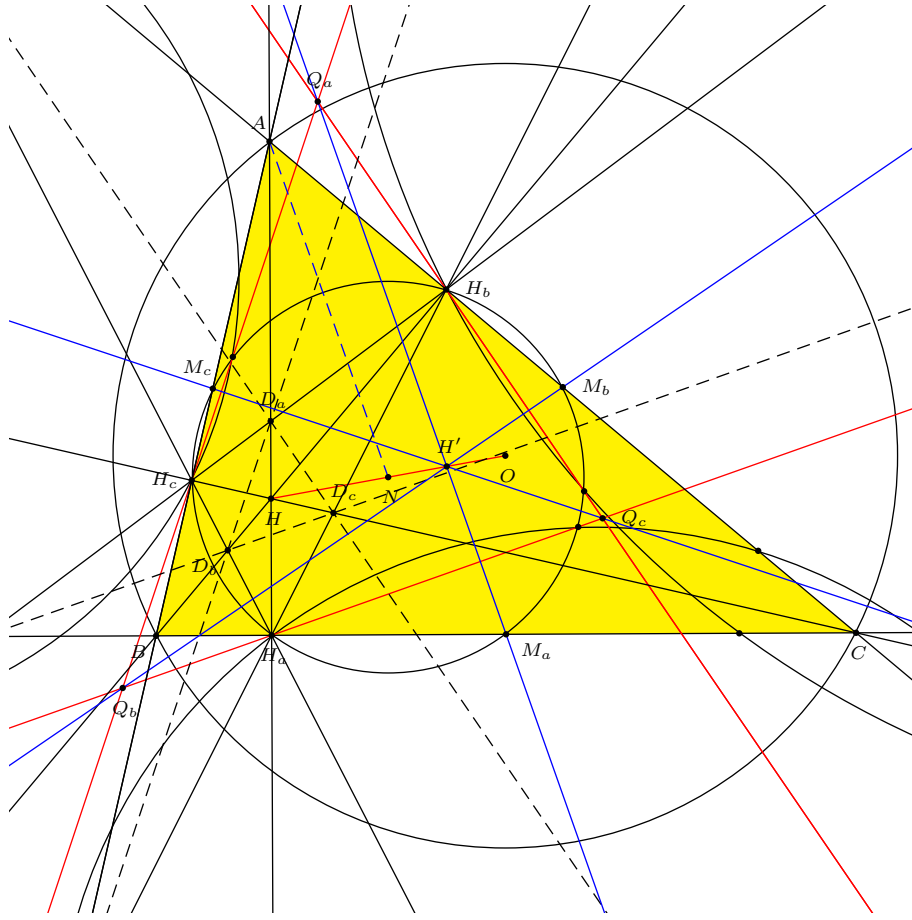**Theorem 11.** *The orthocenter of triangle $Q_aQ_bQ_c$ is the midpoint of ON.*

Figure 9

Proof. It is enough to prove that Q_aM_a is parallel to AN.

Let $D_a = AH \cap H_bH_c$, $D_b = BH \cap H_cH_a$, $D_c = CH \cap H_aH_b$. We claim that D_bD_c is perpendicular to AN. The points D_b and D_c have equal powers with respect to the nine-point circle of ABC and the circumcircle of HBC. Therefore, the line D_bD_c is the radical axis of the these two circles. The circumcenter of HBC is the reflection of O in BC, and form a parallelogram with O, A, H, with N as the common midpoint of the diagonals. Therefore AN is the line joining the centers of the nine-point circle and the center of the circle HBC, and is perpendicular to the radical axis D_bD_c.

The line AN also contains the center N^a of the circle Γ_a. Therefore the radical axes Q_bQ_c and D_bD_c are parallel, and AN is perpendicular to Q_bQ_c.

Now we show that Q_aM_a is parallel to AN.

It is easy to see that $D_aD_bD_c$ is the incentral triangle of $H_aH_bH_c$. (If triangle ABC is obtuse, then the two bisectors not corresponding to obtuse angle have to be replaced by external bisectors; see Remark following Proposition 10). Applying Proposition 10 to the orthic triangle $H_aH_bH_c$, the lines Q_aQ_b and Q_aQ_c are parallel to D_aD_b and D_aD_c respectively, and the midpoint of the arc $H_bH_aH_c$ is M_a, the midpoint of BC. Therefore, Q_aM_a is perpendicular to D_bD_c, which is parallel to Q_bQ_c.

The lines Q_aM_a, Q_bM_b, Q_cM_c are the altitudes of the triangle $Q_aQ_bQ_c$. But these lines are parallel to AN, BN, CN respectively. They are concurrent at the midpoint of ON. $\qquad\square$

Remark. The midpoint of ON is the triangle center $X(140)$ in [3].

References

[1] http://www.artofproblemsolving.com/Forum/viewtopic.php?f=46&t=384694
[2] R. Honsberger, *Episodes in Nineteenth and Twentieth Century Euclidean Geometry*, Math. Assoc. America, 1995.
[3] C. Kimberling, *Encyclopedia of Triangle Centers*, available at
    `http://faculty.evansville.edu/ck6/encyclopedia/ETC.html`.
[4] Y. Zhao, Three Lemmas in Geometry, available at:
    `web.mit.edu/yufeiz/www/olympiad/three_geometry_lemmas.pdf`.

Mehmet Efe Akengin: Istanbul Lisesi (Istanbul High School), Türkocaği Caddesi, No:4, Fatih 34440 Istanbul, Turkey
  E-mail address: `mehmetefeakengin@hotmail.com`

Zeyd Yusuf Köroğlu: Istanbul Lisesi (Istanbul High School), Türkocaği Caddesi, No:4, Fatih 34440 Istanbul, Turkey
  E-mail address: `zeyd.yusuf@gmail.com`

Yiğit Yargiç: Ludwig Maximillian University of Munich, Geschwister-Scholl-Platz 1, 80539 München, Germany
  E-mail address: `yigityargic@hotmail.com`

Intersecting Equilateral Triangles

Colleen Nielsen and Christa Powers

Abstract. In 1980, J. Fickett proposed the following problem: Assume two congruent rectangles R_1 and R_2 intersect in at least one point. Let a be the length of the part of the boundary of R_1 that lies inside R_2 and let b be the length of the part of the boundary of R_2 that lies inside R_1. The conjecture was that the ratio $\frac{a}{b}$ is no smaller than $\frac{1}{3}$ and no larger than 3. This paper presents the solution to the problem when R_1 and R_2 are replaced by equilateral triangles of the same size. We have proved that the ratio $\frac{a}{b}$ is no smaller than $\frac{1}{2}$ and no larger than 2.

In [1], Fickett proposed a problem involving congruent rectangles R_1 and R_2 (including their interiors) in the Euclidean plane and their boundaries ∂R_1 and ∂R_2. The conjecture was that

$$\frac{1}{3} \leq \frac{\text{length } \partial R_1 \cap R_2}{\text{length } \partial R_2 \cap R_1} \leq 3.$$

We show a similar result for equilateral triangles and include a generalization for regular polygons.

Theorem 1. *Let P and Q (including their interiors) be congruent regular $n-$gons, $3 \leq n$, in the Euclidean plane with respective boundaries ∂P and ∂Q.*

(a) *If P and Q intersect in exactly $2n - 1$ or $2n$ boundary points, then* length $\partial P \cap Q = $ length $\partial Q \cap P$.

(b) *If $n = 3$, then* $\dfrac{1}{2} \leq \dfrac{\text{length } \partial P \cap Q}{\text{length } \partial Q \cap P} \leq 2$.

We begin with a useful Lemma.

Lemma 2. *If a_i, b_i are positive real numbers, $2 \leq n$ and $1 \leq i \leq n - 1$, and $\dfrac{a_i}{b_i} = \dfrac{a_{i+1}}{b_{i+1}}$ then $\dfrac{a_i}{b_i} = \dfrac{a_1 + a_2 + \cdots + a_n}{b_1 + b_2 + \cdots + b_n}$.*

Proof. $\dfrac{a_i}{b_i} = \dfrac{a_{i+1}}{b_{i+1}}$ implies that $\dfrac{a_i}{b_i} = \dfrac{a_j}{b_j}$ for $1 \leq i, j \leq n$ and $a_i b_j = b_i a_j$. Thus,

_____

$$a_i b_1 + a_i b_2 + \cdots + a_i b_n = b_i a_1 + b_i a_2 + \cdots + b_i a_n,$$
$$a_i \left(b_1 + b_2 + \cdots + b_n \right) = b_i \left(a_1 + a_2 + \cdots + a_n \right),$$
$$\frac{a_i}{b_i} = \frac{a_1 + a_2 + \cdots + a_n}{b_1 + b_2 + \cdots + b_n}.$$

$\square$

We now prove part (a) of Theorem 1 for $2n$ points. Only an adjustment in the subscripts is needed for the $2n-1$ case. Assume P and Q intersect in $2n$ boundary points with sides labeled as in Figure 1. We must show that $b_0 + b_2 + \cdots + b_{2n-2} = b_1 + b_3 + \cdots + b_{2n-1}$.
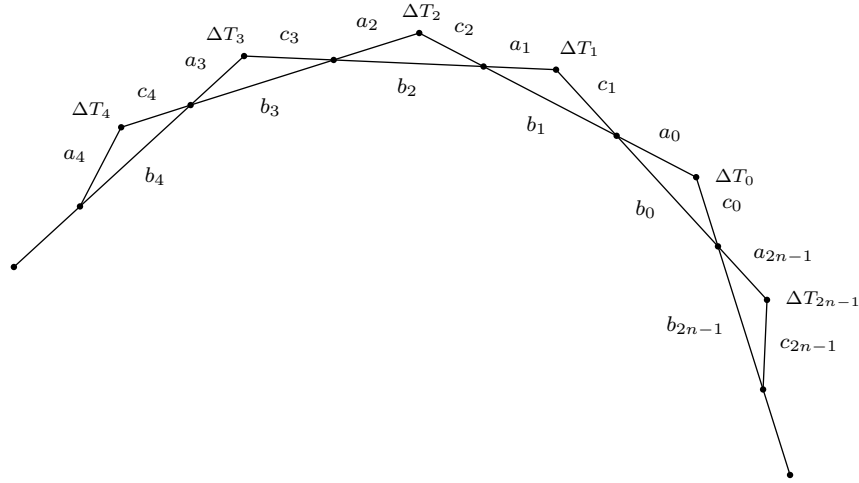
Figure 1

ΔT_i and ΔT_{i+1} both have a $\dfrac{180\,(n-2)}{n}$ degree angle and a pair of congruent vertical angles and so they are similar and more generally, $\Delta T_i \sim \Delta T_k$. This implies that $\dfrac{a_i}{a_j} = \dfrac{b_i}{b_j} = \dfrac{c_i}{c_j}$ and therefore $\dfrac{a_i}{b_i} = \dfrac{a_1}{b_1} = \dfrac{a_3}{b_3} = \cdots = \dfrac{a_{2n-1}}{b_{2n-1}}$ and $\dfrac{a_i}{b_i} = \dfrac{a_0}{b_0} = \dfrac{a_2}{b_2} = \cdots = \dfrac{a_{2n-2}}{b_{2n-2}}$. Using Lemma 1 yields

$$\frac{a_1 + a_3 + \cdots + a_{2n-1}}{b_1 + b_3 + \cdots + b_{2n-1}} = \frac{a_i}{b_i} = \frac{a_0 + a_2 + \cdots + a_{2n-2}}{b_0 + b_2 + \cdots + b_{2n-2}}$$
$$\frac{a_1 + a_3 + \cdots + a_{2n-1}}{a_0 + a_2 + \cdots + a_{2n-2}} = \frac{b_1 + b_3 + \cdots + b_{2n-1}}{b_0 + b_2 + \cdots + b_{2n-2}}$$

Similarly, $\dfrac{a_1 + a_3 + \cdots + a_{2n-1}}{a_0 + a_2 + \cdots + a_{2n-2}} = \dfrac{b_1 + b_3 + \cdots + b_{2n-1}}{b_0 + b_2 + \cdots + b_{2n-2}} = \dfrac{c_1 + c_3 + \cdots + c_{2n-1}}{c_0 + c_2 + \cdots + c_{2n-2}}.$
Again, applying Lemma 1,

$$\frac{b_1 + b_3 + \cdots + b_{2n-1}}{b_0 + b_2 + \cdots + b_{2n-2}} = \frac{a_1 + a_3 + \cdots + a_{2n-1} + c_1 + c_3 + \cdots + c_{2n-1}}{a_0 + a_2 + \cdots + a_{2n-2} + c_0 + c_2 + \cdots + c_{2n-2}}. \quad (1)$$

Assume the sides of the regular polygon are of length 1 and so $a_i + b_{i+1 \ (\mathrm{mod}\ n)} + c_{i+2 \ (\mathrm{mod}\ n)} = 1$ for $1 \leq i \leq n-1$. We find the sum of the sides of each polygon.

$$a_0 + b_1 + c_2 + a_2 + b_3 + c_4 + \cdots + a_{2n-2} + b_{2n-1} + c_0 = n,$$
$$a_0 + a_2 + \cdots + a_{2n-2} + c_0 + c_2 + \cdots + c_{2n-2} = n - (b_1 + b_3 + \cdots + b_{2n-1});$$
$$a_1 + b_2 + c_3 + a_3 + b_4 + c_5 + \cdots + a_{2n-1} + b_0 + c_1 = n,$$
$$a_0 + a_2 + \cdots + a_{2n-1} + c_1 + c_3 + \cdots + c_{2n-1} = n - (b_0 + b_2 + \cdots + b_{2n-2}).$$

These along with (1) yield,

$$\frac{b_1 + b_3 + \cdots + b_{2n-1}}{b_0 + b_2 + \cdots + b_{2n-2}} = \frac{a_1 + a_3 + \cdots + a_{2n-1} + c_1 + c_3 + \cdots + c_{2n-1}}{a_0 + a_2 + \cdots + a_{2n-2} + c_0 + c_2 + \cdots + c_{2n-2}}$$
$$= \frac{n - (b_0 + b_2 + \cdots + b_{2n-2})}{n - (b_1 + b_3 + \cdots + b_{2n-1})}.$$

Let $X = b_1 + b_3 + \cdots + b_{2n-1}$ and $Y = b_0 + b_2 + \cdots + b_{2n-2}$. Substituting $\frac{X}{Y} = \frac{n-Y}{n-X}$, we obtain $nX - X^2 = nY - Y^2$, $(X - Y)(X + Y - n) = 0$.

Now, for each ΔT_i, $b_i < a_i + c_i$, and so

$$2(X + Y) = 2 \sum_{k=0}^{2n-1} b_i < \sum_{k=0}^{2n-1} a_i + b_i + c_i = 2n,$$

which implies that $X + Y < n$. Thus, $X + Y - n \neq 0$, and $X - Y = 0$ or $X = Y$.

Later, we shall need Theorem 1(a) in the special case where $n = 3$ and the two equilateral triangles intersect in exactly five points. We now prove part (b) of Theorem 1 and begin with two preliminary results.

Lemma 3. *If $0 \leq x \leq \frac{\pi}{3}$ then $f(x) = \sin\left(x + \frac{\pi}{3}\right) + \sin x$ has a minimum value of $\frac{\sqrt{3}}{2}$ at $x = 0$ and a maximum value of $\sqrt{3}$ at $x = \frac{\pi}{3}$.*

Proof. For $0 \leq x \leq \frac{\pi}{3}$,

$$f'(x) = \cos\left(x + \frac{\pi}{3}\right) + \cos x = \sqrt{3} \cos\left(x + \frac{\pi}{6}\right) \geq 0,$$

which implies that f is an increasing function on $\left[0, \frac{\pi}{3}\right]$. Thus, $f(0) = \frac{\sqrt{3}}{2}$ is the minimum value of f, and $f\left(\frac{\pi}{3}\right) = \sqrt{3}$ is the maximum value. $\qquad \square$

Proposition 4. *Assume triangle ABC has sides a, b, c and opposite vertices A, B, C, respectively. If $\angle C = 60°$, then $\frac{1}{2} \leq \frac{c}{a+b} < 1$.*

Proof. Using the law of cosines, $c^2 = a^2 + b^2 - 2ab\cos 60° = a^2 + b^2 - ab$. Now,

$$(2c)^2 - (a+b)^2 = 4(a^2 - ab + b^2) - (a^2 + 2ab + b^2) = 3a^2 - 6ab + 3b^2 = 3(a-b)^2 \geq 0.$$

Therefore, $2c \geq a + b$. Since also $c < a + b$, we have $\dfrac{1}{2} \leq \dfrac{c}{a+b} < 1$.   □

To prove part (b) of Theorem 1, we must consider the number of intersection points that are not vertices of a triangle. An intersection point that is a vertex of a triangle will be called a *vertex intersection*. These points will not affect the underlying geometry of what is to follow. If the triangles intersect in fewer than five points, we have four cases to consider (Figure 2).

Case 1: Two intersection points forming a triangle; possibly one vertex intersection.

Case 2: Two intersection points forming a quadrilateral; possibly one or two vertex intersections.

Case 3: Four intersection points forming a quadrilateral.

Case 4: Four intersection points forming a pentagon; possibly two vertex intersections.
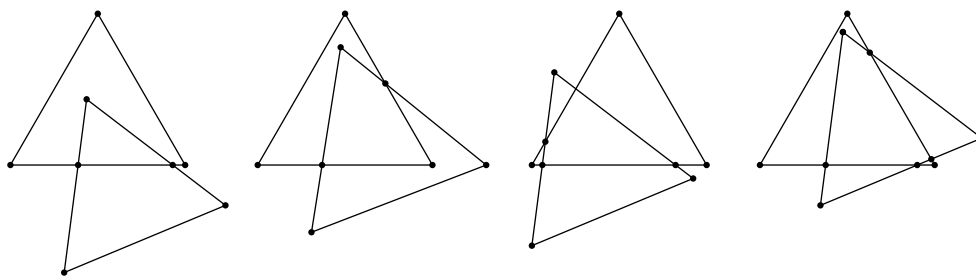
Figure 2

Case 1: In Figure 3, the result follows directly from Proposition 4.
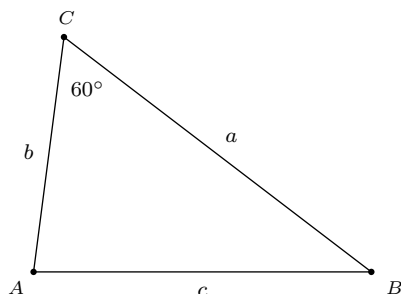
Figure 3
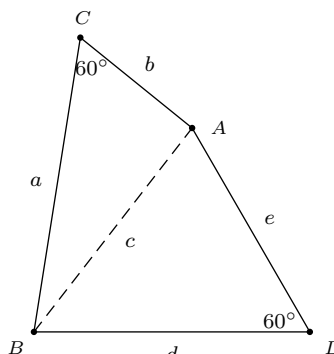
Figure 4

Case 2: We apply the proposition to $\triangle ABC$ and $\triangle ABD$ in Figure 4.

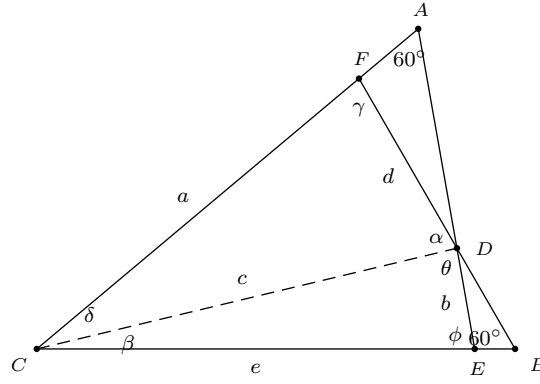Case 3: This case is represented by Figure 5.

Figure 5

We must show that $\dfrac{1}{2} \leq \dfrac{a+b}{d+e} \leq 2$. The angles γ and ϕ are external angles of triangles AFD and BED respectively. Since $\angle FDA = \angle BDE$, $\gamma = \phi$. Applying the law of sines and Lemma 1,

$$\frac{a}{\sin \alpha} = \frac{d}{\sin \delta} = \frac{c}{\sin \gamma} = \frac{c}{\sin \phi} = \frac{b}{\sin \beta} = \frac{e}{\sin \theta},$$

$$\frac{a+b}{\sin \alpha + \sin \beta} = \frac{c}{\sin \gamma} = \frac{d+e}{\sin \delta + \sin \theta}$$

$$\frac{a+b}{d+e} = \frac{\sin \alpha + \sin \beta}{\sin \delta + \sin \theta}.$$

Since α is an external angle of triangle CDB, $\alpha = \beta + 60°$. Similarly, $\theta = \delta + 60°$. Substitution yields

$$\frac{a+b}{d+e} = \frac{\sin (\beta + 60°) + \sin \beta}{\sin \delta + \sin (\delta + 60°)}.$$

Since $\alpha + \delta < 180°$, $\beta + \delta \leq 60°$, and by Lemma 2, $\dfrac{\sin (\beta + 60) + \sin \beta}{\sin \delta + \sin (\delta + 60)}$ will have a minimum value when $\beta = 0$ and $\delta = 60°$ and a maximum value when $\beta = 60°$ and $\delta = 0$. Thus,

$$\frac{\frac{\sqrt{3}}{2}}{\sqrt{3}} \leq \frac{\sin (\beta + 60°) + \sin \beta}{\sin \delta + \sin (\delta + 60°)} \leq \frac{\sqrt{3}}{\frac{\sqrt{3}}{2}} \implies \frac{1}{2} \leq \frac{a+b}{d+e} \leq 2.$$

Case 4: We must now show that $\dfrac{1}{2} \leq \dfrac{a+b+d}{c+e} \leq 2$ and there are two subcases to consider. The first is illustrated by Figure 6.

In Figure 6(a), construct a segment through point A that is parallel to ED and that intersects FD and FE in points D_1 and E_1, respectively. Similarly, construct a segment that is parallel to BC and that intersects AB and AC in points B_1 and C_1, respectively so that triangles AB_1C_1 and D_1E_1F are congruent (Figure 6(b)). By construction, $c_1 < c$, $d_1 > d$, and $e_1 < e$. We apply Theorem 1(a) for
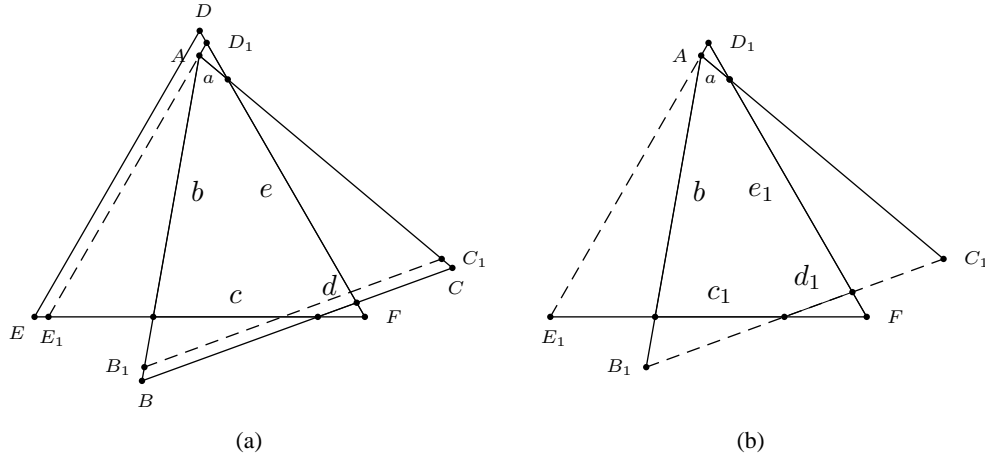
Figure 6

equilateral triangles having five intersection points to Figure 6(b), and obtain

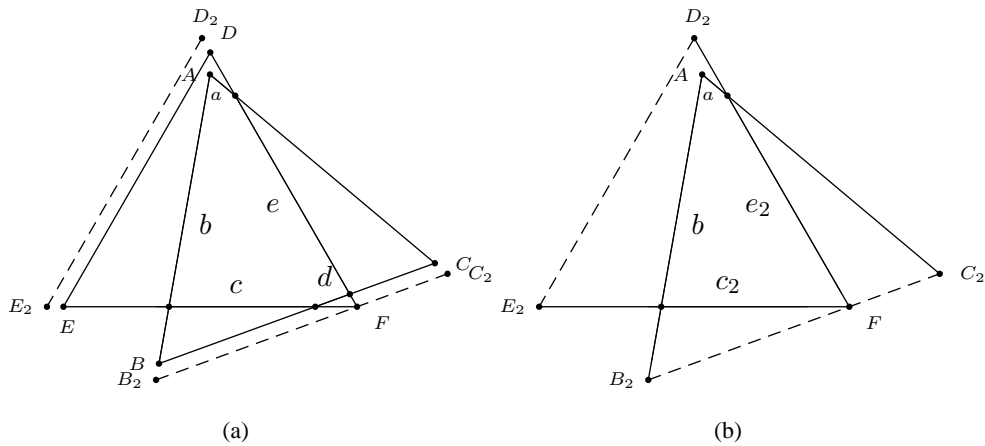$$\frac{a+b+d}{c+e} < \frac{a+b+d_1}{c_1+e_1} = 1 \le 2.$$

Figure 7

The second case is shown in Figure 7(a). Extend AB and AC so that each intersects the line through F parallel to BC at points B_2 and C_2, respectively. Construct a segment that is parallel to ED and that intersects FE and FD in points E_2 and D_2 respectively, so that triangles AB_2C_2 and D_2E_2F are congruent (Figure 7(b)). By construction, $c < c_2$ and $e < e_2$. We apply Case 2 to Figure 7(b) and obtain

$$\frac{1}{2} \le \frac{a+b}{c_2+e_2} < \frac{a+b+d}{c+e}.$$

Combining the inequalities yields $\dfrac{1}{2} \leq \dfrac{a + b + d}{c + e} \leq 2$. This completes the proof of Theorem 1.

Fickett's rectangle problem also appeared in a conjecture that if the congruent polygons were triangles then the maximum ratio would be $\csc \frac{\theta}{2}$ where θ is the smallest angle of the triangle. For equilateral triangles, $\theta = 60°$ and $\csc \frac{\theta}{2} = 2$. This corresponds to our result.

References

[1] J. Fickett, Overlapping congruent convex bodies, *Amer. Math. Monthly*, 87 (1980) 814–815.
[2] H. Croft, K. Falconer, and R. Guy, *Unsolved Problems in Geometry*, Springer-Verlag, New York, 1991. p. 25.

Colleen Nielsen: 15 Parkside Place, Apt. 231, Revere, MA 02151, USA
E-mail address: Cnielsen1022@gmail.com

Christa Powers: Timberlane Regional High School, 36 Greenough Road, Plaistow, NH 03865, USA
E-mail address: cody.christa@yahoo.com

Some Simple Results on Cevian Quotients

Francisco Javier García Capitán

Abstract. We find the loci of the cevian quotients P/Q and Q/P when one of the points is fixed and the other moves along a given line. We also show that, for a given point P, the locus of Q for which the line joining P/Q and Q/P is parallel to PQ is a conic through P and G/P, and give two simple constructions of the conic.

The term cevian quotient was due to John Conway [1]. Given two points $P = (u : v : w)$ and $Q = (x : y : z)$ in homogeneous barycentric coordinates with reference to a triangle ABC, the cevian quotient P/Q is the perspector of the cevian triangle of P and the anticevian triangle of Q. It is the point

$$P/Q = \left(x\left(-\frac{x}{u} + \frac{y}{v} + \frac{z}{w} \right) : y\left(\frac{x}{u} - \frac{y}{v} + \frac{z}{w} \right) : z\left(\frac{x}{u} + \frac{y}{v} - \frac{z}{w} \right) \right).$$

A most basic property of cevian quotient is the following theorem.

Theorem 1 ([2, §2.12], [5, §8.3]). *$P/Q = Q'$ if and only if $P/Q' = Q$.*

This is equivalent to $P/(P/Q) = Q$. It can be proved by direct verification with coordinates. We offer an indirect proof, with the advantage of an explicit construction, for given Q and Q', of a point P with $P/Q = Q'$ and $P/Q' = Q$.

For $Q = (x : y : z)$ and $Q' = (x' : y' : z')$ with anticevian triangles XYZ and $X'Y'Z'$, it is easy to check that the lines QX' and $Q'X$ intersect on the sideline BC, at the point $(0 : xy' + x'y : zx' + z'x) = \left(0 : \frac{1}{zx'+z'x} : \frac{1}{xy'+x'y} \right)$ (see Figure 1). Similarly, the lines QY' and $Q'Y$ intersect on CA at $\left(\frac{1}{yz'+y'z} : 0 : \frac{1}{xy'+x'y} \right)$, and the lines QZ' and $Q'Z$ intersect on AB at $\left(\frac{1}{yz'+y'z} : \frac{1}{zx'+z'x} : 0 \right)$. These form the cevian triangle of the point $P = \left(\frac{1}{yz'+y'z} : \frac{1}{zx'+z'x} : \frac{1}{xy'+x'y} \right)$. It is clear that $P/Q = Q'$ and $P/Q' = Q$.

Remark. The point $P = \left(\frac{1}{yz'+y'z} : \frac{1}{zx'+z'x} : \frac{1}{xy'+x'y} \right)$ is called the cevian product $Q * Q'$ of Q and Q'. Clearly, $Q * Q' = Q' * Q$.

Proposition 2. *Let P be a fixed point. If Q moves along a line $\mathscr{L}$, then the quotient P/Q traverses the bicevian conic of P and the trilinear pole of $\mathscr{L}$.*
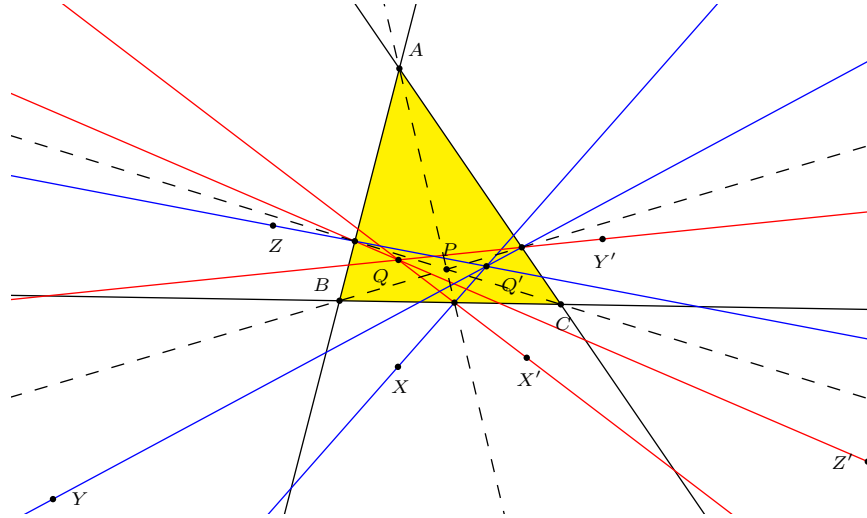
Figure 1.

Proof. Let $P = (u : v : w)$ and Q move along the line $\mathscr{L}$ with line coordinates $[p : q : r]$. If $Q' = P/Q = (x : y : z)$, then $Q = P/Q'$ is on the line $\mathscr{L}$, and

$$px\left(-\frac{x}{u} + \frac{y}{v} + \frac{z}{w}\right) + qy\left(\frac{x}{u} - \frac{y}{v} + \frac{z}{w}\right) + rz\left(\frac{x}{u} + \frac{y}{v} - \frac{z}{w}\right) = 0.$$

Clearing denominators and simplifying, we obtain

$$pvwx^2 + qwuy^2 + ruvz^2 - u(qv + rw)yz - v(rw + pu)zx - w(pu + qv)xy = 0.$$

If $x = 0$, this becomes $u(qy - rz)(wy - uz) = 0$. The conic intersects the line BC at $(0 : v : w)$ and $(0 : r : q)$. Similarly, it intersects CA at $(u : 0 : w)$ and $(r : 0 : p)$, and AB at $(u : v : 0)$ and $(q : p : 0)$. This is the bicevian conic through the traces of P and $\left(\frac{1}{p} : \frac{1}{q} : \frac{1}{r}\right)$, the trilinear pole of $\mathscr{L}$.   □

Corollary 3 ([4])**.** *Let P be a fixed point. The locus of Q for which the cevian quotient P/Q lies on the tripolar of P is the inscribed conic with perspector P.*

Proposition 4. *Let P be a fixed point. If Q moves along a line $\mathscr{L}$, then the cevian quotient Q/P traverses the circumconic of the anticevian triangle of P with perspector $P_{\mathscr{L}}/P$, where $P_{\mathscr{L}}$ is the trilinear pole of $\mathscr{L}$.*

Proof. Let $P = (u : v : w)$ and Q move along the line $\mathscr{L}$ with line coordinates $[p : q : r]$. If $Q'' = Q/P = (x : y : z)$, then $Q = \left(\frac{1}{wy+vz} : \frac{1}{uz+wx} : \frac{1}{vx+uy}\right)$ is on the line $\mathscr{L}$, and

$$\frac{p}{wy + vz} + \frac{q}{uz + wx} + \frac{r}{vx + uy} = 0.$$

Clearing denominators and simplifying, we obtain

$$pvwx^2 + qwuy^2 + ruvz^2 + (pu + qv + rw)(uyz + vzx + wxy) = 0.$$

It is easy to verify that this conic passes through $A' = (-u : v : w)$, $B' = (u : -v : w)$, $C' = (u : v : -w)$. It is a circumconic of the anticevian triangle of P. The tangents to the conic at A', B', C' are the lines $L_a : (qv + rw)x + quy + ruz = 0$, $L_b : pvx + (pu + rw)y + rvz = 0$, $L_c : pwx + qwy + (pu + qv)z = 0$ which intersects $\mathscr{L}$ on BC, CA, AB respectively. This is the conic tangent to the lines $A'X'$, $B'Y'$, $C'Z'$ at A', B', C' respectively. These lines bound a triangle with vertices

$$\left(\frac{qv + rw}{u} : q : r \right), \quad \left(p : \frac{rw + pu}{v} : r \right), \quad \left(p : q : \frac{pu + qv}{w} \right).$$

These form a triangle perspective with the anticevian triangle of P at

$$(u(-pu + qv + rw) : v(pu - qv + rw) : w(pu + qv - rw)),$$

the cevian quotient of $\left(\frac{1}{p} : \frac{1}{q} : \frac{1}{r} \right)$ (the trilinear pole of $\mathscr{L}$) by P. $\square$

Let $\mathscr{L}/P$ be the conic in Proposition 4. This conic is a circle if and only if it is the circumcircle of the anticevian triangle of P. The line $\mathscr{L}$ is the one containing the intercepts of the tangents to this circle at A', B', C' on the respective sidelines of triangle ABC (see Figure 2). This has line coordinates

$$p : q : r = (u(v + w - u)(c^2 v^2 - (b^2 + c^2 - a^2)vw + b^2 w^2)$$
$$v(w + u - v)(a^2 w^2 - (c^2 + a^2 - b^2)wu + c^2 u^2)$$
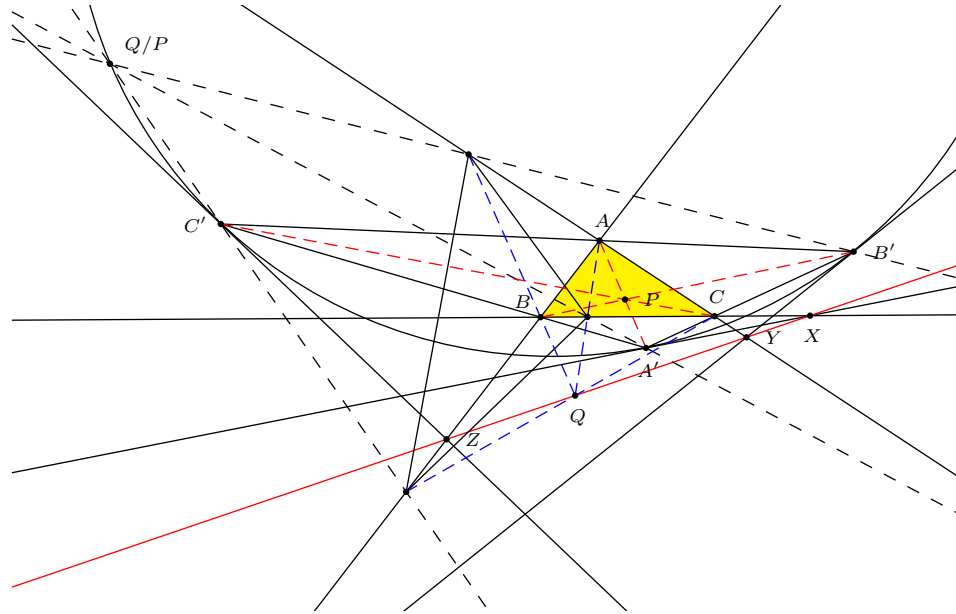$$w(u + v - w)(b^2 u^2 - (a^2 + b^2 - c^2)uv + a^2 v^2).$$

Figure 2.

Here are some simple examples in which $\mathscr{L}/P$ is the circumcircle of the antice-vian triangle of P:

P	$\mathscr{L}$
centroid	$a^2x + b^2y + c^2z = 0$
incenter	line at infinity
symmedian point	$\sum_{\text{cyclic}} a^2(b^2 + c^2 - a^2)x = 0$

Proposition 5. *Let P be a fixed point. The locus of Q for which the line joining (P/Q) to (Q/P) is parallel to PQ is the union of the cevian lines AP, BP, CP and a conic $\Gamma(P)$*

(1) *homothetic to the circumconic with perspector P,*

(2) *passing through P and the cevian quotient G/P, and has*

(3) *the midpoint of P and G/P as center.*

Proof. If $P = (u : v : w)$ and $Q = (x : y : z)$, the line joining P/Q and Q/P contains the infinite point of PQ if and only if

$$\begin{vmatrix} x\left(-\frac{x}{u} + \frac{y}{v} + \frac{z}{w}\right) & y\left(\frac{x}{u} - \frac{y}{v} + \frac{z}{w}\right) & z\left(\frac{x}{u} + \frac{y}{v} - \frac{z}{w}\right) \\ u\left(-\frac{u}{x} + \frac{v}{y} + \frac{w}{z}\right) & v\left(\frac{u}{x} - \frac{v}{y} + \frac{w}{z}\right) & w\left(\frac{u}{x} + \frac{v}{y} - \frac{w}{z}\right) \\ (v+w)x - u(y+z) & (w+u)y - v(z+x) & (u+v)z - w(x+y) \end{vmatrix} = 0.$$

Clearing denominators and simplifying, we obtain

$$2(wy - vz)(uz - wx)(vx - uy)(vwx^2 + wuy^2 + uvz^2 - u^2yz - v^2zx - w^2xy) = 0.$$

Therefore Q lies on one of the lines AP, BP, CP or the conic $\Gamma(P)$ defined by

$$vwx^2 + wuy^2 + uvz^2 - u^2yz - v^2zx - w^2xy = 0.$$

Rewriting this as

$$\Gamma(P): \ (u+v+w)(uyz + vzx + wxy) - (x+y+z)(vwx + wuy + uvz) = 0,$$

it is clear that $\Gamma(P)$ is homothetic to the circumconic with perspector P, and it is routine to verify that it contains P and the cevian quotient $G/P = (u(-u+v+w) : v(u-v+w) : (u+v-w)w)$. The center of the conic is the midpoint of P and G/P, namely,

$$\left(u(u^2 - uv - uw - 2vw) : v(v^2 - uv - 2uw - vw) : w(w^2 - 2uv - uw - vw)\right).$$

$\square$

Remarks. (1) If P is the symmedian point, then $\Gamma(P)$ is the Brocard circle with diameter OK.

(2) If the line PQ contains A, then both cevian quotients P/Q and Q/P are on the same line.

It is easy to note that the conic $\Gamma(P)$ contains the points

$$A_1 = (-u+v+w : v : w), \quad B_1 = (u : u-v+w : w), \quad (u : v : u+v-w)$$

We present two simple constructions of these points, one by Peter Moses [3], and another by Paul Yiu [6].

Construction (Moses)**.** Intersect the cevians AP, BP, CP with the parallels through the centroid G to BC, CA, AB, at X, Y, Z respectively. A_1, B_1, C_1 are the harmonic conjugates of P in AX, BY, CZ respectively.
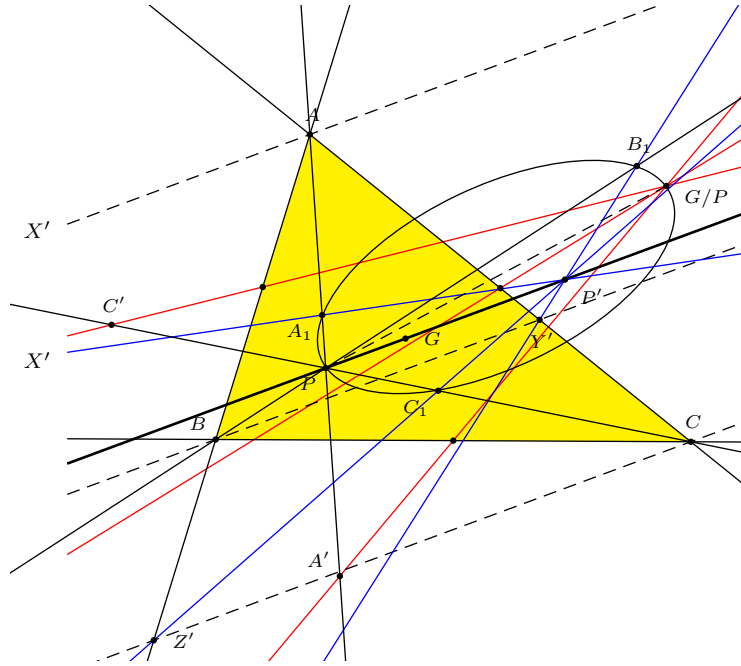

Figure 3.

Construction (Yiu)**.** Let P' be the superior of P, i.e., the point dividing PG in the ratio $PP' : P'G = 3 : -2$. Construct the parallels of the line PG through the vertices A, B, C, to intersect the sidelines BC, CA, AB at X', Y', Z' respectively. Then $A_1 = AP \cap X'P'$, $B_1 = BP \cap Y'P'$, and $C_1 = CP \cap Z'P'$. See Figure 3.

References

[1] J. H. Conway, Hyacinthos message 1018, June 14, 2000.
[2] C. Kimberling, Triangle centers and central triangles, *Congressus Numerantium*, 129 (1998) 1–285.
[3] P. Moses, Private communication, October 19, 2013.
[4] P. Yiu, Hyacinthos message 1030, June 16, 2000.
[5] P. Yiu, *Introduction to the Geometry of the Triangle*, Florida Atlantic University Lecture Notes, 2001; with corrections, 2013, available at
    http://math.fau.edu/Yiu/Geometry.html
[6] P. Yiu, ADGEOM message 728, October 19, 2013.

Francisco Javier García Capitán: Departamento de Matemáticas, I.E.S. Alvarez Cubero, Avda. Presidente Alcalá-Zamora, s/n, 14800 Priego de Córdoba, Córdoba, Spain
E-mail address: garciacapitan@gmail.com

A Vector-based Proof of Morley's Trisector Theorem

Cesare Donolato

Abstract. A proof is given of Morley's trisector theorem using elementary vector analysis and trigonometry. The known expression for the side of Morley's equilateral triangle is also obtained.

Since its formulation in 1899, many proofs of Morley's trisector theorem have appeared, typically based on plane geometry or involving trigonometry; a historical overview of this theorem with numerous references up to the year 1977 can be found in [4]. Some of the more recent geometric proofs are of the "backward" type [2, 5]; a group-theoretic proof was also given [3]. About fifteen different methods that were used to prove Morley's theorem are described in detail in [1], with comments on their specific characteristics. The website [1] also provides the related references, which span from the year 1909 to 2010.

In this note we prove the theorem in two stages. First a lemma is proved by use of the dot product of vectors and trigonometry, then the theorem itself easily follows from elementary geometry.

Morley's Theorem. *In any triangle, the three points of intersection of the adjacent angle trisectors form an equilateral triangle.*
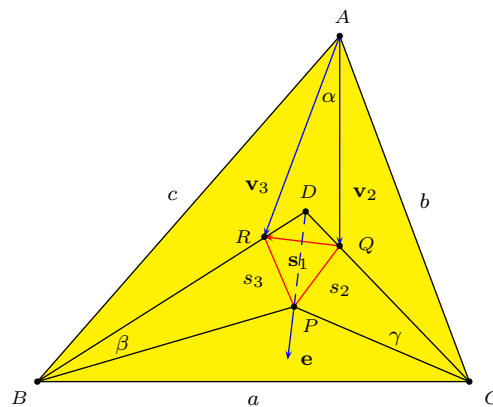

Figure 1

Let the angles of triangle ABC be of amplitude 3α, 3β, 3γ, then $\alpha + \beta + \gamma = 60°$. The adjacent trisectors meet to form Morley's triangle PQR; the line extensions of BR and CQ intersect at D. In triangle BDC the bisector of angle

---

D is concurrent with the other two bisectors BP and CP at P, the incenter of the triangle. First, a lemma is proved, from which the theorem easily follows.

Lemma.   *The line DP is perpendicular to the line RQ.*
Proof. Here use is made of the vector method in conjunction with trigonometry. Let $\mathbf{e}$ be the unit vector along DP and $\mathbf{s}_1$ the vector representing the side QR of triangle PQR. Then the lemma can be restated as saying that the scalar product $\mathbf{s}_1 \cdot \mathbf{e}$ vanishes. Figure 1 shows that $\mathbf{s}_1 = \mathbf{v}_3 - \mathbf{v}_2$ so that we must prove that

$$(\mathbf{v}_3 - \mathbf{v}_2) \cdot \mathbf{e} = 0.$$

In triangle BDC we have $2\beta + 2\gamma = 120° - 2\alpha$, therefore $\angle D = 60° + 2\alpha$. This angle is bisected by the line DP, hence $\angle QDP = \angle RDP = 30° + \alpha$. By the exterior angle theorem $\angle AQD = \alpha + \gamma$ and $\angle ARD = \alpha + \beta$. The angle between the vectors $\mathbf{v}_3$ and $\mathbf{e}$, being the difference between angles RDP and ARD, is $30° - \beta$. Similarly, the angle between $\mathbf{v}_2$ and $\mathbf{e}$ is $30° - \gamma$. From these,

$$\begin{aligned}
(\mathbf{v}_3 - \mathbf{v}_2) \cdot \mathbf{e} &= \mathbf{v}_3 \cdot \mathbf{e} - \mathbf{v}_2 \cdot \mathbf{e} \\
&= v_3 \cos(30° - \beta) - v_2 \cos(30° - \gamma) \\
&= v_3 \sin(60° + \beta) - v_2 \sin(60° + \gamma). \quad (1)
\end{aligned}$$

The magnitudes of $\mathbf{v}_3$ and $\mathbf{v}_2$ can be found by applying the law of sines to triangles ARB and AQC respectively:

$$v_3 = \frac{c \sin \beta}{\sin(\alpha + \beta)} = \frac{c \sin \beta}{\sin(60° - \gamma)}, \qquad v_2 = \frac{b \sin \gamma}{\sin(\alpha + \gamma)} = \frac{b \sin \gamma}{\sin(60° - \beta)}.$$

Substituting these expressions into (1), we obtain

$$\begin{aligned}
(\mathbf{v}_3 - \mathbf{v}_2) \cdot \mathbf{e} &= \frac{c \sin \beta \sin(60° + \beta)}{\sin(60° - \gamma)} - \frac{b \sin \gamma \sin(60° + \gamma)}{\sin(60° - \beta)} \\
&= \frac{c \sin \beta \sin(60° + \beta) \sin(60° - \beta) - b \sin \gamma \sin(60° + \gamma) \sin(60° - \gamma)}{\sin(60° - \beta) \sin(60° - \gamma)} \\
&= \frac{1}{4} \cdot \frac{c \sin 3\beta - b \sin 3\gamma}{\sin(60° - \beta) \sin(60° - \gamma)}
\end{aligned}$$

with the aid of the identity

$$\sin x \sin(60° + x) \sin(60° - x) = \frac{1}{4} \sin 3x, \quad (2)$$

which can be easily proved through the product-to-sum trigonometric formulas.

The law of sines for triangle ABC yields $c \sin 3\beta - b \sin 3\gamma = 0$. Therefore, $(\mathbf{v}_3 - \mathbf{v}_2) \cdot \mathbf{e} = 0$.   □

Proof of Morley's Theorem. Knowing that $DP \perp RQ$, we see that DP divides DQR into two congruent right triangles (with a common leg and a pair of equal acute angles) so that $DQ = DR$. Consequently, triangles DPQ and DPR are also congruent (by SAS), and $s_2 = s_3$. The whole procedure can be used to prove that $s_1 = s_2$. It follows that $s_1 = s_2 = s_3$, and triangle PQR is equilateral. This completes the proof of Morley's theorem.

Remark. Since triangle DQR is composed of two congruent right triangles, and $\angle QDR = 30° + \alpha$, its complement $\angle DQR = 60° - \alpha$.

The side of Morley's triangle. The side length s of the equilateral triangle PQR can be calculated by applying the law of sines to triangle AQR, whose angles are now known. Since $\angle RAQ = \alpha$, and $\angle AQR = \angle AQD + \angle DQR = (\alpha + \gamma) + (60° - \alpha) = 60° + \gamma$, we find that

$$s = \frac{v_3 \sin \alpha}{\sin(60° + \gamma)} = \frac{c \sin \alpha \sin \beta}{\sin(60° + \gamma) \sin(60° - \gamma)}.$$

By multiplying both terms of the last fraction by $\sin \gamma$, and using in the denominator the identity (2), we get the known expression for the side of Morley's triangle

$$s = \frac{4c \sin \alpha \sin \beta \sin \gamma}{\sin 3\gamma} = 8R \sin \alpha \sin \beta \sin \gamma,$$

where $R = \frac{c}{2 \sin 3\gamma}$ is the radius of the circumcircle of triangle ABC.

References

[1] A. Bogomolny, Morley's Miracle, `http://www.cut-the-knot.org/triangle/Morley/index.shtml`
[2] J. H. Conway, The Power of Mathematics, in *Power*, (edited by A. Blackwell and D. MacKay), Cambridge University Press, 2006; pp. 36–50.
[3] A. Connes, A new proof of Morley's theorem, *Publ. Math. IHES*, 88 (1998) 43–46.
[4] C. O. Oakley and J. C. Baker, The Morley Trisector Theorem, *Amer. Math. Monthly*, 85 (1978) 737–745.
[5] B. Stonebridge, A simple geometric proof of Morley's trisector theorem, *Math. Spectrum*, 42 (2009) 2–4.

Cesare Donolato: Via dello Stadio 1A, 36100 Vicenza, Italy
E-mail address: `cesare.donolato@alice.it`